Enhanced Primary Treatment during Wet Weather Flow by Metal-based Coagulants and Ferrate: Coagulation Optimization, Disinfection Kinetics Study, and Micropollutants Oxidation

By

Abdul Rahim Al Umairi

A thesis submitted in partial fulfillment of the requirements for the degree of
Doctor of Philosophy

in

Environmental Engineering

Department of Civil and Environmental Engineering

University of Alberta

Abstract

Wastewater during wet weather flow (WWF) is highly loaded with various pollutants including suspended solids, microorganisms, inorganics, organics, and micropollutants. My research compared different coagulant salts used in the enhanced primary treatment (EPT) during WWF. Then, my project explored ferrate as a coagulant/coagulant aid/disinfectant to be applied during the EPT and as an oxidant to degrade selected micropollutants.

Alum and poly-aluminum chloride surpassed ferric chloride and achieved higher removals of turbidity (90% to 93%) and ortho-phosphate (OP) (73% to 83%). All tested coagulants attained comparable removals of total suspended solids (TSS) (95% to 99%) and chemical oxygen demand (COD) (64% to 71%). The bench and full-scale data were in agreement. The turbidity and percent ultraviolet transmittance showed good correlations with TSS and OP which evokes their use for online process control and monitoring.

Ferrate as a coagulant was evaluated based on a two-level factorial design with an emphasis on the effects of rapid mixing, slow mixing, and polymer addition. At the optimized condition, ferrate (0.5 mg/L Fe) with a cationic polymer (1.25 mg/L) removed 83%, 87%, 70% and 23% of turbidity, TSS, COD, and OP respectively. General linear models were developed to adequately predict the responses. This study thoroughly examined ferrate, in a first application, as a coagulant aid with alum for the EPT. Ferrate (8 mg/L Fe) achieved 2.1 log removal of *E.coli* when used as a coagulant and more than 3 log removal when used as coagulant aid (with alum) or disinfectant (after coagulation/flocculation/settling). The target levels of turbidity (<8 NTU), TSS (< 25 mg/L) and ferrate-induced iron particles (<0.6 mg/L Fe), as well as 5-log removal of *E. coli*, were achieved

at 31 minutes with the optimum ferrate dose 10 mg/L Fe added as coagulant aid along with 6 mg/L Al of alum.

To further investigate the inactivation of *E. coli* in the EPT effluent, different ferrate doses (5, 8 and 10 mg/L Fe) were tested at different temperatures (9 and 19 °C). By increasing the ferrate dose from 5 to 10 mg/L Fe, the *E. coli* inactivation level increased from 1.6 to 4 log removal within 3 minutes at 19 °C. The disinfection kinetics data fit properly into Chick-Watson, Hom and Collins-Selleck models with adjusted R^2 ranging between 0.94 and 0.99. In particular, Chick-Watson's model was the most suitable to model the ferrate disinfection kinetics in the EPT effluent. The inactivation rate constant was less dependent on temperature and more dependent on ferrate dose which was also confirmed by ANOVA. Flow cytometry analysis revealed that ferrate could cause a significant damage to *E. coli* cell membrane whereas a limited damage to DNA was observed. It was also confirmed that hydrogen peroxide was produced *in-situ* during the application of ferrate. Ferrate slightly increased the acute toxicity of the EPT effluent likely due to the formation of toxic by-products.

This research also examined the effect of ferrate on the oxidation of selected micropollutants in a buffered solution. Ferrate exhibited high selectivity on the oxidation of the micropollutants that were classified into three groups: poorly reactive (removal <50%): atrazine (ATZ), fluconazole (FLC), mecoprop (MCPP), moderately reactive (removal>50%): diazinon (DZN), carbendazim (CDZ), perfluorooctanoic acid (PFOA), and highly reactive (removal > 85%): carbamazepine (CBZ), sulfamethoxazole (SMX), trimethoprim (TMP) and clindamycin (CLN). Most poorly and moderately reactive compounds as well as CLN showed less dependence on the pH. In contrast, PFOA was better removed at alkaline pH whereas CBZ, SMX and TMP were better removed at acidic pH. The oxidation kinetics of DZN and CLN were examined for the first-

time using ferrate with pseudo-second order rate constants 0.7314 $\mu M^{-1}s^{-1}$ and 0.0418 $\mu M^{-1}s^{-1}$, respectively. Hydroxyl radicals showed no contribution to the oxidation process in the ferrate system, while superoxide radical did contribute. Interestingly, ferric iron (Fe(III)) (reduced form of ferrate) showed minor contribution (up to 25%) to the overall removal of the tested compounds. The combination of UV/ferrate improved the removal of CDZ by seven times while it hindered the degradation of MCPP with a minor contribution of hydroxyl radical.

Preface

This thesis is an original work by Abdulrahim Alumairi who designed and conducted the experiments, collected and analyzed the data as well as prepared the manuscripts under the supervision of Dr. Mohamed Gamal El-Din. Some colleagues also helped in sample collection, sample preparation or contributed to the final editing as indicated below. Some analyses were done in other departments of the University of Alberta.

- Chapter 1 and 2: Dr. Zuo Tong How, Dr. Pamela Chelme-Ayala contributed to the revision and editing.
- Chapter 3 of this thesis was published as Alameddine, M., Al Umairi, A.R., Zakee Shaikh, M. and Gamal El-Din, M. 2020. Bench to Full-Scale Enhanced Primary Treatment of Municipal Wastewater under Wet Weather Flow for Minimized Pollution Load: Evaluation of Chemical Addition and Process Control Indicators. Canadian Journal of Civil Engineering. With Mirna Alameddine and Abdulrahim Alumairi as dual first author. Dr. Shu Zhu contributed in conducting some experiments related to polymer optimization.
- Chapter 4: Dr. Zuo Tong How, Dr. Pamela Chelme-Ayala contributed to the manuscript revision and editing. SEM and EDX analysis were conducted at NanoFAB labs by Miss Lingjun Meng.
- Chapter 5: Dr. Zuo Tong How, Dr. Pamela Chelme-Ayala contributed on manuscript revision and editing. Dr. Aja Rieger conducted Flow cytometry analysis in the Faculty of Medicine and Dentistry at the University of Alberta.
- Chapter 6: Dr. Zuo Tong How and Dr. Pamela Chelme-Ayala contributed to the manuscript revision and editing. Dr. Zuo Tong How and Dr. Ling Lingling Yang conducted the

micropollutants' analysis using the ultra-performance liquid chromatography time-of-flight mass spectrometry (UPLC-TOF-MS) and liquid chromatography mass spectrometry (LC-MS).

- Chapter 7: Dr. Pamela Chelme-Ayala and Dr. Mirna Alameddine, contributed to the chapter revision and editing.

Acknowledgements

First, I would like to express my sincere and great appreciation to my supervisor, Dr. Mohamed Gamal El-Din for his academic guidance, supervision, and advice without which this thesis could not be possible. My appreciation also goes to Dr. Zuo Tong How for his deep insights and invaluable comments that helped me improve my academic writing skills and opened new windows of thoughts. He indeed revised my thesis thoroughly and showed me always the way to improve. I would also like to thank Dr. Pamela Chelme-Ayala for her proofreading and editing my thesis and her unlimited support. I also appreciate all the other postdoctoral fellows in Dr. Gamal El-Din's research group who helped in the analyses and sample preparation for the analyses.

Thanks are also extended to Dr. Chengjin Wang for ferrate preparation and helpful insights and Miss Lingjun Meng for helping to conduct SEM and EDX analyses. I would like to also extend my thanks to Dr. Muhammad Arslan, Dr. Aja Rieger and Dr. Yanyan Zhang for their assistance and valuable insights regarding the FCM analysis, and to Mr. Yupeng Zhao for providing lab-cultured bacteria for FCM analysis. I also acknowledge the help of Dr. Mirna Alameddine, Mr. Ali Abelrahman, and Miss Lingjun Meng for their assistance in sampling during the disinfection kinetics experiments.

I would like to finally acknowledge the financial support provided by the research grants from Natural Sciences and Engineering Research Council of Canada (NSERC) Collaborative Research and Development (CRD) program and the scholarship from the Government of the Sultanate of Oman.

Table of Contents

List of Tables

List of Figures

List of Abbreviations

ABTS	2,2-azino-bis(3-ethylbenzothiazoline-6sulfonate)
Alum	Aluminum Sulfate
ATZ	Atrazine
CDZ	Carbendazim
CLN	Clindamycin
CMZ	Carbamazepine
C_o	Initial concentration
COD	Chemical oxygen demand
CSO	Combined Sewer Overflow
Ct	Disinfectant residual concentration x contact time
CW	Constructed wet land
DI	Deionized
DOC	Dissolved Organic Carbon
DZN	Diazinon
E. coli	*Escherichia coli*
FCL	fluconazole
FCM	Flow cytometry measurement
Fe(VI)	Ferrate
HRT	Hydraulic Retention Time
KHP	Potassium Hydrogen Phthalate
MCPP	Mecoprop
MPN	Most probable number

MPs	Micropollutants
N_o	Initial bacteria concentration
OP	Ortho Phosphate
pBZQ	*para*-benzoquinone
PFOA	Pentadecfluorooctanoic acid
PI	Primary influent
PPI	propidium iodide
rpm	rotations per minute
SGI	SYBR Green I
SMX	Sulfamethoxazole
TBA	Tert-Butyl Alcohol
TMP	Trimethoprim
TSS	Total Suspended Solids
TVSS	Total Volatile Suspended Solids
UV	Ultraviolet
UVA	Ultraviolet absorbance
UVT%	Ultraviolet Transmittance Percentage
WWTP	Wastewater treatment plant
ZP	Zeta Potential

Chapter 1: General Introduction and Research Objectives

1.1 Background

Wet weather flow (WWF) is associated with high contaminants loading to the surface water bodies through urban runoff, street runoff, agriculture runoff and bypassed water from combined sewer systems (Rechenburg et al., 2006). During WWF condition, the amount of wastewater in combined sewer systems exceed the design capacity of wastewater treatment plants thus excess water either receives partial treatment or is directly bypassed to the nearby receiving water bodies (El Samrani et al., 2008). Studies reported that stormwater and surface runoff increased the levels (2 log higher) of total coliform and pathogens (*Cryptosporidium* species and *E. bieneusi* and *G. duodenalis* genotypes) in surface water (Huang et al., 2017; Passerat et al., 2011; Rechenburg et al., 2006). Furthermore, wastewater during WWF is highly contaminated with pharmaceutical and personal care products (PPCPs), endocrine disrupting compounds (EDCs) and herbicides (Gasperi et al., 2010). As such, in southwest Stuttgart, Germany, wastewater during WWF increased the loading of overall herbicides and polyaromatic hydrocarbons by 90% (Launay et al., 2016). Another study conducted in the USA showed that 40% to 90% of the annual load of hormones and micro-pollutants detected in influent wastewater came from combined sewer during WWF (Phillips et al., 2012). These facts alerted the environmentalists and decision-makers to investigate different methods to curtail WWF impacts. The following section presents the available technologies used to mitigate WWF impacts.

1.1.1 Treatment technologies of wastewater during wet weather flow condition

WWF impacts might be mitigated by either upstream or downstream approaches. Upstream approaches mainly aim to regulate or reduce the influent level sent to the treatment facilities downstream. That includes real-time gate control, porous paving, storage basins and constructed wetlands (CWs) (Lucas and Sample, 2015). In Italy, CWs removed 87% of chemical oxygen demand (COD) and 93% of ammonium ion (NH_4^+) from wastewater during WWF condition (Masi et al., 2017). Under high solid loading condition, CWs may fail to achieve target removal. A study showed that during WWF, the removal of COD in CW had declined by 18% (Avila et al., 2013). While CWs require less operation and maintenance, they require a large footprint and have a low hydraulic rate (Tao et al., 2014). In contrast, downstream approaches that include enhancing the primary treatment using coagulation or enhanced coagulation processes (ballasted flocculation, plate settler), might be more compatible during WWF condition.

The primary treatment might be enhanced by incorporating coagulation/flocculation, before settling, using metal salts such as ferric chloride, alum, polyaluminum chloride (PACl) (Gandhi et al., 2014; Irfan et al., 2017; Jeon et al., 2017; Krupinska, 2018; Mbaeze MC, 2017; McFadden et al., 2017). As such for treating WWF wastewater, PACl (10 mg/L Al) and ferric chloride (35 mg/L) were used as coagulants and were able to remove 100% of turbidity (initial= 114 NTU) and >80% of heavy metals (Zn, Cu, Cr and Pb) (Initial concentration C_o= 25 to 160 µg/L, pH= 6.5 to 7.5, treatment time=40 minutes) (El Samrani et al., 2008). The authors suggested that the removal of turbidity occurred via charge-neutralization and sweep-flocculation mechanisms while heavy metal was removed via sorption onto the formed iron and aluminum hydroxides species. Similarly, both PACl (1.48 mg/L Al) and ferric chloride (2.67 mg/L Fe), spiked individually in WWF wastewater samples, removed >90% of total phosphorus (C_o =3.5 mg/L) and 60% to 70% of COD (C_o= 340 mg/L) and removed 10% to 20% of total nitrogen (C_o =28.6 mg/L) (pH = 7.21, turbidity =130 NTU, treatment time = 40 minutes)(Wang et al., 2016).

Coagulation could be further enhanced by employing a ballasted flocculation technique to increase the floc-settling velocities (Sumant et al., 2016). The ballasted flocculation includes the addition of a ballasting agent (micro-sand) in combination with metal-slat coagulant or polymer to coagulate/flocculate the colloidal particles (El Samrani et al., 2008). Therefore, in bench-scale experiments with WWF wastewater samples, implementing ballasted flocculation after alum coagulation increased the removals of TSS from 20% to 98% (alum= 9.7 to 17.8 mg/L Al, anionic polymer= 1 to 1.8 mg/L, micro-sand=3 g/L of size =300 μm) (Zhu et al., 2007). Likewise, in full-scale treatment, ballasted flocculation removed 80% to 86% of TSS and 83% to 89% of ortho-phosphate, and 50% to 90% of heavy metals (Cu, Zn and Pb) (ferric chloride = 70 to 80 mg/L, micro-sand =3.5 g/L and size= 100-150 μm, anionic polymer = 0.8 to 1.08 mg/L, pH=7) (Gasperi et al., 2012). While the aforementioned techniques were capable of removing the solid contents in the wastewater, they were incapable of reducing the microbial level. Therefore ferrate which is known to be a multifunctional chemical that acts as oxidant/disinfectant and coagulant might be a better choice to mitigate WWF impacts as compared to the conventionally used coagulants (Sharma, 2002). More details about ferrate are presented in the following section.

1.1.2 Ferrate

Ferrate (FeO_4^{2-}) is a powerful oxidant with a redox potential of 2.2 V which is higher than that of ozone (2.1 V) at an acidic condition (pH<2) (Jiang and Lloyd, 2002; Lee et al., 2014; Sharma, 2011). Also, ferrate has higher stability at higher pH thus for instance at pH=8 only 29% of ferrate decomposed in buffer solution compared to 51% at pH=7 after 8 hrs (Jiang and Lloyd, 2002). The self-decay of ferrate in water is explained by equations (1.1-1.6) (Lee et al., 2014). Ferrous species (Fe(V), Fe (IV)) generated by ferrate-decomposition (Fe(VI)) are more reactive than ferrate (Fe(VI)) (Cho et al., 2006; Sharma, 2013; Siskova et al., 2016). Ferrate-decay generates eventually hydroxide/oxide, hydrogen peroxide, and oxygen (Lee et al., 2014).

$$2\mathrm{HFe^{VI}O_4^-} + 4\mathrm{H_2O} \rightarrow 2\mathrm{H_3Fe^{IV}O_4^-} + 2\mathrm{H_2O_2} \qquad (1.1)$$

$$HFe^{VI}O_4^- + H_2O_2 \rightarrow H_3Fe^{IV}O_4^- + O_2 \quad (1.2)$$

$$HFe^{VI}O_4^- + H_2O_2 + H^+ \rightarrow Fe^{II}(OH)_2 + O_2 + 2H_2O \quad (1.3)$$

$$HFe^{VI}O_4^- + Fe^{II}(OH)_2 + H_2O \rightarrow H_2Fe^{V}O_4^- + Fe^{III}(OH)_3 \quad (1.4)$$

$$H_2Fe^{V}O_4^- + H_2O + H^+ \rightarrow Fe^{III}(OH)_3 + H_2O_2 \quad (1.5)$$

$$H_2Fe^{V}O_4^- + H_2O_2 + H^+ \rightarrow Fe^{III}(OH)_3 + O_2 + H_2O \quad (1.6)$$

1.1.2.1 Ferrate as a coagulant

The coagulation property of ferrate is derived from the ferric oxide/hydroxide, the final reduced form of ferrate, which evident to destabilize the colloids in suspension (Jiang et al., 2001). The colloidal particles may destabilize via charge neutralization or sweep-flocculation. In principle, the charge neutralization occurs when the coagulant is applied at low doses not exceeding the solubility limit of metal hydroxide (Duan and Gregory, 2003). Therefore, the cationic hydrolyzed species of the coagulant are adsorbed on the surface of the negatively charged colloid particles. In contrast, the sweep-flocculation occurs when the coagulant is applied in a high concentration exceeding the solubility limit leading to rapid formation hydroxide precipitates which enmesh the colloid particles (Duan and Gregory, 2003). A study showed that, a low dose of Ferrate (0.24 mg/L Fe) was able to remove more than 70% of TSS and COD when used to treat wastewater during WWF (pH=6, COD_o=314±36 mg/L, TSS_o=200±80 mg/L) (Gandhi et al., 2014). The removal of TSS likely occurred due to the coagulation action of ferric species while COD occurred via coagulation of particulate COD by ferric species and oxidation of soluble COD by ferrate reactive species (Gandhi et al., 2014). Ferrate could simultaneously remove heavy metals (Cu, Mn) (>80%) and natural organic matter (NOM) (>86%) via oxidation, precipitation and/or adsorption (heavy metal= 0.1 Mm, ferrate= 0.7 Mm, pH= 6-7, DOC= 10 mg/L) (Lim and Kim, 2010). Ferrate coagulation was positively impacted by increasing the pH which is in favor of forming more ferric hydroxide. Therefore, by increasing pH from 6 to 9, the removal of TSS and COD increased by 30% (Gandhi et al., 2014). The presence of organic matter may interfere with the coagulation process as ferrate oxidizes NOM to a more hydrophilic form generating negatively charged coating adsorbed on iron oxide which inhibits flocs growth (DOC=8 to 10 mg/L, pH=7.5, turbidity=25 NTU, Ferrate=3 mg/L) (Lv et al., 2018). Ferrate coagulation capacity might be enhanced by combination with other coagulants. Therefore, using ferrate with ferric chloride results in rapid flocs formation (fasted coagulation of counter charges of hydrolysis species) and better removal of suspended solids (ferrate =1.7 mg/L Fe, ferric chloride=6.7 mg/L Fe, DOC= 41 mg/L, turbidity=13 NTU, pH=7.8) (Yu et al., 2016).

1.1.2.2 Ferrate as a disinfectant

Ferrate has a biocidal effect with the ability to inactivate a wide variety of microorganisms and a high potential to remove disinfection by-products precursors (Sharma et al., 2005). It was able to inactivate chlorination resisting organisms such as aerobic-forming spores and sulfite-reducing clostridia (Sharma, 2007). Furthermore, using ferrate as a pre-oxidant followed by chlorination or ozonation reduced the formation of trihalomethane and bromate (Gan et al., 2015; Jiang et al., 2016). Therefore, ferrate was considered a competing disinfectant and used to disinfect water and wastewater (Cho et al., 2006; Jiang et al., 2007; Lee et al., 2004). When applied to ballasted water (saline water), ferrate (5 mg/L Fe) achieved > 4-log removal of *Enterococci, E. coli* and *vibrio cholera* (pH=8, DOC=0, N_o=10^5 to 10^7 CFU/mL) (Jessen et al., 2008). In secondary effluent, ferrate (5 mg/L Fe) attained 2.5 log removal of *E. coli* compared to 1 log achieved by chlorine (5 mg/L Cl_2) within 20 minutes (pH= 7.85, COD=7 mg/L, N_o=250 to 500 CFU/mL) (Kwon et al., 2014). Ferrate was examined to disinfect raw WWF wastewater, thus 7 mg/L Fe of ferrate inactivated 3.8 log of *E. coli* within 81 minutes (pH=6.7, TSS=83 mg/L, COD=280 mg/L,

N_o= 2.2 x 10^6 to 2.7 x 10^7 MPN/100mL) (Elnakar and Buchanan, 2019). Ferrate also inactivated 4-log of enteric pathogenic bacteriophage M2S with a dose of 1.25 mg/L Fe within 3 minutes (phosphate buffer, pH= 7, N_o=7.3 x 10^6 plaque forming unit/mL) (Hu et al., 2012).

1.1.2.3 Ferrate as an oxidant

Ferrate is a selective oxidant attacking compounds with electron-rich moieties (ERM) (e.g. phenols, anilines, amines, and olefins) (Jiang, 2015; Lee et al., 2009; Yang et al., 2012). In a secondary effluent spiked with micropollutants (C_o= 0.05 to 0.32 mg/L, pH 6 to 8), ferrate (2 to 5 mg/L Fe) degraded >95% of phenolic containing compounds (e.g. bisphenol A and triclosan) and 85% of amine and olefin containing compounds (e.g. carbamazepine and diclofenac) (Lee et al., 2009). A higher ferrate dose (15 mg/L Fe) was required to degrade 40% of compounds without ERM (iopromide and ibuprofen, bezafibrate). In a mixture of micropollutants (C_o = 100 µg/L) in clean water, ferrate (5 mg/L Fe) also degraded 60% to 80% of diclofenac, sulfamethoxazole and carbamazepine while only 20% of bezafibrate (Zhou and Jiang, 2015). Ferrate (5.5 mg/L Fe) degraded 100% of β-lactam antibiotic (amoxicillin, ampicillin, cloxacillin, and penicillin G) present in secondary effluent wastewater (pH =7 to 8.5, antibiotic= 0.668 mg/L) (Karlesa et al., 2014).

1.2 Research hypotheses

The main hypotheses of this research are:

- Metal salts are capable of destabilizing the suspended collides in WWF samples via different mechanisms including charge-neutralization, sweep-flocculation, inter-particle bridging and precipitation/adsorption. Evaluation of different coagulants based on the removal of the general water quality parameters is very important to achieve the best decision.

- The coagulation/flocculation processes are highly dependent on the coagulant and coagulant aid doses and the mixing condition (rapid mixing/slow mixing) thus optimization of the involved factors is very crucial to achieve effective treatment.
- Ferrate is considered as a strong oxidant and reduced to ferric species which makes it acting simultaneously as an oxidant and coagulant. This might make ferrate a strong candidate to mitigate WWF concerns at a single dosing point.
- Ferrate is a selective oxidant thus effectively oxidizes compounds with electron-rich moieties while compounds without rich moieties may show high persistency. Benchmarking the reactivity of highly detected micropollutants with ferrate provides important information for real application during WWF condition.
- Ferrate-oxidation efficiency depends on the initial concentration of ferrate and the contaminants, Physico-chemical properties of the micropollutants, pH and background demand.
- Ferrate is believed to be more reactive at an acidic medium ($pH \leq 5.2$) where protonated species are predominant.
- The oxidation-process in the ferrate system may occur directly via ferrate (Fe(VI)) and indirectly via intermediate generated reactive species: perferryl (Fe(V)), ferryl (Fe(IV)), hydrogen peroxide (H_2O_2), superoxide radical ($O^{\bullet -}{}_2$) and hydroxyl radical ($^{\bullet}OH$).
- The combination of ferrate/UV is expected to promote the formation of superoxide radical which may benefit the removal of the persistent micropollutants.

1.3 Research scope and objectives

The objectives of this research are:

- To evaluate the efficiencies of different metals salts as primary coagulants for enhanced primary treatment (EPT) during wet weather flow (WWF) (chapter 3). Moreover, to obtain the best operation condition by addressing the effects different operation factors such as initial dose of coagulant/coagulant aid, mixing conditions.

- To thoroughly evaluate ferrate as a coagulant, coagulant aid, and disinfectant for EPT for simultaneously minimizing the levels of solids and bacteria (chapter 4)
- To study ferrate inactivation kinetic when used under environmentally relevant conditions (real wastewater, unadjusted pH, relevant temperature) and finding the important disinfection kinetic parameters for real application (inactivation rate constant, CT) along with ferrate-mode of action during disinfection process (chapter 5).
- To examine the oxidation capacity of ferrate for selected micropollutants under environmentally relevant conditions (concentration in µg/L, spiked in mixture) and the effects of the oxidant dose and pH levels (chapter 6). The oxidation kinetics of selected micropollutants and the contribution of oxygen reactive species were also explored. The combination of UV/ferrate process was investigated against ferrate-persistent micropollutants and radical species contribution was evaluated.

1.4 Thesis organization

This thesis comprises seven chapters as per the following.

- Chapter one provides a general overview about the main theme of the research addressing the concerns associated with treating wastewater during WWF and proposing ferrate as a multifunctional compound able to work as oxidant/disinfectant/coagulant. Chapter one also states the hypotheses, main objectives, and the thesis organization.
- Chapter two represents a detailed literature review regarding the potential hazard of WWF and possible use of ferrate to mitigate the expected effects.

- Chapter three explores the capacity of different coagulants namely alum, aluminum polychloride and ferric chloride to treat WWF wastewater and the optimized conditions obtained based on bench to full-scale experiments.
- Chapter four focuses mainly on ferrate as a coagulant, coagulant aid and disinfectant and explores thoroughly its capacity to treat wastewater during WWF to simultaneously minimize the microbial level and solids contents.
- Chapter five studies ferrate as a disinfectant and evaluates the disinfection-kinetics parameters using different models to describe the obtained data and highlight the effects of temperature and ferrate dose on the inactivation of *E. coli*. Moreover, in chapter five the ferrate-mode of action for inactivating *E. coli* is explored using flow cytometry analysis.
- Chapter six explores the potential of ferrate to oxidize selected micropollutants at environmentally relevant conditions. It shows the effect of pH and the initial dose of ferrate. Furthermore, in chapter six the oxidation-kinetics of a selected micropollutant were examined and the contribution of oxygen reactive species was investigated. Also, the combination of UV/ferrate for the removal of the micropollutant that exhibited low to moderate reactivity with ferrate was also addressed.
- Finally, chapter seven summarizes the conclusions responding to the research objectives and provides recommendations for future works.

1.5 References

Avila, C., Jose Salas, J., Martin, I., Aragon, C. and Garcia, J. 2013. Integrated treatment of combined sewer wastewater and stormwater in a hybrid constructed wetland system in southern Spain and its further reuse. Ecological Engineering 50, 13-20.

Cho, M., Lee, Y., Choi, W., Chung, H.M. and Yoon, J. 2006. Study on Fe(VI) species as a disinfectant: Quantitative evaluation and modeling for inactivating Escherichia coli. Water Research 40(19), 3580-3586.

El Samrani, A.G., Lartiges, B.S. and Villieras, F. 2008. Chemical coagulation of combined sewer overflow: Heavy metal removal and treatment optimization. Water Res. 42(4-5), 951-960.

Elnakar, H. and Buchanan, I. 2019. The role of mixing in potassium ferrate(VI) consumption kinetics and disinfection of bypass wastewater. Journal of Environmental Management 231, 515-523.

Gan, W.H., Sharrna, V.K., Zhang, X., Yang, Y. and Yang, X. 2015. Investigation of disinfection byproducts formation in ferrate(VI) pre-oxidation of NOM and its model compounds followed by chlorination. Journal of Hazardous Materials 292, 197-204.

Gandhi, R., Ray, A.K., Sharma, V.K. and Nakhla, G. 2014. Treatment of Combined Sewer Overflows Using Ferrate (VI). Water Environment Research 86(11), 2202-2211.

Gasperi, J., Laborie, B. and Rocher, V. 2012. Treatment of combined sewer overflows by ballasted flocculation: Removal study of a large broad spectrum of pollutants. Chem. Eng. J. 211, 293-301.

Gasperi, J., Rocher, V., Gilbert, S., Azimi, S. and Chebbo, G. 2010. Occurrence and removal of priority pollutants by lamella clarification and biofiltration. Water Research 44(10), 3065-3076.

Gombos, E., Barkacs, K., Felfoldi, T., Vertes, C., Mako, M., Palko, G. and Zaray, G. 2013. Removal of organic matters in wastewater treatment by ferrate (VI)-technology. Microchemical Journal 107, 115-120.

Hu, L., Page, M.A., Sigstam, T., Kohn, T., Marinas, B.J. and Strathmann, T.J. 2012. Inactivation of Bacteriophage MS2 with Potassium Ferrate(VI). Environmental Science & Technology 46(21), 12079-12087.

Huang, C.C., Hu, Y., Wang, L., Wang, Y.F., Li, N., Guo, Y.Q., Feng, Y.Y. and Xiao, L.H. 2017. Environmental Transport of Emerging Human-Pathogenic Cryptosporidium Species and Subtypes through Combined Sewer Overflow and Wastewater. Applied and Environmental Microbiology 83(16), 11.

Irfan, M., Butt, T., Imtiaz, N., Abbas, N., Khan, R.A. and Shafique, A. 2017. The removal of COD, TSS and colour of black liquor by coagulation-flocculation process at optimized pH, settling and dosing rate. Arabian Journal of Chemistry 10, S2307-S2318.

Jeon, J.C., Jung, Y.J., Kwon, K.H. and Min, K.S. 2017. Enhanced water quality of CSOs with different coagulant treatment. Desalin. Water Treat. 63, 469-477.

Jessen, A., Randall, A., Reinhart, D. and Daly, L. 2008. Effectiveness and Kinetics of Ferrate as a Disinfectant for Ballast Water. Water Environment Research 80(6), 561-569.

Jiang, J.Q. 2015. The role of ferrate(VI) in the remediation of emerging micropollutants: a review. Desalination and Water Treatment 55(3), 828-835.

Jiang, J.Q. and Lloyd, B. 2002. Progress in the development and use of ferrate(VI) salt as an oxidant and coagulant for water and wastewater treatment. Water Research 36(6), 1397-1408.

Jiang, J.Q., Lloyd, B. and Grigore, L. 2001. Preparation and evaluation of potassium ferrate as an oxidant and coagulant for potable water treatment. Environmental Engineering Science 18(5), 323-328.

Jiang, J.Q., Wang, S. and Panagoulopoulos, A. 2007. The role of potassium ferrate(VI) in the inactivation of Escherichia coli and in the reduction of COD for water remediation. Desalination 210(1-3), 266-273.

Jiang, Y.J., Goodwill, J.E., Tobiason, J.E. and Reckhow, D.A. 2016. Bromide oxidation by ferrate(VI): The formation of active bromine and bromate. Water Research 96, 188-197.

Karlesa, A., De Vera, G.A.D., Dodd, M.C., Park, J., Espino, M.P.B. and Lee, Y. 2014. Ferrate(VI) Oxidation of beta-Lactam Antibiotics: Reaction Kinetics, Antibacterial Activity Changes, and Transformation Products. Environmental Science & Technology 48(17), 10380-10389.

Krupinska, I. 2018. Removal of natural organic matter from groundwater by coagulation using prehydrolysed and non- prehydrolysed coagulants. Desalin. Water Treat. 132, 244-252.

Kwon, J.H., Kim, I.K., Park, K.Y., Kim, Y.D. and Cho, Y.H. 2014. Removal of phosphorus and coliforms from secondary effluent using ferrate(VI). Ksce Journal of Civil Engineering 18(1), 81-85.

Launay, M.A., Dittmer, U. and Steinmetz, H. 2016. Organic micropollutants discharged by combined sewer overflows - Characterisation of pollutant sources and stormwater-related processes. Water Res. 104, 82-92.

Lee, Y., Cho, M., Kim, J.Y. and Yoon, J. 2004. Chemistry of ferrate (Fe(VI)) in aqueous solution and its applications as a green chemical. Journal of Industrial and Engineering Chemistry 10(1), 161-171.

Lee, Y., Kissner, R. and von Gunten, U. 2014. Reaction of Ferrate(VI) with ABTS and Self-Decay of Ferrate(VI): Kinetics and Mechanisms. Environmental Science & Technology 48(9), 5154-5162.

Lee, Y., Zimmermann, S.G., Kieu, A.T. and von Gunten, U. 2009. Ferrate (Fe(VI)) Application for Municipal Wastewater Treatment: A Novel Process for Simultaneous Micropollutant Oxidation and Phosphate Removal. Environmental Science & Technology 43(10), 3831-3838.

Lim, M. and Kim, M.-J. 2010. Effectiveness of Potassium Ferrate (K2FeO4) for Simultaneous Removal of Heavy Metals and Natural Organic Matters from River Water. Water Air and Soil Pollution 211(1-4), 313-322.

Lucas, W.C. and Sample, D.J. 2015. Reducing combined sewer overflows by using outlet controls for Green Stormwater Infrastructure: Case study in Richmond, Virginia. Journal of Hydrology 520, 473-488.

Lv, D., Zheng, L., Zhang, H. and Deng, Y. 2018. Coagulation of colloidal particles with ferrate(vi). Environmental Science-Water Research & Technology 4(5), 701-710.

Masi, F., Rizzo, A., Bresciani, R. and Conte, G. 2017. Constructed wetlands for combined sewer overflow treatment: Ecosystem services at Gorla Maggiore, Italy. Ecological Engineering 98, 427-438.

Mbaeze MC, A.V.a.O.N. 2017. Comparative Assessment of Performance of Aluminium Sulphate (Alum) and Ferrous Sulphate as Coagulants in Water Treatment Modern Chemistry & Applications 5(4).

McFadden, M., Loconsole, J., Schockling, A., Nerenberg, R. and Pavissich, J.P. 2017. Comparing peracetic acid and hypochlorite for disinfection of combined sewer overflows: Effects of suspended-solids and pH. Sci. Total Environ. 599, 533-539.

Passerat, J., Ouattara, N.K., Mouchel, J.-M., Rocher, V. and Servais, P. 2011. Impact of an intense combined sewer overflow event on the microbiological water quality of the Seine River. Water Research 45(2), 893-903.

Phillips, P.J., Chalmers, A.T., Gray, J.L., Kolpin, D.W., Foreman, W.T. and Wall, G.R. 2012. Combined Sewer Overflows: An Environmental Source of Hormones and Wastewater Micropollutants. Environ. Sci. Technol. 46(10), 5336-5343.

Rechenburg, A., Koch, C., Classen, T. and Kistemann, T. 2006. Impact of sewage treatment plants and combined sewer overflow basins on the microbiological quality of surface water. Water Science and Technology 54(3), 95-99.

Sharma, V.K. 2002. Potassium ferrate(VI): an environmentally friendly oxidant. Advances in Environmental Research 6(2), 143-156.

Sharma, V.K. 2007. Disinfection performance of Fe(VI) in water and wastewater: a review. Water Science and Technology 55(1-2), 225-232.

Sharma, V.K. 2011. Oxidation of inorganic contaminants by ferrates (VI, V, and IV)-kinetics and mechanisms: A review. Journal of Environmental Management 92(4), 1051-1073.

Sharma, V.K. 2013. Ferrate(VI) and ferrate(V) oxidation of organic compounds: Kinetics and mechanism. Coordination Chemistry Reviews 257(2), 495-510.

Sharma, V.K., Kazama, F., Jiangyong, H. and Ray, A.K. 2005. Ferrates (iron(VI) and iron(V)): Environmentally friendly oxidants and disinfectants. Journal of Water and Health 3(1), 45-58.

Siskova, K.M., Jancula, D., Drahos, B., Machala, L., Babica, P., Alonso, P.G., Travnicek, Z., Tucek, J., Marsalek, B., Sharma, V.K. and Zboril, R. 2016. High-valent iron (Fe-VI, Fe-V, and Fe-IV) species in water: characterization and oxidative transformation of estrogenic hormones. Physical Chemistry Chemical Physics 18(28), 18802-18810.

Sumant, K., Ghosh, N.C. and Kazmi, A.A. 2016. Ballasted sand flocculation for water, wastewater and CSO treatment. Environmental Technology Reviews 5(1), 57-67.

Tao, W.D., Bays, J.S., Meyer, D., Smardon, R.C. and Levy, Z.F. 2014. Constructed Wetlands for Treatment of Combined Sewer Overflow in the US: A Review of Design Challenges and Application Status. Water 6(11), 3362-3385.

Wang, W.-g., Xu, Z.-x., Li, H.-z. and Jin, W. 2016. Coagulation characteristics of organic pollutants removal in cso wastewater treatment. Environmental Engineering and Management Journal 15(1), 75-80.

Yang, B., Ying, G.G., Zhao, J.L., Liu, S., Zhou, L.J. and Chen, F. 2012. Removal of selected endocrine disrupting chemicals (EDCs) and pharmaceuticals and personal care products (PPCPs) during ferrate(VI) treatment of secondary wastewater effluents. Water Research 46(7), 2194-2204.

Yu, W.Z., Yang, Y.J. and Graham, N. 2016. Evaluation of ferrate as a coagulant aid/oxidant pretreatment for mitigating submerged ultrafiltration membrane fouling in drinking water treatment. Chem. Eng. J. 298, 234-242.

Zhou, Z. and Jiang, J.Q. 2015. Reaction kinetics and oxidation products formation in the degradation of ciprofloxacin and ibuprofen by ferrate(VI). Chemosphere 119, S95-S100.

Zhu, W., Seth, R. and Lalman, J. 2007. Evaluation of a micro carrier weighted coagulation flocculation process for the treatment of combined sewer overflow. Environmental Technology 28(7), 761-770.

Chapter 2: Literature Review Wastewater during Wet Weather Flow Condition: Major Concerns and Potential Treatment Technologies

2.1 Introduction

Combined sewer systems (stormwater with sewage) exist in some cities around the world and might be considered a potential risk to the environment (Phillips et al., 2012). During wet weather flow (WWF) conditions, these systems convey tremendous amounts of wastewater which eventually bypass or receive partial treatment due to limited design capacities of wastewater treatment plants (WWTPs). Therefore, during WWF the contaminant loads (e.g. organic, microorganism, heavy metals, toxic chemical) increase dramatically in water bodies and threaten beneficiaries and aquatic lives (Tondera et al., 2016). Detailed studies show that WWF contributed by 40 to 90% to the total load of pharmaceutical and personal care products (PPCPs); endocrine disrupting compounds (EDCs) and herbicides (Launay et al., 2016; Phillips et al., 2012; Ryu et al., 2014). Besides that, conventional WWTPs failed to adapt to these inevitable challenges which unveil the necessity of proposing more efficient techniques to overcome this problem.

In the literature, there are several approaches proposed to curtail WWF impacts such as constructed wetlands, storage basins, rain gardens, real-time control for inlet and outlet gates, enhancement of primary treatment (Lucas and Sample, 2015; Tao et al., 2014). Most surveyed studies did not account equally for the reduction of both microbial contents along with other water quality parameters (e.g. suspended solid, turbidity) and micropollutants. Recently ferrate emerged as a powerful compound that may work effectively as an oxidant/disinfectant and to certain extent as a coagulant (Collivignarelli et al., 2018). Many researchers examined ferrate in lab scale experiments for different water matrices (surface water, ground water, municipal wastewater) and showed promising results (Dong et al., 2019; Rai et al., 2018; Sharma, 2002; Sharma and Bielski, 1991; Sharma et al., 2017; Zhang et al., 2020). Nonetheless, there are limited studies evaluating the efficacy of ferrate for treating wastewater during WWF. More details about ferrate and other available technologies which might be considered to mitigate the effect of WWF are presented in this review.

The main objectives of this review were to introduce WWF problem and major concerns and highlight the characteristics of wastewater during WWF and the contaminants loadings. Also, this review presented the available technologies for mitigating WWF impacts and introduced ferrate either alone or with other technologies to curtail the WWF effects.

2.2 WWF occurrence and pollutant levels

In combined sewer systems, wastewater during WWF is composed of sewage drainages, stormwater, street runoff, roof runoff and garden run off. Therefore, WWF is highly associated with environmental risks due to the imposed contaminant loads. Indeed, WWF wastewater boosts the levels, in the water surface bodies, of total suspended solids (TSS), chemical oxygen demand (COD), biochemical oxygen demand (BOD), along with other organic/inorganic and microbial contents (Launay et al., 2016; Tondera et al., 2016). For instance, a study reported that street runoff in Paris showed a higher contribution (40% to 70%) of organic (TSS, TVSS, COD and BOD) loads during WWF while roof runoff contributed significantly (80%) to the load of heavy metal contaminants (e.g. Pb and Zn) (Gromaire et al., 2001). Similarly in the Greater Milwaukee area, stormwater sourced ≥ 70% of TSS and heavy metals while sanitary sewer contributed ≥ 58% of ammonia (NH_3) (Soonthornnonda and Christensen, 2008). It was reported that the contribution of roof runoff during WWF to the total loading of heavy metals (arsenic, copper and zinc) was correlated to the age of roof materials (≥10 years) and the level of precipitation (McIntyre et al., 2019). In cold countries such as Canada, snowmelt along with wet weather runoffs could contaminate significantly drinking water sources with micropollutants (detected in ng/L to µg/L levels) such as carbamazepine, caffeine and acetaminophen and microorganisms (e.g. *Escherichia coli*) (Madoux-Humery et al., 2013). It was found that, based on a long monitoring assessment (2002-2011), WWF wastewater contributed by 80% to the total *Escherichia coli* (*E.coli*) in surface waters during peak time (500 to 1000 CFU/100mL) (Madoux-Humery et al., 2016). Other studies reported that stormwater and surface runoff increased significantly (2 log higher) the levels of total coliform and pathogenic species (*Cryptosporidium* species and *E. bieneusi* and *G. duodenalis* genotypes) in surface water (Huang et al., 2017; Passerat et al., 2011; Rechenburg et al., 2006).

Storm runoff was also classified as a major source of pesticides (i.e. insecticides, herbicides, fungicides), polycyclic aromatic hydrocarbons (PAHs), and metals. As such, in southwest Stuttgart, Germany, stormwater increased the loading of all herbicides and polycyclic aromatic hydrocarbons (PAHs) by 90% (Launay et al., 2016). Another study conducted in USA unveiled that the WWF wastewater was the main source of 40% to 90% of the annual load of hormones and micropollutants (e.g. benzophenone, caffeine, triclosan) (Phillips et al., 2012). In Seoul, EDCs and PPCPs levels during WWF was 69.8 kg/day compared with 65.1 kg/day during dry weather (Ryu et al., 2014). Moreover, in Copenhagen, the level of PAHs (e.g. indeno (1,2,3-cd) pyrene, pyrene) and pesticides (e.g. glyphosate and aminomethylphsphonic acid) in WWF wastewater was found to be higher than that in stormwater by four times (Birch et al., 2011). Table 2.1 summarizes the concentration of different contaminants in the influents of wastewater treatment plants during WWF and dry weather flow (DWF) wastewaters. These studies revealed the real challenge imposed by WWF conditions and should alert the environmentalists and decision makers to take a big leap to find effective measures for its treatment.

Table 2. 1 Summary of contaminant levels reported in the literature in the influent of wastewater treatment plants during wet weather flow (WWF) and dry weather flow (DWF).

Parameter	WWF	DWF	Reference
Total suspended solid (mg/L)	86.8	284	(Soonthornnonda and Christensen, 2008)
Chemical oxygen demand (mg/L)	138-336	436-539	(Avila et al., 2013)
Biochemical oxygen demand (mg/L)	24	281	Soonthornnonda and Christensen, 2008)
Ammonia (NH_3) (mg/L)	0.831	13.8	Soonthornnonda and Christensen, 2008)
Total phosphorus (mg/L)	0.815	5.45	Soonthornnonda and Christensen, 2008)
Ortho-phosphate (mg/L)	1.2	5.4	(Avila et al., 2013)
***Escherichia coli* (CFU/100mL)**	1.36 x10^5	1.41x10^5	Soonthornnonda and Christensen, 2008)
Fecal coliform (CFU/100mL)	7.3 x10^5	2.14x10^6	Soonthornnonda and Christensen, 2008)
Heavy metals (µg/L)			
Cadmium	2.40	1.58	Soonthornnonda and Christensen, 2008)
Chromium	15.37	43.67	Soonthornnonda and Christensen, 2008)
Copper	26.87	72.67	Soonthornnonda and Christensen, 2008)
Lead	43.17	10.77	Soonthornnonda and Christensen, 2008)
Nickle	9.94	11.17	Soonthornnonda and Christensen, 2008)
Mercury	0.0611	0.1587	Soonthornnonda and Christensen, 2008)
Zink	103.7	164.7	Soonthornnonda and Christensen, 2008)
Micropollutants (µg/L)			
Caffeine	32.9	44.6	(Del Rio et al., 2013)
Ibuprofen	8.51	2.11	(Del Rio et al., 2013)
Carbamazepine	0.03-0.2	0.3-0.9	(Del Rio et al., 2013)
Bezafibrate	0.1-1	0.01-0.11	(Launay et al., 2016)
Sulfamethoxazole	0.005-0.04	0.15-0.8	(Launay et al., 2016)
Naproxen	0.03-38	0.5-55	(Launay et al., 2016)
Mecoprop	0.09-0.4	0.015-0.106	(Launay et al., 2016)
β-Lactams	NA*	4.633	(Segura et al., 2009)
Sulfonamides	NA	11.972	(Segura et al., 2009)
Tetracyclines	NA	11600	(Segura et al., 2009)
Trimethoprim	NA	0.27-1.351	(Segura et al., 2009)

Paracetamol	5.71	0.72	(Del Rio et al., 2013)
Carbendazim	0.01-0.1	0.02-0.04	(Launay et al., 2016)
Diazinon	1.05	0.133	(Koeck-Schulmeyer et al., 2013)
Bisphenol A	0.1-0.4	1-2	(Phillips et al., 2012)
Atrazine	0.081-0.130	0.00124	(Koeck-Schulmeyer et al., 2013)
Estrone	0.004-0.040	0.002-0.010	(Phillips et al., 2012)

*NA not available

2.3 WWF wastewater treatment approaches

Several approaches were reported in the literature to mitigate WWF impacts either upstream or downstream (Autixier et al., 2014; Lucas and Sample, 2015; Tao et al., 2014). The selection of the most effective approach depends on various factors such as water qualities, footprint availability, economic feasibility and water quality compatibility (EPA, 1999). The following sections presented different treatment approaches proposed to mitigate WWF impacts.

Upstream control techniques (e.g. porous paving, real-time gates, off-line treatment) aim to minimize, regulate, or partially treat WWF wastewater conveyed to downstream treatment facilities. As such, porous paving is designed to minimize street runoff by accelerating infiltration of the water during WWF to groundwater through porous paving material (e.g. interlock, bricks, asphalt). For instance, in the city of St. Louis, urban runoff was reduced by 36% to 46% by using permeable concrete and brick paver respectively (Alyaseri and Zhou, 2016). Another upstream approach is real-time gate control which integrates with an automatic control system connected to the storage unit and pump station to regulate WWF influent to WWTPs (Duchesne et al., 2001). In contrast, the off-line treatment approach is partially treating WWF wastewater by diverting excess water to separate units for screening, sedimentation, and storage which proved to remove 25%-75% of TSS (Szabo et al., 2005).

Constructed wetlands (CWs) are composed of water basin with a substrate (e.g. gravel, soil, organic matter) and vascular plant (Avila et al., 2013). The main advantage of CWs is having less operation and maintenance requirements, whereas its main drawback is a large footprint and a low hydraulic rate (Tao et al., 2014). In Italy, CWs had removed 93% of ammonium ion (NH_4^+) from the wastewater during WWF condition (Masi et al., 2017). Another study reported that, the treatment quality of CW for the removal of COD had declined by 18% compared to that during wet weather (Avila et al., 2013).

Downstream treatment approaches are mainly carried out by enhancing the primary treatment of wastewater in WWTP (Haydar and Aziz, 2009). Therefore, different techniques were proposed for enhanced primary treatment (EPT) such as vortex separator, chemical coagulation and enhanced chemical coagulation. In particular, the vortex separator is hydrodynamic unit where the influent is subjected to a high flow rotary regime to extend the resident time and consequently remove suspended solids (Andoh and Saul, 2003). Indeed, a vortex separator is more suitable for particles with high settling characteristics, otherwise chemical coagulation becomes more effective (Kok, 2004).

EPT by chemical coagulation has a high advantage associated with the minimal requirement of infrastructure and maintenance. There were different coagulants examined for EPT such as ferric chloride, alum, polyaluminum chloride (PACl) (Gandhi et al., 2014; Irfan et al., 2017; Jeon et al., 2017; Krupinska, 2018; Mbaeze MC, 2017; McFadden et al., 2017). In one study, PACl (10 mg/L Al) and ferric chloride (35 mg/L) removed 100% of turbidity (initial= 114 NTU) and >80% of heavy metals (Zn, Cu, Cr and Pb) (C_o= 25 to 160 µg/L, pH= 6.5 to 7.5) within 40 minutes (El Samrani et al., 2008). The authors suggested that the removals of heavy metals were owing to the sorption of heavy-metal-carrier compound (e.g. Pb-monosulfide) to the formed hydroxide flocs. Also, both PACl (1.48 mg/L Al) and ferric chloride (2.67 mg/L Fe) removed >90% of total phosphorus (C_o =3.5 mg/L) and 60% to 70% of COD (C_o= 340 mg/L) and 10% to 20% of total nitrogen (C_o =28.6 mg/L) (pH= 7.21, turbidity=130 NTU, treatment time=40 minutes) (Wang et al., 2016b). Alum (20 mg/L) used for EPT during WWF outperformed ferric chloride (20 mg/L) by achieving 60% of UVT% compared to 40% by ferric chloride (20 mg/L) (initial UVT%= 30%, pH=7.1, treatment time=15 minutes) (Gibson et al., 2016). In a comparable study, using WWF wastewater, alum (10 mg/L) removed >90% of TSS (C_o= 150 to 600 mg/L) and DOC (C_o=40 to 60 mg/L), whereas PACl (20 mg/L) or ferric chloride (30 mg/L) was required to achieve the same removal levels (pH=7.1, treatment time=72 minutes) (Exall and Marsalek, 2013).

Indeed EPT coagulation might be further enhanced by the ballasted flocculation technique where settling velocities of formed flocs increase by employing micro-size sand (MS) (Sumant et al., 2016). In bench-scale using WWF sample, ballasted flocculation, preceded by alum coagulation improved the removal of TSS from 19.6% to 98% (alum= 9.7 to 17.8 mg/L Al, anionic polymer= 1 to 1.8 mg/L, MS=3 g/L, size =300 μm) (Zhu et al., 2007). In a full-scale treatment, ballasted flocculation removed (80% to 86%) of TSS and (83% to 89%) of ortho-phosphate, and (50% to 90%) of heavy metals (Cu, Zn and Pb) (ferric chloride = 70 to 80 mg/L, micro-sand =3.5 g/L and size= 100-150 μm, anionic polymer = 0.8 to 1.08 mg/L, pH=7) (Gasperi et al., 2012). The aforementioned studies showed that different techniques might be used for treating wastewater during WWF condition yet all of them were incapable of reducing solids contents and microbial levels simultaneously. Therefore ferrate which is known to be a multifunctional chemical acting as an oxidant/disinfectant and a coagulant might be a better choice to mitigate WWF impacts (Sharma, 2002).

2.4 Ferrate

Ferrate (FeO_4^{2-}) is a hexavalent iron compound with a redox potential of 2.2 V at acidic conditions (pH<2) working as an oxidant/disinfectant and a coagulant (Sharma, 2002). Ferrate can be produced by several methods including wet chemical method, thermal method and electro-chemical method (Jiang and Lloyd, 2002). In the wet method, iron hydroxide is oxidized by concentrated sodium hypochlorite in an alkaline medium resulted in sodium ferrate (Na_2FeO_4) (equation 2.1). When sodium ferrate further reacts with potassium hydroxide (KOH), it generates K_2FeO_4 which is a more stable form of ferrate (equation 2.2) with high purity (98%) (Lee et al., 2004). The wet method is associated with two drawbacks namely chlorine production and a long production process (4 hrs to 6 hrs) (Sharma et al., 2016).

$$\mathrm{2Fe(OH)_3 + 3NaClO + 4NaOH \rightarrow 2Na_2FeO_4 + 3NaCl + 5H_2O} \quad (2.1)$$

$$\mathrm{2Na_2FeO_4 + 2KOH \rightarrow K_2FeO_4 \downarrow + 2NaOH} \quad (2.2)$$

In the thermal method (also called dry method), Na_2FeO_4 salt is produced by heating a mixture of iron oxides with Na_2O_3 at 600 °C (Sharma, 2002; Sharma et al., 2005). The main drawback of this method is the high energy consumption used for heating (Jiang Chengchun, 2008).

The electro-chemical method is more convenient for lab and *in-situ* production and is classified as a green method (Ding et al., 2014; Jiang et al., 2015; Licht and Yu, 2005; Nikolic-Bujanovic et al., 2016). Basically, in an electrolysis cell with concentrated (14 to 16 M) electrolyte solution (e.g. NaOH and KOH), iron metal serves as an anode and is oxidized to ferrate by electrical current (equations 2.3 and 2.4)(Lee et al., 2004; Macova et al., 2009; Sharma et al., 2016; Stanford et al., 2010). The cathode material should be stable in an alkaline medium such as graphite, carbon black, nickel or platinum (Ghernaout and Naceur, 2011). By using the electro-chemical method, ferrate (0.022 g/100 mL) was generated within 25 minutes, with the following conditions: electrical current =36 A/m^2, NaOH =16 M and steel electrode was composed of 99% Fe with a carbon content of 0.11% and cell electric potential of 1.92 V(Alsheyab et al., 2010).

$$\text{Anode: } \mathrm{Fe + 8OH^- \rightarrow FeO_4^{2-} + 4H_2O + 6e^-} \qquad (2.3)$$

$$\text{Cathode: } \mathrm{2H_2O + 2e^- \rightarrow H_2 + 2OH^-} \qquad (2.4)$$

The instability of ferrate is an inherent characteristic affected by the pH of the solution. Therefore ferrate is more stable at pH> 9 and is subjected to faster self-decay at pH < 7(Sharma, 2002). Furthermore, ferrate has three different protonation species in aqueous solution ($\mathrm{H_3Fe^{VI}O_4^+}$, $H_2Fe^{VI}O_4$, $HFe^{VI}O^-_4$) and one deprotonated form ($Fe^{VI}O^{2-}_4$) (equations 2.5, 2.6, 2.7) (Sharma, 2013).

$$\mathrm{H_3Fe^{VI}O_4^+ \rightleftarrows H_2Fe^{VI}O_4 + H^+} \qquad pK_1 = 1.5 \quad (2.5)$$

$$\mathrm{H_2Fe^{VI}O_4 \rightleftarrows HFe^{VI}O_4^- + H^+} \qquad pK_2 = 3.5 \quad (2.6)$$

$$\mathrm{HFe^{VI}O_4^- \rightleftarrows Fe^{VI}O_4^{2-} + H^+} \qquad pK_3 = 7.5 \quad (2.7)$$

Ferrate is subjected to self-decay with faster decomposition at pH= 1.1 to 8.2 (due to the predominant presence of protonated ferrate species) following second order kinetic (e.g. K= 178±18 $M^{-1}s^{-1}$ at pH= 5.5, k= 54 $M^{-1}s^{-1}$ at pH= 7) and slower decomposition at higher pH (≥ 9) following first order kinetic (Lee et al., 2014; Sharma, 2011). The below equations (8-13) describe the proposed pathways for ferrate self-decay (Lee et al., 2014). Therefore, ferrate-self-decay reaction initiates by dimerization two ferrate which undergoes intramolecular oxo-coupling via two-electron-transfer step generating ferryl (Fe(IV)) and liberating hydrogen peroxide (H_2O_2) via two consecutive hydrolysis steps (equation 2.8). Fe(VI) may also react with H_2O_2 and produce ferryl (Fe(VI)) and O_2 via two-electron transfer (equation 2.9). The generated Fe(IV) reacts with H_2O_2 and generate Fe(II) and oxygen via concerted two-electron transfer (equation 2.10). It was also reported that, Fe(IV) may react with H_2O_2 via consecutive one-electron transfer involving superoxide radical ($\bullet O^-_2$) as intermediate product. Fe(VI) may react with the generated Fe(II) and produce perferryl (Fe(V)) and Fe(III) via one-electron transfer (equation 2.11). The generated Fe(V) either decays to Fe(III) and H_2O_2 or react with H_2O_2 and generate Fe(III) and O_2 (equations 2.12 and 2.13). Ferrous species (Fe(V), Fe (IV)) generated from the self-decay of ferrate (Fe(VI)) are known to be more reactive than ferrate (Fe(VI)) (Cho et al., 2006; Sharma, 2013; Siskova et al., 2016). The final products resulted from ferrate decay are ferric hydroxide/oxide, hydrogen peroxide, and oxygen (Lee et al., 2014).

$$2\mathrm{HFe^{VI}O_4^-} + 4\mathrm{H_2O} \rightarrow 2\mathrm{H_3Fe^{IV}O_4^-} + 2\mathrm{H_2O_2} \quad (2.8)$$

$$\mathrm{HFe^{VI}O_4^-} + \mathrm{H_2O_2} \rightarrow \mathrm{H_3Fe^{IV}O_4^-} + \mathrm{O_2} \quad (2.9)$$

$$\mathrm{HFe^{VI}O_4^-} + \mathrm{H_2O_2} + \mathrm{H^+} \rightarrow \mathrm{Fe^{II}(OH)_2} + \mathrm{O_2} + 2\mathrm{H_2O} \quad (2.10)$$

$$\mathrm{HFe^{VI}O_4^-} + \mathrm{Fe^{II}(OH)_2} + \mathrm{H_2O} \rightarrow \mathrm{H_2Fe^{V}O_4^-} + \mathrm{Fe^{III}(OH)_3} \quad (2.11)$$

$$\mathrm{H_2Fe^{V}O_4^-} + \mathrm{H_2O} + \mathrm{H^+} \rightarrow \mathrm{Fe^{III}(OH)_3} + \mathrm{H_2O_2} \quad (2.12)$$

$$\mathrm{H_2Fe^{V}O_4^-} + \mathrm{H_2O_2} + \mathrm{H^+} \rightarrow \mathrm{Fe^{III}(OH)_3} + \mathrm{O_2} + \mathrm{H_2O} \quad (2.13)$$

2.4.1 Ferrate as a coagulant

Ferrate is known to be a multi-function chemical working as a disinfectant/oxidant and a coagulant. Indeed, ferrate coagulation capacity is derived mainly from ferric oxide/hydroxide which is the reduced form of ferrate (Aubertin et al., 1996; Jiang, 2014; Lee et al., 2004). Ferrate was studied previously as a coagulant for EPT during WWF thus ferrate dose of 0.24 mg/L Fe had removed ≥ 70% of TSS (C_o=200±80 mg/L) and COD (C_o=314±36 mg/L) at pH=6 (Gandhi et al., 2014). The former study also showed that the coagulation performance of ferrate improved by increasing the pH where higher removals of TSS and COD (≈ +30%) were attained at higher pH=9. That was mainly attributed to a higher formation of ferric hydroxide at alkaline pH. It is worth mentioning that ferrate-induced iron-particle may interfere with the removal of turbidity due to its poor settling velocity. Therefore, using ferrate as a stand-alone coagulant might not be considered a feasible option (Jun and Wei, 2002; Zheng and Deng, 2016). It was reported that combining ferrate (1 mg/L) with alum (60 mg/L) to treat surface water (pH=7.5) promoted the formation of bigger floc sizes (Jun and Wei, 2002). Moreover, combining ferrate (1.7 mg/L Fe) as a coagulant aid with ferric chloride(6.7 mg/L Fe) reduced the ultrafiltration membrane fouling by 4 times via bacterial inactivation and improved the coagulation process (synthesized surface water, turbidity=13 NTU, pH=7.8) (Yu et al., 2016). Ferrate can also remove heavy metals (Zn^{2+},Cu^{2+} and Mn^{2+}) by ionic bonding with $HFeO^-_4$ and precipitation (pH= 6) or adsorption onto $Fe(OH)_3$ (pH=9). As such ferrate (27 mg/L Fe) removed 73 to 99% of Zn , Cu and Zn along with 86% of organic matter (10 mg/L DOC) after settling /filtration (river water, pH=6, heavy metal= 0.1 mM) (Lim and Kim, 2010).

Ferrate also showed good removal of Ortho-phosphate (OP) in secondary effluent (pH=7) where it reduced OP from 3.6 mg/L to 0.8 mg/L (using a dose of 7 mg/L Fe) (Lee et al., 2009). The removal of OP was affected by the water matrix. Since it was found that a higher dose of ferrate (+4 times) was required in secondary effluent compared to that required in DI to achieve the similar OP removal (Kralchevska et al., 2016). Ferrate removes phosphate via complexation with iron species and precipitation or adsorption onto formed iron hydroxide (equation 2.14 and 2.15) (Lee et al., 2009).

$$\mathrm{Fe(OH)_3 + H_3PO_4 \xrightarrow{alkaline} FePO_4 + 3H_2O} \qquad (2.14)$$

$$\mathrm{Fe^{3+} + H_3PO_4 \xrightarrow{acidic} FePO_4 + 3H^+} \qquad (2.15)$$

Overall, it can be stated that ferrate can work as a coagulant but it may compromise the removal of turbidity and TSS thus combining it with another chemical may improve the overall performance of the process especially during WWF condition.

2.4.2 Ferrate as disinfectant

Wastewater disinfection during WWF is an essential process to reduce microorganisms levels in receiving water bodies. Therefore, numerous disinfectants have been used such as chlorine, ozone, peracetic acid, performic acid and ferrate (Abughararah, 1994; Collivignarelli et al., 2000; Lefevre et al., 1992; Liberti et al., 2000). Ferrate emerged recently as a strong oxidant/disinfectant with a high redox potential of 2.2 V and is known to be an environmentally friendly compound as the final reduced form is the non-toxic ferric species (Sharma et al., 2005). The biocidal effect of ferrate is derived from ferrate reactive species (H_2FeO_4, $HFeO^{-1}{}_4$ and $FeO^{-2}{}_4$) which have higher reactivity at acidic pH (Lee et al., 2004). Ferrate disinfection capacity was tested in different water matrices with low and high organic contents. Therefore, in ballasted water (saline water), ferrate (0.25 to 5 mg/L) reduced *Enterococci* and *E. coli* levels to less than 250 CFU/100 mL and *vibrio cholera* to 1 CFU/100 mL (pH=8, DOC=0, $N_o=10^5$ to 10^7 MPN/mL) (Jessen et al., 2008). In secondary effluent, ferrate (5 mg/L Fe) achieved 2.5 log removal of *E. coli* compared to 1 log by chlorine (5 mg/L) within 20 minutes (pH= 7.85, COD=7 mg/L, N_o=250 to 500 CFU/mL) (Kwon et al., 2014). A recent study examined using ferrate to disinfect raw WWF wastewater. It determined 7 mg/L Fe of ferrate required to remove 3.8 log of *E. coli* within 81 minutes (pH=6.7 ,TSS=83 mg/L, COD=280 mg/L, $N_o= 2.2 \times 10^6$ to 2.7×10^7 MPN/100mL) (Elnakar and Buchanan, 2019). Ferrate is more reactive at lower pH values as such, the inactivation rate of *E. coli* increased significantly from 0.33 to 6.25 L/(mg.min) when the pH decreased from 8.2 to 5.6 in a buffered solution ($N_o= 4 \times 10^5$ to 10^6 CFU/mL) (Cho et al., 2006). Similarly, at acidic pH (pH 5.5) a lower dose of ferrate (4 mg/L Fe) was sufficient to achieve ≥ 4 log removal of *E. coli* whereas at alkaline pH (pH= 7.5) higher dose of 6 mg/L Fe was required to attain similar log removal ($N_o= 3.2 \times 10^8$ CFU/100 mL, tap water) (Jiang et al., 2007). Ferrate also showed a high inactivation level for enteric pathogenic bacteriophage M2S where more than 4-log removal was achieved with a low dose (1.25 mg/L Fe) within 3 minutes (phosphate buffer, pH= 7, N_o=7.3 x 10^6 plaque forming unit/mL) (Hu et al., 2012). Ferrate also competed with ozone for the inactivation of *Bacillus Subtilis* spores. Higher inactivation rate was achieved by ozone as 0.98 L/(mg.min) compared to 0.034 L/(mg.min) by ferrate (phosphate buffer, pH=7, N_o=5 x10^5 CFU/mL, O_3= 1 mg/L, ferrate=90 mg/L) (Makky et al., 2011). The lower performance of ferrate compared to ozone may be attributed to the discrepancy in the involved mechanisms of inactivation for the targeted microorganism.

In fact, chlorine and ozone are strong disinfectants yet they can generate disinfection by-products such as trihalomethanes (THM) caused by chlorine and bromate caused by ozone (Hu et al., 2018; Richardson et al., 2007; von Gunten, 2018). In contrast, ferrate might outweigh other disinfectants such as ozone and chlorine due to its high ability to remove the precursors of disinfection by-products (DBPs) (e.g. natural organic matter (NOM), cyanobacteria). Several studies reported the benefits of using ferrate to reduce the DBPs formation. As such, ferrate (20 mg/L Fe) treated buffered solution spiked with Suwanee river natural organic matter (SRNOM) removed 28% of DOC (pH=7, DOC=3 mg/L) (Gan et al., 2015). In the same study, ferrate pre-oxidation of SRNOM followed by chlorination (20 mg/L Cl_2) for 6 hrs, reduced THM formation by 23%, and both chloral hydrate and haloacetonitriles by 66 % while increased the trichloronitromethane level by 50% due to the reaction with amine groups (ferrate=20 mg/L, pre-oxidation time=360 min). Similarly, the combination of ferrate with coagulation/sedimentation/filtration followed by chlorination reduced the formation of DBPs namely trihalomethanes and trihaloacetic acids by 30% to 45% respectively (pH=7.2, DOC= 3.2 mg/L, ferrate=1.4 mg/L Fe, $FeCl_3$ = 10 mg/L Fe, chlorination time=72 hr, chlorine 3 to 5 mg/L

Cl_2) (Jiang et al., 2016b). Similarly, pre-oxidation of water containing blue-green algae (cynobacteria) by ferrate (8 mg/L Fe) and its subsequent chlorination (30 mg/L Cl) for 72 hrs, reduced the formation of DBPs (trihalomethanes, haloacetic acids, haloketones, chloral hydrate, haloacetonitriles, and trichloronitromethane) by 5.5% to 45.1% (Dong et al., 2019). Furthermore, ferrate (10 mg/L Fe) exhibited a high inactivation rate of the cyanobacterial cell (128-242 $M^{-1}s^{-1}$) and degraded 80% of associated microcystins toxic compound (reservoir water, pH=8.7, DOC=1.7 mg/L) (Fan et al., 2018). Therefore, using ferrate as a disinfectant either alone or in combination with other chemicals might satisfy the target water quality level with minimal toxic by-products.

2.4.3 Ferrate as an oxidant

Ferrate showed an outstanding performance in the removal of a wide range of organic and inorganic compounds in different water matrices (Gombos et al., 2013; Sharma, 2011). Ferrate is also known to be a selective oxidant with a high tendency to attack compounds with ERM (e.g. phenols, anilines, amines, and olefins) (Jiang, 2015; Lee et al., 2009; Yang et al., 2012). In a secondary effluent spiked individually with MPs (C_o= 0.05 to 0.32 mg/L, pH 6 to 8), ferrate (2 to 5 mg/L Fe) removed >95% of phenolic containing compounds (e.g. bisphenol A and triclosan) and 85% of amine and olefin containing compounds (e.g. carbamazepine and diclofenac) (Lee et al., 2009). In contrast, for compounds without ERM (iopromide and ibuprofen, bezafibrate) only 40 % of removal was achieved with a high dose of ferrate (15 mg/L Fe). In another study, in a buffered solution (pH 6 to 9), ferrate (1 to 5 mg/L Fe) removed >70% of ciprofloxacin compared to < 25% of ibuprofen with both compounds spiked in a mixture at an initial concentration of 100 µg/L (Zhou and Jiang, 2015). The high removal of ciprofloxacin by ferrate was attributed to ferrate attack of piperazinyl ring and quinolone moiety of ciprofloxacin leading to cleavage or hydroxylation of the rings. In the same way in a buffered solution spiked with four compounds (C_o

= 100 μg/L), ferrate (5 mg/L Fe) oxidized 60% to 80 % of diclofenac (DCF), SMX and) and only 20% of bezafibrate (BZF) (Zhou and Jiang, 2015). Moreover, it was proposed that SMX was oxidized through oxygen transfer mechanism and hydroxylation while DCF and CBZ oxidized via oxygen and electron transfer mechanisms. In a secondary effluent, ferrate (2.5 to 10 mg/L Fe) removed 90% to 100% of sulfadiazine, sulfapyridine, sulfamethazine, SMX, trimethoprim and ofloxacin detected in the level of 276±26 ng/L (pH=6.88, DOC= 3.03 mg/L) (Yang et al., 2012). Similarly, ferrate (5.5 mg/L Fe) degraded 100% of β-lactam antibiotic (amoxicillin, ampicillin, cloxacillin, and penicillin G) spiked in secondary effluent wastewater (pH =7 to 8.5, antibiotic= 0.668 mg/L) (Karlesa et al., 2014). Ferrate (5.6 mg/L) also removed 50% of metals (Cu, Zn) iminoacetic acid complexed species (C_o=5.94 mg/L) in clean water with pH range of 8 to 12 (Pachuau et al., 2013). The removal was ascribed to the decomplexation of metal iminoacetic acid complexed species which was followed by oxidation of iminoacetic acid and coagulation/adsorption of non-degradable metallic species.

The oxidation of numerous micropollutants in buffered solutions with the effect of pH, concentration of ferrate and pollutants with their rate constants were presented in Table 2. The oxidation process is influenced significantly by different factors: pH, the molar ratio of oxidant and contaminant, reaction time, water matrix, physiochemical properties of oxidant and contaminant. That might explain the difference in the obtained rate constant for different treated model compounds as shown in Table 2.2. The transformation products (TPs) were reported in several studies therefore polishing steps might be recommended for total removal.

Table 2. 2 Previous studies Ferrate treatment of different MPs with effective pH range, rate constant toxicity and oxidation products.

Compounds	**pH**	**molar ratio Ferrate/X**[a]	**rate constant *k* (Ms)$^{-1}$**	**TPs**[b]	**Reference**
polychlorinated diphenyl sulfides	8	20:1	1.37±0.05 x10^3	NA[c]	(Chen et al., 2018)
chloramphenicol	5 to 9	16.3:1 to 81.6:1	2.35x10^3 - 7.25 x10^3	TPs	(Zhou et al., 2017)
amoxicillin, ampicillin	4 to 10	[(Ferrate]=0.1 mM << X	0.03 x10^3-15 x10^3	NA	(Sharma et al., 2013)
acetaminophen	4 to 11	5:1 to 25:1	1.27 x10^3	3 TPs	(Wang et al., 2016a)
diclofenac	7 to 11	5:1 to 30 to 1	2.54 - 11.6	NA	(Wang et al., 2015)
propranolol	9	6:1	3.6 x 10^2	3 TPs	(Anquandah et al., 2013)
bisphenol A	3 to 11	0.1:1 to 8:1	1.9 x10^2 -8.4 x10^2	12 TPs	(Han et al., 2015)
β-lactam antibiotics	6 to 9.5	0.2:1 to 60:1	16 to 150	NA	(Karlesa et al., 2014)
microcystin-LR	7.5 to 10	[Ferrate] <<[X]	8.1± 0.08 - 1.3 ± 0.1x10^2	NA	(Jiang et al., 2014a)
4-tert-octylphenol, 17a-ethynylestradiol	7 to 12	0.3:1 to 3.3:1	90 - 94	NA	(Tiwari et al., 2017)
glycine (GLY), glycylglycine(GLG)	4 to 12.4	[Ferrate] <<[X]	K_{GLY} =14 - 145 K_{GLG} =30 - 822	TPs	(Noorhasan et al., 2010)
bisphenol A (BPA), steroid estrogens (EE)	8.2 to 12	5:1 to 50:1	K_{BPA} =2.8 x10^2 - 7.76 x10^4 K_{EE} =3.05 x10^2 – 5.44 x10^5	9 TPs	(Li et al., 2008)
sucralose, sucrose, glucose, fructose and maltose	9	[(Ferrate] <<[X]	0.1 to .25	NA	(Sharma et al., 2012)
Bisphenol S (BPS) and bisphenol AF (BPAF)	7	51:1 to 30:1	300 to 1300	NA	(Yang et al., 2019)

[a] X the tested compounds, [b] transformation products, [c]Not analyzed

2.5 MPs oxidation technologies

Oxidation and advanced oxidation processes (that involve highly reactive oxidant e.g. $^{\bullet}OH$) are essential to achieve an effective removal of a broad range of MPs detected in water and wastewater. Many oxidants were used individually such as ozone, chlorine, chlorine dioxide or in combination with UV, photocatalysts (e.g. TiO_2, persulfate) (Hamza et al., 2016; Huber et al., 2005b). In bench-scale experiments, ozone and powder activated carbon (PAC) outperformed chlorine by achieving higher removal (40% to 90%) of MPs (e.g. atrazine, ibuprofen, fluorene) spiked in simulated drinking water (MPs= 10 to 250 ng/L, pH=6.8, DOC=3.5 mg/L, O_3=4 mg/L, PAC=1 mg/L, chlorine=6.76 mg/L) (Westerhoff et al., 2005). In the same study, PAC removed 77% of H-17β-Estradiol (C_o= 1360 ng/L) spiked in buffered solution which declined to 45% due to the presence of DOC (pH 8.2, DOC= 3.5 mg/L). Another study revealed that post-ozonation of secondary effluent, removed entirely MPs with aromatic moieties, the double bond and phenol function group (e.g. diclofenac, carbamazepine, sulfamethoxazole) with 0.6 g O_3/ g DOC, pH=7, DOC= 4.2 to 6 mg/L, MPs= 500 to 1500 µg/L) (Hollender et al., 2009). Moreover, in secondary effluent, ozone (0.87 g O_3/ g DOC, contact time=17 min) with granular activated carbon or biological filter bed (BF) removed 80% to 100% of detected MPs (e.g. carbamazepine, diclofenac) (MPs= 1.4 to 3.9 µg/L, DOC=68 mg/L) (Knopp et al., 2016). In pilot-scale study, ozone (2 to 5 mg/L) within 8.4 minutes removed >90% of sulfonamide antibiotics, estrone, naproxen and diclofenac presented in secondary effluent (DOC= 6 to 7.7 mg/L, pH= 6.95 to 7.5, MPs =0.5 to 5 µg/L) (Huber et al., 2005a). In a comparative study where secondary effluent was spiked with MPs (atenolol (ATL), carbamazepine (CBZ), ethinylestradiol EE2, ibuprofen (IBU), and sulfamethoxazole(SMX)) (C_o=0.2 to 1 µM) and treated by selective oxidants: ozone, ferrate, chlorine, chlorine dioxide and non-selective oxidant: hydroxyl radical (UV/H_2O_2) at pH=8 and reaction time of 60 minutes (Lee and von Gunten, 2010). Therefore, lower doses of selective oxidants (3 to 45 µM) were required to remove 90% of EE2 and SMX compared to 45 to 80 µM of $^\bullet$OH to achieve the same removal level. CBZ was poorly removed by chlorine-based oxidants while high removal (90%) was achieved by other oxidants with lower doses (30 to 100 µM) in the order $[O_3]$ <$[HFeO_4]$ <[$^\bullet$OH]. For ATL no removal was observed by chlorine-based oxidants while only 60% of removal achieved by ferrate (150 µM) compared to ≥ 90% by O_3 (40µM) and $^{\bullet}OH$ [85µM]. In contrast, IBU which has no ERM, was removed (≥ 90%) exclusively by $^{\bullet}OH$ [75 µM] and O_3 [120 µM]. Single ozonation (1.4 mg/L) within 30 minutes attained 100% removal for organophosphorus pesticide (diazinon, methyl parathion, and parathion) and completely mineralized diazinon (pH=8, C_o=10 to 30 mg/L) (Wu et al., 2009).

UV-based technologies are used to degrade a wide range of MPs detected in water and wastewater treatment facilities (Rizzo et al., 2018). However, using direct UV photo-degradation might not be considered a feasible option. For instance, in drinking water, direct photodegradation (UV=40 mJ/cm^2) showed poor removal of the tested organic compound thus removed 0.4% of EE2, 27% of diclofenac, 15% of SMX and iopromide (pH=7, DOC= 1.7 to 2 mg/L) (Canonica et al., 2008). In clean water matrix, the required UV dose to remove 90% of mecoprop (C_o=20 mg/L), and CBZ (C_o=7 mg/L) were 910 mJ/cm^2 and 231600 mJ/cm^2 respectively and that dose reduced to 770 mJ/cm^2 and 2250 mJ/cm^2 by using UV/H_2O_2 (25 mg/L) (pH=7) (Shu et al., 2013). The degradation of model compounds in UV-based technologies derived mainly by the direct UV photolysis and the limited generated hydroxyl radical species (Bolton and Linden, 2003). Photo-degradation might be improved by combining UV with H_2O_2 or catalysts such as TiO_2 which is capable of generating more hydroxyl radicals in the system thus increasing the efficacy of the process (Wu et al., 2009). Photocatalysis using UV/TiO_2 removed 39% of diazinon (C_o=11 mg/L) while adding H_2O_2 (i.e. UV/H_2O_2/TiO_2) as an additional source of •OH improved the removal to 51% (pH=4, reaction time=180 min, TiO_2= 2g/L, H_2O_2= 2 g/L) (Alalm et al., 2015).

2.6 Ferrate integrated technologies

The combination of ferrate with other technologies or compounds (e.g. coagulant, UV, ozone, catalyses) may enhance ferrate-oxidation performance especially for recalcitrant contaminants (Acero et al., 2000; Real et al., 2007). Combining ferrate with other coagulants (e.g. aluminum or iron-based coagulants) improved the removal of inorganic and organic compounds via dual action of oxidation/coagulation. For instance, sequential application of ferrate and Alum (1.12 mg/L Fe+0.54 mg/L Al) removed 100% of arsenite (C_o=500 µg/L) presented in drinking water at pH=6.5 (Jain et al., 2009). In the same way, simultaneous dosing of ferrate and PACl (2.35 mg/L Fe /3.24 mg/L Al) removed 36% of the humic-like fluorophore within 25 minutes which surpassed single application of ferrate and PACl or their sequential application (pH=6-7, DOC=3.5 mg/L) (Amano et al., 2018). Ferrate photo-catalyzation with UV/TiO_3 promoted the formation of reactive species (Fe(V)) by scavenging band electron and improved reduction of ammonia, cyanate, microcystins (Sharma et al., 2010). Furthermore, photo-catalyzation of ferrate (0.4 mg/L Fe)/H_2O_2 (9288 mg/L)/UV (403.2 mJ/cm^2) process achieved 5.7 log removal of *Bacillus subtilis spores,* compared to 4.7 log by ferrate (7 mg/L)/H_2O_2 (9846 mg/L) pH=7 (Matin et al., 2018).

The coexistence of some ions and organic compounds in ferrate systems showed catalyzing or restraining impact on the overall ferrate-oxidation system (Kolar et al., 2016). As such, the presence of Mg^{2+} (4.8 mg/L) with ferrate (1.35 mg/L Fe) had improved the removal of acetaminophen (0.5 mg/L) by (+10 %), while other ions (Al^{3+}, PO_4^{3-} ,CO_3^{2-} ,C_o= 5.4 to 19 mg/L) and humic acid (DOC >10 mg/L) declined the removal (-30% to -60 %) at pH= 7 (Wang et al., 2016a). Similarly, the presence of Mn^{2+}, SO_4^{2-} Fe^{2+} and Fe^{3+} (0.03 to 0.038 mg/L) accelerated ferrate (1.344 mg/L Fe) degradation (80%) of diclofenac (0.236 mg/L) within 20 to 40 seconds instead 120 seconds (pH=9) (Zhao et al., 2018a; Zhao et al., 2018b). Furthermore, in the aforementioned studies, the observed enhancement of ferrate-oxidation process was attributed to the catalytic effect of forming Fe(IV)/Fe(V) which is known to be more reactive than ferrate.

The addition of sulfur compounds (e.g. sulfate/sulfite) proved to synergize oxidation processed by forming Fe(V)/Fe(IV) and other reactive species ($SO_4^{\bullet -}$, •OH, $O^{\bullet}{}_2^{-}$). Therefore, ferrate/peroxymonosulfate removed 61% of fluoroquinolones compounds (FQs) (flumequine, enrofloxacin, marbofloxacin, and ofloxacin) within 30 minutes compared to < 10% removal by ferrate alone (ferrate= 5μM, SO_4^{2-}=200 μM, FQs=1 μM, pH=7) (Feng et al., 2017b). Feng et al. (2017 b) ascribed the synergistic effect to the generated reactive $SO_4^{\bullet -}$, •OH, $O^{\bullet}{}_2^{-}$ and ferrate reactive species Fe(V) and Fe(IV) species. Similarly, Zhang et al.(2017) had explored ferrate-sulfite process and reported 85% to ≈ 100% removals of several recalcitrant MPs (benzotriazole, ciprofloxacin, methyl blue, rhodamine B and methyl orange) achieved within 30 seconds (ferrate=50 μM, SO_3^{2-}=250 μM, MPs=5 μM, pH=9)(Zhang et al., 2017). The observed synergistic effect was attributed to the generated reactive species namely $\bullet OH$ / $SO_4^{\bullet -}$ based on quenching experiments and electron spin resonance (ESR) analysis. These two studies had advocated other researches to examine the ferrate/sulfite/sulfate process with different contaminants and testing conditions. As such, Wu et al. (2018) reported that ferrate/sulfate (6 mM/5mM) removed 80% of atrazine (C_o=46 μM) within 20 minutes in surface water (DOC< 4 mg/L C, pH=6) (Wu et al., 2018). Likewise, Feng and Sharma (2018) reported that ferrate/sulfur achieved almost instantaneous removal (15 s) of recalcitrant antibiotics (trimethoprim and flumequine) (pH=7, ferrate: sulfur: antibiotic=5:5:1, antibiotic= 20 μM) (Feng and Sharma, 2018). They confirmed the contribution of radical species ($SO_3^{\bullet -}$, $SO_4^{\bullet -}$, $SO_5^{\bullet -}$ and $\bullet\,OH$) along with ferrate reactive species Fe(IV)/Fe(V). A recent study claimed that the major contribution in ferrate/sulfite systems is mainly attributed to ferrate reactive species Fe(IV)/(V) and minor contribution is attributed to other radical species (e.g. $SO_3^{\bullet -}$,$\bullet$ OH) (Shao et al., 2019). Overall, all studies agreed that ferrate/sulfite/sulfate achieved better removal of the tested contaminants.

The application of the ferrate-ozone process also showed a synergistic impact promoting hydroxyl radical formation reflected by the high reduction of DOC (70.5%), protein (25.6%) and polysaccharide (65.5%) (Liu et al., 2018). Similarly, the ferrate/silica gel process improved the removal (10% higher) of fuel sulfur compounds (benzothiophene, dibenzothiophene, and methyl-dibenzothiophene) and about 50% higher caffeine (pH=8) (Al-Abduly and Sharma, 2014; Manoli et al., 2017a).

Ferrate-acid activation process was hypothesized to promote the formation of ferrate reactive species (Fe(IV)/Fe(V)) which is known to be more reactive than ferrate (Feng et al., 2017a). As such, ferrate/HCl degraded > 90% of acesulfame potassium (ferrate=408 μM, acesulfame potassium=67.8 μM, HCl=798 μM) and caffeine (ferrate=506 μM: caffeine=63 μM, HCl=882 μM) within 1 and 30 minutes respectively instead of several hours without activation pH=7.5-8.1 (Ghosh et al., 2019; Manoli et al., 2017b). In both studies, it was confirmed that the enhancement was due to ferrate activation rather than acid addition based on control experiments. There was no contribution of oxygen reactive species in ferrate-acid activation process based on similar oxidation levels achieved under oxic and anoxic conditions (Manoli et al., 2017b). All the presented studies emphasized that the ferrate performance can be enhanced significantly by different processes however more studies are required to prove the efficiency in real water matrices.

2.7 Ferrate and toxicity concerns

The toxicity impact is a major concern arising with the implementation of any new chemical. With this in mind, several studies investigated the toxicity impact of ferrate application by using different bioassays (e.g. *Vibrio fischeri* luminescent test, zebrafish animal model) (Jiang et al., 2014a; Malachova et al., 2014; Yang et al., 2011). Studies revealed that ferrate may cause the evolution of toxicity during the oxidation of organic compounds. As such, the acute toxicity level (using *Vibrio fischeri*) of the solution during ferrate (16.8 mg/L Fe) oxidation of diclofenac (8.88 mg/L) increased from 15% to 60% in the first 60 minutes and then dropped to 15% after 180 minutes pH=9 (Wang et al., 2015). Likewise, the acute toxicity level during bisphenol A (1 mg/L) degradation by ferrate (2.83 mg/L Fe) had increased (45% to 60%) in the first five minutes and decreased substantially to 25% after 60 minutes at pH=7(Han et al., 2015). The gradual change in the toxicity level was attributed to the toxicity level of the transformation products which might be minimized or removed as a function of reaction time. Based on these observations, the reaction time, during ferrate oxidation of micropollutants, should be optimized to achieve the highest level of degradation and the lowest level of toxicity. Another study reported that the toxicity level was reduced from 63% to 22.8% during ferrate (1.5 mg/L Fe) oxidation of sulfonamide (0.2 mg/L) for 30 minutes prior to chlorination (chlorine 0.9 mg/L, pH=7.4) (Zhang et al., 2018). The toxic compound microcystin-LR (0.33 mg/L) was removed entirely by ferrate (3.7 mg/L Fe) and no toxicity was detected in the treated solution based on the activity of protein phosphate assay (reaction time 30 minutes, pH=8) (Jiang et al., 2014b). Ferrate showed no mortality effect on the Zebrafish embryos model during oxidation of ciprofloxacin (5 μg/L) spiked into secondary wastewater effluent (pH=7.37, COD= 35 mg/L, ferrate =1 to 5 mg/L) (Jiang et al., 2013a).

Bromate is classified as possibly carcinogenic to human by (WHO, 2005) which is most likely formed during oxidation of bromide by ozone. Nevertheless, ferrate (2 mg/L Fe) reduced bromate formation from 95 to 5% when ferrate was used with ozone (2.5 mg/L O_3) to treat bromide (200 μg/L) containing water (pH≤9) (Han et al., 2014). It was found that hydrogen peroxide (generated during ferrate decomposition) reduced active bromine to bromide which eventually suppressed the bromate formation in the ferrate-treatment system (Jiang et al., 2016a; Richardson et al., 2007). In general, ferrate showed benign effects on the environment based on toxicity analyses thus it should be considered as a potential alternative oxidant/disinfectant competing widely used compounds (i.e. ozone and chlorine) which are known to pose toxic effects to the environment.

2.8 Conclusions

WWF is associated with combined sewer flow which threatens the aquatic lives and deteriorates the water quality by increasing the levels of microbial and organic and inorganic contents. Treating WWF wastewater is challenging due to the excess amount of flow which mostly exceeds the capacity of treatment plants. Yet several measures can be implemented either upstream or downstream to curtail the effects. For instance, in upstream, real-time gate control, off-line treatment and storage basin are able to regulate the flow to the treatment facilities. Upstream control measures require a large footprint which might be counted as a drawback. Alternatively, chemical enhancement of primary treatment is easy to retrofit without the need for a new structure. This can be accomplished by using coagulants (e.g. alum, PACl, $FeCl_3$ and ferrate) individually or coupled with other techniques such as lamella plate settlers, ballasted sand, vortex high rate settler. Most of the surveyed studies did not provide a comprehensive process that treat both organic and inorganic contents along with microbial contaminants. Therefore more bench and full-scale studies are necessary for this area to propose more effective measures which can achieve the target water quality levels.

WWF wastewater contributes highly in MPs loading to the influent of WWTPs which are not capable to degrade MPs. Therefore, the existing WWTP should be upgraded with a polishing step that uses a single oxidation unit (e.g. ozone, ferrate) or in combination with other techniques (adsorption or filtration). Moreover, advance oxidation processes (generate radical species e.g.

•OH) using photo-chemical reaction (O_3/UV, ferrate/H_2O_2/UV) or photo-catalyzing reaction (UV/TiO_2) or photo-Fenton ($Fe^{2+/}H_2O_2$/UV) which all showed better removal of MPs than single oxidation.

Ferrate has been recognized as a strong oxidant/disinfectant and its reduced form ferric (Fe(III)) could act as a coagulant. It showed outstanding performance as an oxidant/disinfectant and to a lesser extent as a coagulant with a major concern of increasing the turbidity of treated water. Several studies explored ferrate's capability of removing a broader range of contaminants by using ferrate alone or in combination with other technologies (coagulation, catalyzation, and acidification). Furthermore, toxicity studies revealed that ferrate reduced the toxicity of treated water during the oxidation of pharmaceutical compounds (e.g. diclofenac, bisphenol A). Toxicity screening tests should be used as a complementary analysis for further verification of treatment adequacy. In general, the screened studies showed that ferrate might be used effectively as an oxidant/disinfectant and to a lesser extent as a coagulant to treat water and wastewater with minimal toxic impacts. That being said the screened showed no systematic study examined ferrate simultaneously as a coagulant or disinfectant to treat wastewater during WWF condition.

2.9 References

Abughararah, Z.H. 1994. Effect of temperature on the kinetics of waste-water disinfection using ultraviolet-radiation. Journal of Environmental Science and Health Part a-Environmental Science and Engineering & Toxic and Hazardous Substance Control 29(3), 585-603.

Acero, J.L., Stemmler, K. and Von Gunten, U. 2000. Degradation kinetics of atrazine and its degradation products with ozone and OH radicals: A predictive tool for drinking water treatment. Environmental Science & Technology 34(4), 591-597.

Al-Abduly, A. and Sharma, V.K. 2014. Oxidation of benzothiophene, dibenzothiophene, and methyl-dibenzothiophene by ferrate(VI). Journal of Hazardous Materials 279, 296-301.

Alalm, M.G., Tawfik, A. and Ookawara, S. 2015. Comparison of solar TiO2 photocatalysis and solar photo-Fenton for treatment of pesticides industry wastewater: Operational conditions, kinetics, and costs. Journal of Water Process Engineering 8, 55-63.

Alsheyab, M., Jiang, J.-Q. and Stanford, C. 2010. Electrochemical generation of ferrate (VI): Determination of optimum conditions. Desalination 254(1-3), 175-178.

Alyaseri, I. and Zhou, J. 2016. Stormwater Volume Reduction in Combined Sewer Using Permeable Pavement: City of St. Louis. Journal of Environmental Engineering 142(4).

Amano, M., Lohwacharin, J., Dubechot, A. and Takizawa, S. 2018. Performance of integrated ferrate-polyaluminum chloride coagulation as a treatment technology for removing freshwater humic substances. Journal of Environmental Management 212, 323-331.

Andoh, R.Y.G. and Saul, A.J. 2003. The use of hydrodynamic vortex separators and screening systems to improve water quality. Water Science and Technology 47(4), 175-183.

Anquandah, G.A.K., Sharma, V.K., Panditi, V.R., Gardinali, P.R., Kim, H. and Oturan, M.A. 2013. Ferrate(VI) oxidation of propranolol: Kinetics and products. Chemosphere 91(1), 105-109.

Aubertin, N., Neveux, N., Gerardin, R. and Evrard, O. 1996. Synthesis of potassium sulfatoferrate and its use in wastewater treatment. Revue des Sciences de l'Eau 9(1), 17-30.

Autixier, L., Mailhot, A., Bolduc, S., Madoux-Humery, A.S., Galarneau, M., Prevost, M. and Dorner, S. 2014. Evaluating rain gardens as a method to reduce the impact of sewer overflows in sources of drinking water. Science of the Total Environment 499, 238-247.

Avila, C., Jose Salas, J., Martin, I., Aragon, C. and Garcia, J. 2013. Integrated treatment of combined sewer wastewater and stormwater in a hybrid constructed wetland system in southern Spain and its further reuse. Ecological Engineering 50, 13-20.

Birch, H., Mikkelsen, P.S., Jensen, J.K. and Lutzhoft, H.C.H. 2011. Micropollutants in stormwater runoff and combined sewer overflow in the Copenhagen area, Denmark. Water Science and Technology 64(2), 485-493.

Bolton, J.R. and Linden, K.G. 2003. Standardization of methods for fluence (UV dose) determination in bench-scale UV experiments. Journal of Environmental Engineering-Asce 129(3), 209-215.

Canonica, S., Meunier, L. and Von Gunten, U. 2008. Phototransformation of selected pharmaceuticals during UV treatment of drinking water. Water Research 42(1-2), 121-128.

Chen, J., Xu, X., Zeng, X., Feng, M., Qu, R., Wang, Z., Nesnas, N. and Sharma, V.K. 2018. Ferrate(VI) oxidation of polychlorinated diphenyl sulfides: Kinetics, degradation, and oxidized products. Water Research 143, 1-9.

Cho, M., Lee, Y., Choi, W., Chung, H.M. and Yoon, J. 2006. Study on Fe(VI) species as a disinfectant: Quantitative evaluation and modeling for inactivating Escherichia coli. Water Research 40(19), 3580-3586.

Collivignarelli, C., Bertanza, G. and Pedrazzani, R. 2000. A comparison among different wastewater disinfection systems: Experimental results. Environmental Technology 21(1), 1-16.

Collivignarelli, M.C., Abba, A., Benigna, I., Sorlini, S. and Torretta, V. 2018. Overview of the Main Disinfection Processes for Wastewater and Drinking Water Treatment Plants. Sustainability 10(1), 21.

Del Rio, H., Suarez, J., Puertas, J. and Ures, P. 2013. PPCPs wet weather mobilization in a combined sewer in NW Spain. Science of the Total Environment 449, 189-198.

Ding, L., Liu, T.X. and Li, X.Z. 2014. Removal of CH3SH with in-situ generated ferrate(VI) in a wet-scrubbing reactor. Journal of Chemical Technology and Biotechnology 89(3), 455-461.

Dong, F., Liu, J., Li, C., Lin, Q., Zhang, T., Zhang, K. and Sharma, V.K. 2019. Ferrate(VI) pre-treatment and subsequent chlorination of blue-green algae: Quantification of disinfection byproducts. Environment International 133.

Duchesne, S., Mailhot, A., Dequidt, E. and Villeneuve, J.P. 2001. Mathematical modeling of sewer under surcharge for real time control of combined sewer overflows. Urban Water 3, 241-252.

El Samrani, A.G., Lartiges, B.S. and Villieras, F. 2008. Chemical coagulation of combined sewer overflow: Heavy metal removal and treatment optimization. Water Res. 42(4-5), 951-960.

Elnakar, H. and Buchanan, I. 2019. The role of mixing in potassium ferrate(VI) consumption kinetics and disinfection of bypass wastewater. Journal of Environmental Management 231, 515-523.

EPA .1999. Combined Sewer Overflows Guidelines for Monitoring and Modeling. Agency, W.M.E.P. (ed).

Exall, K. and Marsalek, J. 2013. A Coagulant Survey for Chemically Enhanced Primary Treatment of Synthetic CSOs. Water Air and Soil Pollution 224(2), 9.

Fan, J., Lin, B.H., Chang, C.W., Zhang, Y. and Lin, T.F. 2018. Evaluation of potassium ferrate as an alternative disinfectant on cyanobacteria inactivation and associated toxin fate in various waters. Water Research 129, 199-207.

Feng, M., Cizmas, L., Wang, Z. and Sharma, V.K. 2017a. Activation of ferrate(VI) by ammonia in oxidation of flumequine: Kinetics, transformation products, and antibacterial activity assessment. Chemical Engineering Journal 323, 584-591.

Feng, M., Cizmas, L., Wang, Z. and Sharma, V.K. 2017b. Synergistic effect of aqueous removal of fluoroquinolones by a combined use of peroxymonosulfate and ferrate(VI). Chemosphere 177, 144-148.

Feng, M. and Sharma, V.K. 2018. Enhanced oxidation of antibiotics by ferrate(VI)-sulfur(IV) system: Elucidating multi-oxidant mechanism. Chemical Engineering Journal 341, 137-145.

Gan, W.H., Sharrna, V.K., Zhang, X., Yang, Y. and Yang, X. 2015. Investigation of disinfection byproducts formation in ferrate(VI) pre-oxidation of NOM and its model compounds followed by chlorination. Journal of Hazardous Materials 292, 197-204.

Gandhi, R., Ray, A.K., Sharma, V.K. and Nakhla, G. 2014. Treatment of Combined Sewer Overflows Using Ferrate (VI). Water Environment Research 86(11), 2202-2211.

Gasperi, J., Laborie, B. and Rocher, V. 2012. Treatment of combined sewer overflows by ballasted flocculation: Removal study of a large broad spectrum of pollutants. Chem. Eng. J. 211, 293-301.

Ghernaout, D. and Naceur, M.W. 2011. Ferrate(VI): In situ generation and water treatment - A review. Desalination and Water Treatment 30(1-3), 319-332.

Ghosh, M., Manoli, K., Renaud, J.B., Sabourin, L., Nakhla, G., Sharma, V.K. and Ray, A.K. 2019. Rapid removal of acesulfame potassium by acid-activated ferrate(VI) under mild alkaline conditions. Chemosphere 230, 416-423.

Gibson, J., Farnood, R. and Seto, P. 2016. Chemical pretreatment of combined sewer overflows for improved UV disinfection. Water Science and Technology 73(2), 375-381.

Gombos, E., Barkacs, K., Felfoldi, T., Vertes, C., Mako, M., Palko, G. and Zaray, G. 2013. Removal of organic matters in wastewater treatment by ferrate (VI)-technology. Microchemical Journal 107, 115-120.

Gromaire, M.C., Garnaud, S., Saad, M. and Chebbo, G. 2001. Contribution of different sources to the pollution of wet weather flows in combined sewers. Water Research 35(2), 521-533.

Hamza, R.A., Iorhemen, O.T. and Tay, J.H. 2016. Occurrence, impacts and removal of emerging substances of concern from wastewater. Environmental Technology & Innovation 5, 161-175.

Han, Q., Wang, H.J., Dong, W.Y., Liu, T.Z. and Yin, Y.L. 2014. Suppression of bromate formation in ozonation process by using ferrate(VI): Batch study. Chemical Engineering Journal 236, 110-120.

Han, Q., Wang, H.J., Dong, W.Y., Liu, T.Z., Yin, Y.L. and Fan, H.K. 2015. Degradation of bisphenol A by ferrate(VI) oxidation: Kinetics, products and toxicity assessment. Chemical Engineering Journal 262, 34-40.

Haydar, S. and Aziz, J.A. 2009. Characterization and treatability studies of tannery wastewater using chemically enhanced primary treatment (CEPT)-A case study of Saddiq Leather Works. Journal of Hazardous Materials 163(2-3), 1076-1083.

Hollender, J., Zimmermann, S.G., Koepke, S., Krauss, M., McArdell, C.S., Ort, C., Singer, H., von Gunten, U. and Siegrist, H. 2009. Elimination of Organic Micropollutants in a Municipal Wastewater Treatment Plant Upgraded with a Full-Scale Post-Ozonation Followed by Sand Filtration. Environmental Science & Technology 43(20), 7862-7869.

Hu, J., Chu, W., Sui, M., Xu, B., Gao, N. and Ding, S. 2018. Comparison of drinking water treatment processes combinations for the minimization of subsequent disinfection by-products formation during chlorination and chloramination. Chem. Eng. J. 335, 352-361.

Hu, L., Page, M.A., Sigstam, T., Kohn, T., Marinas, B.J. and Strathmann, T.J. 2012. Inactivation of Bacteriophage MS2 with Potassium Ferrate(VI). Environmental Science & Technology 46(21), 12079-12087.

Huang, C.C., Hu, Y., Wang, L., Wang, Y.F., Li, N., Guo, Y.Q., Feng, Y.Y. and Xiao, L.H. 2017. Environmental Transport of Emerging Human-Pathogenic Cryptosporidium Species and Subtypes through Combined Sewer Overflow and Wastewater. Applied and Environmental Microbiology 83(16), 11.

Huber, M.M., Gobel, A., Joss, A., Hermann, N., Loffler, D., McArdell, C.S., Ried, A., Siegrist, H., Ternes, T.A. and von Gunten, U. 2005a. Oxidation of pharmaceuticals during ozonation of municipal wastewater effluents: A pilot study. Environmental Science & Technology 39(11), 4290-4299.

Huber, M.M., Korhonen, S., Ternes, T.A. and von Gunten, U. 2005b. Oxidation of pharmaceuticals during water treatment with chlorine dioxide. Water Research 39(15), 3607-3617.

Irfan, M., Butt, T., Imtiaz, N., Abbas, N., Khan, R.A. and Shafique, A. 2017. The removal of COD, TSS and colour of black liquor by coagulation-flocculation process at optimized pH, settling and dosing rate. Arabian Journal of Chemistry 10, S2307-S2318.

Jain, A., Sharma, V.K. and Mbuya, O.S. 2009. Removal of arsenite by Fe(VI), Fe(VI)/Fe(III), and Fe(VI)/Al(III) salts: Effect of pH and anions. Journal of Hazardous Materials 169(1-3), 339-344.

Jeon, J.C., Jung, Y.J., Kwon, K.H. and Min, K.S. 2017. Enhanced water quality of CSOs with different coagulant treatment. Desalin. Water Treat. 63, 469-477.

Jessen, A., Randall, A., Reinhart, D. and Daly, L. 2008. Effectiveness and Kinetics of Ferrate as a Disinfectant for Ballast Water. Water Environment Research 80(6), 561-569.

Jiang Chengchun, L.C., and Wang Shichao (2008) Ferrates Synthesis, Properties, and Applications in Water and Wastewater Treatment. K.Sharma, V. (ed), pp. 94-101, American Chemical Society.

Jiang, J.-Q., Zhou, Z., Patibandla, S. and Shu, X. 2013. Pharmaceutical removal from wastewater by ferrate(VI) and preliminary effluent toxicity assessments by the zebrafish embryo model. Microchemical Journal 110, 239-245.

Jiang, J.Q. 2014. Advances in the development and application of ferrate(VI) for water and wastewater treatment. Journal of Chemical Technology and Biotechnology 89(2), 165-177.

Jiang, J.Q. 2015. The role of ferrate(VI) in the remediation of emerging micropollutants: a review. Desalination and Water Treatment 55(3), 828-835.

Jiang, J.Q., Durai, H.B.P., Winzenbacher, R., Petri, M. and Seitz, W. 2015. Drinking water treatment by in situ generated ferrate(VI). Desalination and Water Treatment 55(3), 731-739.

Jiang, J.Q. and Lloyd, B. 2002. Progress in the development and use of ferrate(VI) salt as an oxidant and coagulant for water and wastewater treatment. Water Research 36(6), 1397-1408.

Jiang, J.Q., Wang, S. and Panagoulopoulos, A. 2007. The role of potassium ferrate(VI) in the inactivation of Escherichia coli and in the reduction of COD for water remediation. Desalination 210(1-3), 266-273.

Jiang, W., Chen, L., Batchu, S.R., Gardinali, P.R., Jasa, L., Marsalek, B., Zboril, R., Dionysiou, D.D., O'Shea, K.E. and Sharma, V.K. 2014a. Oxidation of Microcystin-LR by Ferrate(VI): Kinetics, Degradation Pathways, and Toxicity Assessments. Environmental Science & Technology 48(20), 12164-12172.

Jiang, W.J., Zhu, L.F., Sharma, V.K., Batchu, S.R., Gardinali, P.R., Dionysiou, D.D. and O'Shea, K.E. 2014b. Oxidation of microcystin-LR by ferrate(VI): Intermediates, degradation pathways, and toxicity assessments. Abstracts of Papers of the American Chemical Society 247, 1.

Jiang, Y.J., Goodwill, J.E., Tobiason, J.E. and Reckhow, D.A. 2016a. Bromide oxidation by ferrate(VI): The formation of active bromine and bromate. Water Research 96, 188-197.

Jiang, Y.J., Goodwill, J.E., Tobiason, J.E. and Reckhow, D.A. 2016b. Impacts of ferrate oxidation on natural organic matter and disinfection byproduct precursors. Water Research 96, 114-125.

Jun, M. and Wei, L. 2002. Effectiveness of ferrate (VI) preoxidation in enhancing the coagulation of surface waters. Water Research 36(20), 4959-4962.

Karlesa, A., De Vera, G.A.D., Dodd, M.C., Park, J., Espino, M.P.B. and Lee, Y. 2014. Ferrate(VI) Oxidation of beta-Lactam Antibiotics: Reaction Kinetics, Antibacterial Activity Changes, and Transformation Products. Environmental Science & Technology 48(17), 10380-10389.

Knopp, G., Prasse, C., Ternes, T.A. and Comel, P. 2016. Elimination of micropollutants and transformation products from a wastewater treatment plant effluent through pilot scale ozonation followed by various activated carbon and biological filters. Water Research 100, 580-592.

Koeck-Schulmeyer, M., Villagrasa, M., Lopez de Alda, M., Cespedes-Sanchez, R., Ventura, F. and Barcelo, D. 2013. Occurrence and behavior of pesticides in wastewater treatment plants and their environmental impact. Science of the Total Environment 458, 466-476.

Kok, S. 2004. Wet-weather flow management in the Great Lakes Areas of Concern. Water Quality Research Journal of Canada 39(4), 319-330.

Kolar, M., Novak, P., Siskova, K.M., Machala, L., Malina, O., Tucek, J., Sharma, V.K. and Zboril, R. 2016. Impact of inorganic buffering ions on the stability of Fe(VI) in aqueous solution: role of the carbonate ion. Physical Chemistry Chemical Physics 18(6), 4415-4422.

Kralchevska, R.P., Prucek, R., Kolarik, J., Tucek, J., Machala, L., Filip, J., Sharma, V.K. and Zboril, R. 2016. Remarkable efficiency of phosphate removal: Ferrate(VI)-induced in situ sorption on core-shell nanoparticles. Water Res. 103, 83-91.

Krupinska, I. 2018. Removal of natural organic matter from groundwater by coagulation using prehydrolysed and non- prehydrolysed coagulants. Desalin. Water Treat. 132, 244-252.

Kwon, J.H., Kim, I.K., Park, K.Y., Kim, Y.D. and Cho, Y.H. 2014. Removal of phosphorus and coliforms from secondary effluent using ferrate(VI). Ksce Journal of Civil Engineering 18(1), 81-85.

Launay, M.A., Dittmer, U. and Steinmetz, H. 2016. Organic micropollutants discharged by combined sewer overflows: Characterization of pollutant sources and stormwater-related processes. Water Res. 104, 82-92.

Lee, Y., Cho, M., Kim, J.Y. and Yoon, J. 2004. Chemistry of ferrate (Fe(VI)) in aqueous solution and its applications as a green chemical. Journal of Industrial and Engineering Chemistry 10(1), 161-171.

Lee, Y., Kissner, R. and von Gunten, U. 2014. Reaction of Ferrate(VI) with ABTS and Self-Decay of Ferrate(VI): Kinetics and Mechanisms. Environmental Science & Technology 48(9), 5154-5162.

Lee, Y. and von Gunten, U. 2010. Oxidative transformation of micropollutants during municipal wastewater treatment: Comparison of kinetic aspects of selective (chlorine, chlorine dioxide, ferrate(VI), and ozone) and non-selective oxidants (hydroxyl radical). Water Research 44(2), 555-566.

Lee, Y., Zimmermann, S.G., Kieu, A.T. and von Gunten, U. 2009. Ferrate (Fe(VI)) Application for Municipal Wastewater Treatment: A Novel Process for Simultaneous Micropollutant Oxidation and Phosphate Removal. Environmental Science & Technology 43(10), 3831-3838.

Lefevre, F., Audic, J.M. and Ferrand, F. 1992. Peracetic-acid disinfection of secondary effluents discharged off coastal seawater. Water Science and Technology 25(12), 155-164.

Li, C., Li, X.Z., Graham, N. and Gao, N.Y. 2008. The aqueous degradation of bisphenol A and steroid estrogens by ferrate. Water Research 42(1-2), 109-120.

Liberti, L., Lopez, A., Notarnicola, M., Barnea, N., Pedahzur, R. and Fattal, B. 2000. Comparison of advanced disinfecting methods for municipal wastewater reuse in agriculture. Water Science and Technology 42(1-2), 215-220.

Licht, S. and Yu, X.W. 2005. Electrochemical alkaline Fe(VI) water purification and remediation. Environmental Science & Technology 39(20), 8071-8076.

Lim, M. and Kim, M.-J. 2010. Effectiveness of Potassium Ferrate (K2FeO4) for Simultaneous Removal of Heavy Metals and Natural Organic Matters from River Water. Water Air and Soil Pollution 211(1-4), 313-322.

Liu, J., Zhang, Z.H., Chen, Q.H. and Zhang, X.H. 2018. Synergistic effect of ferrate (VI)-ozone integrated pretreatment on the improvement of water quality and fouling alleviation of ceramic UF membrane in reclaimed water treatment. Journal of Membrane Science 567, 216-227.

Lucas, W.C. and Sample, D.J. 2015. Reducing combined sewer overflows by using outlet controls for Green Stormwater Infrastructure: Case study in Richmond, Virginia. Journal of Hydrology 520, 473-488.

Macova, Z., Bouzek, K., Hives, J., Sharma, V.K., Terryn, R.J. and Baum, J.C. 2009. Research progress in the electrochemical synthesis of ferrate(VI). Electrochimica Acta 54(10), 2673-2683.

Madoux-Humery, A.-S., Dorner, S., Sauve, S., Aboulfadl, K., Galarneau, M., Servais, P. and Prevost, M. 2013. Temporal variability of combined sewer overflow contaminants: Evaluation of wastewater micropollutants as tracers of fecal contamination. Water Research 47(13), 4370-4382.

Madoux-Humery, A.-S., Dorner, S., Sauve, S., Aboulfadl, K., Galarneau, M., Servais, P. and Prevost, M. 2016. The effects of combined sewer overflow events on riverine sources of drinking water. Water Research 92, 218-227.

Makky, E.A., Park, G.-S., Choi, I.-W., Cho, S.-I. and Kim, H. 2011. Comparison of Fe(VI) (FeO42-) and ozone in inactivating Bacillus subtilis spores. Chemosphere 83(9), 1228-1233.

Malachova, K., Sezimova, H. and Rozinek, R. 2014. Detection of genotoxicity and toxicity of wastewater treatment plant (WTP) effluents after pretreatment with ferrate (VI). Toxicol. Lett. 229, S117-S118.

Manoli, K., Nakhla, G., Feng, M., Sharma, V.K. and Ray, A.K. 2017a. Silica gel-enhanced oxidation of caffeine by ferrate(VI). Chemical Engineering Journal 330, 987-994.

Manoli, K., Nakhla, G., Ray, A.K. and Sharma, V.K. 2017b. Oxidation of Caffeine by Acid-activated Ferrate(VI): Effect of Ions and Natural Organic Matter. Aiche Journal 63(11), 4998-5006.

Masi, F., Rizzo, A., Bresciani, R. and Conte, G. 2017. Constructed wetlands for combined sewer overflow treatment: Ecosystem services at Gorla Maggiore, Italy. Ecological Engineering 98, 427-438.

Matin, A.R., Yousefzadeh, S., Ahmadi, E., Mahvi, A., Alimohammadi, M., Aslani, H. and Nabizadeh, R. 2018. A comparative study of the disinfection efficacy of H2O2/ferrate and UV/ H2O2/ferrate processes on inactivation of Bacillus subtilis spores by response surface methodology for modeling and optimization. Food and Chemical Toxicology 116, 129-137.

Mbaeze MC, A.V.a.O.N. 2017. Comparative Assessment of Performance of Aluminium Sulphate (Alum) and Ferrous Sulphate as Coagulants in Water Treatment Modern Chemistry & Applications 5(4).

McFadden, M., Loconsole, J., Schockling, A., Nerenberg, R. and Pavissich, J.P. 2017. Comparing peracetic acid and hypochlorite for disinfection of combined sewer overflows: Effects of suspended-solids and pH. Sci. Total Environ. 599, 533-539.

McIntyre, J.K., Winters, N., Rozmyn, L., Haskins, T. and Stark, J.D. 2019. Metals leaching from common residential and commercial roofing materials across four years of weathering and implications for environmental loading. Environmental Pollution 255.

Nikolic-Bujanovic, L., Cekerevac, M., Tomic, M. and Zdravkovic, M. 2016. Ibuprofen removal from aqueous solution by in situ electrochemically generated ferrate(VI): proof-of-principle. Water Science and Technology 73(2), 389-395.

Noorhasan, N., Patel, B. and Sharma, V.K. 2010. Ferrate(VI) oxidation of glycine and glycylglycine: Kinetics and products. Water Research 44(3), 927-935.

Pachuau, L., Lee, S.M. and Tiwari, D. 2013. Ferrate(VI) in wastewater treatment contaminated with metal(II)-iminodiacetic acid complexed species. Chemical Engineering Journal 230, 141-148.

Passerat, J., Ouattara, N.K., Mouchel, J.-M., Rocher, V. and Servais, P. 2011. Impact of an intense combined sewer overflow event on the microbiological water quality of the Seine River. Water Research 45(2), 893-903.

Phillips, P.J., Chalmers, A.T., Gray, J.L., Kolpin, D.W., Foreman, W.T. and Wall, G.R. 2012. Combined Sewer Overflows: An Environmental Source of Hormones and Wastewater Micropollutants. Environmental Science & Technology 46(10), 5336-5343.

Rai, P.K., Lee, J., Kailasa, S.K., Kwon, E.E., Tsang, Y.F., Ok, Y.S. and Kim, K.-H. 2018. A critical review of ferrate(VI)-based remediation of soil and groundwater. Environmental Research 160, 420-448.

Real, F.J., Benitez, F.J., Acero, J.L. and Gonzalez, M. 2007. Removal of diazinon by various advanced oxidation processes. Journal of Chemical Technology and Biotechnology 82(6), 566-574.

Rechenburg, A., Koch, C., Classen, T. and Kistemann, T. 2006. Impact of sewage treatment plants and combined sewer overflow basins on the microbiological quality of surface water. Water Science and Technology 54(3), 95-99.

Richardson, S.D., Plewa, M.J., Wagner, E.D., Schoeny, R. and DeMarini, D.M. 2007. Occurrence, genotoxicity, and carcinogenicity of regulated and emerging disinfection by-products in drinking water: A review and roadmap for research. Mutation Research-Reviews in Mutation Research 636(1-3), 178-242.

Rizzo, L., Lofrano, G., Gago, C., Bredneva, T., Lannece, P., Pazos, M., Krasnogorskaya, N. and Carotenuto, M. 2018. Antibiotic contaminated water treated by photo driven advanced oxidation processes: Ultraviolet/H2O2 vs ultraviolet/peracetic acid. Journal of Cleaner Production 205, 67-75.

Ryu, J., Oh, J., Snyder, S.A. and Yoon, Y. 2014. Determination of micropollutants in combined sewer overflows and their removal in a wastewater treatment plant (Seoul, South Korea). Environmental Monitoring and Assessment 186(5), 3239-3251.

Segura, P.A., Francois, M., Gagnon, C. and Sauve, S. 2009. Review of the Occurrence of Anti-infectives in Contaminated Wastewaters and Natural and Drinking Waters. Environmental Health Perspectives 117(5), 675-684.

Shao, B., Dong, H., Sun, B. and Guan, X. 2019. Role of Ferrate(IV) and Ferrate(V) in Activating Ferrate(VI) by Calcium Sulfite for Enhanced Oxidation of Organic Contaminants. Environmental Science & Technology 53(2), 894-902.

Sharma, V.K. 2002. Potassium ferrate(VI): an environmentally friendly oxidant. Advances in Environmental Research 6(2), 143-156.

Sharma, V.K. 2011. Oxidation of inorganic contaminants by ferrates (VI, V, and IV)-kinetics and mechanisms: A review. Journal of Environmental Management 92(4), 1051-1073.

Sharma, V.K. 2013. Ferrate(VI) and ferrate(V) oxidation of organic compounds: Kinetics and mechanism. Coordination Chemistry Reviews 257(2), 495-510.

Sharma, V.K. and Bielski, B.H.J. 1991. Reactivity of ferrate(vi) and ferrate(v) with amino-acids. Inorganic Chemistry 30(23), 4306-4310.

Sharma, V.K., Chen, L. and Zboril, R. 2016. Review on High Valent Fe-VI (Ferrate): A Sustainable Green Oxidant in Organic Chemistry and Transformation of Pharmaceuticals. Acs Sustainable Chemistry & Engineering 4(1), 18-34.

Sharma, V.K., Chen, L. and Zboril, R. 2017. Review on High Valent Fe-VI (Ferrate): A Sustainable Green Oxidant in Organic Chemistry and Transformation of Pharmaceuticals (vol 4, pg 18, 2016). Acs Sustainable Chemistry & Engineering 5(3), 2781-2781.

Sharma, V.K., Graham, N.J.D., Li, X.Z. and Yuan, B.L. 2010. Ferrate(VI) enhanced photocatalytic oxidation of pollutants in aqueous TiO2 suspensions. Environmental Science and Pollution Research 17(2), 453-461.

Sharma, V.K., Kazama, F., Jiangyong, H. and Ray, A.K. 2005. Ferrates (iron(VI) and iron(V)): Environmentally friendly oxidants and disinfectants. Journal of Water and Health 3(1), 45-58.

Sharma, V.K., Liu, F., Tolan, S., Sohn, M., Kim, H. and Oturan, M.A. 2013. Oxidation of beta-lactam antibiotics by ferrate(VI). Chemical Engineering Journal 221, 446-451.

Sharma, V.K., Sohn, M., Anquandah, G.A.K. and Nesnas, N. 2012. Kinetics of the oxidation of sucralose and related carbohydrates by ferrate(VI). Chemosphere 87(6), 644-648.

Shu, Z.Q., Bolton, J.R., Belosevic, M. and El Din, M.G. 2013. Photodegradation of emerging micropollutants using the medium-pressure UV/H2O2 Advanced Oxidation Process. Water Research 47(8), 2881-2889.

Siskova, K.M., Jancula, D., Drahos, B., Machala, L., Babica, P., Alonso, P.G., Travnicek, Z., Tucek, J., Marsalek, B., Sharma, V.K. and Zboril, R. 2016. High-valent iron (Fe-VI, Fe-V, and Fe-IV) species in water: characterization and oxidative transformation of estrogenic hormones. Physical Chemistry Chemical Physics 18(28), 18802-18810.

Soonthornnonda, P. and Christensen, E.R. 2008. Source apportionment of pollutants and flows of combined sewer wastewater. Water Research 42(8-9), 1989-1998.

Stanford, C., Jiang, J.Q. and Alsheyab, M. 2010. Electrochemical Production of Ferrate (Iron VI): Application to the Wastewater Treatment on a Laboratory Scale and Comparison with Iron (III) Coagulant. Water Air and Soil Pollution 209(1-4), 483-488.

Sumant, K., Ghosh, N.C. and Kazmi, A.A. 2016. Ballasted sand flocculation for water, wastewater and CSO treatment. Environmental Technology Reviews 5(1), 57-67.

Szabo, J.G., Buchberger, S.G. and Bishop, P.L. 2005. Performance of wet weather treatment facility for control of combined sewer overflows: Case study in Cincinnati, Ohio. Journal of Environmental Engineering-Asce 131(3), 375-386.

Tao, W.D., Bays, J.S., Meyer, D., Smardon, R.C. and Levy, Z.F. 2014. Constructed Wetlands for Treatment of Combined Sewer Overflow in the US: A Review of Design Challenges and Application Status. Water 6(11), 3362-3385.

Tiwari, D., Sailo, L., Choi, S.I., Yoon, Y.Y. and Lee, S.M. 2017. Efficient oxidative removal of 4-tert-octylphenol and 17 alpha-ethynylestradiol from aqueous solutions using ferrate(VI). Korean Journal of Chemical Engineering 34(3), 734-740.

Tondera, K., Klaer, K., Koch, C., Hamza, I.A. and Pinnekamp, J. 2016. Reducing pathogens in combined sewer overflows using performic acid. Int. J. Hyg. Environ. Health. 219(7), 700-708.

von Gunten, U. 2018. Oxidation Processes in Water Treatment: Are We on Track? Environ. Sci. Technol. 52(9), 5062-5075.

Wang, H.Y., Liu, Y.B. and Jiang, J.Q. 2016a. Reaction kinetics and oxidation product formation in the degradation of acetaminophen by ferrate (VI). Chemosphere 155, 583-590.

Wang, W.G., Xu, Z.X., Li, H.Z. and Jin, W. 2016b. Coagulation characteristics of organic pollutants removal in cso wastewater treatment. Environmental Engineering and Management Journal 15(1), 75-80.

Wang, Y.L., Liu, H.J., Liu, G.G., Xie, Y.H. and Gao, S.Y. 2015. Oxidation of diclofenac by potassium ferrate (VI): Reaction kinetics and toxicity evaluation. Science of the Total Environment 506, 252-258.

Westerhoff, P., Yoon, Y., Snyder, S. and Wert, E. 2005. Fate of endocrine-disruptor, pharmaceutical, and personal care product chemicals during simulated drinking water treatment processes. Environmental Science & Technology 39(17), 6649-6663.

WHO, W.H.O. 2005 Bromate in Drinking Water.

Wu, J.G., Lan, C.Y. and Chan, G.Y.S. 2009. Organophosphorus pesticide ozonation and formation of oxon intermediates. Chemosphere 76(9), 1308-1314.

Wu, S.H., Li, H.R., Li, X., He, H.J. and Yang, C.P. 2018. Performances and mechanisms of efficient degradation of atrazine using peroxymonosulfate and ferrate as oxidants. Chemical Engineering Journal 353, 533-541.

Yang, B., Ying, G.G., Zhao, J.L., Zhang, L.J., Fang, Y.X. and Nghiem, L.D. 2011. Oxidation of triclosan by ferrate: Reaction kinetics, products identification and toxicity evaluation. Journal of Hazardous Materials 186(1), 227-235.

Yang, B., Ying, G.G., Zhao, J.L., Liu, S., Zhou, L.J. and Chen, F. 2012. Removal of selected endocrine disrupting chemicals (EDCs) and pharmaceuticals and personal care products (PPCPs) during ferrate(VI) treatment of secondary wastewater effluents. Water Research 46(7), 2194-2204.

Yang, T., Wang, L., Liu, Y., Huang, Z., He, H., Wang, X., Jiang, J., Gao, D. and Ma, J. 2019. Comparative study on ferrate oxidation of BPS and BPAF: Kinetics, reaction mechanism, and the improvement on their biodegradability. Water Research 148, 115-125.

Yu, W.Z., Yang, Y.J. and Graham, N. 2016. Evaluation of ferrate as a coagulant aid/oxidant pretreatment for mitigating submerged ultrafiltration membrane fouling in drinking water treatment. Chem. Eng. J. 298, 234-242.

Zhang, H., Zheng, L., Li, Z., Pi, K. and Deng, Y. 2020. One-step Ferrate(VI) treatment as a core process for alternative drinking water treatment. Chemosphere 242.

Zhang, J., Zhu, L., Shi, Z. and Gao, Y. 2017. Rapid removal of organic pollutants by activation sulfite with ferrate. Chemosphere 186, 576-579.

Zhang, T., Dong, F., Luo, F. and Li, C. 2018. Degradation of sulfonamides and formation of trihalomethanes by chlorination after pre-oxidation with Fe(VI). Journal of Environmental Sciences 73, 89-95.

Zhao, J., Liu, Y., Wang, Q., Fu, Y., Lu, X. and Bai, X. 2018a. The self-catalysis of ferrate (VI) by its reactive byproducts or reductive substances for the degradation of diclofenac: Kinetics, mechanism and transformation products. Separation and Purification Technology 192, 412-418.

Zhao, J., Wang, Q., Fu, Y., Peng, B. and Zhou, G. 2018b. Kinetics and mechanism of diclofenac removal using ferrate(VI): roles of Fe3+, Fe2+, and Mn2+. Environmental Science and Pollution Research 25(23), 22998-23008.

Zheng, L. and Deng, Y. 2016. Settleability and characteristics of ferrate(VI)-induced particles in advanced wastewater treatment. Water Research 93, 172-178.

Zhou, J.H., Chen, K.B., Hong, Q.K., Zeng, F.C. and Wang, H.Y. 2017. Degradation of chloramphenicol by potassium ferrate (VI) oxidation: kinetics and products. Environmental Science and Pollution Research 24(11), 10166-10171.

Zhou, Z. and Jiang, J.Q. 2015. Reaction kinetics and oxidation products formation in the degradation of ciprofloxacin and ibuprofen by ferrate(VI). Chemosphere 119, S95-S100.

Zhu, W., Seth, R. and Lalman, J. 2007. Evaluation of a micro carrier weighted coagulation flocculation process for the treatment of combined sewer overflow. Environmental Technology 28(7), 761-770.

Chapter 3: Bench to Full-Scale Enhanced Primary Treatment of Municipal Wastewater under Wet Weather Flow for Minimized Pollution Load: Evaluation of Chemical Addition and Process Control Indicators

3.1 Introduction

Wastewater collection networks represent a fundamental component of a city's infrastructure and its wastewater treatment process. In areas where those networks are designed to accommodate stormwater runoffs in addition to regular domestic and industrial wastewaters, they become known as combined sewers. Their operation thus varies seasonally, reaching its full capacity during events of heavy rain and intensive snow melts. In such cases, wastewater treatment plants (WWTPs) to which those networks are connected become unable to contain the excess wastewater during wet weather conditions. Consequently, untreated wastewater ends up overflowing to the closest water stream as per the combined sewer system design. According to the USEPA (2018), this is known as combined sewer overflow (CSO) and it includes regular untreated wastewater diluted by stormwater. The volume of poorly treated or untreated CSO and the frequency of its discharge will essentially contribute to the concentration of pollutants (including pathogens, organic and inorganic chemicals) in the receiving water body, and consequently will affect its suitability for drinking or recreational purposes. Problems with the discharge of untreated CSO can transcend, impacting the aquatic ecosystem and public health with detrimental waterborne diseases (Jalliffier-Verne et al. 2015). It is reported that in Canada, 87% of the population is connected via a wastewater collection network to a certain type of treatment and that only few treatment plants undertake the initiative to store and treat CSO. As such, direct discharges from CSO have not been routinely monitored (Canada 2019, CWN 2018).

CSO is commonly characterized in terms of its mass loading of macropollutants. Some of its major constituents include around 83-600 mg/L of total suspended solids (TSS), 30-180 mg/L of biochemical oxygen demand (BOD), 80-200 mg/L of chemical oxygen demand (COD), 80-190 mg/L of total phosphorus, and 30-50 mg/L of ortho-phosphate (ortho-P) (El Samrani et al. 2008a, Gasperi et al. 2008, Li et al. 2004). CSOs can also be as a relevant source of micropollutants (MPs) (pharmaceuticals, personal care products, herbicides and pesticides) as WWTPs (Kay et al. 2016, Phillips et al. 2012) and thus imply similar adverse effects on aquatic and terrestrial fauna and flora (Shu et al. 2016). Ryu et al. (2014) estimated that physical, chemical and biological processes in a WWTP can decrease the MPs in the effluent by 28% as compared to 97% decrease in suspended solids and 86% decrease in COD. This relatively low removal sheds the light on the importance of screening and modeling approaches to estimate the overall load of MPs in the environment and mitigate their cost-prohibitive and impractical quantification (Arlos et al. 2014, Johnson and Williams 2004, Launay et al. 2016, Mutzner et al. 2016, Tolouei et al. 2019).

In wet weather conditions, El Samrani et al. (2008a) demonstrated that the aluminum-based coagulant PACl was more efficient than $FeCl_3$ for CSO treatment. It had a lower optimum dose and allowed a pronounced reduction of turbidity and associated metals such as copper, lead, zinc and chromium. Gibson et al. (2016) reported a similar effect on turbidity removal with alum coupled with a cationic polymer; yet, no major impact on TSS removal or percent ultraviolet transmittance (% UVT) was observed.

The addition of a coagulant that comes as a natural or synthetic polymer or a metal salt, initiates the colloidal destabilization and aggregation resulting in the formation of larger particles able to settle out. Different mechanisms can be involved in the particles removal depending on the water quality and coagulant dose (Pourrezaei et al. 2011). Particularly, during coagulation with aluminum-based salts, the salt hydrolysis product is responsible for particle destabilization (Exall and Marsalek 2013). Two important precipitation reactions take place when alum is added to the wastewater. The first one occurs between alum and calcium bicarbonate and produces aluminum hydroxide precipitate that can enmesh and remove colloids (equation 3.1). The second one occurs between alum and phosphorus and produces insoluble aluminum phosphate (equation 3.2) (Cao et al. 2010).

$$\boldsymbol{Al_2(SO_4)_3 \cdot 18\,H_2O + 3\,Ca(HCO_3)_2 \leftrightarrow 3\,CaSO_4 + 2\,Al(OH)_3 + 6\,CO_2 + 18\,H_2O} \quad (3.1)$$

$$\boldsymbol{Al^{3+} + PO_4{}^{3-} \leftrightarrow AlPO_4} \quad (3.2)$$

Following coagulation, larger particles or flocs are formed during flocculation by colloidal aggregation. This process is induced by mixing and polymer addition to strengthen the formed flocs (Young et al. 2000). Settling entails the separation of solids from the liquid and is the last step in the process. In real applications, settling can take place in sedimentation tanks often enhanced by plate settlers that promote the large surface area and short settling distance. While the role of plate settlers is to maximize the particles removal, their efficiency remains a function of their geometric design, the wastewater quality and flow conditions (Sarkar et al. 2007).

To the best of our knowledge, no study on the treatment of wet weather primary influent (PI) or CSO has comprehensively addressed the upscaling of coagulation conditions and the evaluation of process control indicators. Most studies were limited to the bench or pilot-scale levels (El Samrani et al. 2008b, Exall and Marsalek 2013, Li et al. 2003, Zhu et al. 2007). Evidence of full-scale application of the optimum coagulant dose is also scarce in the literature (Baghvand et al. 2010, El Samrani et al. 2008b, Guida et al. 2007, Wang et al. 2015b). Few studies only evaluated the performance of disinfectants at a full-scale level using performic acid and peracetic acid (Chhetri et al. 2016, Chhetri et al. 2015, Chhetri et al. 2014). In this study, we undertook a practical approach towards the EPT of CSO to maximize the output, i.e. the quality of the effluent, while minimizing the chemical input.

The main objective of this work was to evaluate the performance of different coagulants and coagulant aids for the enhanced primary treatment of municipal wastewater during wet weather conditions at a bench-scale level. The application of those compounds at a full-scale level was investigated in order to optimize the EPT at the WWTP, its online process control, and the overall discharge of suspended solids and ortho-phosphate into the receiving environment.

3.2 Material and methods

3.2.1 Wastewater

Samples of municipal wastewater were collected in 20 L plastic pails from the influent stream (i.e., primary influent (PI)) to the Enhanced Primary Treatment (EPT) unit of a WWTP in central Edmonton between November 2016 and March 2017 and between August and October 2017 (Figure 3.1). The collected grab samples of PI during wet weather flow were transported to the laboratory for a preliminary characterization for TSS. During dry weather, PI samples were diluted with deionized water to the desired TSS concentration to emulate the average TSS value during wet weather flow. The obtained wastewater was immediately used in the coagulation/flocculation experiments.

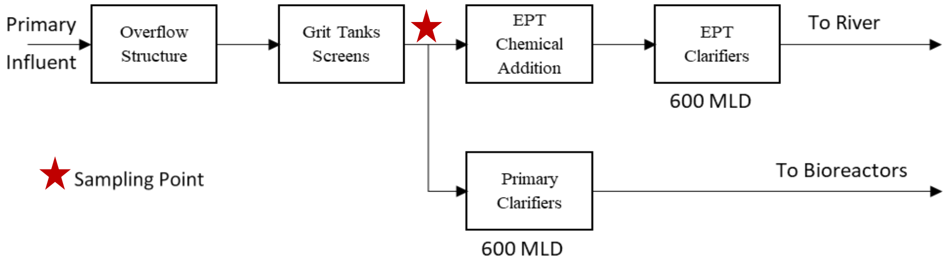

Figure 3. 1 Simplified representation of the EPT system.

3.2.2 Coagulants and polymers

All coagulants and chemicals used in the laboratory analyses were purchased from Fisher Scientific, except PACl which was obtained from ClearTech in the form of a stock solution of 4.6 mol/L. Polymers were purchased from SNF Inc., BASF, Kemira and AS Paterson. Stock solutions of coagulants and polymers were prepared in the laboratory by dissolving the respective solutes in deionized water to the desired concentration; they were then stored at 4°C for up to four days until used in the jar test.

3.2.3 Jar test

During the coagulant and polymer optimization studies, three B-KER^2 Jar Test apparatuses with 3-inch wide Phipps & Bird stirrers were used for each mixing condition to cater for duplicate test runs. Jars and stirrers were thoroughly cleaned with a phosphate-free detergent and rinsed with deionized water before and after each use. At the beginning of each experiment, jars were filled with 2 L of homogenized wastewater, then the designated doses of coagulants and polymers were consecutively added to the jars before turning the impellers on. In all experiments, one jar remained free of chemical addition to represent the effect of mixing only. Rapid and slow mixing were performed sequentially before stopping the impellers and carefully removing the stirrers in each apparatus to avoid any media disturbance. Settling was then allowed for one hour after which the supernatant was collected with syringes immersed at 2 inches below the surface. Samples were stored in dark glass bottles at 4°C for analysis.

A 2^3 factorial design was adopted to determine the impact of rapid and slow mixing conditions and coagulant doses on the coagulation/flocculation process of the wastewater (Table 3.1). These factors were selected due to their influence on the destabilization and aggregation process as well as their easy manipulation at a bench-scale level. Keeping in mind that these factors are among the most important ones impacting the coagulation/flocculation efficiency and that various other factors have also been studied such at pH and temperature (Afzal et al. 2011, Chelme-Ayala et al. 2012, Chelme-Ayala et al. 2011, Pourrezaei et al. 2010). In total, there were four replicates for each measurement performed in the factorial design. Three different coagulants were tested: alum, PACl and $FeCl_3$.

Table 3. 1 Details of the 2^3 factorial design used for the coagulants assessment.

Factor	High Level	Low Level
Rapid Mixing Gt	68400 (300 rpm – 3 min)	9300 (150 rpm – 1 min)
Slow Mixing Gt	27600 (30 rpm – 20 min)	6000 (15 rpm – 10 min)
Coagulant Dose	125 mg/L Alum (10.14 mg Al/L) 105 mg/L PACl (10.14 mg Al/L) 61 mg/L $FeCl_3$ (20.95 mg Fe/L)	50 mg/L Alum (4.05 mg Al/L) 42 mg/L PACl (4.05 mg Al/L) 24 mg/L $FeCl_3$ (8.38 mg Fe/L)

Literature was screened to identify the most common applicable doses of alum in the treatment of wet weather PI. In general, doses ranged between 25 and 200 mg/L, with 100 mg/L alum being identified for maximum COD removal and % UVT (Gibson et al. 2016, Jung et al. 2015, Wang et al. 2015b). Accordingly, the alum doses decided upon in this study were 50 and 125 mg/L as they represent a reasonable range of values. Metal-equivalent doses were then calculated to identify the corresponding doses of PACl and $FeCl_3$ (Table A.1). They were elaborated based on the molar equivalent for the consumption of the same amount of alkalinity (equation 3.1 and 3.3), according to which 2 moles of $FeCl_3$ are equivalent to 1 mole of alum. 1.25 mg/L cationic polymer was also uniformly added in all jars along with the coagulant. Two levels of rapid mixing with Gt values 68400 and 9300 and two levels of slow mixing with Gt values 27600 and 6000 were applied. Where "G" is the velocity gradient and "t" is the mixing time. Conversions from rpm-min to Gt are presented in Table A.2.

$$2FeCl_3 + 6\,H_2O + 3\,Ca(HCO_3)_2 \leftrightarrow 3\,CaCl_2 + 2\,Fe(OH)_3 + 6\,CO_2 + 12\,H_2O$$

(3.3)

Eight anionic polymers (labeled A to H) and one cationic polymer were arbitrarily selected and their performances as coagulant aids were evaluated at a bench scale using a jar test with alum as the primary coagulant (Table A.3). Similar mixing conditions were applied with all polymers were uniformly injected with alum. After one hour of settling time, samples were collected from the supernatant. They were screened for TSS, turbidity and ortho-P. The polymer that revealed the highest removals was selected and investigated under a range of dose combinations to identify the optimum condition for full-scale operation. All polymers were prepared from stock solutions and applied with a ratio of 100:1 as coagulant: polymer.

3.2.4 Full-scale application of alum/polymer

Different dose combinations of alum and polymer were tested at the existing EPT plant at the WWTP. The coagulant was dosed with mixing in the channel connected to the primary clarifier and the flocculent was dosed downstream with mixing in the channel connected to the flocculation chambers (Figure 3.1). Settling took place in the primary clarifier equipped with plate settlers for a retention time of approximately one to two hours.

3.2.5 Analytical methods

Samples were analyzed according to the Standard Methods for the Examination of Water and Wastewater (2012) for TSS (APHA (2012): Method 2540 D, using 0.45 µm filter paper), and COD (Method 5220 D). HACH method was used to measure ortho-P in filtered samples (HACH 8114 based on Standard Method 4500-P C). pH and turbidity were determined using Accumet Research AR20 pH/conductivity meter (Fischer-Scientific) and T-100 handheld Oakton Turbidity meter, respectively. UV absorbance (UVA) was measured at 254 nm using Thermo Scientific

GENESYS 10S UV-Vis Spectrophotometer, and the % UV Transmittance (% UVT) was calculated using Equation 3.4. Data was analyzed using Microsoft Excel® which was also used to run the Three-Factor ANOVA statistical test.

$$\% \text{ UVT} = 100 \times 10^{-\text{UVA}} \tag{3.4}$$

3.3 Results and Discussion

3.3.1 Wastewater quality

As part of this study, samples of PI during real wet weather conditions were collected at different rain occasions and analyzed for TSS. The average obtained TSS value was 150 mg/L. Accordingly; during dry weather, PI samples were diluted with deionized water to emulate real wastewater in wet weather flow. Also, under wet weather conditions and a flow rate of 1000 MLD, the recorded turbidity and ortho-phosphate values were 128 NTUs and 6.6 mg PO_4^{3-}/L respectively, while at a lower flow rate of 276 MLD, those values increased to 212 NTUs and 12.7 mg PO_4^{3-}/L. The sampling period extended for two years with a total of 12 samples. Details on all parameters are included in Table 3.2.

Table 3. 2 Water quality parameters of the untreated diluted primary influent (PI) used in the bench-scale experiment and the influent wastewater to the WWTP in the full-scale runs.

		pH	**Turbidity (NTU)**	**TSS (mg/L)**	**% UVT**	**COD (mg O_2/L)**	**Ortho-P (mg PO_4^{3-}/L)**
Bench-scale	**Range**	7.17-7.88	43-110	98-167	*N.M.*	160-361	2.10-6.35
	Average (±STDEV)	7.38 (±0.22)	88 (±22)	137 (±29)	*N.M.*	293 (±71)	4.48 (±1.88)
Full-scale	**Range**	6.71-7.29	87-192	138-364	33-57	*N.M.*	0.88-11.10
	Average (±STDEV)	7.13 (±0.16)	150 (±31)	224 (±59)	44 (±6.85)	*N.M.*	6.54 (±2.44)

***N.M. = Not measured**

3.3.2 Performance assessment of coagulants

In general, the capacity of each coagulant to eliminate pollutants varied with the dose and mixing conditions. Neither mixing conditions nor coagulant type and dose affected the final pH of the wastewater which dropped slightly upon coagulant addition. At lower coagulant doses, the pH ranged between 6.90-7.21 for alum, 7.16-7.34 for PACl and 7.11-7.29 for $FeCl_3$. At higher coagulant doses, the pH of treated samples ranged between 6.35-6.99 for alum, 6.85-7.21for PACl and 6.74-7.10 for $FeCl_3$.

According to Figure 3.2, turbidity removal ranged widely between 75% and to 96%. Indeed, alum and PACl showed comparable performance in the removal of turbidity and achieved 95% and 96% removals respectively compared to 85% by $FeCl_3$ at the high dose. It was also noticeable that higher coagulant doses achieved higher turbidity removal with the best performance attained at the low level of rapid mixing and slow mixing.

Results of TSS removal indicated that all three coagulants showed comparable efficiencies with the best removal achieved at the low level of rapid mixing and high level of slow mixing. At low doses of coagulants and optimal mixing conditions, $FeCl_3$ removed 95% of TSS while alum and PACl attained ≥ 98% removal. Mixing showed different impacts on TSS removal with PACl mainly because the flocs formed with PACl are more sensitive to breakage, and their settling velocity changes inversely with Gt (Dempsey et al. 1985, Yu et al. 2009). The best removal of TSS by both dose levels of PACl was achieved at the low level of rapid mixing and high level of slow mixing while the lowest removal attained at the high level of both rapid mixing and slow mixing. This might be ascribed to that PACl form hydroxide flocs rapidly and extensive rapid mixing leads flocs breakage thus inhibiting suspended solids removal (Wang et al. 2015a). In contrast, higher slow mixing promotes larger flocs formation with higher settling velocities resulted in better removal of suspended solids. It is worth noting that in all cases, the final recorded TSS value was less than the target value set by the WWTP (30 mg/L).

With COD removal, the tested coagulant doses and mixing conditions turned out to have different effects. The condition of low-level rapid mixing with high-level slow mixing was consistently the most favorable for all three coagulants at the low dose level. At the low dose level, the tested coagulants achieved comparable removal of COD while at a high dose level, PACl in most cases revealed better COD removal reaching up to 79%. In fact, PACl is expected to exceed alum as it is a pre-polymerized coagulant that brings pre-formed stable aluminum hydroxide polymeric species to the matrix upon its addition. These species are also formed when alum is used and they are the product of alum hydrolysis (Jiang and Graham 2010). Yet, with PACl application, they are readily available for a longer time which justifies their higher potential for charge neutralization. Studies have demonstrated that for these reasons, PACl has a high capacity to adsorb and thus remove dissolved organic carbon which would also imply the removal of natural organic matter and lower COD (Jiang and Graham 2010, Smoczynski et al. 2014). Alternatively, studies suggested increasing the dose of alum to improve COD removal (Zhou et al. 2008).

The removal of ortho-P was best achieved with alum under all mixing conditions and doses, with the highest removal being 100%. Similar to the results above, high coagulant doses lead to a higher percentage of removal and $FeCl_3$ remained the least efficient among the three coagulants. The mixing intensity impacted positively on the removal of ortho-P. Such observation can be associated with the formation of phosphate complexes that are influenced by pH and coagulant dose. When Al-based coagulants are applied, aluminum monomer species that form by the coagulant hydrolysis have the dominant effect on the formation of phosphate complexes (Trinh and Kang 2015). It has been reported that iron-based coagulants are more effective for the removal of phosphate, while aluminum-based coagulants are more effective for the removal of COD (Smoczynski et al. 2014). This is not supported by our results that showed that $FeCl_3$ was less effective for the removal of both ortho-P and COD when applied in iron-equivalent doses comparable to those of the aluminum-based coagulants. This disagreement regarding the efficiency of both metal-based coagulants can be due to the different experimental conditions applied in both studies. As such, Smoczynski et al. (2014) used synthetic wastewater along with higher doses of aluminum and iron-based coagulant doses: 235 mg Al/L and 452 mg Fe/L, while we applied lower doses of both coagulants (10.14 mg Al/L and 20.95 mg Fe/L, equivalent to 0.37 mM of metal) on real wastewater.

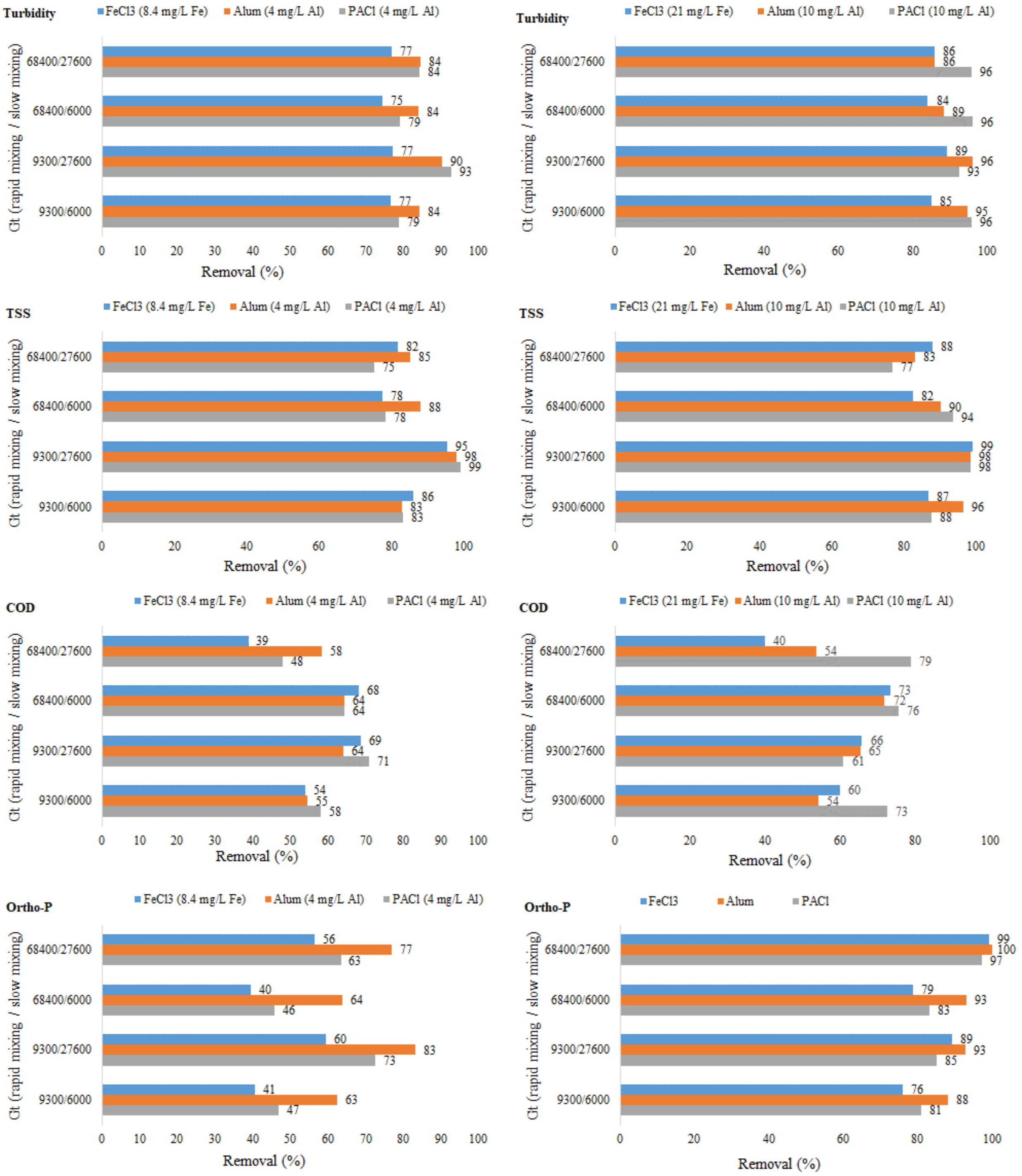

Figure 3. 2 Percentage removal (%) of the tested parameters by FeCl3, alum and PACl at high and low coagulant doses. The effect of mixing and settling on the removal was excluded in the calculation. In untreated wastewater, the parameters ranged as follows: Turbidity 47.2-106.0 NTU; TSS 99-167 mg/L; COD 160-361 mg O_2/L; and Ortho-P 2.10-6.35 mg P/L.

The two components of mixing addressed in this study: intensity and time are generally capable of mitigating the effect of each other. On one hand, studies have demonstrated that intense mixing provokes the breakage of flocs which results in small hard to settle particles and thus high turbidity (Yukselen and Gregory 2004). On the other hand, long mixing time could reverse flocs breakage, yet this is not always guaranteed and tends to be less significant in metal-based coagulants (Yu et al. 2011, Yukselen and Gregory 2004). For all those reasons added to the extra power requirements for mixing, high-level rapid mixing conditions are generally not favored.

Since, during the analysis of variance, the effects with values near-zero are generally attributed to experimental error or noise (Anderson 2015), factors in the current ANOVA showing such effects were considered negligible regardless of their p-values. Overlooking all three coagulants, it could be noticed that while turbidity removal was unilaterally impacted by coagulant dose, there was no agreement on the factors, impacting the removal of TSS, COD and ortho-P across the studied coagulants (Table A.4). As such, factors affecting TSS removal by alum and the extent of this effect differed from those with PACl and $FeCl_3$. Similar results were obtained by Zhu et al. (2010) during the treatment of liquid swine manure. COD removal by alum was mostly affected by slow mixing alone and slow mixing and coagulant dose combined, while with PACl and $FeCl_3$ slow mixing was the most impactful. Factors affecting the removal of ortho-P by alum and PACl were the same (coagulant dose only and slow mixing and coagulant dose). It must be highlighted that slow mixing and/or coagulant dose combined unveiled the highest effect for the removal of ortho-P and COD across all three coagulants. So, to maximize the removal of the contaminants, these factors must be optimized.

The following ANOVA models can be developed to predict the percent removal of TSS with factors at two levels; models for the removal of other contaminants are available in Table A.5.

TSS % Removal by:

Alum: 90.29 – 7.32 A + 3.52 C – 6.78 AB – 3.47 AC + 4.35 BC

PACl: 86.36 – 5.40 A + 4.89 C – 10.35 AB + 8.98 AC – 5.95 BC

$FeCl_3$: 85.66– 5.93 B + 9.48 AC – 12.76 BC

3.3.3 Optimization of the alum dose

The above analysis deemed alum and PACl comparable for the removal of contaminants, yet alum is more cost-efficient than PACl (with approximately 300 USD /MT of alum compared to 600 - 715 USD /MT of PACl), so it can be considered the best coagulant for full-scale application. In order to further optimize its dosage, a jar test was performed with a broader range of alum doses (0 to 150 mg/L) that were evaluated for the removal of TSS (Figure 3.3). Results demonstrated that with an alum dose of 75 mg/L, the final average TSS was 33 mg/L. Further increasing the alum dose decreased the TSS to below the target value of 30 mg/L to reach near a plateau. Therefore, we recommended 75 mg/L alum as the typical dose because higher doses would incur higher costs with minimal returns.

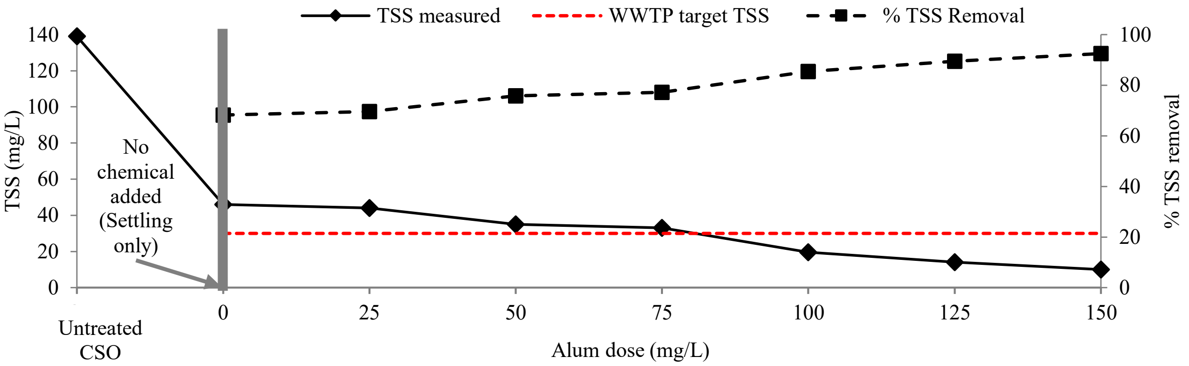

Figure 3. 3 Effect of alum dosage on the removal of TSS from wastewater at wet weather conditions.

3.3.4 Effect of polymer type on the performance of alum in the treatment of wastewater during wet weather flow

As alum was deemed the best coagulant for wastewater treatment, an attempt was made to further improve its performance under the effect of different types of polymers. The WWTP is currently implementing anionic polymer A along with alum. Therefore, 7 other types of anionic polymers and 1 cationic polymer were put to test to assess the role of polymer addition. The chemical and physical properties of all polymers are available in Table A.35. The dose ratios of coagulant: polymer were maintained constant at 100:1 and the mixing conditions were fixed at 300 rpm - 1 min for rapid mixing and 30 rpm - 20 minutes for slow mixing. Following the previous set of experiments, it was decided to investigate the performance of 75 mg/L alum applied with 0.75 mg/L polymer in terms of turbidity, TSS and ortho-P removal. The obtained results (summarized in Figure 3.4) showed that while all tested polymers exhibited comparable performances, Alum with the anionic polymers A and B showed the best removal for all three tested parameters. All treated samples met the TSS and UVT % design values for the EPT effluent (30 mg/L and 40% respectively).

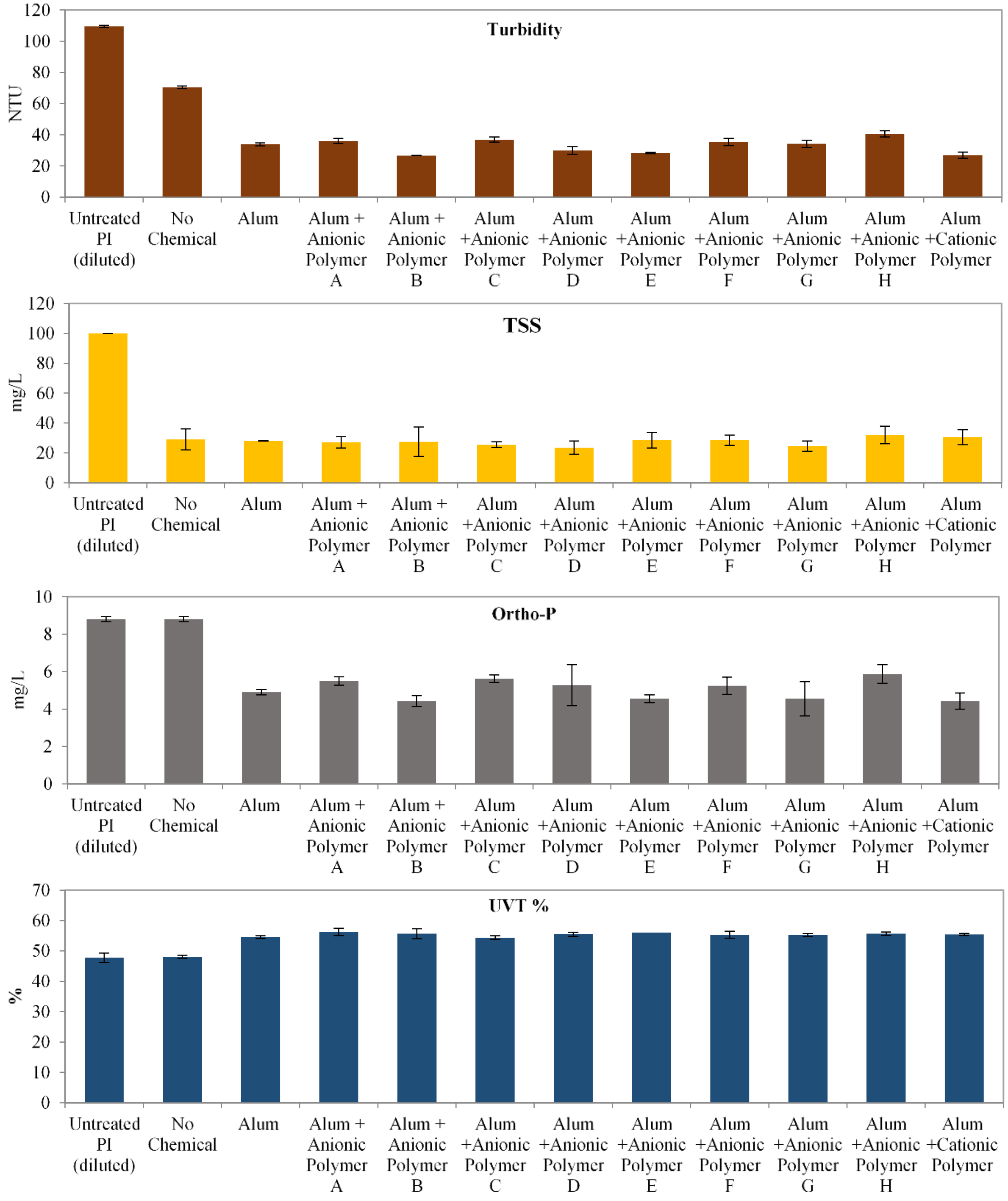

Figure 3. 4 Effect of polymer addition on turbidity, TSS, ortho-P and % UVT (applied alum dose is 75 mg /L and polymer dose is 0.75 mg/L).

The addition of anionic polymer was further evaluated, and the experiments were limited to polymer A which the WWTP was using in its operations at the time of this study. Thus, alum was applied with and without polymers A, (in doses ranging between 25/0.25 and 150/1.5 mg/L as alum/polymer (mg/L)) during a jar test and samples were analyzed for turbidity, TSS and ortho-P removal (Figure 3.5). With mixing only and no chemical addition, turbidity and TSS were significantly reduced compared to ortho-P. Adding alum only without polymers led to better removals compared to adding alum with a polymer which is in line with findings from another study (Aguilar et al. 2005). An average alum dose of 75 mg/L achieved the target EPT effluent TSS value set by the WWTP (30 mg/L). Increasing the doses of alum and polymer did not efficiently improve the removals as samples treated with 125:1.25 alum/polymer could barely reach a final TSS value close to 30 mg/L. This may be referred to a mechanism of re-stabilization of particles in suspension due to the tremendous increase in the positively charged aluminum species (Saritha et al. 2017).

The removal of ortho-P is usually influenced by the wastewater quality including: initial ortho-P concentration, TSS, and pH, in addition to the type and dose of chemical added, and mixing conditions (Hussain et al. 2011). The pH of all tested samples was between 7.13 and 7.22 without adjustment, which is the optimum pH for ortho-P removal by alum and iron-based coagulants. During the coagulation process, different aluminum and phosphate complexes are formed under specific pH values. It is reported that phosphorus adsorbs onto the hydrolysis products of the metal-based coagulants, this chemisorption results in precipitates that separate easily from the liquid. Changes in the pH can affect the favorable conditions for the formation of phosphate-aluminum complexes and the adsorption and desorption mechanisms (Smoczynski et al. 2014). The solubility diagram of aluminum hydroxide shows that pH dictates the form of hydrolysis products which are positively charged at low pH and negatively charged at high pH. It was found that the favorable pH for ortho-P removal by precipitation of aluminum phosphate ($AlPO_4$) is between 6 and 8 (David

Jenkins and Menar 1970). In this study, the removal of ortho-P was noticed to improve when higher chemical doses were applied; however less improvement was observed when alum doses exceeded 125 mg/L (Figure 3.5). Moreover, the application of anionic polymer might be hindering the removal of ortho-P as alum alone was able to achieve better removal.

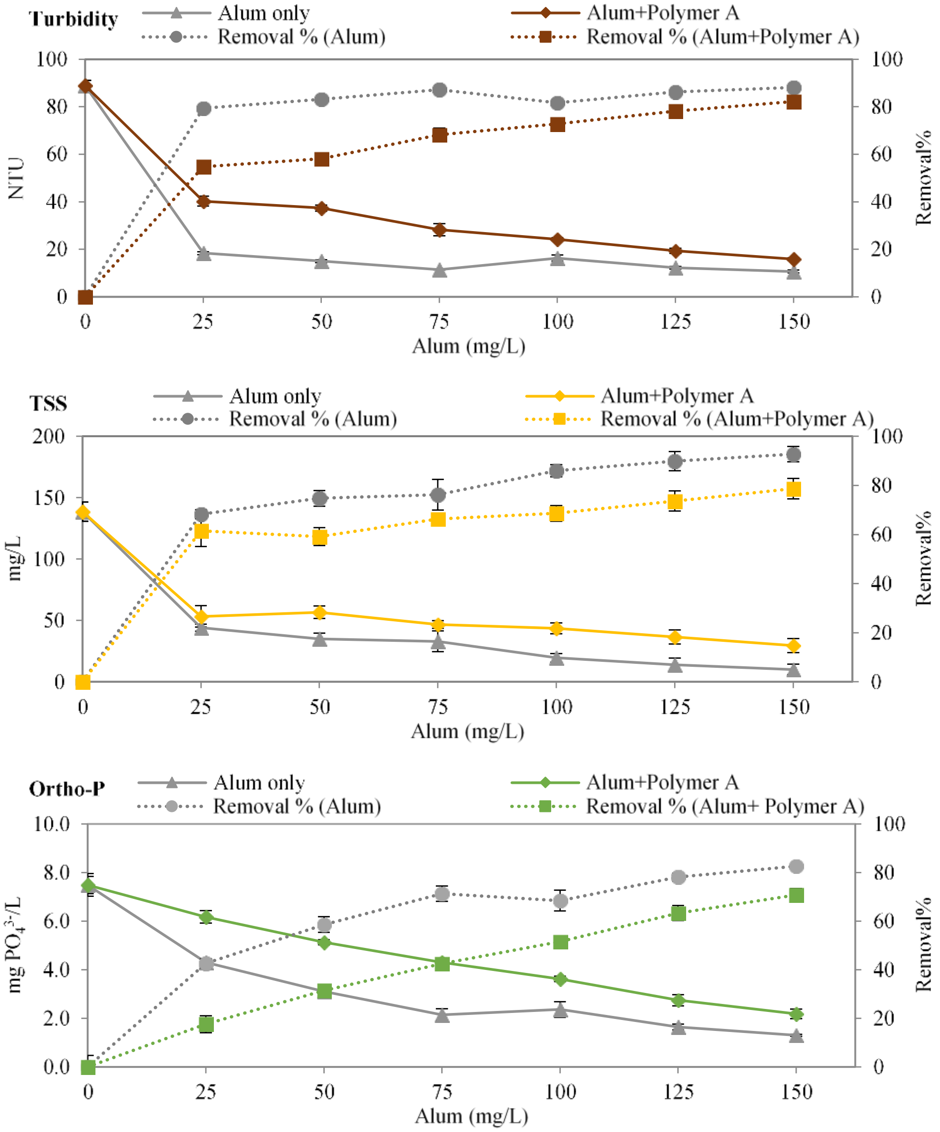

Figure 3. 5 Impact of alum dose applied with anionic polymer A in a fixed dose ratio of 100:1 (as alum: polymer in mg/L) on the removal of turbidity, TSS and Ortho-P.

3.3.5 Effect of alum and polymer addition during full-scale application

A detailed description of water quality parameters in the influent and effluent of the WWTP is available in Table A.6. The initial TSS values for all events from the full-scale application ranged from 168 to 296 mg/L. As shown in Figure 3.6, the results of coagulant addition were in line with the findings from the jar test confirming that 100 mg/L of alum was capable of achieving the target TSS design value (30 mg/L). In fact, this is expected since the primary clarifier is provided with lamella plate settlers to maximize the removal of suspended solids. Moreover, better removal was achieved with the lower dose of alum: polymer A 75/0.75 mg/L when the initial TSS was less than 200 mg/L. Yet, when initial TSS exceeded 200 mg/L, the same alum dose of 75 mg/L was unable to achieve the required removal even when increasing the polymer dose to 1.1 mg/L. It is therefore preferable to adjust the alum dose when the TSS values in the incoming PI are higher than 200 mg/L. Pollutant removals induced by the application of chemicals were evaluated against removals under the effect of lamella plate settlers (indicated by "No chemicals" in Fig.3.6). Results showed that the chemical addition is crucial for ortho-P reduction whereas the effect of lamella settler alone was almost null because ortho-P removal is mainly associated with precipitation (Gasperi et al. 2010, Mohammed and Shanshool 2009). However, there was a noticeable reduction in TSS and turbidity where the main mechanism of removal is settling. In some cases, the effects of lamella settler on TSS reduction were comparable with the values obtained when chemicals were added. These findings are comparable to those reported by the effect of mixing only in the jar tests.

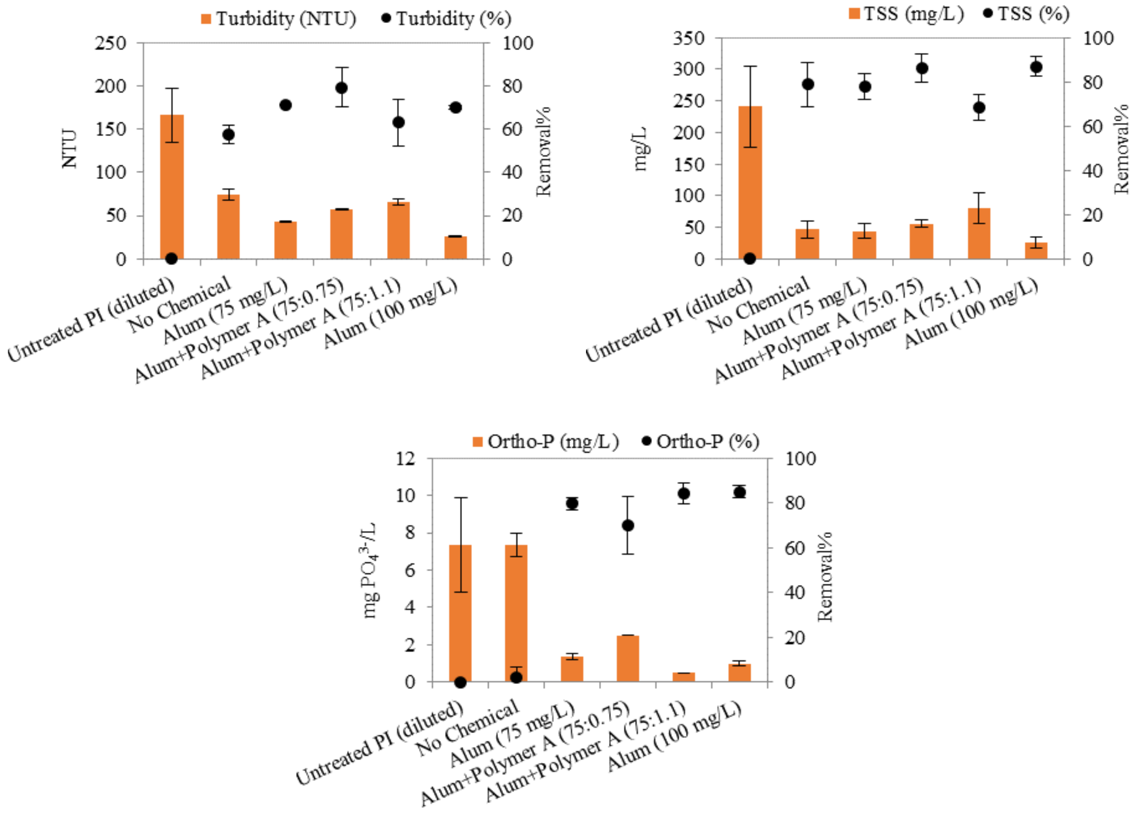

Figure 3. 6 Removal of turbidity, TSS and ortho-P during the full-scale application of alum and alum + polymer A.

There are multiple physical and chemical factors affecting the process of coagulation/flocculation such as the dose and type of chemical and its application point, reactor type, background effects and mixing intensities and times. In fact, it is possible to compare bench -scale with full-scale experiments by using the mean velocity gradient G or Gt values assuming the mixing environments will be the same under constant G or Gt (Cornwell and Bishop 1983). Yet, during the jar tests, both chemicals were simultaneously added at the beginning of rapid mixing with known mixing intensities while during full-scale operation, the coagulant is mixed with the inflow to the coagulation tank and the polymer is mixed later with the outflow into the flocculation chamber. In addition, on either scale the temperature was not controlled, it varied between 5 and 20°C at full scale while room temperature was maintained during jar tests. Indeed, the comparison between bench and full-scale was strictly based upon the chemical addition. So, although the jar test could not mimic the exact operation conditions, our results acquired from bench-scale experiments were comparable to the results of the full-scale operation in terms of contaminants removals on a mass basis (Figure 3.7). Bench-scale data showed that polymer addition had no impact on the removal of tested parameters while at full-scale polymer addition showed slight improvement (Figures 3.5&3.6). That might be ascribed to the discrepancy in the addition point of polymer in which at bench-scale the polymer was added simultaneously with coagulant at the beginning of rapid mixing while at full-scale the polymer was added at the beginning of slow mixing. The effects of polymer addition point was not covered in this study and that might be considered in future work.

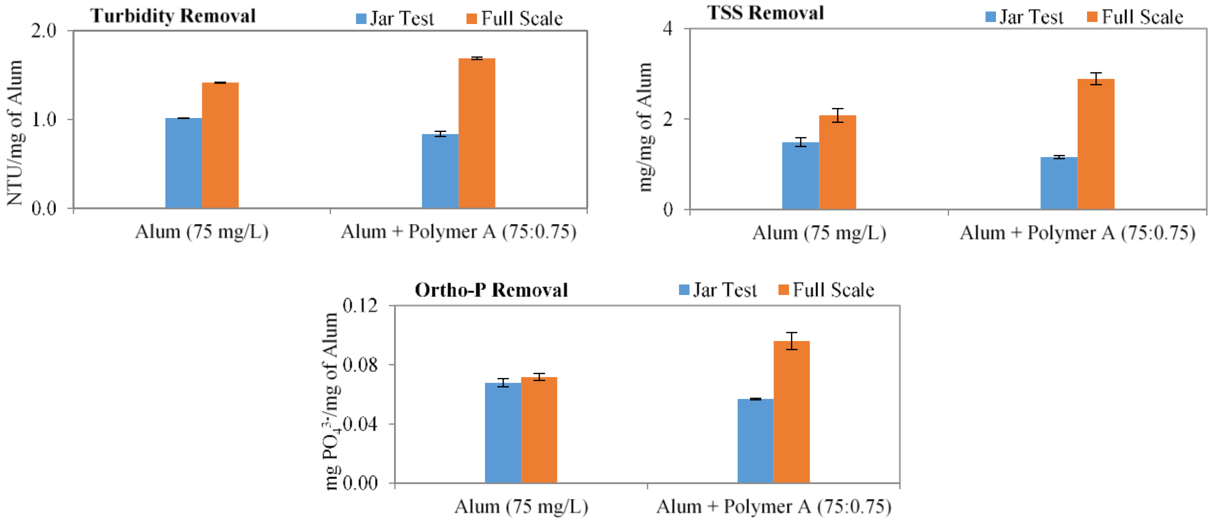

Figure 3. 7 Comparison between bench-scale and full-scale applications of 75 mg/L alum only and 75 mg/L alum + 0.75 mg/L polymer for the removal of turbidity, TSS and ortho-P.

3.3.6 Effective parameters for online process control

Investigating the correlation between different wastewater parameters is technically and economically beneficial. According to Ratnaweera and Fettig (2015), pH, turbidity, TSS, UVA and ortho-P are relevant parameters to evaluate the coagulation/flocculation/sedimentation process, and they are typically monitored by online sensors. Ortho-P is occasionally measured to monitor the influent and effluent quality. For these reasons, correlations between the different parameters were studied to investigate downsizing the analysis to the most effective parameter for online process control.

Results obtained from the full-scale analysis revealed no strong association between the influent flow rate and any of the measured parameters. So, the flow rate cannot be a reliable indicator for process control. Also, besides the redundant correlation between TSS and turbidity, there was a strong correlation between % UVT and ortho-P (Figure 3.8). This signifies that measuring turbidity and UVA during operation can help predict rough estimates of TSS and ortho-P and adjust the required coagulant dose without the hassle of multiple sample analyses. This is known as a feed-forward control scheme where the quality of the influent is monitored to adjust the chemical dosing. (Ratnaweera and Fettig 2015). Mass removal ratios can be used here to approximate the required coagulant dose.

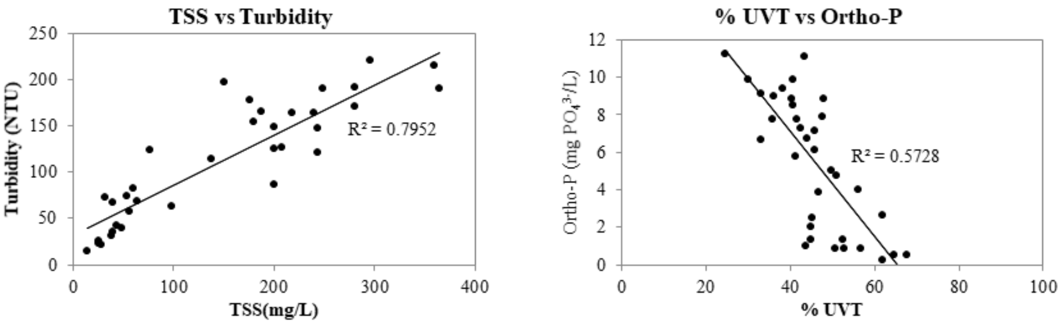

Figure 3. 8 Correlations between contaminants measured at the full-sale level.

At the bench-scale level, our results showed a good correlation between turbidity and TSS, TSS and COD, and COD and ortho-P (Figure 3.9). The strongest linear correlations were between turbidity and TSS at both full-scale and bench-scale levels, where the R^2 values were 0.80 and 0.85 respectively (Figures 3.8&3.9). These results comply with those obtained by Grayson et al. (1996)

who studied the correlation between turbidity and TSS and turbidity and total phosphorus in samples collected from a river catchment area and identified strong linear correlations with R^2 values of 0.86 and 0.90, respectively. It is noteworthy that the strength of such correlations is site-specific and changes according to the tested wastewater matrix (Hannouche et al. 2011). Nevertheless, more data is essential to reduce the uncertainty and validate those correlations.

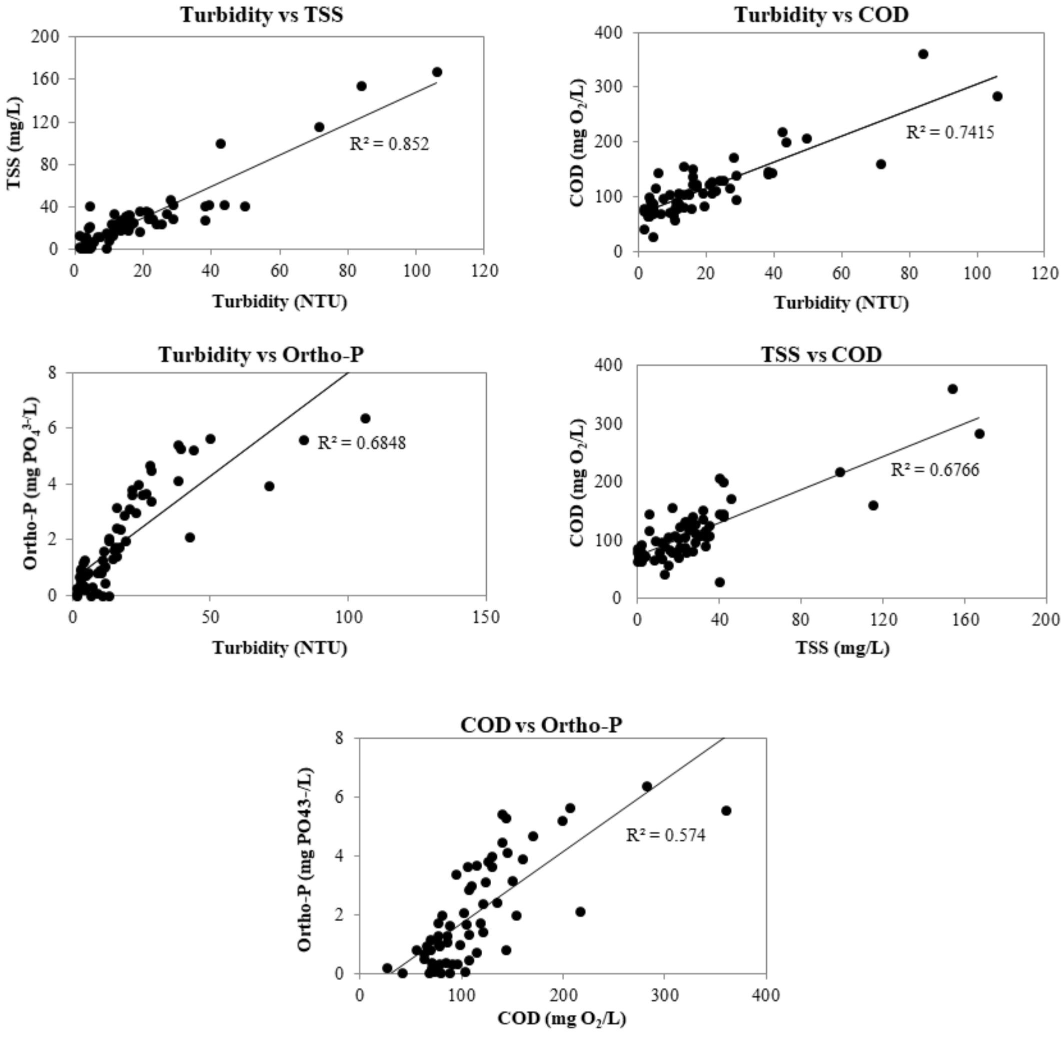

Figure 3. 9 Correlations between contaminants measured at bench-scale level.

3.3.7 Implications of these removals on the monitoring of micropollutants

As discussed previously, CSOs are a considerable source of micropollutants. So, in order to assess the overall efficiency of the EPT and the need for any additional treatment, it is important to monitor not only conventional pollutants, but also micropollutants of concern. Thus, in order to estimate the elimination of MPs during EPT, the correlation between differential UVA_{254} (ΔUVA_{254}) and removal of MPs was surveyed from different studies. In the present study we project that UVA can serve not only for process control, but also as a surrogate parameter to estimate the removal of micropollutants during the EPT of CSO. Micropollutants removal correlates with ΔUVA_{254}in advanced oxidation and adsorption processes where an increase in ΔUVA_{254} is associated with higher removal of trace organics reaching up to 95% depending on the chemical structure and properties of the compound (Altmann et al. 2016, Altmann et al. 2015, Ning et al. 2007, Sui et al. 2010, Zhang et al. 2015, Ziska et al. 2016). In coagulation/flocculation/sedimentation processes, UVA_{254} was found to be an accurate surrogate parameter for trihalomethane formation in alum-treated waters (Pifer and Fairey 2014). In the current study, ΔUVA_{254} ranged between 15% and 40% with the use of 75 mg/L alum at the bench and full-scale levels. This range can be associated with up to complete removal of some trace organics by ozonation (Chys et al. 2017). In this WWTP final effluent, Shu et al. (2013) and Kerr et al. (2008) reported on the occurrence of some micropollutants such as carbamazepine, diclofenac, ibuprofen, gemfibrozil, mecoprop, diazinon and others at varying concentrations. In contrast, CSO contributes up to 10% of the total discharged load of trace organic compounds with low removal efficiency in a WWTP and up to 90% of those with high removal efficiency (Phillips et al. 2012). As such, we anticipate that the EPT of CSO can still achieve some removal of those compounds that have low water solubility, which entails hydrophobic interactions and sorption onto particulate matter (Margot et al. 2015). Other hydrophilic compounds can also aggregate with metal ions during the treatment with alum. Alum treatment can as such remove up to 75% of some micropollutants (Kim and Zoh 2016) which can translate in higher ΔUVA_{254}. Moreover, the removal of selected MPs by different oxidants will be investigated extensively in other phases of this study.

3.3.8 Recommended future interventions

The local municipality projects that by 2020, the WWTP would contribute around 10% of the total TSS loading to the adjacent river among which 10 % (2700 Kg/d) would be attributed to the EPT effluent (at a concentration of 30 mg/L) compared to 72% to the final effluent (at a concentration of 7 mg/L) and 18% to the combined bypasses. Thus, the EPT was put under the Combined Sewer Overflow Control Strategy set by the city to control the discharges into the river (City-of-Edmonton 2009). Despite prioritizing TSS, several macro and micropollutants can implicate detrimental effect to the environment receiving the EPT effluent. It is believed that the discharge of CSO cumulatively increases the level of *E. coli* in the aquatic environment by 0.5 to 2 log (Madoux-Humery et al. 2016). The disinfection of CSOs was effectively achieved by ultraviolet irradiation (Tondera et al. 2015, Wojtenko et al. 2001a), ozone (Tondera et al. 2015, Wojtenko et al. 2001b), performic acid (Chhetri et al. 2015, Chhetri et al. 2014, Tondera et al. 2016), and peracetic acid (Chhetri et al. 2016, Chhetri et al. 2014, Coyle et al. 2014). Therefore, further polishing steps will be required for disinfection and oxidation purposes to minimize the environmental impact of the EPT effluent.

3.4 Conclusions

This study provided a practical solution for the enhanced primary treatment of municipal primary influent under wet weather conditions and proposed the best parameters for online process control. It demonstrated that alum is the best coagulant for the EPT. In fact, alum and PACl were both capable of maximizing the removal of major macropollutants under different mixing scenarios. However, the former had the advantage of cost efficiency and was therefore considered for further optimization. A dose of 75 mg/L alum (6 mg/L Al) without any polymer was guaranteed to achieve the target levels of TSS and reduce turbidity by 87% and ortho-P by 71%.

Overall, bench and full-scale applications of coagulant and coagulant aid, despite their dissimilarities, unveiled comparable results especially for turbidity and TSS removal. The role of temperature in the overall optimization of the treatment process can be further investigated particularly where major seasonal and diurnal fluctuations are forecasted. The removal of macropollutants presented in this study correlated with that of micropollutants can serve as a guide for additional treatment with a small footprint and high efficiency in order to refine the EPT of CSO. This treatment should consider sustainable options for disinfection and oxidation.

3.5 References

Afzal, A., Pourrezaei, P., Ding, N., Moustafa, A., Hwang, G., Drzewicz, P., Kim, E.S., Pérez-Estrada, L.A., Chelme-Ayala, P., Liu, Y. and Gamal-El-Din, M. (2011) Physico-Chemical Processes. Water Environ. Res. 83(10), 994-1091.

Aguilar, M.I., Saez, J., Llorens, M., Soler, A., Ortuno, J.F., Meseguer, V. and Fuentes, A. (2005) Improvement of coagulation-flocculation process using anionic polyacrylamide as coagulant aid. Chemosphere 58(1), 47-56.

Altmann, J., Massa, L., Sperlich, A., Gnirss, R. and Jekel, M. (2016) UV_{254} absorbance as real-time monitoring and control parameter for micropollutant removal in advanced wastewater treatment with powdered activated carbon. Water Res 94, 240-245.

Altmann, J., Zietzschmann, F., Geiling, E.-L., Ruhl, A.S., Sperlich, A. and Jekel, M. (2015) Impacts of coagulation on the adsorption of organic micropollutants onto powdered activated carbon in treated domestic wastewater. Chemosphere 125.

Anderson, M.J. (2015) Design of Experiments Simplified, Boca Raton, FL: CRC Press is an imprint of the Taylor & Francis Group, an Informa business.

APHA (2012) Standard Methods for the Examination of Water and Wastewater, APHA, AWAA, WEF, Washington, DC.

Arlos, M.J., Braggb, L.M., Servos, M.R. and Parker, W.J. (2014) Simulation of the fate of selected pharmaceuticals and personal care products in a highly impacted reach of a Canadian watershed. Science of the Total Environment, 193-204.

Baghvand, A., Zand, A.D., Mehrdadi, N. and Karbassi, A. (2010) Optimizing coagulation process for low to high turbidity waters using aluminum and iron salts. American Journal of Environmental Sciences 6(5), 442-448.

Canada, E. (2019) Municipal Wastewater Status in Canada.

Cao, B., Gao, B., Xu, C., Fu, Y. and Liu, X. (2010) Effects of pH on coagulation behavior and floc properties in Yellow River water treatment using ferric based coagulants. Chinese Science Bulletin 55(14), 1382-1387.

Chelme-Ayala, P., Afzal, A., Ding, N., Moustafa, A.M.A., Pourrezaei, P., Alpatova, A., Drzewicz, P., Hwang, G., Kim1, E.-S., Liu, Y. and Gamal-El-Din, M. (2012) Physico-Chemical Processes. Water Environ. Res. 84(10), 971-1028.

Chelme-Ayala, P., Gamal-El-Din, M., R., R.S. and Leonard, C. (2011) Advanced treatment of liquid swine manure using physico-chemical treatment. J. Hazard. Mater. 186, 1632-1638.

Chhetri, R.K., Bonnerup, A. and Andersen, H.R. (2016) Combined Sewer Overflow pretreatment with chemical coagulation and a particle settler for improved peracetic acid disinfection. Journal of Industrial and Engineering Chemistry 37, 372-379.

Chhetri, R.K., Flagstad, R., Munch, E.S., Hørning, C., Berner, J., Kolte-Olsen, A., Thornberg, D. and Andersen, H.R. (2015) Full scale evaluation of combined sewer overflows disinfection using performic acid in a sea-outfall pipe. Chemical Engineering Journal 270, 133-139.

Chhetri, R.K., Thornberg, D., Berner, J., Gramstad, R., Ojstedt, U., Sharma, A.K. and Andersen, H.R. (2014) Chemical disinfection of combined sewer overflow waters using performic acid or peracetic acids. Sci Total Environ 490, 1065-1072.

Chys, M., Audenaert, W.T.M., Deniere, E., Mortier, S.v.T.r.s.F.C., Langenhove, H.V., Nopens, I., Demeestere, K. and Hulle, S.W.H.V. (2017) Surrogate-Based Correlation Models in View of Real-Time Control of Ozonation of Secondary Treated Municipal Wastewater - Model Development and Dynamic Validation. Environmental Science and Technology 51, 14233-14243.

City-of-Edmonton (2009) City of Edmonton Total Loadings Plan City of Edmonton Edmonton.

Cornwell, D.A. and Bishop, M.M. (1983) Determining velocity gradients in laboratory and full-scale systems. American Water Works Association Journal 75(9), 470-475.

Coyle, E.E., Ormsbee, L.E. and Brion, G.M. (2014) Peracetic Acid as an Alternative Disinfection Technology for Wet Weather Flows. Water Environment Research 86(8), 687-697.

CWN (2018) Canada’s Challenges and Opportunities to Address Contaminants in Wastewater Supporting Document 2

Wastewater Treatment Practice and Regulations in Canada and Other Jurisdictions, Environment and Climate Change Canada.

David Jenkins, J.F.F., And Arnold and Menar, B. (1970) Review Paper:Chemical Processes for Phosphate Removal, pp. 369-389., Water Research Pergamon Press.

Dempsey, B.A., Sheu, H., Tanzeer Ahmed, T.M.T. and Mentink, J. (1985) Polyaluminum Chloride and Alum Coagulation of Clay-Fulvic Aicd Suspensions. American Water Works Association 77(3), 74-80.

Ebeling, J.M. and Ogden, S.R. (2004) Application of chemical coagulation aids for the removal of suspended solids (TSS) and phosphorus from the microscreen effluent discharge of an intensive recirculating aquaculture system. North American Journal of Aquaculture 66(3), 198-207.

El Samrani, A.G., Lartiges, B.S. and Villieras, F. (2008a) Chemical coagulation of combined sewer overflow: heavy metal removal and treatment optimization. Water Res 42(4-5), 951-960.

El Samrani, A.G., Lartiges, B.S. and Villieras, F. (2008b) Chemical coagulation of combined sewer overflow: Heavy metal removal and treatment optimization. Water Research 42(4-5), 951-960.

Exall, K. and Marsalek, J. (2013) A Coagulant Survey for Chemically Enhanced Primary Treatment of Synthetic CSOs. Water Air and Soil Pollution 224(2), 9.

Gasperi, J., Garnaud, S., Rocher, V. and Moilleron, R. (2008) Priority pollutants in wastewater and combined sewer overflow. Sci Total Environ 407(1), 263-272.

Gasperi, J., Rocher, V., Gilbert, S., Azimi, S. and Chebbo, G. (2010) Occurrence and removal of priority pollutants by lamella clarification and biofiltration. Water Research 44(10), 3065-3076.

Gibson, J., Farnood, R. and Seto, P. (2016) Chemical pretreatment of combined sewer overflows for improved UV disinfection. Water Sci Technol 73(2), 375-381.

Grayson, R.B., Finlayson, B.L., Gippel, C.J. and Hart, B.T. (1996) The potential of field turbidity measurements for the computation of total phosphorus and suspended solids loads. Journal of Environmental Management 47(3), 257-267.

Guida, M., Mattei, M., Della Rocca, C., Melluso, G. and Meric, S. (2007) Optimization of alum-coagulation/flocculation for COD and TSS removal from five municipal wastewater. Desalination 211(1-3), 113-127.

Hannouche, A., Chebbo, G., Ruban, G., Tassin, B., Lemaire, B.J. and Joannis, C. (2011) Relationship between turbidity and total suspended solids concentration within a combined sewer system. Water Science and Technology 64(12), 2445-2452.

Hussain, S., Aziz, H.A., Isa, M.H., Ahmad, A., Van Leeuwen, J., Zou, L., Beecham, S. and Umar, M. (2011) Orthophosphate removal from domestic wastewater using limestone and granular activated carbon. Desalination 271(1-3), 265-272.

Jalliffier-Verne, I., Leconte, R., Huaringa-Alvarez, U., Madoux-Humery, A.S., Galarneau, M., Servais, P., Prevost, M. and Dorner, S. (2015) Impacts of global change on the concentrations and dilution of combined sewer overflows in a drinking water source. Science of the Total Environment 508, 462-476.

Jiang, J.K. and Graham, N.J.D. (2010) Enhanced Coagulation Using Al/Fe(III) Coagulants: Effect of Coagulant Chemistry on the Removal of Colour-Causing NOM. Environmental Technology 17, 937-950.

Johnson, A.C. and Williams, R.J. (2004) A Model To Estimate Influent and Effluent Concentrations of Estradiol, Estrone, and Ethinylestradiol at Sewage Treatment Works. Environmental Science and Technology 38, 3649-3658.

Jung, C., Oh, J. and Yoon, Y. (2015) Removal of acetaminophen and naproxen by combined coagulation and adsorption using biochar: influence of combined sewer overflow components. Environ Sci Pollut Res Int 22(13), 10058-10069.

Kay, P., Hughes, S.R., Ault, J.R., Ashcroft, A.E. and Brown, L.E. (2016) Widespread, routine occurrence of pharmaceuticals in sewage effluent, combined sewer overflows and receiving waters. Environmental Pollution 220, 1447e1455.

Kerr, J.L., Guo, Z., Smith, D.W., Goss, G.G. and Belosevic, M. (2008) Use of goldfish to monitor wastewater and resue water for xenobiotics. Journal of Environmental Engineering and Science 7.

Kim, M.-K. and Zoh, K.-D. (2016) Occurrence and removals of micropollutants in water environment. Environmental Engineering Research 21(4), 319-332.

Launay, M.A., Dittmer, U. and Steinmetz, H. (2016) Organic micropollutants discharged by combined sewer overflowseCharacterisation of pollutant sources and stormwater-related processes. Water Res 104, 82-92.

Li, J.G., Dhanvantari, S., Averill, D. and Biswas, N. (2003) Windsor combined sewer overflow treatability study with chemical coagulation. Water Quality Research Journal of Canada 38(2), 317-334.

Li, J.G., Horneck, H., Averill, D., McCorquodale, J.A. and Biswas, N. (2004) High-Rate Retention Treatment Basins for CSO Control in Windsor, Ontario. Water Quality Research Journal of Canada 39(4), 449–456.

Madoux-Humery, A.S., Dorner, S., Sauve, S., Aboulfadl, K., Galarneau, M., Servais, P. and Prevost, M. (2016) The effects of combined sewer overflow events on riverine sources of drinking water. Water Res 92, 218-227.

Margot, J., Rossi, L., Barry, D.A. and Holliger, C. (2015) A review of the fate of micropollutants in wastewater treatment plants. Wiley Interdisciplinary Reviews: Water 2(5), 457-487.

Mohammed, S. and Shanshool, H.A. (2009) Phosphorus Removal from Water and Waste Water by Chemical Precipitation Using Alum and Calcium Chloride.

Mutzner, L., Staufer, P. and Ort, C. (2016) Model-based screening for critical wet-weather discharges related tomicropollutants from urban areas. Water Res 104.

Ning, B., Graham, N., Zhang, Y., Nakonechny, M. and Gamal El-Din, M. (2007) Degradation of Endocrine Disrupting Chemicals by Ozone/AOPs. Ozone: Science & Engineering 29(3), 153-176.

Phillips, P.J., Chalmers, A.T., Gray, J.L., Kolpin, D.W., Foreman, W.T. and Wall, G.R. (2012) Combined sewer overflows: an environmental source of hormones and wastewater micropollutants. Environ Sci Technol 46(10), 5336-5343.

Pifer, A.D. and Fairey, J.L. (2014) Suitability of Organic Matter Surrogates to Predict Trihalomethane Formation in Drinking Water Sources. Environemntal Engineering Science 31.

Pourrezaei, P., Afzal, A., Ding, N., Islam, M.S., Moustafa, A., Drzewicz, P., Chelme-Ayala, P. and Gamal-El-Din, M. (2010) Physico-Chemical Processes. Water Environ. Res. 82(10), 997-1072.

Pourrezaei, P., Drzewicz, P., Wang, Y., Gamal-El-Din, M., Perez-Estrada, L.A., Martin, J.W., Anderson, J., Wiseman, S., Liber, K. and Giesy, J.P. (2011) The Impact of Metallic Coagulants on the Removal of Organic Compounds from Oil Sands Process-Affected Water. Environ. Sci. Technol. 45(19), 8452-8459.

Ratnaweera, H. and Fettig, J. (2015) State of the Art of Online Monitoring and Control of the Coagulation Process. Water 7(11), 6574-6597.

Ryu, J., Oh, J., Snyder, S.A. and Yoon, Y. (2014) Determination of micropollutants in combined sewer overflows and their removal in a wastewater treatment plant (Seoul, South Korea). Environ Monit Assess 186(5), 3239-3251.

Saritha, V., Srinivas, N. and Vuppala, S. (2017) Analysis and optimization of coagulation and flocculation process. Applied Water Science 7, 451-460.

Sarkar, S., Kamilya, D. and Mal, B.C. (2007) Effect of geometric and process variables on the performance of inclined plate settlers in treating aquacultural waste. Water Res 41, 993-1000.

Shu, Z., Bolton, J.R., Belosevic, M. and Gamal-El-Din, M. (2013) Photodegradation of emerging micropollutants using the medium-pressure UV/H_2O_2 Advanced Oxidation Process. Water Res 47, 2881-2889.

Shu, Z., Singh, A., Klamerth, N., McPhedran, K., Bolton, J.R., Belosevic, M. and Gamal-El-Din, M. (2016) Pilot-Scale UV/H2O2 Advanced Oxidation Process for Municipal Reuse Water: Assessing Micropollutant Degradation and Estrogenic Impacts on Goldfish (Carassius auratus L.). Water Res 101, 157-166.

Smoczynski, L., Munska, K.T., Kosobucka, M. and Pierozynski, B. (2014) Phosphorus and COD Removal from Chemically and Electrichemically Coagualated Wastewater. Environmental Protection ENgineering 40(3), 63-73.

Sui, Q., Huang, J., Deng, S., Yu, G. and Fan, Q. (2010) Occurrence and removal of pharmaceuticals, caffeine and DEET in wastewater treatment plants of Beijing, China. Water Res 44(2), 417-426.

Tolouei, S., Jean-Baptiste Burneta, Autixiera, L., Taghipoura, M., Bonsteelb, J., Duy, S.V., Sauve, S., Prevost, M. and Dorner, S. (2019) Temporal variability of parasites, bacterial indicators, and wastewatermicropollutants in a water resource recovery facility under variousweather conditions. Water Res 148, 446-458.

Tondera, K., Klaer, K., Gebhardt, J., Wingender, J., Koch, C., Horstkott, M., Strathmann, M., Jurzik, L., Hamza, I.A. and Pinnekamp, J. (2015) Reducing pathogens in combined sewer overflows using ozonation or UV irradiation. Int J Hyg Environ Health 218(8), 731-741.

Tondera, K., Klaer, K., Koch, C., Hamza, I.A. and Pinnekamp, J. (2016) Reducing pathogens in combined sewer overflows using performic acid. Int J Hyg Environ Health 219(7 Pt B), 700-708.

Trinh, T.K. and Kang, L.S. (2015) Coagulation of phosphorus: effects of Al(III) species (Al-a, Al-b, and Al-c). Desalination and Water Treatment 53(2), 485-492.

USEPA (2018) Combined Sewer Overflows (CSOs).

Wang, C., Alpatova, A., McPhedran, K.N. and Gamal-El-Din, M. (2015a) Coagulation/flocculation process with polyaluminum chloride for theremediation of oil sands process-affected water: Performance andmechanism study. J. Environ. Manage. 160, 254-262.

Wang, W., Xu, Z., Li, H. and Jin, W. (2015b) Optimization of coagulation–flocculation process for combined sewer overflow wastewater treatment using response surface methodology. Desalination and Water Treatment 57(32), 14824-14832.

Wei, N., Zhang, Z.G., Liu, D., Wu, Y., Wang, J. and Wang, Q.H. (2015) Coagulation behavior of polyaluminum chloride: Effects of pH and coagulant dosage. Chinese Journal of Chemical Engineering 23(6), 1041-1046.

Wojtenko, I., Stinson, M.K. and Field, R. (2001a) Challenges of Combined Sewer Overflow Disinfection by Ultraviolet Light Irradiation. Critical Reviews in Environmental Science and Technology 31(3), 223-239.

Wojtenko, I., Stinson, M.K. and Field, R. (2001b) Performance of Ozone as a Disinectant for Combined Sewer Overflow. Critical Reviews in Environmental Science and Technology 31(4), 295-309.

Young, S., Stanley, S.J. and Smith, D.W. (2000) Effect of mixing on the kinetics of polymer-aided flocculation. Journal of Water Services Research and Technology-Aqua 49(1), 1-8.

Yu, W.-z., Gregory, J., Campos, L. and Li, G. (2011) The role of mixing conditions on floc growth, breakage and re-growth. Chemical Engineering Journal 171(2), 425-430.

Yu, W., Li, G., Xu, Y. and Yang, X. (2009) Breakage and re-growth of flocs formed by alum and PACl. Powder Technology 189(3), 439-443.

Yukselen, M.A. and Gregory, J. (2004) The effect of rapid mixing on the break-up and re-formation of flocs. Journal of Chemical Technology & Biotechnology 79(7), 782-788.

Zhang, K., Deletic, A., Page, D. and McCarthy, D.T. (2015) Surrogates for herbicide removal in stormwater biofilters. Water Res 81, 64-71.

Zhou, Y., Liang, Z. and Wang, Y. (2008) Decolorization and COD removal of secondary yeast wastewater effluents by coagulation using aluminum sulfate. Desalination 225(1-3), 301-311.

Zhu, K., Gama-El-Din, M., Moawad, A.K. and Bromley, D. (2010) Physical and Chemical Processes for Removing Suspended Solids and Phosphorus from Liquid Swine Manure. Environmental Technology 25(10), 1177-1187.

Zhu, W., Seth, R. and Lalman, J. (2007) Evaluation of a micro carrier weighted coagulation flocculation process for the treatment of combined sewer overflow. Environmental Technology 28(7), 761-770.

Ziska, A.D., Park, M., Anumol, T. and Snyder, S.A. (2016) Predicting trace organic compound attenuation with spectroscopic parameters in powdered activated carbon processes. Chemosphere 156, 163-171.

Chapter 4: Enhanced Primary Treatment during Wet Weather Flow Condition Using Ferrate as a Coagulant, Coagulant Aid and Disinfectant

4.1 Introduction

Ideally, sewage drainage and stormwater drainage are disconnected for better management and treatment of both water types. However, some cities in the United States, Canada and Europe have combined sewer systems, where the sewage drainage and stormwater drainage are combined. Most of the wastewater treatment plants (WWTPs) are not adapted to treat the high volumes of influent wastewater during wet weather flow (WWF) (Phillips et al., 2012). In Canada, as of 2016, the total numbers of combined sewer systems were 269. They discharged 120 million m^3 of wet weather flow (WWF) wastewater in receiving water bodies (e.g. rivers, lakes) without proper treatment according to Environment and Climate Change Canada (ECCC, 2019a). In Alberta, there is only one combined sewer system which discharges an annual average of 5.4 million m^3 of WWF wastewater to the surface water (ECCC, 2019b). This practice tremendously increases the contaminants' levels (bacteria, inorganic/organic matter, heavy metals, PAHs) in surface waters thus endangers the aquatic lives and beneficiaries (Gromaire et al., 2001; Marsalek and Rochfort, 2004). Therefore, to minimize the impact of WWF, many approaches have been used such as constructed wetlands, rain gardens, real-time gate control, and enhanced primary treatment (EPT) (Autixier et al., 2014; Lucas and Sample, 2015; Tao et al., 2014). EPT is easier to retrofit where chemical intervention (i.e. coagulation/flocculation) is used to destabilize organic and solid contents, which are subsequently removed by sedimentation. For instance, a cationic polymer with alum and silica micro-sand were employed for treating WWF wastewater and removed 98% of the total suspended solids (TSS) (Zhu et al., 2007). Furthermore, it was reported that alum and ferric chloride were used along with lamella plate settlers for treating WWF wastewater and removed 80%, 60%, 85% and 75% of TSS, chemical oxygen demand (COD), total phosphorous and heavy metals, respectively (El Samrani et al., 2008). Nonetheless, the aforementioned techniques for treating WWF wastewater might fail to achieve target levels of microbial reduction thus exploring new approaches becomes more essential.

Ferrate ($\mathrm{FeO_4^{2-}}$) has emerged as a multifunctional compound that acts as both an oxidant/disinfectant and a coagulant with the highest reduction potential (2.2 V) among the non-radical oxidants (Amano et al., 2018; Cho et al., 2006; Gandhi et al., 2014). In fact, ferrate has been classified as an environmentally friendly compound of the non-toxic final reduced form of ferric oxide/hydroxide which could act as a coagulant (Yates et al., 2014). As such, ferrate has been proposed as a suitable chemical to treat the wastewater during WWF condition.

Many studies examined ferrate as an oxidant, disinfectant and coagulant in pure water, drinking water and wastewater matrices (Goodwill et al., 2015; Karlesa et al., 2014; Lan et al., 2016; Sharma, 2011; Xu et al., 2007; Yu et al., 2013). For instance, ferrate (8 to 15 mg/L Fe) was applied in secondary effluent where it removed 80% of COD, and 99.9% of total coliform (Jiang and Lloyd, 2002). For primary influent wastewater, ferrate (<1 mg/L Fe) surpassed ferric chloride and removed 60% of TSS ($C_o = 432 \pm 169$ mg/L), 40% of total phosphorus (TP) ($C_o = 14.3\pm3.6$ mg/L) and 80% of COD ($C_o = 946 \pm 307$ mg/L) (Stanford et al., 2010). Moreover, ferrate (3 mg/L Fe) removed 16% of dissolved organic carbon (DOC) (C_o= 4.43 mg/L) in surface water at pH = 5.8 (Song et al., 2016).

Ferrate is also a strong disinfectant and has demonstrated high biocidal effects against different microorganisms such as total coliform, fecal coliform, *Escherichia coli (E. coli), Giardia* and *Cryptosporidium* (Gombos et al., 2013; Jiang, 2014; Makky et al., 2011; Sharma et al., 2016). In secondary wastewater effluent, ferrate (5 mg/L Fe) inactivated 100% of heterotrophic bacteria ($N_o = 2.58 \times 10^4$ to 8×10^6 CFU/mL) at pH=7.31 to 7.91 (Gombos et al., 2013). In the same study, ferrate (4 mg/L Fe) surpassed sodium hypochlorite (10 mg/L Cl_2) by achieving 100% inactivation of *E. coli* ($N_o = 3 \times 10^6$ CFU/mL). In fact, ferrate is more effective as a disinfectant at acidic pH due to the presence of protonated species (e.g. $HFeO^-_4$, H_2FeO_4) (Sharma, 2002). Therefore, ferrate (1.5 mg/L Fe) achieved 4 log removal of *E. coli* at pH 7.2 compared to 1.7 log removal at pH= 8.2 in deionized (DI) water ($N_o = 2.58 \times 10^4$ to 8×10^6 CFU/mL) (Cho et al., 2006).

The wastewater treatment approaches during WWF should consider the reduction of both conventional water quality parameters (e.g. TSS, COD) and bacterial level (e.g. total coliform, *E. coli*). However, numerous studies have been limited to either coagulation or disinfection/oxidation of wastewater during WWF. For example, treating the wastewater during WWF by coagulation or enhanced coagulation was proposed while disinfection was overlooked (El Samrani et al., 2008; Exall and Marsalek, 2013; Gasperi et al., 2012; Jeon et al., 2017; Jolis and Ahmad, 2004; Li et al., 2003; Sumant et al., 2016; Wang et al., 2016b; Zhu et al., 2007). In contrast, other studies had evaluated different disinfectants (peracetic acid, formic acid, and hypochlorite) during WWF and ignored the pre-treatment (McFadden et al., 2017; Ravi Kumar Chhetri, 2016; Tondera et al., 2016). That being said, limited studies investigated coagulation/sedimentation with disinfection during WWF (Chhetri et al., 2016; Gibson et al., 2016). To the best of the authors' knowledge, only limited studies proposed ferrate for treating the wastewater during WWF condition (Elnakar and Buchanan, 2019; Gandhi et al., 2014). However, Gandhi et al. (2014) explored ferrate only as a coagulant with dose optimization and pH impact. While Elnakar and Buchanan (2019) only focused on ferrate as a disinfectant and highlighted the role of mixing. Therefore, this study was designed to systematically evaluate the capacity of ferrate to minimize both suspended solids and microbial levels in the wastewater during WWF condition. Specifically, ferrate coagulation and disinfection behaviors were evaluated simultaneously when ferrate was used alone as a coagulant or as a coagulant aid with alum to treat the raw WWF samples. Moreover, the disinfection effects of ferrate at post-dosing (after coagulation/sedimentation) were also examined. Some studies showed that ferrate can be used effectively as a coagulant (Graham et al., 2010; Jiang and Lloyd, 2002; Jiang et al., 2001; Jiang et al., 2006) while other studies reported an inefficient performance of ferrate for coagulation (Goodwill et al., 2015; Jun and Wei, 2002; Yates et al., 2014; Yu et al., 2016; Zheng and Deng, 2016). The main objectives of this study were: (i) to evaluate ferrate capacity as a coagulant/coagulant aid/disinfectant for enhanced primary treatment during WWF; (ii) to optimize ferrate coagulation operation conditions (rapid mixing, slow mixing, polymer addition) using two-level factorial design; (iii) to evaluate ferrate as a coagulant aid with alum as primary coagulant; (iv) to examine ferrate as a disinfectant at different dosing points.

4.2 Materials and Methods

4.2.1 WWF sampling and chemicals

Raw WWF or sewage samples were collected from a wastewater treatment plant located in Alberta, Canada in high-density polyethylene pails (20 liters). The samples were preserved at 4 °C before the analysis. All analyses were conducted within a week while bacterial analysis was completed within the 24 hrs following sampling. During WWF events, the samples without further modification were used for analysis, while during dry weather, raw samples were diluted using deionized (DI) water to reach the same TSS concentration of real WWF samples. The water quality parameters of the WWF and diluted raw samples during dry weather are presented in Table B.1.

Potassium ferrate (K_2FeO_4) (purity 76%) was prepared by wet method and stored in a desiccator isolated from moisture for more than one year (Thompson et al., 1951). Ferrate stock solution was freshly prepared by dissolving potassium ferrate (K_2FeO_4) in DI water (pH= 9.2) and was used within 30 minutes. The ferrate concentration was measured by the direct spectrophotometric method using a UV−vis spectrophotometer (Thermo Scientific). Firstly, the absorbance was measured at 510 nm, after filtration with 0.2 µm nylon filters (Thermo Scientific) to remove any interferences from ferric particles and impurities. Then the absorbance was divided by an absorptive coefficient (1150 M^{-1}) (Luo et al., 2011).

The cationic polymer (Praestol™ Flocculants) used in this study was freshly prepared by dissolving the liquid stock in DI before each experimental run. Aluminum sulfate (alum) was purchased from Sigma Aldrich and supplied in powder form of 100% purity. The stock solution of alum was prepared freshly before every experimental run.

4.2.2 pH, turbidity,TSS, UVT% and alkalinity

pH was measured using Accumet Research AR20 pH/conductivity meter (Fisher Scientific). Turbidity was measured by OAKTON turbid meter T-100. TSS was measured following the standard method 2540 D and samples were filtered using a glass fiber filter (GF/F Whatman). The ultraviolet absorbance UV was measured at wavelength 254 nm using a Genesys 10S UV−vis. spectrophotometer (Thermo Scientific). Samples were filtered with a 0.45 µm nylon filter (Thermo Scientific). The percent ultraviolet transmittance (UVT%) was calculated using equation (4.1):

$$\mathrm{UVT\%} = 10^{2-\mathrm{A}} \qquad (4.1)$$

where A is the absorbance measured in cm^{-1}.

The alkalinity was measured following the standard method 2320B (APHA, 2017). Titration was conducted using a Mettler Toledo autotitrator with standardized sulfuric acid used as a titrant. The titration was stopped at pH 4.5 and alkalinity was calculated using equation (4.2):

$$Alkalinity, mg\ Ca\,CO_3/L = \frac{A \times N \times 50000}{mL\ sample} \qquad (4.2)$$

where: A = mL titrant used, N = normality of titrant, and mL sample = volume of used sample.

4.2.3 Measurement of COD and orthophosphate

COD was measured according to the closed reflux, colorimetric method (standard method 5220D) (APHA, 2017). Orthophosphate (OP) was measured according to the standard method (4500-P C) using HACH 8114. Therefore, 10 mL of the sample was filtered with a 0.2 µm nylon filter and transferred to glass vials. Then 0.5 mL of phosphate reagent (Molybdovanadate reagent) was added. After 7 minutes, OP concentration was measured using a spectrophotometer (at 430 nm wavelength) (HACH DR 3900). All vials were cleaned by phosphate-free detergents.

4.2.4 Measurement of E. coli

E. coli was measured according to the standard method 9222B membrane filtration techniques for members of the coliform group (APHA, 2017). The colony-forming unit was counted and reported as colony-forming unit/100 mL (CFU/100 mL) as per the standard procedures.

4.2.5 Zeta potential (ZP), iron residual and ferrate generated flocs

Zeta potential (ZP) analysis was conducted by using a Nanobrook Omni instrument (Brook Haven Instrument) where 2 mL of sample was placed in a disposable polystyrene cuvette. Phase analysis light scattering (PALS) was used and the reported reading was measured as an average of two runs with 30 cycles of each using the Particle Solution software. Iron concentration was measured by using inductively coupled plasma mass spectrometry (ICP-MS).

The morphology of generated flocs after coagulation and sedimentation was characterized by scanning electron microscopy (SEM) and elemental distribution measured by energy-dispersive X-ray (EDX) using Zeiss EVO M10 SEM W/EDX. The flocs were collected by borosilicate glass drop pipette from generated sludge 50 mL of wet sludge and subsequently dried at 104 °C.

The samples were coated with a thin golden film layer using the Denton Sputtering system before SEM and EDX analyses.

4.2.6 Experimental design and setup

In this study, ferrate was tested as a coagulant, coagulant aid, and disinfectant following different treatment trains through bench-scale experiments using PB-700^{TM} JARTESTER (PHIPPS&BIRD^{TM}) jar test apparatus (Figure 4.1). In treatment train 1, ferrate was used a coagulant with and without cationic polymer addition. The coagulant dose, polymer addition and mixing conditions were optimized based on a two-level factorial design (Table 4.1). In treatment train 2, ferrate was evaluated as a coagulant aid and applied simultaneously with alum (primary coagulant) at the beginning of rapid mixing. In treatment train 3, ferrate was dosed as a disinfectant after completion of the coagulation/flocculation/settling process. All experiments were performed in duplicates and average values were presented.

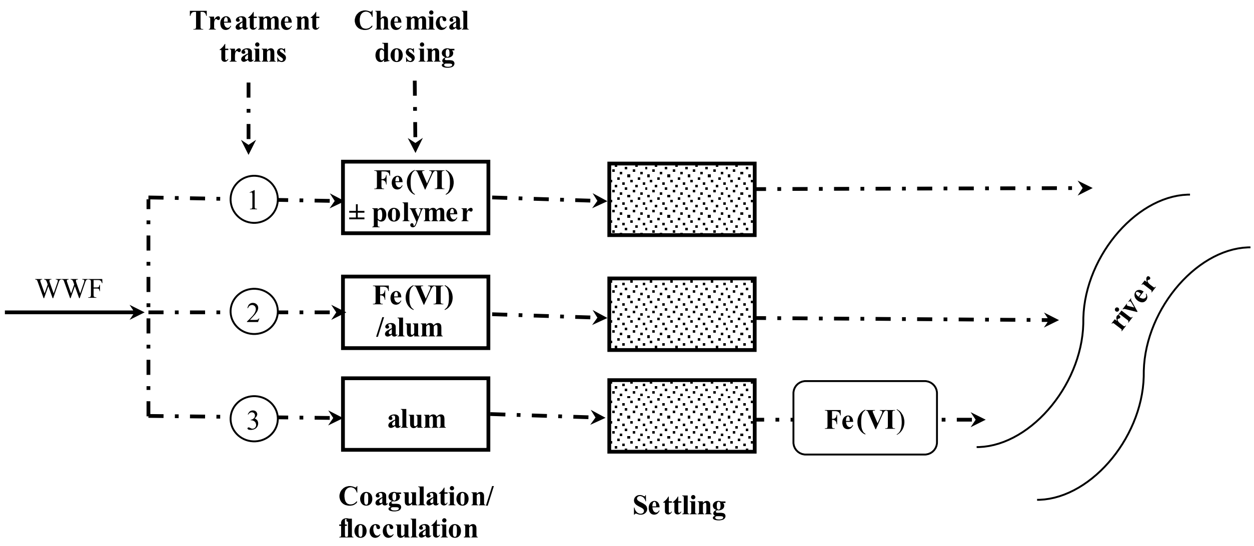

Figure 4. 1 General schematic of different treatment trains (TR) (1, 2 and 3) that were used in this study for testing ferrate as a coagulant, coagulant aid and disinfectant during wastewater treatment during wet weather flow (WWF) in bench-scale level. At the coagulation/flocculation point, the chemical was added at the beginning of rapid mixing followed by slow mixing (flocculation) and then the settling process. In TR (1) WWF samples were treated by ferrate a coagulant with or without cationic polymer while in TR (2) the treatment was carried out by ferrate as a coagulant aid with alum. In TR (3) alum was added to WWF at the coagulation/flocculation point and ferrate was added as a disinfectant to the supernatant after settling.

Table 4. 1 Two-levels factorial design with three factors rapid mixing, slow mixing and coagulant dose.

Experiment	**Rapid mixing (rpm/min)**	**Slow mixing (rpm/min)**	**Gt[a] (rapid/slow)**	**Mixing level**	**Ferrate doses (mg/L Fe)**	**Polymer doses (mg/L)**
1	300/3	30/20	(68400/27600)	(1/1)[b]	(0.5/8)[c]	(0/1.25)[d]
2	300/3	15/10	(68400/6000)	(1/-1)	(0.5/8)	(0/1.25)
3	150/1	30/20	(9300/27600)	(-1/1)	(0.5/8)	(0/1.25)
4	150/1	15/10	(9300/6000)	(-1/-1)	(0.5/8)	(0/1.25)

[a] Velocity gradient in s^{-1} and t is mixing time, [b] High level/low level of mixing, [c] Low dose of ferrate/high dose of ferrate, [d] polymer dose level.

4.3 Results and Discussion

4.3.1 Ferrate as a coagulant

Ferrate was evaluated as a coagulant based on treatment train 1 where ferrate was used to treat the wastewater during WWF condition (Figure 4. 1). Two-level (high and low) factorial design (Table 4. 1) was implemented to optimize the operation conditions. The tested factors were polymer addition, ferrate dose, and mixing conditions (rapid/slow). The low level of ferrate dose was 0.5 mg/L Fe, while the high level was 8 mg/L Fe. The low polymer level was set at 0 mg/L and the high level was 1.25 mg/L. Mixing levels were selected based on the screened literature and the most common conditions in practice (El Samrani et al., 2008; Exall and Marsalek, 2013; Gibson et al., 2016). In principle, the efficiency of the coagulation and flocculation process is highly dependent on coagulant and coagulant aid level and mixing intensity (i.e. rapid mixing, slow mixing) (Young et al., 2000). Coagulation is initiated by rapid mixing upon the addition of coagulant and coagulant aid to assure an effective dispersion of chemicals. That is followed by slow mixing to promote flocs growth before sedimentation (Saritha et al., 2017).

pH and alkalinity levels of treated samples had average values of 7.4 ± 0.1 and 195 ± 16 mg/L $CaCO_3$, respectively (Table B. 2, B. 3). Ferric hydroxide, the reduced form of ferrate (equation 4.3) which is insoluble at pH 6-8, is considered to carry out the coagulation process (Jiang and Lloyd, 2002; Lee et al., 2014; Lv et al., 2018).

$$2FeO_4^{-2} + 5H_2O \rightarrow 2\ Fe(OH)_3 + 4OH^- + 1.5O_2 \uparrow \qquad (4.3)$$

Results unveiled that the low dose of ferrate (0.5 mg/L Fe) with polymer surpassed the high dose (8 mg/L Fe) and removed 83% of turbidity, 87% of TSS, 87% of TVSS, and 70% of COD (Figure 4. 2 and Table B. 4). Moreover, the addition of cationic polymer with ferrate (0.5 mg/L Fe) improved the removals of turbidity by 19% and 11% approximately for TSS and COD respectively (Figure 4. 2). The performance of ferrate as a coagulant at a higher dose (8 mg/L Fe) declined possibly due to the presence of ferrate-induced particles (iron residuals) (Figure 4.3 a). Residual iron was found to be 0.255 mg/L Fe and 1.945 mg/L Fe induced by ferrate doses 0.5 mg/L Fe and 8 mg/L Fe without polymer, respectively. Other studies revealed that ferrate-residual iron particles had nano-particle sizes with poor settling properties (e.g. 18% settled after 72 hr) which may affect the turbidity of the wastewater (Jun and Wei, 2002; Yuan et al., 2002; Zheng and Deng, 2016). In this study, the cationic polymer (1.25 mg/L) reduced the residual iron by 41% to 63% (Figure 4.3 a) when combined with ferrate doses 0.5 and 8 mg/L Fe respectively, likely via adsorption and agglomeration entailed by settling (Onen et al., 2018). Indeed, iron particles under oxic conditions might form rust-color silts and result in the growth of iron-bacteria when the concentration exceeds 0.6 mg/L Fe (ECCC, 2019c). Moreover, the magnitudes of zeta potentials for the untreated and ferrate-treated water (using 0.5 and 8 mg/L Fe with polymer) remained unchanged (-19±1 mV) (Figure 4.3, 1b). This indicated that the residual iron particles have high stability in suspension.

The average removals of TSS and COD achieved by ferrate at 0.5 mg/L Fe were slightly lower than that achieved by alum (4 mg/L Al) and ferric chloride (8.4 mg/L Fe) reported in a previous study (Alameddine et al., 2020). In particular, ferrate 0.5 mg/L Fe achieved 80% of TSS and 57% of COD while alum (4 mg/L Al) and ferric chloride achieved 84% to 86% of TSS and 66% to 68% of COD respectively when all coagulants were injected with same polymer dose (1.25 mg/L). The discrepancies in the performance among the three coagulants might be attributed to the involved coagulation mechanisms (Duan and Gregory, 2003; Lv et al., 2018). The lower performance of ferrate compared to ferric chloride might be ascribed to the different pathways underwent by each chemical to form ferric hydroxides/oxides (Goodwill et al., 2015; Jiang et al., 2015a; Sharma et al., 2015; Yu et al., 2016). Actually, ferrate forms ferric precipitates via crystallization (slow aging process, smaller floc size) while ferric chloride is subjected to the stepwise hydrolyzing process (forming bigger floc sizes) (Goodwill et al., 2015; Yu et al., 2016).

The surface morphology of the resulting flocs was characterized by SEM and showed rough texture covered with the adsorbed impurities (Figure B. 1). In fact, the surface roughness might increase the adsorption capacity of the floc due to the effective void space in the created microspheres (Vuong and Monson, 1998). This provides a suitable condition for enmeshment of suspended particles which was also reported for the removal of colloidal kaolin particles and aqueous arsenate precipitates (Lv et al., 2018; Wang et al., 2020). Furthermore, EDX analysis showed almost similar elemental distribution in floc induced by the high and low dose of ferrate (Table B. 5). In contrast, the percentage of iron weight in flocs came in line with the initial dose of ferrate and was found to be 4.2% and 10.7% corresponding to the ferrate doses 0.5 and 8 mg/L, respectively.

A ferrate dose of 8 mg/L Fe with polymer achieved higher removal of OP (28.6%) in average, compared to 17.4% by ferrate at 0.5 mg/L Fe with polymer (Table B. 6). It was also found in another study that OP (C_o= 3.4 mg/L) removal improved from 10% to 30% by increasing the ferrate dose from 0.12 to 0.6 mg/L Fe in simulated WWF wastewater (Gandhi et al., 2014). In another study, a ferrate dose of 15 mg/L Fe was required to achieve 100% removal of OP (C_o=0.252 mg/L) when applied to secondary effluent (Kwon et al., 2014). Ferric chloride (8 mg/L Fe) achieved higher removal of OP (83%) than that achieved by ferrate (8 mg/L Fe) under similar testing conditions (Alameddine et al., 2020). A comparative study showed that ferric chloride and ferrate have different precipitation mechanisms, which may determine the overall performance in phosphate removal (Goodwill et al., 2015). In fact, the removal of the OP might occur via the formation of ferric phosphate precipitation or adsorption of phosphate species to ferric hydroxide (Bunce et al., 2018; Lee et al., 2009). The latter mechanism might be the dominant mechanism in this study where the obtained pH 7.3±0.37 promoted the formation of ferric hydroxide (Lv et al., 2018). EDX analysis showed that there was a traceable amount of phosphorus ions present in sludge samples of ferrate (8 mg/L Fe) (Table B. 5). That being said, a more in-depth study might be required to explore the phosphate removal mechanism by ferrate.

Ferrate even at the higher dose, did not improve UVT% (an indicator of dissolved organic matter) (Table B. 7). That might be attributed to two reasons: firstly, the affinity of ferrate to attack the hydrophobic portion of NOM which may contribute insignificantly to the total UVT% value compared to the hydrophilic portion (Deng et al., 2018). Also, the presence of dissolved ferric species might interfere with the UVT% measurement which was also confirmed on UV measurement within the wavelength of 220 to 400 nm (Doane and Horwath, 2010; Xiao et al., 2013).

The mixing level affected differently the removal of turbidity, TSS and COD. The highest removal of turbidity and TSS was achieved at the high level of rapid mixing and low level of slow mixing as 83% and 87%, respectively (Figure 4. 2 a & b). Of note, unlike ferrate, alum (4 mg/L Al) and ferric chloride (8.4 mg/L Fe) achieved the best removal of turbidity at the high-level for both rapid and slow mixing (1/1) whereas for TSS the best removal achieved by alum and ferric chloride was at low-level rapid mixing and high-level slow mixing (1/-1) (Alameddine et al., 2020). Interestingly, for ferrate, the highest removal of COD was attained at the high-level of both rapid and slow mixing (Figure 4. 2 c) which was also reported for ferric chloride (Alameddine et al., 2020). The observed discrepancies on the influence of the mixing intensity (Gt) might be attributed to the differences in the characteristic of formed flocs and mechanisms of removal of the tested parameters. It was reported that charge-neutralization-induced flocs showed more resistance to shear breakage (Rong et al., 2013). Also, floc properties (floc size, strength, settling properties, break-up factors) are influenced significantly by Gt and coagulant type (Marques and Ferreira Filho, 2017; Zhan et al., 2011). A high level of mixing during the flocculation stage might break the formed flocs leading to lower removals of turbidity and TSS (Young et al., 2000). Also, ferrate removed total COD via two processes: oxidation of soluble COD and coagulation of particulate COD (Jiang et al., 2006). Therefore, a higher mixing intensity advocated the oxidation and coagulation, which resulted eventually in higher removal of total COD (Cho et al., 2006; Kralchevska et al., 2016; Sharma, 2013).

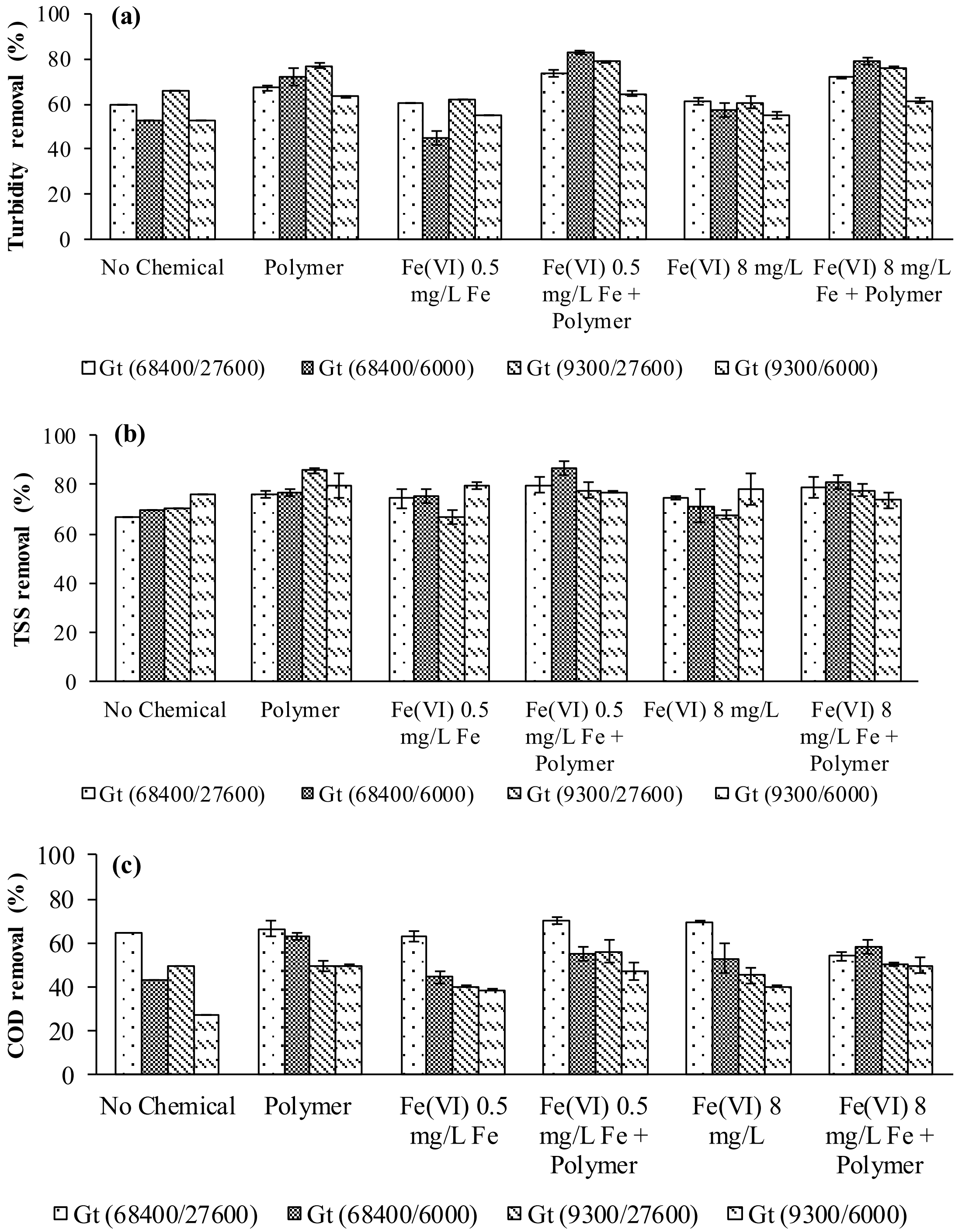

Figure 4. 2 The percentage of removals for a) turbidity and b) TSS, c) COD at different testing conditions after coagulation and sedimentation when ferrate used as a coagulant (the cationic polymer concentration fixed as 1.25 mg/L).

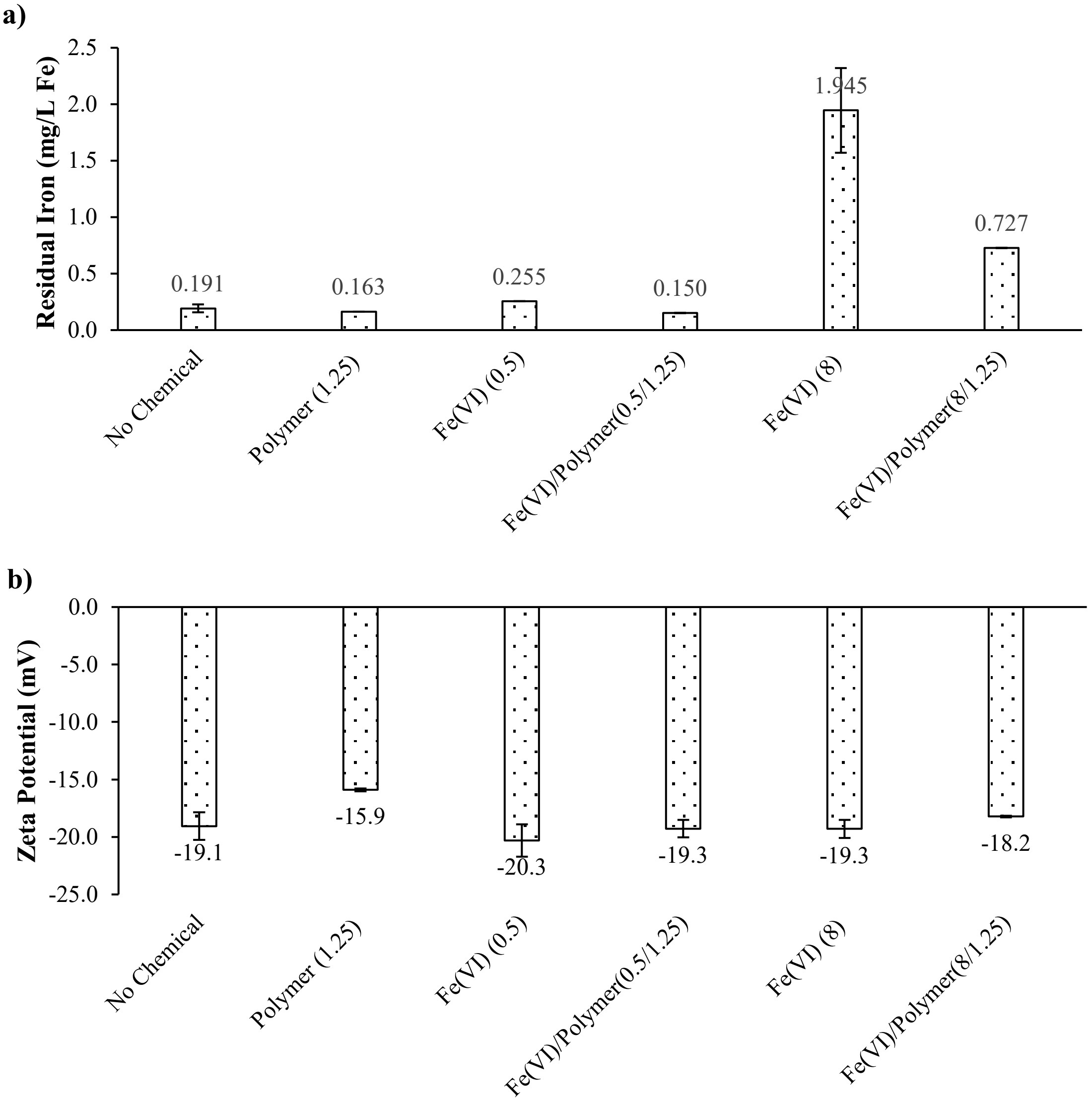

Figure 4. 3 The impact of ferrate dose and polymer addition on a) the residual iron levels and b) zeta potential. The number between brackets is the concentration in mg/L.

The experimental data unveiled clearly that the low dose of ferrate (0.5 mg/L Fe) surpassed the high dose for the removal of turbidity, TSS, and COD. Moreover, polymer addition exhibited positive impacts. The level of rapid mixing and slow mixing showed different influences on the tested parameters. Therefore, to understand the interaction effects of the three factors (i.e. polymer addition, rapid mixing, and slow mixing), thorough factorial analyses were conducted.

4.3.2 *Two-level full factorial design (2^3) analyses*

The experimental data obtained by using ferrate low dose (0.5 mg/L Fe) were further analyzed based on the factorial design as per the following procedures. Firstly, the effects of the main factors (A= rapid mixing, B= slow mixing, and C = polymer addition) and their interactions (AB, AC, BC, ABC) were calculated based on measured responses in the standard coded matrix (Table B. 8) using equation 4.4. Secondly, ANOVA was employed to evaluate the statistical significance level of effects with a p-value =0.05. Therefore, the effect was considered significant if the p-value was < 0.05 (i.e. rejecting the null hypothesis) and insignificant with a p-value ≥ 0.05. Finally, constructing and validating general linear model equations for predicting the response of each selected indicator (i.e. turbidity, TSS, and COD) base on the general form of linear equation (4.5).

$$effect = \frac{\sum Y_+}{n_+} - \frac{\sum Y_-}{n_-} \tag{4.4}$$

Y= the corresponding response at a high level (Y_+) or low level (Y_-)

n = number of data points collected for each level

$$Y=\beta_o+\beta_1A_1+\beta_2B_2+\beta_3C_3+\beta_{12}A_1B_2+\beta_{13}A_1C_3+\beta_{23}B_2C_3+\beta_{123}A_1B_2C_3 \tag{4.5}$$

Y is predicted response

β_o overall mean

β_1, β_2, β_3 effect coefficient for the main effect of factor (A, B, C)

β_{12}, β_{23}, β_{123} effect coefficient for interaction effects of the factors

The effects coefficients of all three factors (i.e. rapid mixing, slow mixing, and polymer addition) were calculated based on equation (4.4) (Anderson, 2015), and their statistical significance was evaluated via two-way ANOVA (Tables B. 9-B. 11).

As such, the factors showed different impacts on the overall coagulation process quantitatively (magnitude) and qualitatively (positive/ negative). In general, polymer addition (C) showed a statistical significant effect for the removal of turbidity, TSS and COD which also came in agreement with experimental observations (Tables B. 9-B. 11). It is noteworthy, the apparent main effect coefficients of other factors (A, B) are not necessarily reflected on the final responses due to interaction effects (i.e. AB, AC, BC, etc.). For instance, slow mixing (B) showed a positive main effect on turbidity removal while rapid mixing (A) showed an insignificant effect (Table B. 9) yet the experimental data revealed that the highest removal was achieved at (+A/-B) and the lowest at (-A/-B) (Figure 4.2 a). The general model equation incorporated the main and interaction effect to describe the experimental data properly. Therefore, three model equations were established to predict the removals of turbidity, TSS and COD (equations 4.6, 4.7, and 4.8). The factors (A, B or C) should be substituted with (+1) for high level and (–1) for low level while interaction effect (e.g. AB) depend on the sign of parent main effect (e.g. A=-1, B=1, AB=-1).

$$\text{Turbidity Removal (\%)} = 67+10.359B+15.910C-7.250AB+9.844AC-7.775BC \tag{4.6}$$

$$\text{TSS Removal (\%)} = 78-2.936A-5.89B+5.899C-5.11ABC \tag{4.7}$$

$$\text{COD Removal (\%)} = 54+14.008A+10.159B+11.360C+5.178AB-4.108ABC \tag{4.8}$$

The model equations (equations 4.6, 4.7, and 4.8) were validated by diagnosing residuals to normal distribution. Therefore, the residuals of all tested model equations appeared to be normally distributed (Figure B. 2). This supports the assumption of residuals was normally distributed and independent with a constant variance. By checking the residual of each equation, it was noticed that a high residual range was observed from turbidity and COD prediction as (20 to -15) and (13 to -21) respectively. In contrast, TSS prediction had a lower residual range (9 to -11). That might occur due to significant interaction effects of other tested factors on turbidity and COD which reflected eventually as overestimation or underestimation (Shah and Pathak, 2010).

In this phase, the low dose of ferrate (0.5 mg/L Fe) with polymer (1.25 mg/L) reduced the level of TSS from 143 mg/L to 19 mg/L (Figure 4.4) which complied with Alberta guidelines for surface water discharge (TSS ≤ 25 mg/L) (Government of Alberta, 2018). However, the same dose of ferrate could not achieve the target value for the turbidity level as 8 NTU.

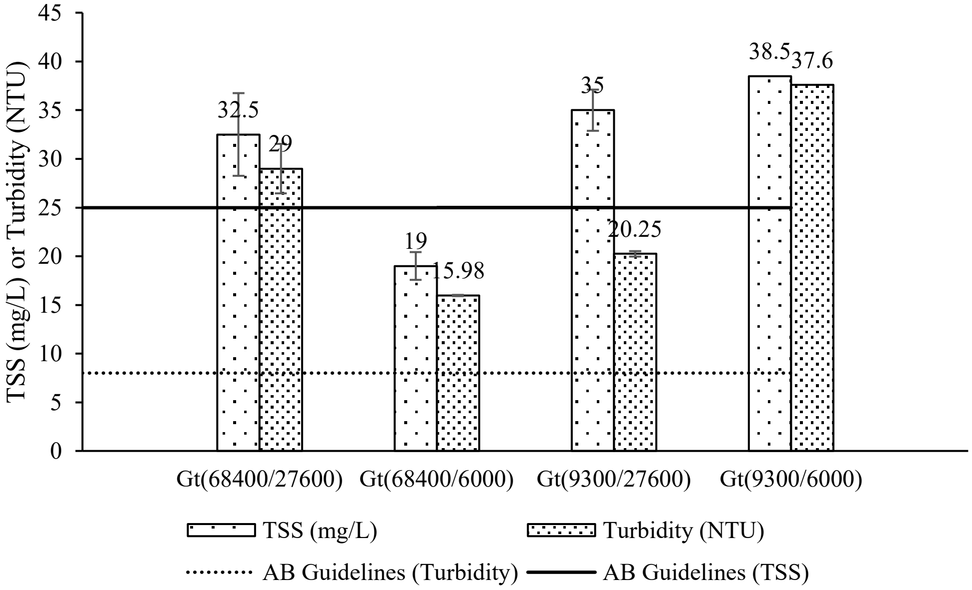

Figure 4. 4 TSS and turbidity levels achieved by using ferrate 0.5 mg/L Fe with 1.25 mg/L of the cationic polymer under different mixing conditions compared with Alberta (AB) guidelines for surface water discharge.

4.3.3 Ferrate as a coagulant aid

Ferrate was explored as a coagulant aid when applied simultaneously with alum (alum/ ferrate) during rapid mixing (treatment train 2, Figure 4. 1). Ferrate doses varied from 1 to 20 mg/L Fe with a fixed alum dose of 6 mg/L Al which was reported as an optimum dose in another study by the group (Alameddine et al., 2020). The results revealed that alum alone removed 94%, 84%, and 76% of turbidity, TSS, and COD, respectively (Figure 4. 5). In contrast, alum/ferrate (ferrate doses 1 to 10 mg/L Fe), improved TSS removal by 12.5% on average while no improvement was observed for the removal of turbidity and COD. Indeed, ferrate can aid alum coagulation by forming ferric species which may remove colloidal particles via complexation and adsorption (Lim and Kim, 2010). The benefit of ferrate as a coagulant aid was also reported elsewhere in the ferrate-ferric chloride system where better removal of suspended solids (+16%) was observed during the treatment of surface water (ferric chloride = 6.7 mg/L Fe, ferrate=1.68 mg/L Fe, pH= 8, DOC=41 mg/L) (Yu et al., 2016). The authors reported that the induced flocs by ferrate-ferric chloride were bigger than those generated by single dosing of ferrate or ferric chloride.

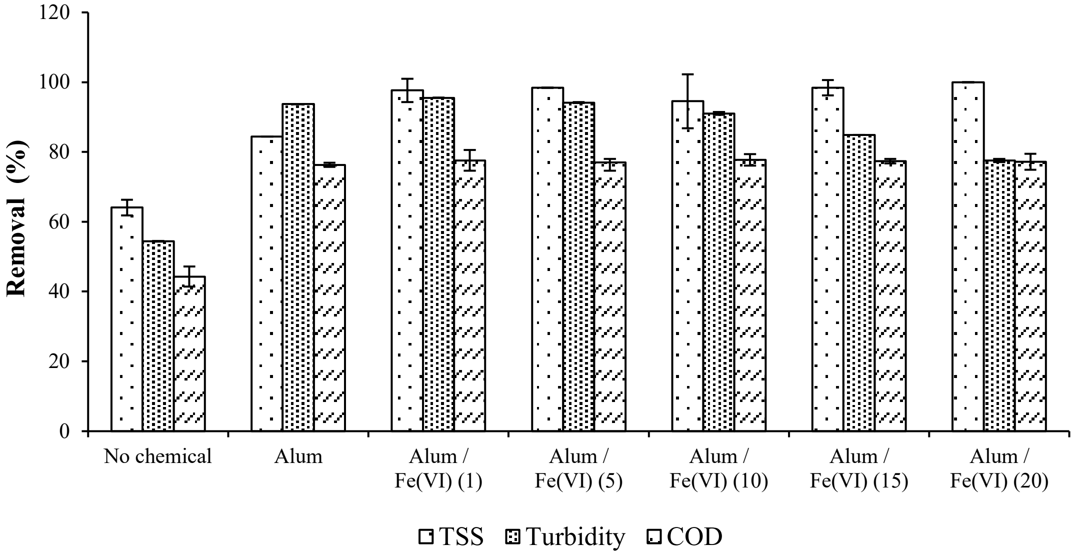

Figure 4. 5: Removal percentages of turbidity, TSS and COD when ferrate (Fe(VI)) used as a coagulant aid with alum. Alum dose was fixed at 6 mg/L Al. The number between bracket indicate ferrate concentration in mg/L Fe.

UVT% was improved from 70.6% at 6 mg/L Al of alum to 72.2% by alum/ferrate with 10 mg/L Fe (Table 4. 2). A previous study also showed that, combining ferrate and polyaluminum chloride (PACl) improved the removal of humic substances (UVT% used as an indicator) present in natural water (DOC=3.38 mg/L, pH = 6-7, ferrate= 2.5 mg/L Fe, PACl=20 mg/L) (Amano et al., 2018).

Table 4. 2 Average obtained values of pH, UVT% and COD during the simultaneous application of ferrate and alum.

sample ID	pH	Turbidity (NTU)	TSS (mg/L)	UVT%	COD (mg/L)
WWF[a]	7.39	74.3	106.7	66.6	278.3
No chemical	7.43	33.9	38.3	66.4	155.1
Alum[b]	7.20	4.7	16.7	70.6	65.9
Alum / Fe(VI) 1[c]	7.14	3.3	2.5	46.5	62.4
Alum / Fe(VI) 5	7.30	4.3	1.7	47.7	63.9
Alum / Fe(VI) 10	7.65	6.7	5.8	72.2	61.9
Alum / Fe(VI) 15	7.97	11.2	0.0	71.6	62.9
Alum / Fe(VI) 20	8.17	16.7	5.0	72.1	63.4

[a] wet weather flow sample, [b] alum dose fixed at 6 mg/L Al, [c] ferrate concentration in mg/L Fe

The negligible improvement in turbidity and COD removal with an alum/ferrate dose <10 mg/L Fe and reversal effects at higher dose >10 mg/L Fe of ferrate, might be implied by ferrate-induced particles and competition of alum and ferrate to particulate COD.

Alum/ferrate integrated process (6 mg/L Al 10 mg/L Fe) reduced ferrate-induced iron particles in the treated water by 70% approximately with a final concentration of 0.52 mg/L Fe (Figure 4. 6 a). The reduction of ferrate-induced iron particles by alum might reduce soluble iron (negatively charge) likely by charge neutralization and sweep flocculation (Duan and Gregory, 2003). As per the Canadian guidelines for drinking water, the acceptable level of iron concentration should be ≤ 0.6 mg/L (ECCC, 2019c). Previous studies had reported the presence of iron particles but did not propose a method of removal after ferrate addition (Goodwill et al., 2015; Jiang et al., 2006; Lv et al., 2018; Yuan et al., 2002).

Zeta potential measurement was performed to understand the behavior of alum and ferrate in the coagulation processes (Figure 4. 6 b). As such, alum (6 mg/L Al) reduced the negativity of zeta potential from -17.9 mV (no chemical) to -8.9 mV (Figure 4 b). That might be ascribed to partial charge neutralization via aluminum hydrolysis products $Al(OH)^{+}_{2}$ and subsequently adsorption to aluminum hydroxides which may be present at the pH range 7.20 to 7.65 of the tested samples (Table 4. 2) (Duan and Gregory, 2003). In contrast, ferrate (10 mg/L Fe) addition increased slightly the negativity of zeta potential from -17.9 mV to -19.93 mV due to the increase in the level of negatively-charged residual iron particles ($Fe(OH)^{-}_{4}$)(Jiang et al., 2006).

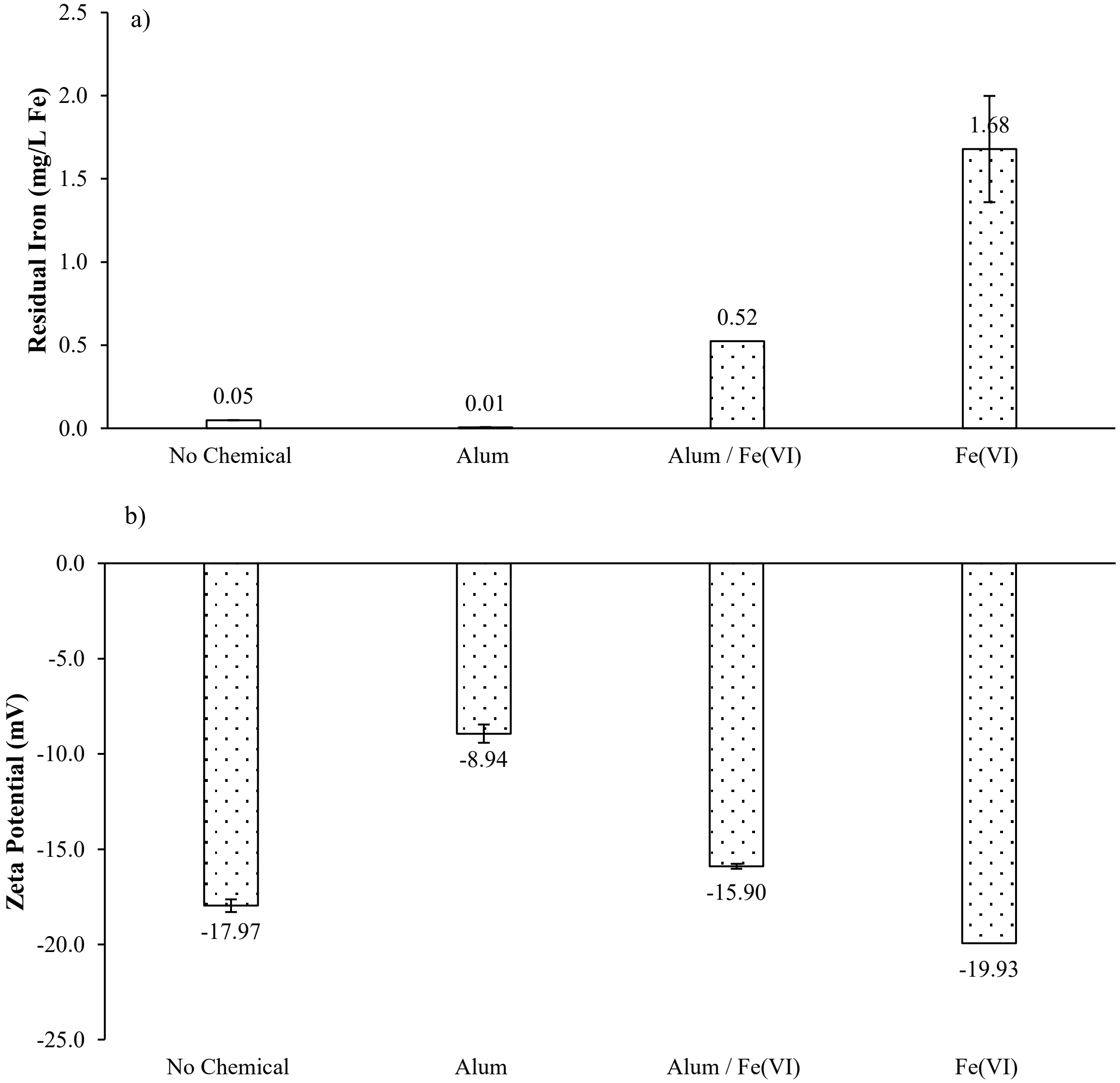

Figure 4. 6 a) residual iron levels and b) zeta potential levels (mV) for selected dosing condition: Alum (6 mg/L Al), Alum / Fe(VI) (6 mg/L Al/10 mg/L Fe), and ferrate alone (Fe(VI) (10 mg/L Fe)

The removal of OP was also measured and alum combined with ferrate (10 mg/L Fe) removed 100% of OP compared to 92% to 96% by a single application of alum and ferrate (10 mg/L Fe), respectively (Figure 4. 7). Basically, in the iron and aluminum-based coagulants, the major species involved in phosphorus removal are $Fe(OH)^{+}$, Fe(OH), $AlOH^{2+}$, $Al(OH)^{+}_{2}$ and $Al(OH)_3$ (Yang et al., 2010). Therefore, the removal of OP was expected to occur via complexation of dissolved phosphate species entailed by aluminum phosphate or ferric phosphate precipitates adsorption and sedimentation (Kralchevska et al., 2016).

Combining alum and ferrate showed a slight improvement in the removal of TSS while no improvements were observed in the removal of turbidity and COD. Moreover, alum (6 mg/L Al) and ferrate (10 mg/L Fe) achieved the recommended levels of turbidity (<8 NTU) and TSS (< 25 mg/L) as per Alberta guidelines for surface water discharge (Government of Alberta, 2018). In fact, alum and ferrate combination might become more feasible especially for the wastewater treatment during WWF if the ferrate disinfection effect was considered as discussed in section 4.3.5

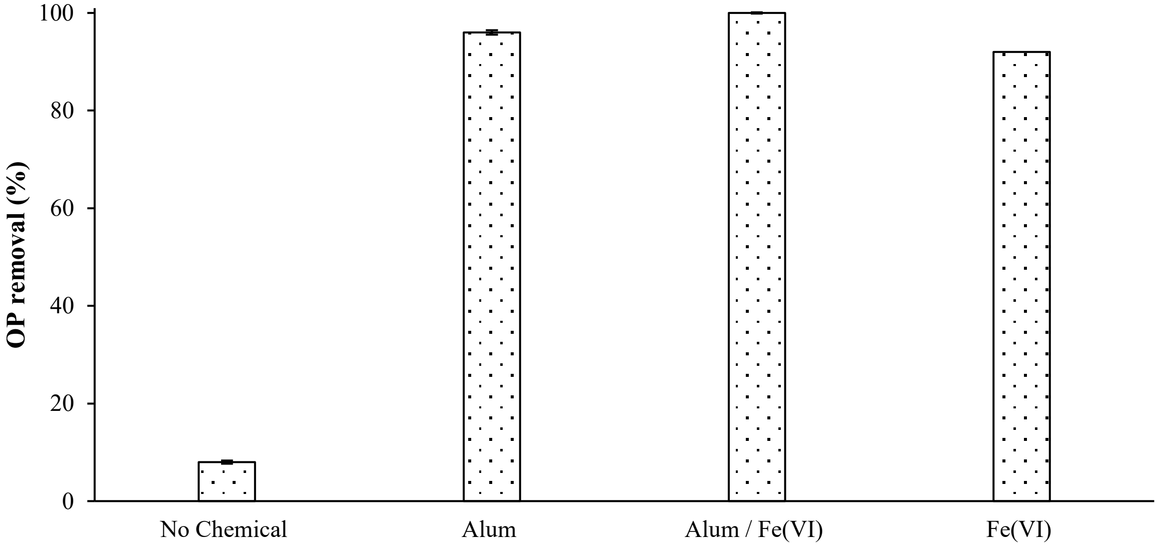

Figure 4. 7 OP % removal for selected dosing condition: Alum (6 mg/L Al), Alum / Fe(VI) (6 mg/L Al/10 mg/L Fe), and ferrate alone (Fe(VI) (10 mg/L Fe).

4.3.4 Settling time optimization

The settling time was optimized for the optimum doses of ferrate as a coagulant (ferrate 0.5 mg/L, polymer 1.25 mg/L) and ferrate as a coagulant aid (ferrate 10 mg/L Fe, alum 6 mg/L Al) based on turbidity measurement. Turbidity was selected as an indicator for settling time optimization as it correlated properly with other parameters such as TSS and COD (Alameddine et al., 2020). The results revealed that by the end of slow mixing the turbidity was reduced from 87 to 32 (NTU) for ferrate as a coagulant while minor reduction (98 to 92 NTU) was observed when ferrate used as coagulant aid at the same time (Figure 4. 8). The major reduction of turbidity was observed after 10 min settling time (21 minutes of treatment) and reached 8 and 4 NTU when ferrate was used as a coagulant and a coagulant aid respectively. That was expected because the flocs size and growth rate for both ferrate and alum achieved a plateau within 5 to 10 minutes thus a considerable turbidity reduction was observed afterward (Rong et al., 2013; Yu et al., 2016). At 20 minutes of settling time (31 minutes of treatment), turbidity dropped to 8.4 and 1.8 NTU when ferrate was used as a coagulant and a coagulant aid respectively. By observing the turbidity level after 40 to 60 minutes, there was no considerable reduction in turbidity levels. Based on these observations, the optimized settling time was fixed for 20 minutes. In addition, the optimized settling time for the alum/ferrate process also achieved the target turbidity level (≤ 8 NTU) as per Alberta guidelines for surface water discharge (Government of Alberta, 2018).

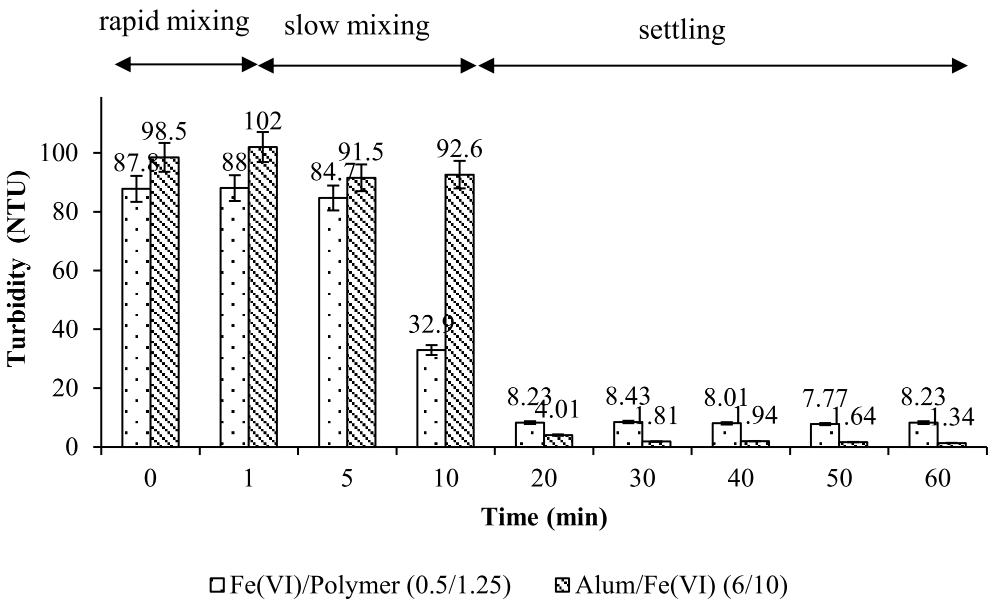

Figure 4. 8 Turbidity change (Y-axis) over time (X-axis) for using ferrate as a coagulant denoted as Fe(VI)/Polymer and ferrate as coagulant aid denoted as alum/Fe(VI). The numbers between the brackets indicate the concentration in mg/L.

4.3.5 Ferrate disinfection performance

This section presents the performance of ferrate as a disinfectant throughout the three different treatment trains: ferrate alone as a coagulant (train 1), ferrate used as a coagulant aid with alum (train 2) and ferrate applied after coagulation/flocculation/settling (train 3) (Figure 4. 1). The total contact time was selected to be 31 minutes based on the findings in section 4.3.4. The initial concentration of *E. coli* was $2.97\times10^6 \pm 0.40\times10^6$ (CFU/100 mL). Figure 4. 9 a depicted the performance of ferrate as a disinfectant at the aforementioned dosing points. To achieve similar inactivation (2.1-log removal) of *E. coli*, 8 mg/L Fe of ferrate was required when used as a coagulant compared to only 1 mg/L Fe of ferrate as a coagulant aid with alum. That can be attributed to the effective alum reduction of background demand (organic matter, ammonia, phosphorus, etc.) thus increasing ferrate availability for *E. coli* inactivation (Barbeau et al., 2005).

Of note, comparable inactivation levels were achieved by using ferrate either as a coagulant aid (combined with alum) or as a disinfectant (after coagulation/flocculation /sedimentation). For example, ferrate (8 mg/L Fe) as a coagulant aid achieved 3.5-log removal (~ 0.8 log removal contributed by alum) compared to 3-log removals when used only as a disinfectant. These findings have a very important implementation in the full-scale practice where coagulation/flocculation/disinfection is initiated at a single unit without compromising the target treatment level.

The findings of this study were consistent with those of previous studies using WWF wastewaters. As such, 7 mg/L Fe of ferrate inactivated 2-log of *E. coli* presented in WWF sample (Elnakar and Buchanan, 2019). To achieve 3-log removal of *E. coli* in WWF sample within 30 minutes, 12 to 24 mg/L of performic acid were required (Tondera et al., 2016). In simulated WWF sample, high UV-doses of 214.1 to 428.7 mJ cm^{-1} were applied to achieve 2.2±2 log removal of *E. coli* while 8.4 to 12.8 mg/L of ozone was required to achieve 3.4 ± 2.1 log removal within 15 min (Tondera et al., 2015). Indeed, ferrate (10 mg/L Fe) with alum (6 mg/L Al) as coagulant aid removed > 5-log of *E. coli* within 31 minutes which complied with Alberta guidelines for surface water quality discharge (*E. coli* ≤ 100 CFU/100 mL) (Government of Alberta, 2018). As such, ferrate might be proposed as an effective approach for treating the wastewater during WWF condition.

It is hypothesized that the protonated species of ferrate (H_xFeO_4) are more reactive and predominantly available at acidic pH < 7.3 (pK_a=7.3) (Cho et al., 2006). As such, ferrate disinfection performance was evaluated at two different pH values (6 and 7.3) for practical implementation. In this study, no remarkable change in the inactivation level was noticed within the tested pH values (6 and 7.3). For instance, ferrate (8 mg/L Fe) had achieved 2.6 log removal of *E. coli* at pH=6 compared to 3.5 log removal at pH= 7.3 and similar inactivation level at higher doses (Figure 4. 9, b). A similar observation was also reported where the change of pH from 9 to 6 caused an insignificant change in ferrate inactivation of sewer biofilm (Yan et al., 2020). The authors ascribed that to the corresponding narrow change in the fraction of $HFeO_4^-$ (0.4% to 5%). However, another study showed that, by changing the pH from 7.5 to 5.5, the required dose of ferrate to achieve the same level of *E. coli* inactivation was reduced by one-third (Jiang et al., 2007). Therefore, for practical implementation, it is not feasible to lower the pH (strong acidic condition ≤5.5) to achieve the target inactivation level. Alternatively, increasing the ferrate dose might be more favorable to achieve the target level of inactivation and comply with the required pH (6.5 to 9) of the treated effluent wastewater (Government of Alberta, 2018).

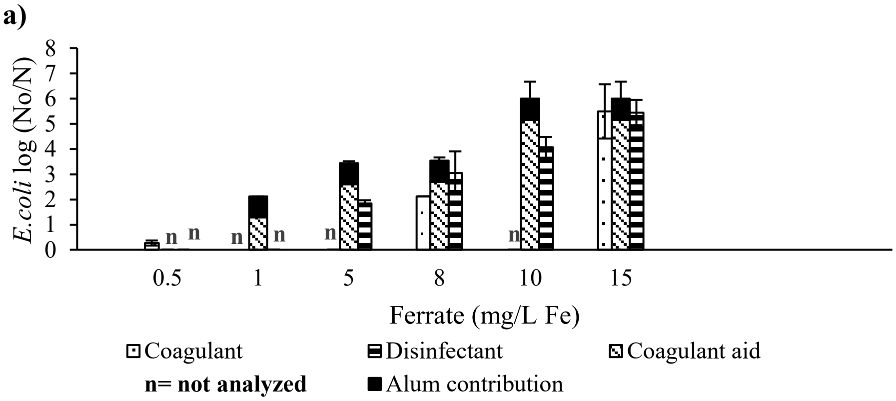

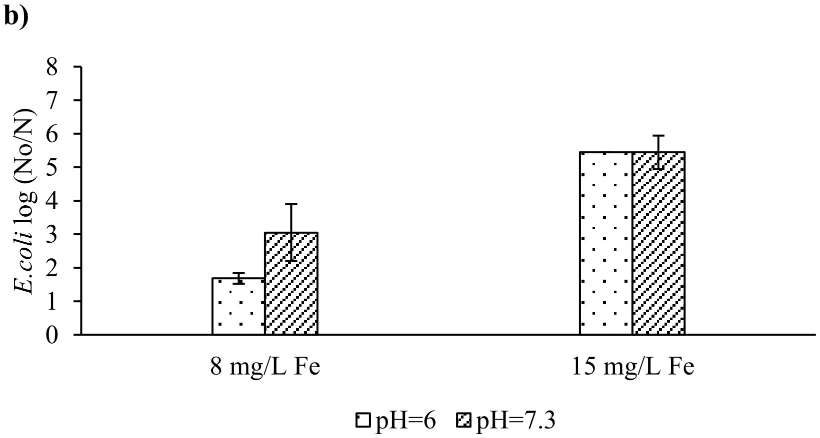

Figure 4. 9 a) The effect of dosing points on the *E. coli* removal by ferrate when used as coagulant/disinfectant injected alone, as coagulant aid/disinfectant injected with alum and as a disinfectant injected after coagulation/flocculation/sedimentation b) pH impact (original sample pH = 7.3 and adjusted pH = 6) when ferrate as a disinfectant.

4.4 Conclusions

The main objective of this study was to investigate the use of ferrate as a coagulant, coagulant aid, and disinfectant for enhanced primary treatment during wet weather flow. A two-level factorial design was used to optimize ferrate dose, polymer addition, and mixing conditions (rapid/slow). The experimental data showed that ferrate as a coagulant, applied with a cationic polymer (1.25 mg/L), achieved the best removals of turbidity, TSS and, COD at a low dose (0.5

mg/L Fe) at the high level of rapid mixing. ANOVA revealed that polymer addition and slow mixing had significant effects on the removal of turbidity, TSS and COD. General linear model equations were established and showed acceptable adequacy of fitting the obtained data to predict the removals. Ferrate applied as a coagulant at optimized conditions (ferrate dose =0.5 mg/L Fe, polymer dose=1.25 mg/L, high level of rapid mixing/low level of slow mixing) achieved the target level of TSS <25 mg/L but failed to reduce turbidity level to < 8 NTU Alum outperformed ferrate in the removal of turbidity and TSS when both were tested under similar conditions.

For the first time, this study explored ferrate as a coagulant aid with alum for treating the wastewater during WWF condition. The optimum dose of ferrate as 10 mg/L Fe was applied with 6 mg/L Al. At the optimum dose of alum/ferrate, the levels of TSS and turbidity and ferrate-induced iron particles were reduced and complied with the Alberta guidelines for surface water quality discharge.

The role of ferrate for disinfection was evaluated at three dosing points: first, added as a coagulant to raw WWF sample; second added as a coagulant aid with alum to raw WWF sample and third, added as a disinfectant to the primary effluent (after coagulation/flocculation/settling). A ferrate dose of 8 mg/L Fe achieved 2.1-log removal of *E. coli* when applied as a coagulant, 3.5-log removal when applied as a coagulant aid, and 3-log removal when applied as a disinfectant to the primary effluent.

In conclusion, this study found that using ferrate as a coagulant aid as a one-step treatment is a novel and effective approach for the enhanced primary treatment of wastewater during WWF conditions achieving the target level of TSS, turbidity, iron residual and *E.coli* removal collectively within 31 minutes.

4.5 References

Alameddine, M., Al Umairi, A.R., Zakee Shaikh, M. and Gamal El-Din, M. 2020. Bench to Full-Scale Enhanced Primary Treatment of Municipal Wastewater under Wet Weather Flow for Minimized Pollution Load: Evaluation of Chemical Addition and Process Control Indicators. Canadian Journal of Civil Engineering.

Government of Alberta. 2018. Environmental Quality Guidelines for Alberta Surface Waters. Water Policy Branch, Alberta Evironment and Parks. Government of Alberta, Edmonton,Alberta.

Amano, M., Lohwacharin, J., Dubechot, A. and Takizawa, S. 2018. Performance of integrated ferrate-polyaluminum chloride coagulation as a treatment technology for removing freshwater humic substances. Journal of Environmental Management 212, 323-331.

Anderson, M.J. 2015. Design of Experiments Simplified, Boca Raton, FL: CRC Press is an imprint of the Taylor & Francis Group, an Informa business.

American Public Health Association (APHA). 2017. Standard Methods for the Examination of Water and Wastewater, Washington, DC, USA.

Autixier, L., Mailhot, A., Bolduc, S., Madoux-Humery, A.-S., Galarneau, M., Prevost, M. and Dorner, S. 2014. Evaluating rain gardens as a method to reduce the impact of sewer overflows in sources of drinking water. Science of the Total Environment 499, 238-247.

Barbeau, B., Desjardins, R., Mysore, C. and Prevost, M. 2005. Impacts of water quality on chlorine and chlorine dioxide efficacy in natural waters. Water Research 39(10), 2024-2033.

Bunce, J.T., Ndam, E., Ofiteru, I.D., Moore, A. and Graham, D.W. 2018. A Review of Phosphorus Removal Technologies and Their Applicability to Small-Scale Domestic Wastewater Treatment Systems. Frontiers in Environmental Science 6.

Chhetri, R.K., Bonnerup, A. and Andersen, H.R. 2016. Combined Sewer Overflow pretreatment with chemical coagulation and a particle settler for improved peracetic acid disinfection. Journal of Industrial and Engineering Chemistry 37, 372-379.

Cho, M., Lee, Y., Choi, W., Chung, H.M. and Yoon, J. 2006. Study on Fe(VI) species as a disinfectant: Quantitative evaluation and modeling for inactivating Escherichia coli. Water Research 40(19), 3580-3586.

Deng, Y., Jung, C., Liang, Y., Goodey, N. and Waite, T.D. 2018. Ferrate(VI) decomposition in water in the absence and presence of natural organic matter (NOM). Chemical Engineering Journal 334, 2335-2342.

Doane, T.A. and Horwath, W.R. 2010. Eliminating interference from iron(III) for ultraviolet absorbance measurements of dissolved organic matter. Chemosphere 78(11), 1409-1415.

Duan, J.M. and Gregory, J. 2003. Coagulation by hydrolysing metal salts. Advances in Colloid and Interface Science 100, 475-502.

El Samrani, A.G., Lartiges, B.S. and Villieras, F. 2008. Chemical coagulation of combined sewer overflow: Heavy metal removal and treatment optimization. Water Res. 42(4-5), 951-960.

Elnakar, H. and Buchanan, I. 2019. The role of mixing in potassium ferrate(VI) consumption kinetics and disinfection of bypass wastewater. Journal of Environmental Management 231, 515-523.

Environment and Climate Change Canada (ECCC). 2019a. Wastewater Systems Effluent Regulations-2016 Status Report. Environment Canada, Gatineau, Quebec.

Environment and Climate Change Canada (ECCC). 2019b. Wastewater Systems Effluent Regulations Reported Data Environment. Canada, Gatineau, Quebec.

Environment and Climate Change Canada (ECCC). 2019c. Canadian Environmental Protection Act, 1999, Federal Environmental Quality Guidelines – Iron. National Guidelines and Standards Office, Environment Canada, Gatineau, Quebec.

Exall, K. and Marsalek, J. 2013. A Coagulant Survey for Chemically Enhanced Primary Treatment of Synthetic CSOs. Water Air and Soil Pollution 224(2), 9.

Fang, R., Cheng, X. and Xu, X. 2010. Synthesis of lignin-base cationic flocculant and its application in removing anionic azo-dyes from simulated wastewater. Bioresource Technology 101(19), 7323-7329.

Feng, M., Cizmas, L., Wang, Z. and Sharma, V.K. 2017. Activation of ferrate(VI) by ammonia in oxidation of flumequine: Kinetics, transformation products, and antibacterial activity assessment. Chemical Engineering Journal 323, 584-591.

Gandhi, R., Ray, A.K., Sharma, V.K. and Nakhla, G. 2014. Treatment of Combined Sewer Overflows Using Ferrate (VI). Water Environment Research 86(11), 2202-2211.

Gasperi, J., Laborie, B. and Rocher, V. 2012. Treatment of combined sewer overflows by ballasted flocculation: Removal study of a large broad spectrum of pollutants. Chemical Engineering Journal 211, 293-301.

Gibson, J., Farnood, R. and Seto, P. 2016. Chemical pretreatment of combined sewer overflows for improved UV disinfection. Water Science and Technology 73(2), 375-381.

Gombos, E., Barkacs, K., Felfoldi, T., Vertes, C., Mako, M., Palko, G. and Zaray, G. 2013. Removal of organic matters in wastewater treatment by ferrate (VI)-technology. Microchemical Journal 107, 115-120.

Goodwill, J.E., Jiang, Y.J., Reckhow, D.A., Gikonyo, J. and Tobiason, J.E. 2015. Characterization of Particles from Ferrate Preoxidation. Environmental Science & Technology 49(8), 4955-4962.

Government of Alberta 2018 Environmental Quality Guidelines for Alberta Surface Waters, Water Policy Branch Alberta Environment and Parks Edmonton, Alberta.

Graham, N.J.D., Khoi, T.T. and Jiang, J.Q. 2010. Oxidation and coagulation of humic substances by potassium ferrate. Water Science and Technology 62(4), 929-936.

Gromaire, M.C., Garnaud, S., Saad, M. and Chebbo, G. 2001. Contribution of different sources to the pollution of wet weather flows in combined sewers. Water Research 35(2), 521-533.

Jeon, J.C., Jung, Y.J., Kwon, K.H. and Min, K.S. 2017. Enhanced water quality of CSOs with different coagulant treatment. Desalination and Water Treatment 63, 469-477.

Jiang, J.Q. 2014. Advances in the development and application of ferrate(VI) for water and wastewater treatment. Journal of Chemical Technology and Biotechnology 89(2), 165-177.

Jiang, J.Q., Durai, H.B.P., Winzenbacher, R., Petri, M. and Seitz, W. 2015a. Drinking water treatment by in situ generated ferrate(VI). Desalination and Water Treatment 55(3), 731-739.

Jiang, J.Q. and Lloyd, B. 2002. Progress in the development and use of ferrate(VI) salt as an oxidant and coagulant for water and wastewater treatment. Water Research 36(6), 1397-1408.

Jiang, J.Q., Lloyd, B. and Grigore, L. 2001. Preparation and evaluation of potassium ferrate as an oxidant and coagulant for potable water treatment. Environmental Engineering Science 18(5), 323-328.

Jiang, J.Q., Wang, S. and Panagoulopoulos, A. 2006. The exploration of potassium ferrate(VI) as a disinfectant/coagulant in water and wastewater treatment. Chemosphere 63(2), 212-219.

Jiang, Y., Goodwill, J.E., Tobiason, J.E. and Reckhow, D.A. 2015b. Effect of Different Solutes, Natural Organic Matter, and Particulate Fe(III) on Ferrate(VI) Decomposition in Aqueous Solutions. Environmental Science & Technology 49(5), 2841-2848.

Jolis, D. and Ahmad, M.L. 2004. Evaluation of high-rate clarification for wet-weather-only treatment facilities. Water Environment Research 76(5), 474-480.

Jun, M. and Wei, L. 2002. Effectiveness of ferrate (VI) preoxidation in enhancing the coagulation of surface waters. Water Research 36(20), 4959-4962.

Karlesa, A., De Vera, G.A.D., Dodd, M.C., Park, J., Espino, M.P.B. and Lee, Y. 2014. Ferrate(VI) Oxidation of beta-Lactam Antibiotics: Reaction Kinetics, Antibacterial Activity Changes, and Transformation Products. Environmental Science & Technology 48(17), 10380-10389.

Kralchevska, R.P., Prucek, R., Kolarik, J., Tucek, J., Machala, L., Filip, J., Sharma, V.K. and Zboril, R. 2016. Remarkable efficiency of phosphate removal: Ferrate(VI)-induced in situ sorption on core-shell nanoparticles. Water Research 103, 83-91.

Kwon, J.H., Kim, I.K., Park, K.Y., Kim, Y.D. and Cho, Y.H. 2014. Removal of phosphorus and coliforms from secondary effluent using ferrate(VI). Ksce Journal of Civil Engineering 18(1), 81-85.

Lan, B.Y., Wang, Y.X., Wang, X., Zhou, X.T., Kang, Y. and Li, L.S. 2016. Aqueous arsenic (As) and antimony (Sb) removal by potassium ferrate. Chemical Engineering Journal 292, 389-397.

Lee, Y., Cho, M., Kim, J.Y. and Yoon, J. 2004. Chemistry of ferrate (Fe(VI)) in aqueous solution and its applications as a green chemical. Journal of Industrial and Engineering Chemistry 10(1), 161-171.

Lee, Y., Kissner, R. and von Gunten, U. 2014. Reaction of Ferrate(VI) with ABTS and Self-Decay of Ferrate(VI): Kinetics and Mechanisms. Environmental Science & Technology 48(9), 5154-5162.

Lee, Y., Zimmermann, S.G., Kieu, A.T. and von Gunten, U. 2009. Ferrate (Fe(VI)) Application for Municipal Wastewater Treatment: A Novel Process for Simultaneous Micropollutant Oxidation and Phosphate Removal. Environmental Science & Technology 43(10), 3831-3838.

Li, J.G., Dhanvantari, S., Averill, D. and Biswas, N. 2003. Windsor combined sewer overflow treatability study with chemical coagulation. Water Quality Research Journal of Canada 38(2), 317-334.

Lim, M. and Kim, M.-J. 2010. Effectiveness of Potassium Ferrate (K2FeO4) for Simultaneous Removal of Heavy Metals and Natural Organic Matters from River Water. Water Air and Soil Pollution 211(1-4), 313-322.

Lucas, W.C. and Sample, D.J. 2015. Reducing combined sewer overflows by using outlet controls for Green Stormwater Infrastructure: Case study in Richmond, Virginia. J. Hydrol. 520, 473-488.

Luo, Z.Y., Strouse, M., Jiang, J.Q. and Sharma, V.K. 2011. Methodologies for the analytical determination of ferrate(VI): A Review. Journal of Environmental Science and Health Part a-Toxic/Hazardous Substances & Environmental Engineering 46(5), 453-460.

Lv, D., Zheng, L., Zhang, H. and Deng, Y. 2018. Coagulation of colloidal particles with ferrate(vi). Environmental Science-Water Research & Technology 4(5), 701-710.

Makky, E.A., Park, G.-S., Choi, I.-W., Cho, S.-I. and Kim, H. 2011. Comparison of Fe(VI) (FeO42-) and ozone in inactivating Bacillus subtilis spores. Chemosphere 83(9), 1228-1233.

Marques, R.d.O. and Ferreira Filho, S.S. 2017. Flocculation kinetics of low-turbidity raw water and the irreversible floc breakup process. Environmental Technology 38(7), 901-910.

Marsalek, J. and Rochfort, Q. 2004. Urban wet-weather flows: Sources of fecal contamination impacting on recreational waters and threatening drinking-water sources. Journal of Toxicology and Environmental Health-Part a-Current Issues 67(20-22), 1765-1777.

McFadden, M., Loconsole, J., Schockling, A., Nerenberg, R. and Pavissich, J.P. 2017. Comparing peracetic acid and hypochlorite for disinfection of combined sewer overflows: Effects of suspended-solids and pH. Science of the Total Environment 599, 533-539.

Onen, V., Beyazyuz, P. and Yel, E. 2018. Removal of Turbidity from Travertine Processing Wastewaters by Coagulants, Flocculants and Natural Materials. Mine Water and the Environment 37(3), 482-492.

Phillips, P.J., Chalmers, A.T., Gray, J.L., Kolpin, D.W., Foreman, W.T. and Wall, G.R. 2012. Combined Sewer Overflows: An Environmental Source of Hormones and Wastewater Micropollutants. Environmental Science & Technology 46(10), 5336-5343.

Ravi Kumar Chhetri, D.T., Jesper Berner, Robin Gramstadd, Ulrik Öjstedt, Anitha Kumari Sharma, Henrik Rasmus Andersena 2016 Chemical disinfection of combined sewer overflow waters using performic acid or peracetic acids pp. 1065-1072, Elsevier B.V.

Rong, H., Gao, B., Dong, M., Zhao, Y., Sun, S., YanWang, Yue, Q. and Li, Q. 2013. Characterization of size, strength and structure of aluminum-polymer dual-coagulant flocs under different pH and hydraulic conditions. Journal of Hazardous Materials 252, 330-337.

Saritha, V., Srinivas, N. and Vuppala, S. 2017. Analysis and optimization of coagulation and flocculation process. Applied Water Science 7, 451-460.

Shah, M. and Pathak, K. 2010. Development and Statistical Optimization of Solid Lipid Nanoparticles of Simvastatin by Using 2(3) Full-Factorial Design. Aaps Pharmscitech 11(2), 489-496.

Shao, B., Dong, H., Feng, L., Qiao, J. and Guan, X. 2020. Influence of sulfite / Fe(VI) molar ratio on the active oxidants generation in Fe(VI)/sulfite process. Journal of hazardous materials 384, 121303-121303.

Shao, B., Dong, H., Sun, B. and Guan, X. 2019. Role of Ferrate(IV) and Ferrate(V) in Activating Ferrate(VI) by Calcium Sulfite for Enhanced Oxidation of Organic Contaminants. Environmental Science & Technology 53(2), 894-902.

Sharma, V.K. 2002. Potassium ferrate(VI): an environmentally friendly oxidant. Advances in Environmental Research 6(2), 143-156.

Sharma, V.K. 2011. Oxidation of inorganic contaminants by ferrates (VI, V, and IV)-kinetics and mechanisms: A review. Journal of Environmental Management 92(4), 1051-1073.

Sharma, V.K. 2013. Ferrate(VI) and ferrate(V) oxidation of organic compounds: Kinetics and mechanism. Coordination Chemistry Reviews 257(2), 495-510.

Sharma, V.K., Chen, L. and Zboril, R. 2016. Review on High Valent Fe-VI (Ferrate): A Sustainable Green Oxidant in Organic Chemistry and Transformation of Pharmaceuticals. Acs Sustainable Chemistry & Engineering 4(1), 18-34.

Sharma, V.K., Zboril, R. and Varma, R.S. 2015. Ferrates: Greener Oxidants with Multimodal Action in Water Treatment Technologies. Accounts of Chemical Research 48(2), 182-191.

Song, Y.L., Deng, Y. and Jung, C.I. 2016. Mitigation and degradation of natural organic matters (NOMs) during ferrate(VI) application for drinking water treatment. Chemosphere 146, 145-153.

Stanford, C., Jiang, J.Q. and Alsheyab, M. 2010. Electrochemical Production of Ferrate (Iron VI): Application to the Wastewater Treatment on a Laboratory Scale and Comparison with Iron (III) Coagulant. Water Air and Soil Pollution 209(1-4), 483-488.

Sumant, K., Ghosh, N.C. and Kazmi, A.A. 2016. Ballasted sand flocculation for water, wastewater and CSO treatment. Environmental Technology Reviews 5(1), 57-67.

Tao, W.D., Bays, J.S., Meyer, D., Smardon, R.C. and Levy, Z.F. 2014. Constructed Wetlands for Treatment of Combined Sewer Overflow in the US: A Review of Design Challenges and Application Status. Water 6(11), 3362-3385.

Thompson, G.W., Ockerman, L.T. and Schreyer, J.M. 1951. Preparation and purification of potassium ferrate .6. Journal of the American Chemical Society 73(3), 1379-1381.

Tondera, K., Klaer, K., Gebhardt, J., Wingender, J., Koch, C., Horstkott, M., Strathmann, M., Jurzik, L., Hamza, I.A. and Pinnekamp, J. 2015. Reducing pathogens in combined sewer overflows using ozonation or UV irradiation. International Journal of Hygiene and Environmental Health 218(8), 731-741.

Tondera, K., Klaer, K., Koch, C., Hamza, I.A. and Pinnekamp, J. 2016. Reducing pathogens in combined sewer overflows using performic acid. International Journal of Hygiene and Environmental Health 219(7), 700-708.

Vuong, T. and Monson, P.A. 1998. Surface roughness effects in molecular models of adsorption in heterogeneous porous solids. Langmuir 14(17), 4880-4886.

Wang, H.Y., Liu, Y.B. and Jiang, J.Q. 2016a. Reaction kinetics and oxidation product formation in the degradation of acetaminophen by ferrate (VI). Chemosphere 155, 583-590.

Wang, K.M., Shu, J., Wang, S.J., Hong, T.Y., Xu, X.P. and Wang, H.Y. 2020. Efficient electrochemical generation of ferrate(VI) by iron coil anode imposed with square alternating current and treatment of antibiotics. Journal of Hazardous Materials 384.

Wang, W.-g., Xu, Z.-x., Li, H.-z. and Jin, W. 2016b. Coagulation characteristics of organic pollutants removal in cso wastewater treatment. Environmental Engineering and Management Journal 15(1), 75-80.

Xiao, Y.H., Sara-Aho, T., Hartikainen, H. and Vahatalo, A.V. 2013. Contribution of ferric iron to light absorption by chromophoric dissolved organic matter. Limnology and Oceanography 58(2), 653-662.

Xu, Z.H., Wang, J.M., Shao, H.B., Tang, Z. and Zhang, J.Q. 2007. Preliminary investigation on the physicochemical properties of calcium ferrate(VI). Electrochemistry Communications 9(3), 371-377.

Yan, X., Sun, J., Kenjiahan, A., Dai, X., Ni, B.-J. and Yuan, Z. 2020. Rapid and strong biocidal effect of ferrate on sulfidogenic and methanogenic sewer biofilms. Water Research 169.

Yang, K., Li, Z., Zhang, H., Qian, J. and Chen, G. 2010. Municipal wastewater phosphorus removal by coagulation. Environmental Technology 31(6), 601-609.

Yates, B.J., Zboril, R. and Sharma, V.K. 2014. Engineering aspects of ferrate in water and wastewater treatment - a review. Journal of Environmental Science and Health Part a-Toxic/Hazardous Substances & Environmental Engineering 49(14), 1603-1614.

Young, S., Stanley, S.J. and Smith, D.W. 2000. Effect of mixing on the kinetics of polymer-aided flocculation. Journal of Water Services Research and Technology-Aqua 49(1), 1-8.

Yu, M.R., Chang, Y.Y., Keller, A.A. and Yang, J.K. 2013. Application of ferrate for the treatment of metal-sulfide. Journal of Environmental Management 116, 95-100.

Yu, W.Z., Yang, Y.J. and Graham, N. 2016. Evaluation of ferrate as a coagulant aid/oxidant pretreatment for mitigating submerged ultrafiltration membrane fouling in drinking water treatment. Chemical Engineering Journal 298, 234-242.

Yuan, B.L., Qu, J.H. and Fu, M.L. 2002. Removal of cyanobacterial microcystin-LR by ferrate oxidation-coagulation. Toxicon 40(8), 1129-1134.

Zhan, X., Gao, B., Wang, Y. and Yue, Q. 2011. Influence of velocity gradient on aluminum and iron floc property for NOM removal from low organic matter surfacewater by coagulation. Chemical Engineering Journal 166(1), 116-121.

Zheng, L. and Deng, Y. 2016. Settleability and characteristics of ferrate(VI)-induced particles in advanced wastewater treatment. Water Research 93, 172-178.

Zhu, W., Seth, R. and Lalman, J. 2007. Evaluation of a micro carrier weighted coagulation flocculation process for the treatment of combined sewer overflow. Environmental Technology 28(7), 761-770.

Chapter 5: Ferrate as a Potential Disinfectant for Enhanced Primary Treatment Effluent during Wet Weather Flow Condition: Kinetic Study, Mode of Action, Hydrogen Peroxide *in-situ* Production and Toxicity Analysis

5.1 Introduction

Wastewater discharge during wet weather flow (WWF) could significantly increase the microbial and contaminant loads (organic and inorganic) in the receiving surface water bodies (Marsalek and Rochfort, 2004; Wojtenko et al., 2001). For instance, in cold country like Canada, snowmelt along with wet weather runoff contaminate significantly drinking water sources with micropollutants (e.g. carbamazepine, caffeine and acetaminophen) and microorganisms (e.g. *Escherichia coli* (*E. coli*)) (Madoux-Humery et al., 2013). Moreover, WWF proved to increase the levels of total coliform and pathogenic species (*Giardia*, *Cryptosporidium*, *Enterocytozoon bieneusi*) in surface water (Huang et al., 2017; Rechenburg et al., 2006). Therefore, to protect the aquatic lives and end-users during WWF, effective treatments are required for microbial inactivation. Numerous techniques are used for microbial reduction such as ultra-membrane filtration (UF), ultraviolet radiation (UV), chemical disinfection (e.g. ozonation, chlorination). UF and UV are not suitable for WWF wastewater treatment due to high solids contents in the water resulting in membrane fouling and impairing UV absorbance (Li et al., 2017b; Zondervan and Roffel, 2007). While ozone and chlorine are powerful disinfectants, they may generate regulated disinfection by-products (DBPs) such as trihalomethane, chlorate and bromate (Chhetri et al., 2014; Jessen et al., 2008; Lee et al., 2016). In the past decades, ferrate has emerged as a potential alternative disinfectant used for water and wastewater treatment (Cho et al., 2006; Fan et al., 2018; Ghernaout and Naceur, 2011). Ferrate is subjected to step-wise self-decay reactions and form reactive intermediate species (Fe (V), Fe(IV), radical species ($^{\bullet}OH$, $O_2^{\bullet-}$), hydrogen peroxide which may contribute in oxidation and disinfection process (Cho et al., 2006;

Jiang et al., 2006; Lee et al., 2014). Several studies demonstrated that ferrate effectively inactivated total coliform, fecal coliform, and *E. coli* in drinking water and municipal wastewater (Cho et al., 2006; Jessen et al., 2008; Kwon et al., 2014). In addition, there has been evidence on the effect of ferrate for the removal of DBPs precursors (e.g. natural organic matter and bromide, cyanobacteria), which may give an advantage for ferrate over chlorine and ozone (Dong et al., 2019; Fan et al., 2018; Jiang et al., 2016; Makky et al., 2011). However, there have been limited studies (Gandhi et al., 2014; Elnakar and Buchanan, 2019) on ferrate as an alternative disinfectant/coagulant for WWF wastewater treatment.

The disinfection kinetic of ferrate were mostly studied in clean water matrices (Cho et al., 2006; Fan et al., 2018; Hu et al., 2012b; Jessen et al., 2008; Jiang et al., 2007; Makky et al., 2011) and to a lesser extent in real wastewater (Elnakar and Buchanan, 2019; Fan et al., 2018; Kwon et al., 2014; Manoli et al., 2020). The impact of temperature on ferrate inactivation kinetic was studied previously using Bacillus subtilis spores (Makky et al., 2011) or Bacteriophage MS2 (Hu et al., 2012b). However, no study evaluated temperature effect on inactivation of fecal indicator bacteria by ferrate. Such a study is important for a better understanding of the efficacy of ferrate for wastewater treatment during WWF occurring under different temperatures.

This study aimed to evaluate ferrate as an alternative disinfectant for the enhanced primary treatment (EPT) effluent during WWF. Disinfection kinetic experiments were performed, and the effect of temperature was assessed. *E. coli* was used as an indicator for the bacterial inactivation. Three different kinetic models were examined, namely Chick-Watson, Hom and Collins-Selleck and their adequacies were examined by comparing the measured inactivation levels versus the predicted values and obtaining the adjusted R^2 (includes only variables which improve the prediction of regression model). Moreover, flow cytometry analysis was conducted to propose a mode of action for ferrate during *E. coli* inactivation by evaluating membrane integrity and DNA damage. Nonetheless, this study shed the light on the potential benefits of *in-situ* produced hydrogen peroxide and acute toxicity of ferrate treated samples using *vibrio fischeri* bioassay. Ultimately, this work provided vital information about the behaviors of ferrate as a disinfectant and gave a better understanding to scale-up its application.

5.2 Materials and method

5.2.1 Sampling and jar test

Primary influent wastewater samples were collected from a wastewater treatment plant (WWTP) located in Alberta. The samples were diluted by deionized (DI) water (to the ratio 1:1) to mimic the condition of WWF. They were then treated with alum (75 mg/L) using a Jar tester (PB-700^{TM} JARTESTER (PHIPPS&BIRD^{TM}) with rapid mixing at 150 rpm (rotations per minute) for 1 minute and slow mixing at 15 rpm for 10 minutes followed by settling for 20 minutes. The wastewater characteristics are presented in Table 1. Samples were collected from the supernatant and transferred to a beaker (2 L) for the kinetic study. The beaker was provided with a magnetic stirrer to maintain a sufficient dispersion of ferrate during the experiment. A ferrate stock solution (purity >76%) was freshly prepared in potassium hydroxide (KOH) solution at pH= 9 before each run and was used within 30 minutes to minimize the effect of self-decomposing.

Table 5. 1 Water quality parameters average values ± standard deviation of enhanced primary treatment effluent during wet weather flow used for disinfection kinetic study

Parameter	**Values**
pH	7.21 ± 0.2
Turbidity (NTU)	8.97 ± 0.7
COD (mg/L)	49.16 ± 23.8
UVT %	74.9 ± 6.93
OP (mg/L)	2.15 ± 0.1
***E. coli* (MPN/100mL)**	$2.1 \times 10^4 \pm 9.3 \times 10^3$

5.2.2 Measurement of time-dependent ferrate concentration

The concentration of ferrate stock solution was obtained by the direct spectrophotometric method according to which the absorbance was measured at 510 nm using Genesys 10S UV−vis. spectrophotometer (Thermo Scientific) and divided by a coefficient of absorptivity (1150 $M^{-1}cm^{-1}$)(Hernandez et al., 2017). Three doses of ferrate (5, 8 and 10 mg/L Fe) were used to evaluate the dose-effect on inactivation of *E. coli.* Throughout each run, two sets of samples were collected at pre-determined time intervals the first set was used to measure ferrate residual and the second set for *E. coli* quantification. Ferrate residual concentration was determined by using 2,2-azino-bis(3-ethylbenzothiazoline-6sulfonate (ABTS) spectrophotometric method (detection range 0.00168 to 1.96 mg/L Fe) with molar absorptivity of 34000 $M^{-1}cm^{-1}$ at 415 nm. ABTS reacted with ferrate rapidly ($t_{1/2}$=0.1 s) and form green radical cation ($ABTS\bullet^{+}$) which is very stable for several hours (10 hr) (Lee et al., 2005). The measurement accuracy was verified by comparing the results of the ABTS method with those of the direct spectrophotometric method. Ferrate concentration was calculated using equation 1 below (Luo et al., 2011).

$$[\text{Ferrate}]_{\text{sample}}=A_{415}V_{\text{final}} / \varepsilon V_{\text{sample}} \qquad (5.1)$$

Where A_{415} is the absorbance at 415 nm, V_{final} is the final volume after addition all solutions (ABTS reagent, ABTS buffer, DI water and sample), ε is molar absorptivity $(3.4 \pm 0.05) \times 10^4$ $M^{-1}cm^{-1}$ and V_{sample} is actual sample volume before adding ABTS reagents and DI water.

The preparation of all chemicals for the ABTS method was carried out based on the described method by Lee and the co-authors (Lee et al., 2005). Briefly, ABTS reagent stock solution was prepared by dissolving 1 g of diammonium-ABTS salt (Aldrich) into 1 liter of deionized (DI) water to produce a final concentration of 1.82 mM which then stored at 4 °C. The ABTS buffer (all chemicals were purchased from Fisher Scientific) of pH 4.1 was prepared by adding 34.3 mL of acetic acid (CH_3COOH), 6.9 g of sodium dihydrogen phosphate monohydrate ($NaH_2PO_4.H_2O$) and 26.7 g of disodium monohydrogen phosphate dihydrate ($Na_2HPO_4.2H_2O$) into 1 liter of DI to produce 0.6 M of acetate and 0.2 M phosphate solution.

5.2.3 E. coli quantification

IDEXX™ method was used for *E. coli* quantification throughout this study. All accessories for the quantification was purchased from IDEXX™. The sample was collected in sterilized plastic vessels (100 mL) provided with sodium thiosulfate to quench residual ferrate. They were topped by DI water as per the required dilution factor and transferred to quanti-tray plates (Quaniti-Tray®/2000). After, the incubation period (18 hr at 35±0.5 ˚C), blue fluorescing wells (exposed to 6-watt fluorescent UV lamp at 365 nm) were counted as positive and accordingly most probable number (MPN) was obtained. To investigate the effect of temperature, one set of experiments were conducted at room temperature (19 °C) and another at 9 °C in a temperature-controlled room. All experiments were conducted in duplicates and average results were reported.

5.2.4 Inactivation kinetic modelling

In this study, the inactivation of *E. coli* by ferrate was described by three different models namely: Chick-Watson, Hom and Collins-Selleck which were used successfully to describe the inactivation of total coliform, fecal coliform and *E. coli* (Cho et al., 2006; Gyurek and Finch, 1998; Henao et al., 2018; Najm, 2006). Chick-Watson model assumes a linear correlation of log reduction and time (equation 5.2). The dose coefficient (n) expresses the concentration importance relative to time thus n>1 indicates that concentration is more important than time to cause the inactivation (Ganguly et al., 2018). The disinfection rate constant (*k*) and n are calculated by linear regression (Lambert et al., 1999):

$$\log\left(\frac{N}{N_o}\right) = -k\mathrm{C}^{\mathrm{n}}\mathrm{t} \qquad (5.2)$$

Where; N survival bacteria at any time, N_o= initial population of bacteria, *k* is inactivation rate constant (L/(mg.min)), C is the disinfectant concentration (mg/L), n is dilution factor and t is contact time (minute)

Hom model (equation 5.3) accounts for non-linear correlation of log reduction versus time by modifying equation 5.2 and incorporating a time coefficient (h) in which h>1 indicates the presence of shoulder and h<1 indicates tailing-off effect (Haas and Karra, 1984).

$$\log\left(\frac{N}{N_o}\right) = -k\mathrm{C}^{\mathrm{m}}\mathrm{t}^{\mathrm{h}} \qquad (5.3)$$

The values of k, m and h were obtained by using multiple linear regression analysis and setting log (-log N/N_o) as the dependent variable while log C and log t as an independent variable (Lambert et al., 1999).

Collins-Selleck model (equation 5.4,) was used to account for initial lag and deceleration in the inactivation process. It was found to fit properly the bacterial inactivation kinetics data using different disinfectants (e.g. chlorine, peracetic acid, ozone) with d as an empirical coefficient (unitless) and k as the lag coefficient (mg min/L) (Gyurek and Finch, 1998; Haas and Karra, 1984). Collins-Selleck model accounts for initial lag at Ct> k indicates the lag presence (equation 5.4 = 0) and k > Ct expressed by equation 5.4 (Hassaballah et al., 2019).

$$\log(\frac{N}{N_o}) = -d\log(\frac{Ct}{k}) \qquad (5.4)$$

5.2.5 Flow Cytometry (FCM) Analysis

Flow cytometry (FCM) analysis was conducted with double staining method (SYBR Green I (SGI), propidium iodide (PPI)) to evaluate the bacterial cell viability and membrane and DNA damage after ferrate treatment. SGI can bind with DNA of bacteria with an intact or damaged cell membrane (Berney et al., 2006; Lee et al., 2016). By contrast, PPI binds only with the DNA of bacterial cells with a damaged membrane (i.e. dead cell) (Berney et al., 2008b). Moreover, when both dyes are combined (SGI/PPI), a distinct pattern of membrane integrity and cell viability can be seen under given conditions (Berney et al., 2007). This method was used previously to identify the membrane integrity and cell viability of *E. coli*, *bacillus subtilis,* and heterotrophic bacteria in pure, fresh and marine water matrices (Barbesti et al., 2000; Gregori et al., 2001; Ramseier et al., 2011). As such, a lab-cultured bacteria *E. coli* strain (ATCC25922) (purchased from ATCC) was spiked into phosphate-buffer solution (25 mM, pH=7.2) to mimic the alkaline medium of real wastewater samples. The presence of *E. coli* in the control sample (ferrate =0 mg/L Fe) was verified using the IDEXX™ method and the initial concentration was 1.09 x 10^4 (MPN/ 100 mL). Samples were treated with different doses of ferrate: 1, 3 and 5 mg/L Fe for 20 minutes of contact time. The staining procedures for FCM analysis were performed according to the method described previously (Berney et al., 2008a; Lee et al., 2016). Briefly, a working solution of SYBR® Green I (SGI) (Sigma-Aldrich) was prepared by diluting the SGI (10,000 x DMSO) 100-fold using anhydrous dimethyl sulfoxide (DMSO). A mixture of SGI and propidium iodide (PPI) was prepared by mixing the SGI working solution with a 1.5 mM PPI (Sigma-Aldrich, 1g/L with MW=668.39 g/mole) to a final PPI concentration of 0.6 mM. All working solutions of dyes (SGI and SGI/PPI mixture) were stored in dark at -20 °C until use. Every 1 ml of sample was stained with 10 µL of SGI or SGI/PPI. Before FCM analysis, the samples were incubated in a dark environment for 15 min. FCM was conducted using (BD LRSFortess^{TM} X-20 Flow Cytometer) where the red fluorescence collected at 586 nm and green fluorescence collected at 530 nm.

5.2.6 Hydrogen peroxide quantification and acute toxicity analysis

The measurement of hydrogen peroxide was conducted by using the spectrophotometric method. Titanium oxysulfate was added to the sample (2 mL of sample + 0.2 mL of titanium oxysulfate) which instantaneously form a yellow complex and absorbance intensity measured at 410 nm and compared with the calibration curve. Absorbance was measured using Genesys 10S UV−vis. spectrophotometer (Thermo Scientific).

Acute toxicity was evaluated by Microtox® 500 Analyzer (Azur Environmental, Carlsbad, USA) and 81.9% screen test protocol was followed. The bioluminescence indicator was *vibrio fischeri* which reconstituted and inoculated into tested samples. The change in the luminescence was measured after 15 minutes of incubation. The inhibition percentage was calculated with reference to the control sample.

5.3 Results and Discussion

5.3.1 Dose and temperature effect on ferrate-decay and the bacterial inactivation

E. coli inactivation was tested using different doses of ferrate (5, 8 and 10 mg/L Fe) under different temperatures (9 and 19 °C) at a fixed contact time of 20 (Figure 5. 1, a and b). The decomposition of ferrate was observed under different temperatures and the stability of ferrate reduced with temperature increment (Figure 5. 1, a and b). As such, at a lower temperature (9 °C) after 3 minutes, lower consumption of ferrate doses 5, 8 and 10 mg/L Fe were observed as 88%, 74% and 73% respectively (Figure 5.1 a). In contrast, at a higher temperature (19 °C) after 3 minutes, higher consumption of ferrate doses 5, 8 and 10 mg/L Fe were observed as 94%, 88% and 78% respectively (Figure 5.1, b).

The effect of ferrate dose and temperature on the level of *E. coli* inactivation is presented in Figure 5. 1 c and d. Both ferrate dose and temperature affected bacterial inactivation positively. In specific, by increasing the ferrate dose from 5 to 10 mg/L Fe, the inactivation levels increased from less than 2 log removal to more than 3.5 log removals regardless of the temperature. Likewise, by increasing the temperature from 9 °C to 19 °C, the inactivation level corresponding to ferrate doses 8 and 10 mg/L Fe increased by 0.5 log removal. This was confirmed by using statistical analysis using ANOVA that showed that, both dose level and temperature have significant effects on inactivation levels (Table C. 1). Previous studies also reported that the level of inactivation increased by increasing temperatures during the inactivation of Bacteriophage MS2 (virus) and bacillus subtilis spores (protozoa indicator) using ferrate(Hu et al., 2012b; Makky et al., 2011).

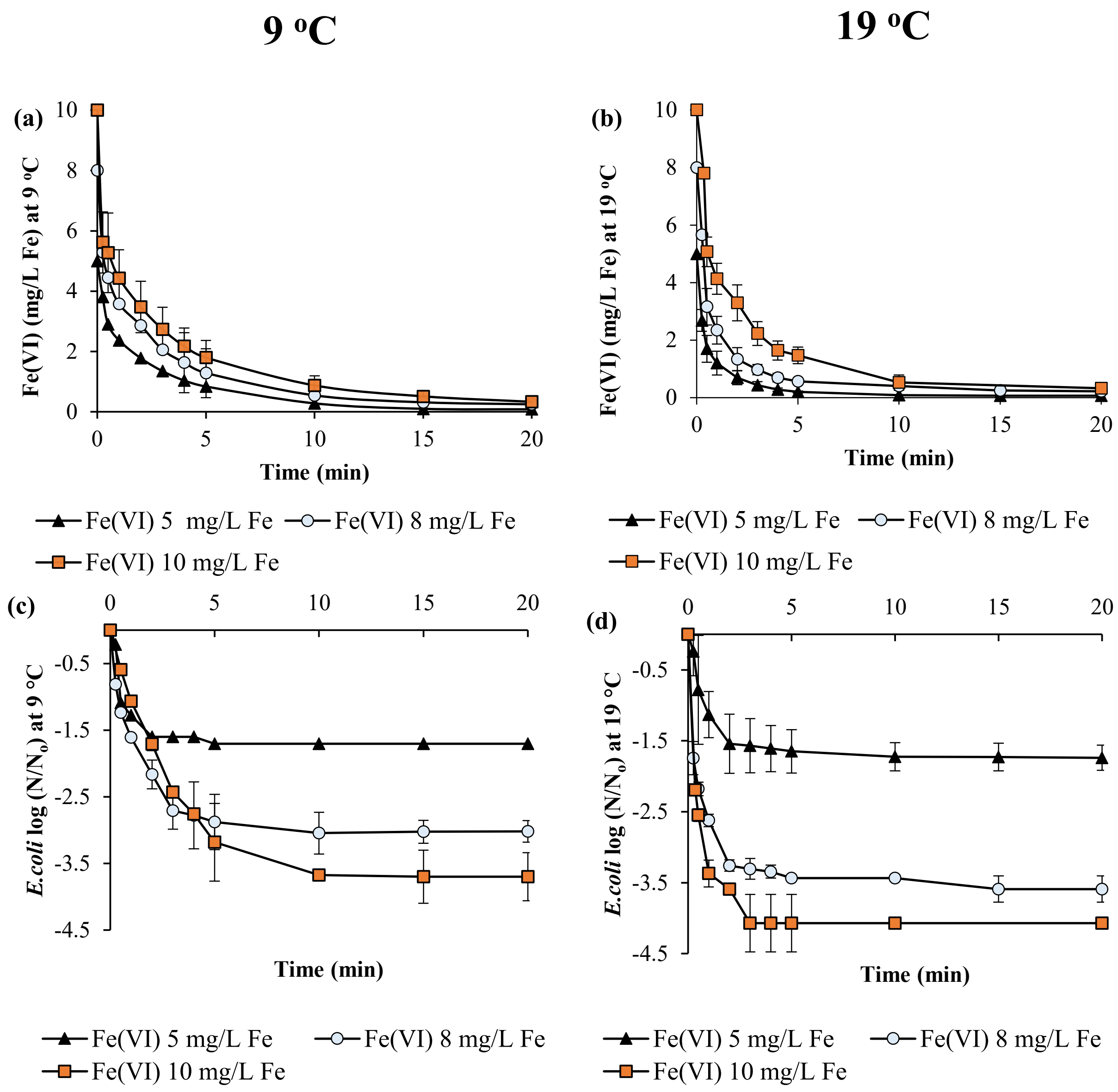

Figure 5. 1 Ferrate degradation (5,8 and 10 mg/L Fe): a) temperature 9 °C, b) temperature 19 °C and *E. coli inactivation :* c) temperature 9 °C, d) temperature 19 °C during disinfection kinetic experiments (20 minutes contact time) treating effluent of enhanced primary treatment during wet weather flow.

The contact time is a very important factor for the disinfection process: under lower temperature longer contact time is required to achieve higher inactivation levels (Figure 5. 2 a and b). Therefore, at a lower temperature (9 °C) by increasing the contact time from 3 minutes to 10 minutes the log removal increased from 2.4 to 3.7 corresponding to 10 mg/L Fe of ferrate (Figure 5. 2, a).

The water matrix has significant impacts on the efficacy of the used disinfectant. As such, using EPT effluent during WWF condition (COD= 49 mg/L Fe, ferrate= 8 mg/L Fe, 19 °C), 3.6 log removal was achieved in this study, compared to 2 log removal achieved in raw WWF wastewater (COD= 623 mg/L, ferrate 7 mg/L Fe, 25±1 °C) (Elnakar and Buchanan, 2019) within approximately 20 minutes of contact time in both studies. Other studies showed that lower ferrate doses (4 to 6.25 mg/L Fe) achieved ≥ 3 log removal of *E. coli* suspended in a buffered solution with a contact time that varied between 1 and 30 minutes (Cho et al., 2006; Jiang et al., 2007). The aforementioned discrepancies in the performance of ferrate can be attributed to the differences in the experimental condition (i.e. wastewater matrices, pH, and the initial microbial concentration and ferrate dose level).

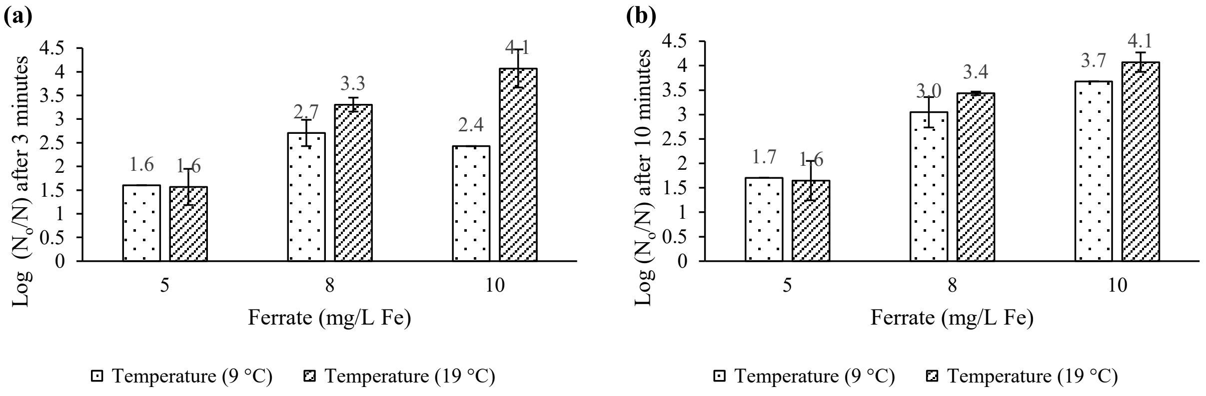

Figure 5. 2 Effect of contact time on log removal level under two different temperatures (19 °C and 9 °C): a) 3 minutes contact time, b) 10 minutes contact time treating effluent of enhanced primary treatment during wet weather flow.

5.3.2 Kinetic modeling of ferrate-decay

Figure 5. 3 (a to f) shows the kinetic modeling of ferrate-decay corresponding to different doses 5, 8 and 10 mg/L Fe under two different temperatures: 9 and 19 ˚C. The obtained data fit properly into a second-order kinetic model with high R^2 (0.98-0.99) for all tested ferrate doses (5, 8, and 10 mg/L Fe). Other studies also reported that the second-order kinetic model fits properly the ferrate-decay during bacterial inactivation (Cho et al., 2006; Elnakar and Buchanan, 2019). The ferrate-decay rate constant obtained in this study was 0.98 (L/(mg.min)) for ferrate dose of 5 mg/L was comparable to that reported in secondary effluent as 1.571(L/(mg.min)) (pH=7.5, COD=31.5 mg/L)(Zheng and Deng, 2016). Of note, the reported rate constants in phosphate-buffered solutions (0.102 to 0.135 (L/(mg.min) (Cho et al., 2006; Hu et al., 2012b) were lower than those obtained in real wastewater matrices (EPT effluent (this study), secondary effluent Zheng and Deng (2016)). That may ascribe to the phosphate complexation with ferric species which proved to inhibit ferrate-decay (Jiang et al., 2015). Temperature showed insignificant effects on the obtained ferrate-decay rate constants and that was further supported by ANOVA findings (Table C. 2). For instance, ferrate rate constant for dose of 10 mg/L Fe was 0.1525 (L/(mg.min)) at 19 °C which dropped slightly to 0.1395 (L/(mg.min)) at lower temperature (9 °C). Similarly, in a previous study, it was also reported that ferrate-decay rate constant slightly change with temperature (5 to 30 °C) (e.g. $k_{10\ °C}$= 0.073, $k_{20\ °C}$ =0.083 (L/(mg.min)) (Hu et al., 2012b). In principle, the increase in temperature was expected to increase the collision energy of reactant molecules thus increase the rate constant (Laidler, 1984). Ferrate- rate constant showed independency of temperature, which might be ascribed to lower steric factor (effective collision/total collision) (Yao and Haag, 1991). In fact, verification of this hypothesis is not in the scope of this study and an in-depth study might be required to uncover this concept. The half-lives

corresponding to the ferrate-decay rate constants were calculated and depicted in Table C. 3. In general, the half-lives of ferrate were inversely correlated with temperature thus at the higher temperature, a lower half-life was obtained and vice versa. The half-life might also be affected by the pH of the solution: at pH of 7.2, the half-life of ferrate found to be 17 minutes whereas at pH 8.2 it was 190 min during inactivation of murine norovirus tested in phosphate buffer solution (10 mM) (ferrate =1.05-1.16 mg/L Fe, N_o= 917-935 PFU/mL) (Manoli et al., 2020).

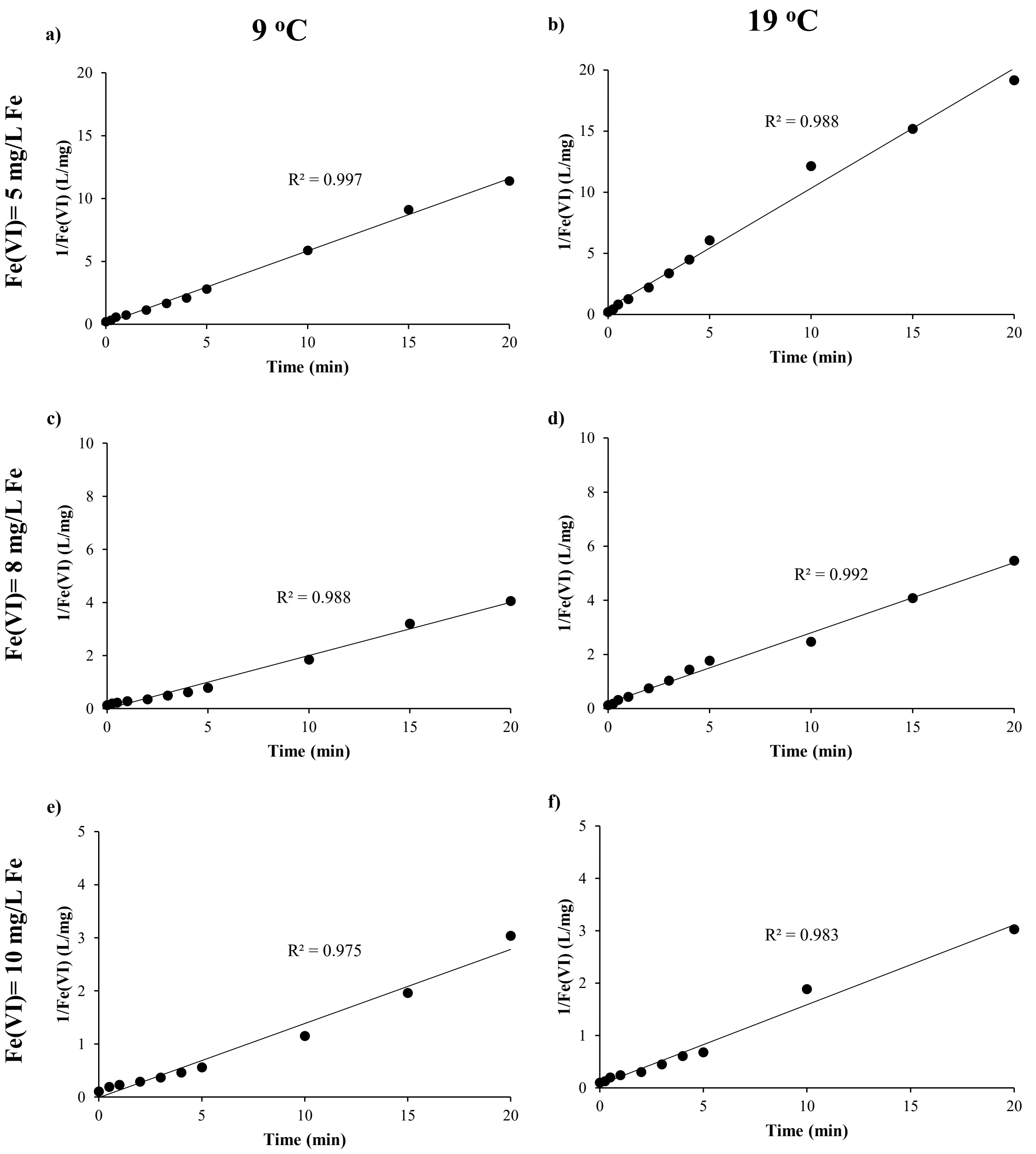

Figure 5. 3 Ferrate decay follows second order during *E. coli* inactivation presented in effluent of enhanced primary treatment during wet weather flow for different doses of ferrate and temperatures: ferrate dose 5 mg/L Fe; a) temperature 9 °C and b) temperature 19 °C; ferrate dose 8 mg/L Fe; c) temperature 9 °C and d) temperature 19 °C; ferrate dose 10 mg/L Fe; e) temperature 9 °C and f) temperature 19 °C.

5.3.3 *E. coli inactivation kinetic modeling*

The tested models could successfully describe the obtained data in the following order: Chick-Watson ≈ Hom > Collins-Selleck model with adjusted $R^2 \geq 0.94$ (Table 5.2). All three models were validated by comparing the measured inactivation levels with the predicted levels (Figure 5. 4). The goodness of fit test (based on the Anderson-Darling test) showed that the differences between the measured and the predicted data were normally distributed (Table C 4). In this study, ferrate-decay was predicted by the second-order kinetic model and based on that the instantaneous concentration of ferrate was included in the used disinfection kinetic models. The obtained data showed that there was no lag-phase in the ferrate disinfection of *E. coli* and that depicted in Figure 5. 4. That indeed came in agreement with findings of other studies when ferrate was applied to different water matrices for inactivating total coliform, fecal coliform, *E. coli* and Bacteriophage MS2 (buffered solution, secondary effluent and saline water) (Cho et al., 2006; Hu et al., 2012a; Kwon et al., 2014). Of note, the Collins-Selleck model obtained the lowest adjusted R^2 compared to the other tested models because it showed lag-phase (Figure 5.4, circled by red line) which makes it deviated from the measured data. The tailing-off became more significant as ferrate dose decreased under both temperatures, yet the used models fitted the obtained data adequately (Figure 5. 4). Different hypotheses might explain the presence of tailing-off. Firstly, the decrease in the biocidal effect of the disinfectant, which became more obvious with lower initial dose and lower temperature (Figures 5. 3 and 5. 4). It was also suggested that tailing-off might be related to shielding effect of microbial clumping which provide protection from disinfectant (Campo et al., 2020; Liang et al., 2013). Moreover, the ability of microorganism to change their properties and developing resistance potency might also explain tailing effect (Sigstam et al., 2014).

In this study, the *E. coli* inactivation rate constant (*k*) was 1.328 (L/(mg.min)) (Chick-Watson, 19 ˚C, ferrate= 5 mg/L) which was higher than that reported in saline water *k*= 0.39 (L/(mg.min)) (pH= 8, ferrate=0.25 to 5 mg/L Fe, N_o= 1x10^7 MPN/ml) (Jessen et al., 2008) or in phosphate buffer solution as 0.625 (L/(mg.min)) (pH=7.2, ferrate dose=1.4-6.25 mg/L Fe, N_o= 4 x 10^5 to 1x10^6 CFU/ mL) (Cho et al., 2006). Similar observation was reported in a previous study in which ferrate achieved higher inactivation rate constant (2 times higher) in secondary effluent compared to that achieved in phosphate buffer solution (Manoli et al., 2020). That might be attributed to the inhibition impact of buffer solution (e.g. phosphate) on the ferrate-decomposition and formation of reactive species (Fe(V), Fe(IV)) thus reduced ferrate reactivity (i.e. lower *k*) (Jiang et al., 2015; Wang et al., 2016). In this study, the calculated lag coefficient (*k*) based on Collins-Selleck model was 0.54 (mg.min/L) (ferrate = 5 mg/L at 19˚C) compared to 1.1(mg.min/L) when peracetic acid (PAA) used in secondary effluent (PAA=2 to 6 mg/L, N_o=10^4 to 10^5 CFU/100 mL, pH=7.1, TOC=13 mg/L) (Hassaballah et al., 2019). Indeed, a higher lag coefficient indicates a weaker disinfectant. The efficiency of the disinfection process depends on the targeted microorganism, water matrix, physiochemical properties of the disinfectant (Li et al., 2017a). A summary of different inactivation kinetic studies corresponding to ferrate and other disinfectants were presented in Table C. 5. In general ferrate showed a better performance than other disinfectants such as peracetic acid and performic acid (Campo et al., 2020) and comparable performance with chlorine (Owoseni et al., 2017). Ozone surpassed ferrate and achieved higher inactivation rate of *E. coli* (1.92 x 10^3 (L/(mg.min)) (Czekalski et al., 2016) and *bacillus subtilis* spores (0.9 (L/(mg.min)) (Makky et al., 2011). Table 5. 3 summarizes the predicted CT (mg/L. min) based on the Chick-Watson model to achieve 1-4 log removal of *E. coli* by ferrate (this study) and compared to that achieved by other disinfectants (ozone, performic acid (PFA), peracetic acid

(PAA) and free chlorine). It was clear that ozone outperformed other disinfectants by achieving the target log removal with lower CT values. For example, ozone achieved 3-log removal with CT value of 0.0016 mg/L. min while CT should be 4 mg/L. min by ferrate and > 12 mg/L. min by other disinfectants. As per the summarized studies the effectiveness of disinfectant came in order from O_3>Fe(VI)> PFA ~ chlorine> PAA. That being stated, ferrate might be considered as a promising disinfectant because of its outstanding performance and benign impacts on the environment (i.e. no DBPs) (Hu et al., 2018).

Table 5. 2 summary of the three tested disinfection models with corresponding parameters and R^2 obtained for different doses under different temperatures

Parameter / Model							
Ferrate dose	mg/L Fe	**5**		**8**		**10**	
Temperature	°C	**9 °C**	**19 °C**	**9 °C**	**19 °C**	**9 °C**	**19**
Ferrate-decay rate constant	**k'** (L/(mg.min))	0.58	0.98	0.2	0.26	0.14	0.15
Chick-Watson	**n**	1.01	0.89	0.94	1.04	0.72	1.12
	k (L/(mg.min))	1.04	1.33	0.61	1	0.46	0.7
	Adjusted R^2	>0.99	>0.99	>0.99	>0.99	0.95	>0.99
Hom	**m**	1.03	2.76	1.21	0.85	2.66	0.85
	h	1.02	2.73	1.22	0.84	2.66	0.79
	k (L/(mg.min))	1.03	1.85	0.45	1.2	0.02	1.02
	Adjusted R^2	0.96	>0.99	0.98	0.98	0.98	0.97
Collins-Selleck	**d**	2.97	6.85	5.91	5.08	13.12	4.56
	k ((mg.min)/L)	0.45	0.56	1.48	0.75	3.64	0.76
	Adjusted R^2	0.96	0.98	0.94	0.97	0.94	0.95

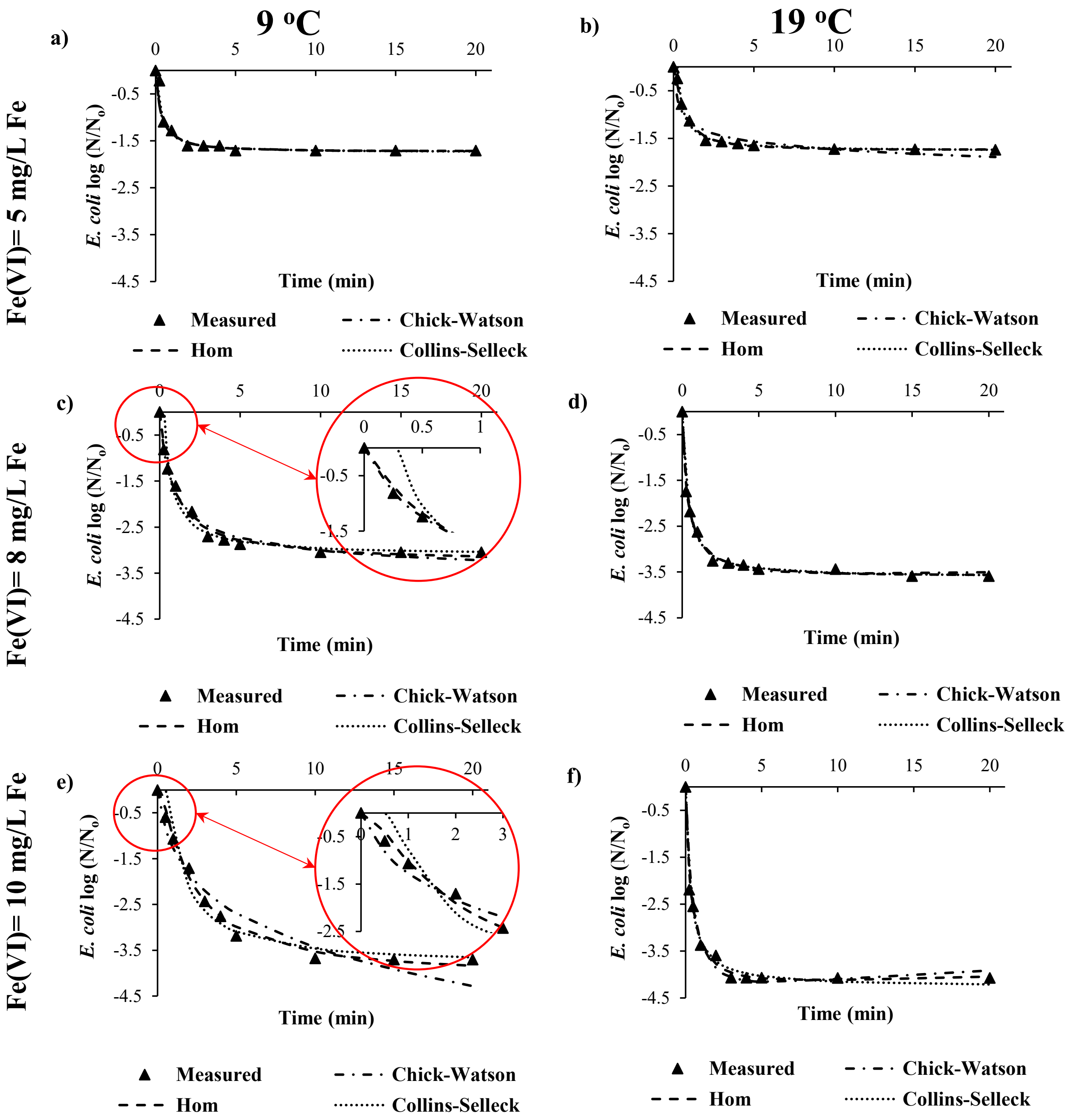

Figure 5. 4 Comparisons between measured and predicted log removal using three models Chick-Watson, Hom and Collins-Selleck models for different doses of ferrate: 5 mg/L Fe (a, b), 8 mg/L Fe (b, c) and 10 mg/L Fe for (e, f) and different temperatures 19 ˚C (left side of figure) and 9 ˚C (right side of the figure).

Table 5. 3 CT values predicted by Chick-Watson model required for 1,2,3 and 4-log removal of E. coli by Fe(VI) (in enhanced primary effluent) compared to those by ozone (O_3), performic acid, peracetic acid (PAA) and free chlorine in municipal secondary effluent wastewater.

Disinfectant	**CT(mg/L.min)**				**Reference**
	1-log	2-log	3-log	4-log	
Fe (VI)	1.4	2.6	3.8	4.9	Current study
O_3	0.0005	0.001	0.0016	0.0021	(Czekalski et al., 2016)
PFA	7	12	12	15	(Campo et al., 2020)
PAA	45	50	70	75	(Campo et al., 2020)
Chlorine	6	11	17	22	(Owoseni et al., 2017)

5.3.4 Temperature effect on inactivation rate constants

The temperature impact on the rate constant was described by the Arrhenius equation (5.5) which hypothesized that any major increment in temperature (exceeding the activation energy) will increase available energy for collision in the system and thus reaction rate (Li et al., 2001).

$$k=Ae^{-Ea/RT} \qquad (5.5)$$

Where k is the rate constant, A is the frequency factor, E_a is the activation energy (J/mol), R is the universal gas constant (8.31 J/(mol.k)) and T is the temperature in kelvin.

In this study the average activation energy based on obtained rate constants using the Chick-Watson model found to be 27±10 (kJ/mol) as compared to other studies: 39±6 (kJ/mol) and 67 (kJ/mol) related to bacteriophage M2S and *bacillus subtill spore* inactivation respectively (Hu et al., 2012a; Makky et al., 2011). In particular, the effects of temperature change can be expressed by a fraction of molecules ($e^{-Ea/RT}$) that have an energy equal to or more than the activation energy in the system (Laidler, 1984; Lambert, 2003). Based on that notion every increment of 10 °C would cause ~1.5 increment in the rate constant in this study. That came in agreement with the obtained k of this study (e.g. $k_{19\text{ C, Fe(VI)=8}}$ =1.0, $k_{9\text{ C, Fe(VI)=8}}$ =0.61 mg/Lmin) (Table 5. 2). The observed increment in the inactivation rate constant was statistically insignificant as per ANOVA (Table C. 6). That might be ascribed to the low dependence of ferrate-decay rate constant on temperature (Table C. 2). The effect of temperature on the rate of inactivation might vary depending on the target microorganism and used disinfectant. As such ferrate-inactivation rate constant of bacteriophage MS2 and *bacillus subtilis spores* increased twice by an increment of every13 ˚C and 10 ˚C of temperature respectively (Hu et al., 2018; Makky et al., 2011). In contrast, in another study it was found that a temperature change by 10 °C caused 2.5 increments on the inactivation rate of *Cryptosporidium parvum oocysts* by ozone (Li et al., 2001).

5.3.5 Flow Cytometry (FCM) analysis

The lab-cultured *E. coli* (ATCC25922) was spiked into phosphate buffer and treated with different doses of ferrate (1, 3 and 5 /L Fe). Tow set of ferrate-treated samples were prepared one set was stained with the SGI and the second with a combination of PPI and SGI. In this study, when only SGI was used, the green fluorescence presented in Q4-1 (blue dots) indicated the total cell count (TCC= intact cell + damaged cell) while the black dots likely to be debris, proteins/contaminant from the media (Figure 5.5: a – d). In particular, the ferrate dose of 1 mg/L Fe reduced slightly the TCC level by 20%, while higher doses (3 and 5 mg/L Fe) caused a noticeable reduction in TCC as 35.4% and 60.1% respectively (Figures 5.5 and 5.6). The observed reduction in the TCC level might be ascribed to the DNA oxidation with the notion that SGI can bind with the DNA regardless of cell viability status (Ramseier et al., 2011). The double staining (SGI/PPI) of bacterial cells provided distinct discrimination of damaged cells and intact cells. In Figure 5.5(e to h), Q1-1 represents the damaged cells (damaged membrane) while blue dots represent the intact cells. As such, the intact cell reduced significantly with a low dose of ferrate (1 mg/L Fe) while further increment in ferrate dose caused a slight reduction in the damaged cell count (Figures 5.5 and 5.6).

That might be ascribed to the high reactivity of ferrate with cell membrane components (e.g. amino acids, phospholipids) (Gan et al., 2015; Sharma, 2013; Sharma and Bielski, 1991). It was reported that ferrate oxidized deoxyribonucleosides to different extents thus ferrate oxidized 62% and 100% of deoxycytidine and deoxyguanosine compared to 13% to 25% of deoxyadenosine and thymidine (pH= 8) (Sharma, 2013). In a previous study, it was reported that ferrate could cause damage to the cell membrane of native drinking water bacteria cells and no damage of DNA was observed (Ramseier et al., 2011). The discrepancy between the findings of that study and this study might be due to the differences in the water matrix (a mixture of lake water, groundwater, tap water versus phosphate buffered); used bacterial indicator (native drinking water bacteria versus lab-cultured bacteria); initial TCC (26 x 10^7 cell/L versus 4.5 x 10^6 cell/L); TOC (0.8 mg/L C versus 0 mg/L C); and pH of the samples (8.2 versus 7.2). Furthermore, it was reported ferrate mode of inactivating *Microcystis aeruginosa* affected by NOM and coexisting cations (e.g. manganese) (pH= 7.6, DOC=2.02 mg/L, Mn=0.368 mg/L)(Fan et al., 2018). In addition, the ferrate mode of action might also be impacted by the pH of the solution because ferrate protonated species ($HFeO_4^-$, pK_a=7.2) are proved to be more reactive than deprotonated species (FeO_4^{2-}) (Cho et al., 2006).

Nonetheless, cell membrane destruction is a widely accepted criterion for determining inactivated bacteria (Berney et al., 2008a; Gombos et al., 2012; Ramseier et al., 2011). In this study, the colony counting method (i.e. based on bacterial cultivation) showed that ferrate achieved 4-log removal of *E. coli* while FCM revealed that only 1.3-log of intact cells were removed. This difference could be attributed to the presence of viable but not-cultivatable bacteria (i.e. *E. coli*) which might occur generally due to sub-lethal injury, the inadequacy of temperature or time to grow (Antonelli et al., 2006; Gillespie et al., 2014). This further emphasized that the cultivation-independent techniques (microscopy, flow cytometry or molecular biological techniques) might be used as a complementary tool for evaluating the disinfectant effectiveness.

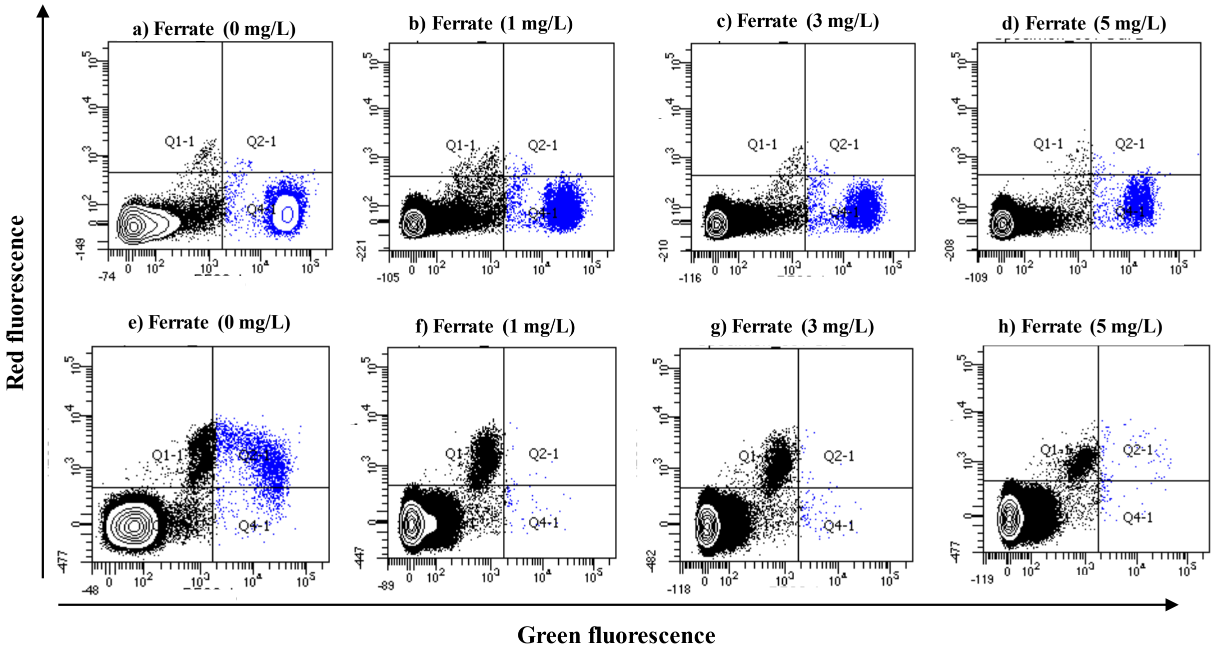

Figure 5. 5 The representative FCM density plots (X-axis 530 nm, Y-axis 586 nm) of lab-cultured E. coli (1.09 x 10^4 MPN/100mL) spiked in phosphate-buffered solution (pH=7.2) and treated with different doses of ferrate (0, 1, 3, and 5 mg/L). The first row (a, b, c and d) samples were stained with SYRB Green I (SGI) represent total cell count (intact cell + damaged cell) and second row samples were stained with SGI+ Propidium Iodide (PPI) for distinct classification of cells (intact cell and damaged cell).

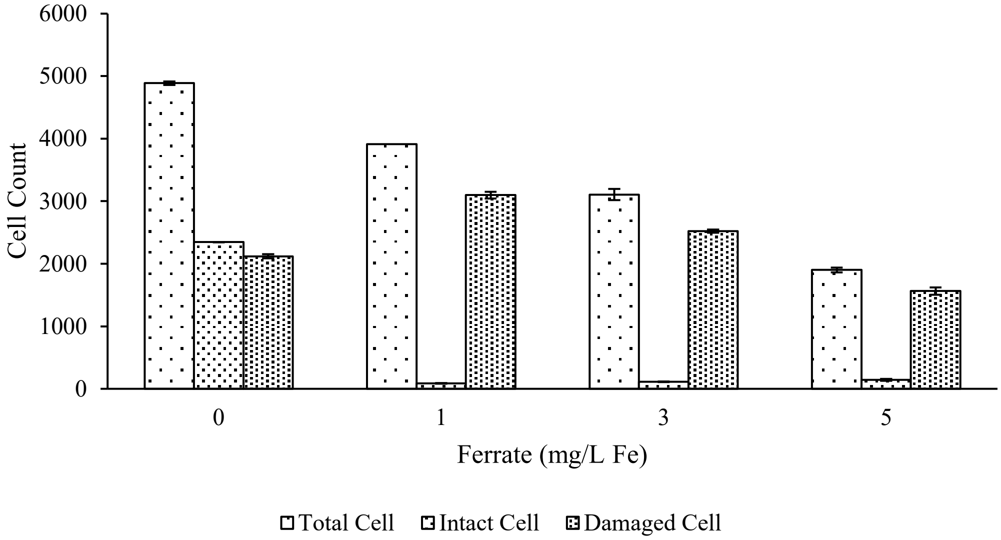

Figure 5. 6 Total cell count derived from SGI staining cells and intact cell number and damaged cells derived from double staining SGI/PPI for *E. coli* suspended in phosphate buffer solution (pH = 7.2) treated by different doses of ferrate (0, 1, 3, and 5 mg/L Fe).

5.3.6 Hydrogen peroxide (H_2O_2) in-situ production

Hydrogen peroxide (H_2O_2) is an oxidant/disinfectant with a redox potential of 1.8 V had been used alone or in combination with other technologies in the water and wastewater treatment field (Jimenez-Del-Rio et al., 2010; Lambert et al., 1999; Lin and Lo, 1997).

In fact, this study had investigated the *in-situ* production of hydrogen peroxide as a byproduct of ferrate dissociation chemistry which might provide a feasible alternative source for the commercial hydrogen peroxide (Asghar et al., 2015). Therefore, as part of ferrate dissociation chemistry different iron species are formed (e.g. $H_2Fe^{V}O_4^-$, $H_3Fe^{IV}O_4^-$, Fe^{2+}, Fe^{3+}) along with hydrogen peroxide (H_2O_2) and dissolved oxygen (O_2) (equation 5.6-5.11)(Lee et al., 2004; Lee et al., 2014).

$$2HFe^{VI}O_4^- + 4H_2O \rightarrow 2H_3Fe^{IV}O_4^- + 2H_2O_2 \qquad (5.6)$$

$$HFe^{VI}O_4^- + H_2O_2 \rightarrow H_3Fe^{IV}O_4^- + O_2 \qquad (5.7)$$

$$HFe^{VI}O_4^- + H_2O_2 + H^+ \rightarrow Fe^{II}(OH)_2 + O_2 + 2H_2O \quad (5.8)$$

$$HFe^{VI}O_4^- + Fe^{II}(OH)_2 + H_2O \rightarrow H_2Fe^{V}O_4^- + Fe^{III}(OH)_3 \quad (5.9)$$

$$H_2Fe^{V}O_4^- + H_2O + H^+ \rightarrow Fe^{III}(OH)_3 + H_2O_2 \quad (5.10)$$

$$H_2Fe^{V}O_4^- + H_2O_2 + H^+ \rightarrow Fe^{III}(OH)_3 + O_2 + H_2O \quad (5.11)$$

The level of hydrogen peroxide was monitored during ferrate-decomposition corresponded to ferrate doses (5, 8 and 10 mg/L Fe) for 20 minutes (Figure 5. 7, a). Therefore, the produced H_2O_2 was equivalent to 20 to 26% of the ferrate initial dose within pH (7.3 to 8.4) (Figure 5. 7, b). This percentage was comparable with what was reported previously as generated hydrogen peroxide equal 26% of initial ferrate dose at pH= 8.8 (Lee et al., 2014). The produced hydrogen peroxide was stable in the tested system and no major reduction was observed over 120 min (data not shown). The presence of hydrogen peroxide in the treated effluent is an environmental concern and a proper method of control is required. Different approaches were proposed in the literature to control residual of hydrogen peroxide such as granular activated carbon (GAC), chlorine, and sulfur compounds (Huang et al., 2018; Olmez-Hanci et al., 2014; Wang et al., 2019). In the pilot and lab-scale experiments, it was reported that GAC could effectively quench H_2O_2 (4 to 10 mg/L) presented in UV/H_2O_2 treated surface water within 4 to 20 minutes approximately (pH=6.9 to 7.76, TOC=1.95-3.32 mg/L) (Huang et al., 2018). The author suggested that the H_2O_2 decomposition occurred via the generation of radical species with the reactive surface layer of GAC or it may involve the transfer of functional group between GAC and H_2O_2. In the lab-scale experiment, it was suggested using chlorine as a quenching agent of H_2O_2, therefore greater than 95% of H_2O_2 (5 to 10 mg/L) was quenched by chlorine within 0.4 to 14 minute (molar ratio of chlorine:H_2O_2: 1:1, pH= 6.2-7.2)(Wang et al., 2019). Nonetheless, using chlorine for the full-scale application required more investigation. Sodium sulfite and sodium thiosulfate were not recommended for full-scale application due to slow reaction or high molar ratio requirement (e.g. 10 mg/L of $Na_2S_2O_3$ for quenching 1 mg/L of H_2O_2)(Keen et al., 2013). Exploring other techniques for quenching residual H_2O_2 deduced by the ferrate process is very crucial.

The *in-situ* generated H_2O_2 might be used in the advance oxidation process: firstly, Fenton process (H_2O_2/Fe (III)) and secondly UV-based process (UV/H_2O_2). As such, in both options hydroxyl radicals ($OH^{\bullet}$, redox=2.8 V) could be formed by the reaction of H_2O_2 with transition metals (e.g. iron (Fe^{2+}, Fe^{3+})) or UV/H_2O_2 photolysis (equation 5.12) (De Laat and Gallard, 1999; Zaharia et al., 2009). In particular, ferric (also generated by ferrate) reacts with hydrogen peroxide and form ferric hydroperoxy complex ($Fe - OOH^{2+}$) which further decompose to form hydroxyl radical (equations 5.13-5.15) at acidic medium (pH < 4). Thus, at higher pH (alkaline), ferrous (Fe^{2+}) (Fenton reagent) may promote ferric hydroxo complex formation and ferric (Fe^{3+}) precipitation may occur, which eventually hindered hydroxyl radical formation (De Laat and Gallard, 1999). Based on all of that using hydrogen peroxide for Fenton (UV/Fe(III)) might not be feasible as it is required an acidic medium (pH <4) (out of typical pH (6 to 9) for water and wastewater treatment) and high concentration of H_2O_2 ($[Fe^{2+}]/[H_2O_2] \ll 1$ (Yoon et al., 2001).

$$H_2O_2 + h\upsilon \rightarrow 2OH\bullet + OH^- \qquad (5.12)$$

$$Fe^{3+} + H_2O_2 \rightarrow Fe\text{-}OOH^{2+} + H^+ \qquad (5.13)$$

$$Fe\text{-}OOH^{2+} \rightarrow HO_2\bullet + Fe^{2+} \qquad (5.14)$$

$$Fe^{2+} + H_2O_2 \rightarrow Fe^{3+} + OH\bullet + OH^- \qquad (5.15)$$

$$Fe^{2+} + OH\bullet \rightarrow Fe^{3+} + OH^- \qquad (5.16)$$

The second option (UV/H_2O_2) might be more practical for oxidation or disinfection processes in the context of the treated water. For instance, H_2O_2/UV (10 mg/L)/(5 mJ/cm^2) could inactivate 4-logs of *E. coli* (10^6 CFU/ mL) spiked into buffer solution (pH=7.5, DOC= 6 mg/L) compared to 3 log achieved by UV alone (Teksoy et al., 2011). Moreover, photo-degradation of pesticides (e.g. chlorfenvinphos, 2,4 D, aldrin) using UV/H_2O_2/air had exhibited high removal (80% to 99.5%) for bench-scale and pilot-scale application in industrial wastewater (UV-radiation time=40 min, pesticide=1.5 mg/L)(Kowalska et al., 2004). UV/H_2O_2 -process (1056 (mJ/cm^2)/ 340 mg/L) also showed high removal (> 90%) of endocrine disruptive compounds (EDCs) (n-butylparaben (BP) and4-tert-octylphenol (OP)) presented in buffered and pure water solution (pH range 5 to 8, compounds=1.7 x 10^{-4} to 5 x 10^{-8} M) (Bledzka et al., 2010). Indeed, in all mentioned studies, high doses of hydrogen peroxide were required to achieve the target removals thus it is recommended to conduct a feasibility study for the application of *in-situ* produced hydrogen peroxide.

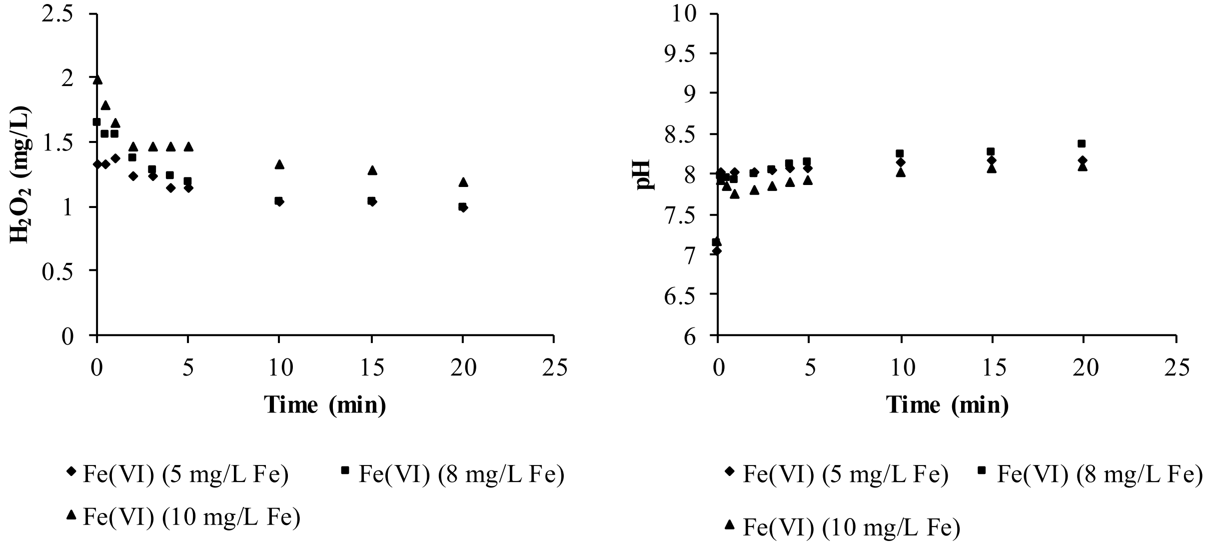

Figure 5. 7 The measured hydrogen peroxide levels (a) and pH change (b) during the decomposing of different doses of ferrate (5, 8 and 10 mg/L Fe) for treating enhanced primary treatment effluent during wet weather flow.

5.3.7 Acute toxicity analysis

In this study, acute toxicity was measured based on the change of luminescence emission of *vibrio fischeri* (Figure 5.8). Therefore, the acute toxicity of the untreated WWF sample was 60% which was likely due to the original constituents of wastewater (Figure 5.8). Interestingly, the toxicity level declined to zero after coagulation/sedimentation (denoted as EPT effluent) which may attribute to alum efficiency in removing a wide range of organic and inorganic contaminants (El Samrani et al., 2008; Kelly et al., 2004). That indeed came in agreement with another study which also reported that that alum and poly-aluminum chloride reduced effectively acute toxicity (*vibrio fischeri*) of secondary effluent of municipal wastewater (Petala et al., 2006). In this study ferrate (5, 8 and 10 mg/L Fe) induced apparent toxic effects (10 to 25%) of treated samples. The observed toxicity by ferrate might be explained by ferrate-oxidation of presented contaminants and consequently formation of toxic by-products. Similar observations were also reported when ferrate was used to oxidize diclofenac and bisphenol A (Han et al., 2015; Wang et al., 2015). In overall, the obtained results indicated that a more in-depth study was required to further explore the source of toxicity in the ferrate treatment system.

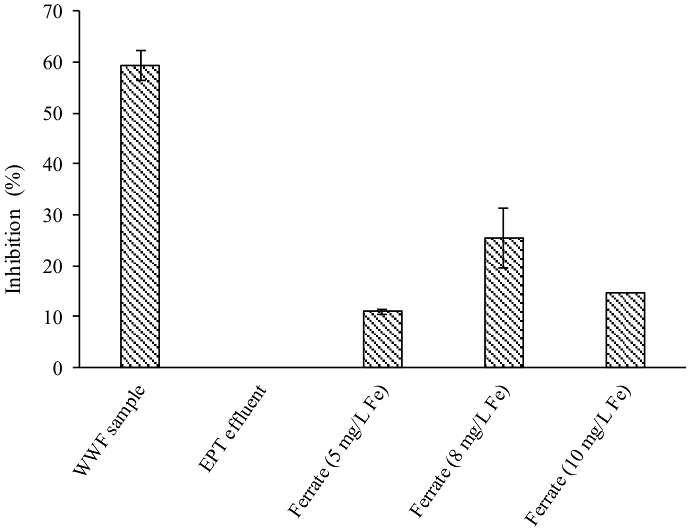

Figure 5. 8 Inhibition percentage of *vibrio fischeri* for different samples before and after treatments. Notes: WWF sample represents raw wet weather flow sample. EPT (enhanced primary treatment) effluent was treated by alum (75 mg/L). Different ferrate doses (5, 8 and 10 mg/L Fe) were applied into EPT effluent samples used for disinfection experiments.

5.4 Conclusions

This study demonstrated that ferrate is efficient to inactivate *E. coli* presented in the effluent of enhanced primary treatment during wet weather flow. The impacts of temperature and ferrate doses were evaluated comprehensively. Ferrate dose of 10 mg/L Fe effectively removed 3.6 to 4 log of *E. coli* within 3 to 10 minutes at the tested temperatures. The temperature change from 9 to 19 °C had increased slightly log-removal by approximately 0.5 log. Ferrate-degradation was observed during the inactivation kinetic study and fit into a second-order kinetic model. No lag was observed in the inactivation process of *E. coli* by ferrate, yet tailing-off was observed. Chick-Watson, Hom and Selleck models were successfully fit the inactivation kinetic data with adjusted $R^2 \geq 0.94$. Interestingly, Chick-Watson and Hom model exhibited comparable performances to fit the experimental data while Collins-Selleck showed inferior performance. The increment in temperature from 9 to 19 ºC caused an approximate increment of 1.5 in the inactivation rate constant.

Flow cytometry (FCM) analysis revealed that, ferrate could inactivate *E. coli* by damaging the cell membrane and to a lower extent cause DNA damage. The *in-situ* production of hydrogen peroxide was verified in this study and it was found to equal 20 to 26% of ferrate initial dose. Using ferrate should be always adapted with a proper method of control as the generated H_2O_2 cannot be discharged directly.

The acquired acute toxicity results exhibited a high reduction in the toxicity of raw wet weather flow samples after the coagulation sedimentation process. Furthermore, ferrate imposed slight toxicity effects on the treated samples, which might be ascribed to the oxidation process. Further study is recommended to further explore the source of toxicity in the ferrate treatment process. In overall, this method provides important insights on overall ferrate performance as a disinfectant and therefore ferrate might be suggested to be an alternative disinfectant for treating the EPT effluent during WWF. Additionally, it is worth mentioning that these experiments were conducted at a bench-scale level thus full-scale application was warranted for further optimization of operating conditions.

5.5 References

Antonelli, M., Rossi, S., Mezzanotte, V. and Nurizzo, C. 2006. Secondary effluent disinfection: PAA long term efficiency. Environmental Science & Technology 40(15), 4771-4775.

Asghar, A., Raman, A.A.A. and Daud, W.M.A.W. 2015. Advanced oxidation processes for in-situ production of hydrogen peroxide/hydroxyl radical for textile wastewater treatment: a review. Journal of Cleaner Production 87, 826-838.

Barbesti, S., Citterio, S., Labra, M., Baroni, M.D., Neri, M.G. and Sgorbati, S. 2000. Two and three-color fluorescence flow cytometric analysis of immunoidentified viable bacteria. Cytometry 40(3), 214-218.

Berney, M., Hammes, F., Bosshard, F., Weilenmann, H.-U. and Egli, T. 2007. Assessment and interpretation of bacterial viability by using the LIVE/DEAD BacLight kit in combination with flow cytometry. Applied and Environmental Microbiology 73(10), 3283-3290.

Berney, M., Vital, M., Huelshoff, I., Weilenmann, H.-U., Egli, T. and Hammes, F. 2008a. Rapid, cultivation-independent assessment of microbial viability in drinking water. Water Research 42(14), 4010-4018.

Berney, M., Vital, M., Hulshoff, I., Weilenmann, H.U., Egli, T. and Hammes, F. 2008b. Rapid, cultivation-independent assessment of microbial viability in drinking water. Water Research 42(14), 4010-4018.

Berney, M., Weilenmann, H.-U. and Egli, T. 2006. Flow-cytometric study of vital cellular functions in Escherichia coli during solar disinfection (SODIS). Microbiology-Sgm 152, 1719-1729.

Bledzka, D., Gryglik, D., Olak, M., Gebicki, J.L. and Miller, J.S. 2010. Degradation of n-butylparaben and 4-tert-octylphenol in H2O2/UV system. Radiation Physics and Chemistry 79(4), 409-416.

Campo, N., De Flora, C., Maffettone, R., Manoli, K., Sarathy, S., Santoro, D., Gonzalez-Olmos, R. and Auset, M. 2020. Inactivation kinetics of antibiotic resistant Escherichia coli in secondary wastewater effluents by peracetic and performic acids. Water research 169, 115227.

Chhetri, R.K., Thornberg, D., Berner, J., Gramstad, R., Ojstedt, U., Sharma, A.K. and Andersen, H.R. 2014. Chemical disinfection of combined sewer overflow waters using performic acid or peracetic acids. Sci. Total Environ. 490, 1065-1072.

Cho, M., Chung, H., Choi, W. and Yoon, J. 2004. Linear correlation between inactivation of E-coli and OH radical concentration in TiO2 photocatalytic disinfection. Water Research 38(4), 1069-1077.

Cho, M., Lee, Y., Choi, W., Chung, H.M. and Yoon, J. 2006. Study on Fe(VI) species as a disinfectant: Quantitative evaluation and modeling for inactivating Escherichia coli. Water Res. 40(19), 3580-3586.

Czekalski, N., Imminger, S., Salhi, E., Veljkovic, M., Kleffel, K., Drissner, D., Hammes, F., Burgmann, H. and von Gunten, U. 2016. Inactivation of Antibiotic Resistant Bacteria and Resistance Genes by Ozone: From Laboratory Experiments to Full-Scale Wastewater Treatment. Environmental Science & Technology 50(21), 11862-11871.

De Laat, J. and Gallard, H. 1999. Catalytic decomposition of hydrogen peroxide by Fe(III) in homogeneous aqueous solution: Mechanism and kinetic modeling. Environmental Science & Technology 33(16), 2726-2732.

Dong, F., Liu, J., Li, C., Lin, Q., Zhang, T., Zhang, K. and Sharma, V.K. 2019. Ferrate(VI) pre-treatment and subsequent chlorination of blue-green algae: Quantification of disinfection byproducts. Environment International 133.

El Samrani, A.G., Lartiges, B.S. and Villieras, F. 2008. Chemical coagulation of combined sewer overflow: Heavy metal removal and treatment optimization. Water Research 42(4-5), 951-960.

Elnakar, H. and Buchanan, I. 2019. The role of mixing in potassium ferrate(VI) consumption kinetics and disinfection of bypass wastewater. Journal of Environmental Management 231, 515-523.

Fan, J., Lin, B.-H., Chang, C.-W., Zhang, Y. and Lin, T.-F. 2018. Evaluation of potassium ferrate as an alternative disinfectant on cyanobacteria inactivation and associated toxin fate in various waters. Water Research 129, 199-207.

Faria, E.C., Brown, B.J.T. and Snook, R.D. 2004. Water toxicity monitoring using Vibrio fischeri: a method free of interferences from colour and turbidity. Journal of Environmental Monitoring 6(2), 97-102.

Gan, W.H., Sharrna, V.K., Zhang, X., Yang, Y. and Yang, X. 2015. Investigation of disinfection byproducts formation in ferrate(VI) pre-oxidation of NOM and its model compounds followed by chlorination. Journal of Hazardous Materials 292, 197-204.

Gandhi, R., Ray, A.K., Sharma, V.K. and Nakhla, G. 2014. Treatment of Combined Sewer Overflows Using Ferrate (VI). Water Environment Research 86(11), 2202-2211.

Ganguly, P., Byrne, C., Breen, A. and Pillai, S.C. 2018. Antimicrobial activity of photocatalysts: Fundamentals, mechanisms, kinetics and recent advances. Applied Catalysis B-Environmental 225, 51-75.

Ghernaout, D. and Naceur, M.W. 2011. Ferrate(VI): In situ generation and water treatment - A review. Desalination and Water Treatment 30(1-3), 319-332.

Gillespie, S., Lipphaus, P., Green, J., Parsons, S., Weir, P., Juskowiak, K., Jefferson, B., Jarvis, P. and Nocker, A. 2014. Assessing microbiological water quality in drinking water distribution systems with disinfectant residual using flow cytometry. Water Research 65, 224-234.

Gombos, E., Felfoeldi, T., Barkacs, K., Vertes, C., Vajna, B. and Zaray, G. 2012. Ferrate treatment for inactivation of bacterial community in municipal secondary effluent. Bioresource Technology 107, 116-121.

Gregori, G., Citterio, S., Ghiani, A., Labra, M., Sgorbati, S., Brown, S. and Denis, M. 2001. Resolution of viable and membrane-compromised bacteria in freshwater and marine waters based on analytical flow cytometry and nucleic acid double staining. Applied and Environmental Microbiology 67(10), 4662-4670.

Gyurek, L.L. and Finch, G.R. 1998. Modeling water treatment chemical disinfection kinetics. Journal of Environmental Engineering-Asce 124(9), 783-793.

Haas, C.N. and Karra, S.B. 1984. Kinetics of microbial inactivation by chlorine .2. Kinetics in the presence of chlorine demand. Water Research 18(11), 1451-1454.

Han, Q., Wang, H.J., Dong, W.Y., Liu, T.Z., Yin, Y.L. and Fan, H.K. 2015. Degradation of bisphenol A by ferrate(VI) oxidation: Kinetics, products and toxicity assessment. Chemical Engineering Journal 262, 34-40.

Hassaballah, A.H., Nyitrai, J., Hart, C.H., Dai, N. and Sassoubre, L.M. 2019. A pilot-scale study of peracetic acid and ultraviolet light for wastewater disinfection. Environmental Science-Water Research & Technology 5(8), 1453-1463.

Henao, L.D., Cascio, M., Turolla, A. and Antonelli, M. 2018. Effect of suspended solids on peracetic acid decay and bacterial inactivation kinetics: Experimental assessment and definition of predictive models. Science of the Total Environment 643, 936-945.

Hernandez, M.A.C., May, A., Bonakdapour, A., Mohseni, M. and Wilkinson, D.P. 2017. Analytical quantification of electrochemical ferrates for drinking water treatments. Canadian Journal of Chemistry 95(1), 105-112.

Hu, J., Chu, W., Sui, M., Xu, B., Gao, N. and Ding, S. 2018. Comparison of drinking water treatment processes combinations for the minimization of subsequent disinfection by-products formation during chlorination and chloramination. Chemical Engineering Journal 335, 352-361.

Hu, L., Page, M.A., Sigstam, T., Kohn, T., Marinas, B.J. and Strathmann, T.J. 2012a. Inactivation of Bacteriophage MS2 with Potassium Ferrate(VI). Environmental Science & Technology 46(21), 12079-12087.

Hu, L., Page, M.A., Sigstam, T., Kohn, T., Mariñas, B.J. and Strathmann, T.J. 2012b. Inactivation of Bacteriophage MS2 with Potassium Ferrate(VI). Environ. Sci. Technol. 46(21), 12079-12087.

Huang, C.C., Hu, Y., Wang, L., Wang, Y.F., Li, N., Guo, Y.Q., Feng, Y.Y. and Xiao, L.H. 2017. Environmental Transport of Emerging Human-Pathogenic Cryptosporidium Species and Subtypes through Combined Sewer Overflow and Wastewater. Applied and Environmental Microbiology 83(16), 11.

Huang, Y., Nie, Z., Wang, C., Li, Y., Xu, M. and Hofmann, R. 2018. Quenching H2O2 residuals after UV/H2O2 oxidation using GAC in drinking water treatment. Environmental Science-Water Research & Technology 4(10), 1662-1670.

Jessen, A., Randall, A., Reinhart, D. and Daly, L. 2008. Effectiveness and Kinetics of Ferrate as a Disinfectant for Ballast Water. Water Environment Research 80(6), 561-569.

Jiang, J.Q., Wang, S. and Panagoulopoulos, A. 2006. The exploration of potassium ferrate(VI) as a disinfectant/coagulant in water and wastewater treatment. Chemosphere 63(2), 212-219.

Jiang, J.Q., Wang, S. and Panagoulopoulos, A. 2007. The role of potassium ferrate(VI) in the inactivation of Escherichia coli and in the reduction of COD for water remediation. Desalination 210(1-3), 266-273.

Jiang, Y.J., Goodwill, J.E., Tobiason, J.E. and Reckhow, D.A. 2015. Effect of Different Solutes, Natural Organic Matter, and Particulate Fe(III) on Ferrate(VI) Decomposition in Aqueous Solutions. Environmental Science & Technology 49(5), 2841-2848.

Jiang, Y.J., Goodwill, J.E., Tobiason, J.E. and Reckhow, D.A. 2016. Impacts of ferrate oxidation on natural organic matter and disinfection byproduct precursors. Water Research 96, 114-125.

Jimenez-Del-Rio, M., Suarez-Cedeno, G. and Velez-Pardo, C. 2010. Using Paraquat to Generate Anion Free Radicals and Hydrogen Peroxide in In Vitro: Antioxidant Effect of Vitamin E a procedure to teach theoretical and experimental principles of reactive oxygen species biochemistry. Biochemistry and Molecular Biology Education 38(2), 104-109.

Keen, O.S., Dotson, A.D. and Linden, K.G. 2013. Evaluation of Hydrogen Peroxide Chemical Quenching Agents following an Advanced Oxidation Process. Journal of Environmental Engineering-Asce 139(1), 137-140.

Kelly, C.J., Tumsaroj, N. and Lajoie, C.A. 2004. Assessing wastewater metal toxicity with bacterial bioluminescence in a bench-scale wastewater treatment system. Water Research 38(2), 423-431.

Kowalska, E., Janczarek, M., Hupka, J. and Grynkiewicz, M. 2004. H2O2/UV enhanced degradation of pesticides in wastewater. Water Science and Technology 49(4), 261-266.

Kwon, J.H., Kim, I.K., Park, K.Y., Kim, Y.D. and Cho, Y.H. 2014. Removal of phosphorus and coliforms from secondary effluent using ferrate(VI). Ksce Journal of Civil Engineering 18(1), 81-85.

Laidler, K.J. 1984. The development of the arrhenius equation. Journal of Chemical Education 61(6), 494-498.

Lambert, R.J.W. 2003. A model for the thermal inactivation of micro-organisms. Journal of Applied Microbiology 95(3), 500-507.

Lambert, R.J.W., Johnston, M.D. and Simons, E.A. 1999. A kinetic study of the effect of hydrogen peroxide and peracetic acid against Staphylococcus aureus and Pseudomonas aeruginosa using the Bioscreen disinfection method. Journal of Applied Microbiology 87(5), 782-786.

Lee, Y., Cho, M., Kim, J.Y. and Yoon, J. 2004. Chemistry of ferrate (Fe(VI)) in aqueous solution and its applications as a green chemical. J. Ind. Eng. Chem. 10(1), 161-171.

Lee, Y., Imminger, S., Czekalski, N., von Gunten, U. and Hammes, F. 2016. Inactivation efficiency of Escherichia coli and autochthonous bacteria during ozonation of municipal wastewater effluents quantified with flow cytometry and adenosine tri-phosphate analyses. Water Research 101, 617-627.

Lee, Y., Kissner, R. and von Gunten, U. 2014. Reaction of Ferrate(VI) with ABTS and Self-Decay of Ferrate(VI): Kinetics and Mechanisms. Environ. Sci. Technol. 48(9), 5154-5162.

Lee, Y., Yoon, J. and von Gunten, U. 2005. Spectrophotometric determination of ferrate (Fe(Vl)) in water by ABTS. Water Research 39(10), 1946-1953.

Li, C., Dong, F., Feng, L., Zhao, J., Zhang, T., Cizmas, L. and Sharma, V.K. 2017a. Bacterial community structure and microorganism inactivation following water treatment with ferrate(VI) or chlorine. Environmental Chemistry Letters 15(3), 525-530.

Li, H., Gyurek, L.L., Finch, G.R., Smith, D.W. and Belosevic, M. 2001. Effect of temperature on ozone inactivation of Cryptosporidium parvum in oxidant demand-free phosphate buffer. Journal of Environmental Engineering-Asce 127(5), 456-467.

Li, X., Liu, Y., Liu, F., Liu, A. and Feng, Q. 2017b. Comparison of ferric chloride and aluminum sulfate on phosphorus removal and membrane fouling in MBR treating BAF effluent of municipal wastewater. Journal of Water Reuse and Desalination 7(4), 442-448.

Liang, Y.M., Zhang, Z.L., Yang, X. and Liu, W. 2013. Effect of Suspended Solids on the Sequential Disinfection of Secondary Effluent by UV Irradiation and Chlorination. Journal of Environmental Engineering 139(12), 1482-1487.

Lin, S.H. and Lo, C.C. 1997. Fenton process for treatment of desizing wastewater. Water Research 31(8), 2050-2056.

Luo, Z.Y., Strouse, M., Jiang, J.Q. and Sharma, V.K. 2011. Methodologies for the analytical determination of ferrate(VI): A Review. J. Environ. Sci. Health Part A-Toxic/Hazard. Subst. Environ. Eng. 46(5), 453-460.

Madoux-Humery, A.-S., Dorner, S., Sauve, S., Aboulfadl, K., Galarneau, M., Servais, P. and Prevost, M. 2013. Temporal variability of combined sewer overflow contaminants: Evaluation of wastewater micropollutants as tracers of fecal contamination. Water Research 47(13), 4370-4382.

Makky, E.A., Park, G.-S., Choi, I.-W., Cho, S.-I. and Kim, H. 2011. Comparison of Fe(VI) (FeO42-) and ozone in inactivating Bacillus subtilis spores. Chemosphere 83(9), 1228-1233.

Malachova, K., Sezimova, H. and Rozinek, R. 2014. Detection of genotoxicity and toxicity of wastewater treatment plant (WTP) effluents after pretreatment with ferrate (VI). Toxicology Letters 229, S117-S118.

Malik, S.N., Ghosh, P.C., Vaidya, A.N., Waindeskar, V., Das, S. and Mudliar, S.N. 2017. Comparison of coagulation, ozone and ferrate treatment processes for color, COD and toxicity removal from complex textile wastewater. Water Science and Technology 76(5), 1001-1010.

Manoli, K., Maffettone, R., Sharma, V.K., Santoro, D., Ray, A.K., Passalacqua, K.D., Carnahan, K.E., Wobus, C.E. and Sarathy, S. 2020. Inactivation of Murine Norovirus and Fecal Coliforms by Ferrate(VI) in Secondary Effluent Wastewater. Environmental Science & Technology 54(3), 1878-1888.

Marsalek, J. and Rochfort, Q. 2004. Urban wet-weather flows: Sources of fecal contamination impacting on recreational waters and threatening drinking-water sources. Journal of Toxicology and Environmental Health-Part a-Current Issues 67(20-22), 1765-1777.

Najm, I. 2006. An alternative interpretation of disinfection kinetics. Journal American Water Works Association 98(10), 93-+.

Olmez-Hanci, T., Arslan-Alaton, I. and Dursun, D. 2014. Investigation of the toxicity of common oxidants used in advanced oxidation processes and their quenching agents. Journal of Hazardous Materials 278, 330-335.

Owoseni, M.C., Olaniran, A.O. and Okoh, A.I. 2017. Chlorine Tolerance and Inactivation of Escherichia coli recovered from Wastewater Treatment Plants in the Eastern Cape, South Africa. Applied Sciences-Basel 7(8).

Petala, M., Samaras, P., Kungolos, A., Zouboulis, A., Papadopoulos, A. and Sakellaropoulos, G.P. 2006. The effect of coagulation on the toxicity and mutagenicity of reclaimed municipal effluents. Chemosphere 65(6), 1007-1018.

Ramseier, M.K., von Gunten, U., Freihofer, P. and Hammes, F. 2011. Kinetics of membrane damage to high (HNA) and low (LNA) nucleic acid bacterial clusters in drinking water by ozone, chlorine, chlorine dioxide, monochloramine, ferrate(VI), and permanganate. Water Research 45(3), 1490-1500.

Rechenburg, A., Koch, C., Classen, T. and Kistemann, T. 2006. Impact of sewage treatment plants and combined sewer overflow basins on the microbiological quality of surface water. Water Science and Technology 54(3), 95-99.

Sharma, V.K. 2013. Ferrate(VI) and ferrate(V) oxidation of organic compounds: Kinetics and mechanism. Coordination Chemistry Reviews 257(2), 495-510.

Sharma, V.K. and Bielski, B.H.J. 1991. Reactivity of ferrate(vi) and ferrate(v) with amino-acids. Inorganic Chemistry 30(23), 4306-4310.

Sigstam, T., Rohatschek, A., Zhong, Q.X., Brennecke, M. and Kohn, T. 2014. On the cause of the tailing phenomenon during virus disinfection by chlorine dioxide. Water Research 48, 82-89.

Stampi, S., De Luca, G. and Zanetti, F. 2001. Evaluation of the efficiency of peracetic acid in the disinfection of sewage effluents. Journal of Applied Microbiology 91(5), 833-838.

Teksoy, A., Alkan, U., Eleren, S.C., Topac, B.S., Sagban, F.O.T. and Baskaya, H.S. 2011. Comparison of indicator bacteria inactivation by the ultraviolet and the ultraviolet/hydrogen peroxide disinfection processes in humic waters. Journal of Water and Health 9(4), 659-669.

Wang, C.J., Hofmann, M., Safari, A., Viole, I., Andrews, S. and Hofmann, R. 2019. Chlorine is preferred over bisulfite for H_2O_2 quenching following UV-AOP drinking water treatment. Water Research 165, 6.

Wang, W.-g., Xu, Z.-x., Li, H.-z. and Jin, W. 2016. Coagulation characteristics of organic pollutants removal in cso wastewater treatment. Environmental Engineering and Management Journal 15(1), 75-80.

Wang, Y.L., Liu, H.J., Liu, G.G., Xie, Y.H. and Gao, S.Y. 2015. Oxidation of diclofenac by potassium ferrate (VI): Reaction kinetics and toxicity evaluation. Science of the Total Environment 506, 252-258.

Wojtenko, I., Stinson, M.K. and Field, R. 2001. Performance of ozone as a disinectant for combined sewer overflow. Critical Reviews in Environmental Science and Technology 31(4), 295-309.

Yao, C.C.D. and Haag, W.R. 1991. Rate constants for direct reactions of ozone with several drinking-water contaminants. Water Research 25(7), 761-773.

Yoon, J., Lee, Y. and Kim, S. 2001. Investigation of the reaction pathway of OH radicals produced by Fenton oxidation in the conditions of wastewater treatment. Water Science and Technology 44(5), 15-21.

Zaharia, C., Suteu, D., Muresan, A., Muresan, R. and Popescu, A. 2009. Textile wastewater treatment by homogeneous oxidation with hydrogen peroxide. Environmental Engineering and Management Journal 8(6), 1359-1369.

Zheng, L. and Deng, Y. 2016. Settleability and characteristics of ferrate(VI)-induced particles in advanced wastewater treatment. Water Research 93, 172-178.

Zondervan, E. and Roffel, B. 2007. Evaluation of different cleaning agents used for cleaning ultra tiltration membranes fouled by surface water. Journal of Membrane Science 304(1-2), 40-49.

Chapter 6: Elimination of Selected Pesticides and Pharmaceutical Model Compounds by Ferrate and Ferrate-UV Processes: pH Impact, Kinetics Study and Hydroxyl Radical and Superoxide Radical Contributions

6.1 Introduction

Contaminants of emerging concern (CECs) (e.g. pharmaceutical and personal care products or pesticides) are detected in ng/L to µg/L in surface water, wastewater influent/effluents and agriculture runoff, endangering the aquatic life and human health (Petrie et al., 2015). While limited regulation is available for the discharge of the CECs in wastewater, the potential risk of CECs to the environment and public health is still of high concern for environmental researchers and decision-makers. Between 2006 and 2007, an extensive study conducted by Benotti et al., (2009), investigated the occurrence of more than 51 CECs in different water sources including: tap water, drinking water sources, finished water and wastewater treated effluent. They concluded that, the mostly detected ECs were: Atenolol, *N,N*-diethyl-m-toluamide, estrone, meprobamate, atrazine, trimethoprim, sulfamethoxazole, carbamazepine, phenytoin, naproxen, gemfibrozil and tris-2-chloroethyl phosphate. Among 14 surveyed countries for occurrence and fate of a wide range of CECs, it was found that antibiotic, anti-inflammatory drugs were found to have the highest concentration (up to µg/L) in surface water and sewage effluents of Canada, UK and Japan (Jiang et al., 2013). Some compounds were detected frequently in surface water and may serve as an indicator for the occurrence of CECs such as atrazine (ATZ), mecoprop (MCPP), and carbamazepine (CBZ) (Benotti et al., 2009; Martinez et al., 2016). Atrazine is a herbicide used to kill weeds with global annual consumption of 70,000 tonnes and detected in surface water with a concentration > 0.1 µg/L (Tankiewicz et al., 2010; Wu et al., 2018). Mecoprop is a chloro-phenoxy herbicide used to control chickweeds, lawn and weeds of other cereal crops with annual use of 500,000 tons detected more frequently in surface water with a concentration of 0.1 µg/L (Martinez et al., 2016). In contrast, CBZ is a pharmaceutical compound used as a mood stabilizer and anti-convulsant with a detected level in surface water of up to 6 μg/L.

Conventional wastewater treatment plants (WWTPs) (biodegradation/coagulation/ filtration) showed deficiency to remove CECs (Hamza et al., 2016; Westerhoff et al., 2005). Alternatively, oxidation processes (direct oxidation or advance oxidation) showed higher efficiencies to degrade the broader range of CECs (Acero et al., 2000; Huber et al., 2005). For instance, ozone, a strong oxidant (redox potential=2.1 V) effectively removed CECs with electron-rich moieties (e.g. ibuprofen, sulfamethoxazole) whereas showing moderate removal for other CECs (e.g. caffeine, iopromide) (Knopp et al., 2016). Photolysis oxidation process via UV could degrade effectively CECs with high quantum yield (e.g. sulfamethoxazole, diclofenac) while UV/H_2O_2 process showed better performance due to the generation of non-selective hydroxyl radical (e.g. ibuprofen degradation) (Trapido et al., 2014).

Ferrate recently emerged as a powerful oxidant (redox potential =2.2 V) with a high capacity to degrade a broad range of CECs (Gombos et al., 2013; Jiang, 2013; 2015; Karlesa et al., 2014; Lee et al., 2009; Sharma, 2013; Sharma et al., 2016; Sun et al., 2016; Yang et al., 2012; Zhang et al., 2015). In fact, ferrate is known to be more reactive at acidic pH (due to the presence of protonated species) and more stable at alkaline condition (Sharma, 2002). Ferrate had shown to effectively remove several pharmaceutical compounds such as carbamazepine and metoprolol in different water matrices (pure water and hospital wastewater effluent, pH = 10) (Peings et al., 2017). Also, ferrate (C_o=22.4 mg/L Fe) had removed significantly polychlorinated diphenyl sulfides (C_o=3.72 mg/L) within minutes at pH=8.2 (Chen et al., 2018). The synergistic effect was reported when peroxymonosulfate was added to ferrate during the degradation of fluroquinolone

(Feng et al., 2017). It was also found that ferrate could be activated by acid to removed recalcitrant compounds (acesulfame potassium, caffeine, atenolol) (Manoli et al., 2017).

This paper attempted to evaluate ferrate efficiency for degrading selected CECs serve as indicators for CECs presence in water and wastewater with environmental relevant conditions. Therefore, to benchmarking the reactivity of CECs, a mixture of selected model compounds was treated by different doses of ferrate under different pH (5.2, 7.2 and 9.2). Some of the selected model compounds were treated by ferrate for the first time such as fluconazole, mecoprop, diazinon, carbendazim, perfluorooctanoic acid, and clindamycin. The oxidation kinetic experiments for the degradation of carbendazim and fluconazole were performed, and the contribution of hydroxyl radical and superoxide radical was explored. Furthermore, this study also investigated the combination of UV/Ferrate process to treat the compounds with poor or moderate reactivity with ferrate alone and obtained kinetic parameters. In overall, this study added new information about ferrate oxidation efficiency toward newly tested model compounds and the potential of the ferrate-photo assisted process (UV/ferrate) and the role of radical species in ferrate technology.

6.2 Material and method

6.2.1 Chemicals and reagents

All tested model compounds were purchased from Sigma Aldrich (analytical grade) namely carbendazim (CDZ), atrazine (ATZ), sulfamethoxazole (SMX), carbamazepine (CMZ), trimethoprim (TMP), mecoprop (MCPP), diazinon (DZN), fluconazole (FCL), clindamycin (CLN) and pentadecfluorooctanoic acid (PFOA). The individual model compound stock solution was prepared by adding a measured amount of each compound and dissolved in a known volume of ultrapure water (resistance ≥18.2 MΩ, Millipore) in an amber glass bottle and mixed with a magnetic stirrer overnight. All stock solutions were stored at 4 ˚C. The concentration of each stock solution was prepared to have a concentration below its water solubility to avoid direct precipitation. The details of stock solution concentrations were provided in Table D. 1.

6.2.2 Classification of CECs reactivity to ferrate oxidation

The mixture of model compounds (50 µg/L) was spiked into different buffered solutions to examine pH impact on the degradation process. The phosphate buffer solution was used for pH=5.2 and 7.2 while the carbonate buffer solution was used for pH=9.2. The degradation of model compounds experiments was conducted in batch reactors and continuously stirred using a magnetic stirrer at room temperature 20 ± 1 ˚C. The reaction was initiated by adding ferrate into the solution and allowed to react for 30 minutes. At the end of the reaction, the samples were filtered using a 0.2 µm pore size nylon filter (Fisher Scientific). The CECs were analyzed using ultra-performance liquid chromatography – quadrupole time-of-flight mass spectrometry (Xevo G2-S, Waters), operated in positive or negative mode. Chromatographic separation was achieved using ACQUITY UPLC BEH C18, 50×2.1 mm column, at 50 °C with an injection volume of 10 µL.

6.2.3 Kinetic experiment

The kinetic oxidation experiments were conducted for two model compounds CDZ and CLN which tested for the first-time using ferrate treatment. Ferrate was added into buffered solution (potassium phosphate 10 mM, pH=7.2) containing individual targeted model compound and the reaction lasted for 30 minutes in a batch reactor. Ferrate was added in excess compared to the model compounds assuming pseudo-order kinetic condition. During the reaction course time, two samples were collected from the reaction solution at predetermined time intervals one sample quenched by sodium thiosulphate (1 mM) and the second by 2,20-azino-bis (3-ethylbenzothiazoline-6-sulfonate) (ABTS) (1.82 mM) to determine the concentrations of the model compound and ferrate respectively. The ferrate concentration was determined using the ABTS method spectrophotometric method (Lee et al., 2005). Radical scavengers *tert*-butyl alcohol (TBA) and *para*-benzoquinone (*p*BZQ) were used to identify the contribution of hydroxyl radical and superoxide radical, respectively. The concentration of radical scavengers used was 1 mM.

6.2.4 UV photolysis experiment

In this study, the combination of UV/Ferrate process was examined to treat the compounds with poor or moderate reactivity with ferrate. The selected model compounds (50 μg/L) spiked into phosphate buffer solution (pH=7.2) to mimic the pH of water and wastewater in the treatment plants. One set of samples treated by UV alone and another using UV/ Ferrate. To examine the contribution of hydroxyl radical, the reaction solution was spiked by radical scavengers TBA. Ferrate dose was fixed as 10 mg/L Fe (179 μM). Different doses of UV were used by exposing the samples to fixed radiation intensity for variable predetermined time intervals. The samples were quenched by sodium thiosulfate to stop the reaction and stored directly into amber vials and prevent any photodegradation due to the light. The samples were filtered using a 0.2 μm pore size nylon filter and the concentration was quantified using qTOF MS. A quasi-collimated beam UV apparatus (Model PSI-120, Calgon Carbon Corporation) was provided with a medium pressure mercury-lamp (Calgon Carbon Corporation). The irradiance was measured by a UV detector (International Light, Model SED240) connected with a radiometer (International Light, Model IL 1400A). The samples were placed into a glass beaker size 80 mL provided with a magnetic stirrer, with a testing solution depth of 3.8 cm and an internal diameter of 5.2 cm. The distance from the UV source and surface of the testing solution was fixed as 26 cm and UV irradiance maintained as 2.3 mW/cm^2. A small portion of the test solution was collected at different time intervals as per the required UV dose and consequently placed into an amber vial for further analysis.

6.3 Results

The degradation of the selected model compounds by ferrate was divided in different phases. Phase one aimed to classify the reactivity of the tested model compounds using different doses of ferrate under different pH. Phase two examined the kinetic of the indicator model compounds from groups 2 and 3 to obtain the rate constants and the contribution of radical species (hydroxyl radical and superoxide radical). In the third phase, the combination of ferrate -UV photolysis process was explored for the degradation of recalcitrant model compounds indicator and contribution of hydroxyl radical species was also reported. The concentrations of the model compounds in this study were selected to be environmentally relevant to mimic the real water matrix condition.

6.3.1 Classification of model compounds reactivity with ferrate

The physicochemical properties of all tested model compounds are presented in Table D. 2. The selected model compounds can be divided into two main groups: pesticides/surfactant and pharmaceutical model compounds. The pesticides/surfactant includes: ATZ, FCL, MCPP, DZN, CDZ and PFOA. The pharmaceutical compounds include: CBZ, SMX, TMP and CLN. The model compounds were spiked as a mixture in a buffer solution with an initial concentration of 50 μg/L. Different doses of ferrate doses were used (10, 20 and 30 mg/L Fe) to evaluate the reactivity of the selected model compounds.

In general, based on overall removal, the compounds were categorized into three groups: group 1 poorly reactive includes ATZ, FCL and MCPP, group 2 moderately reactive includes DNZ and CDZ and group3 highly reactive includes PFOA, CBZ, SMX, TMP and CLN (Figure 6. 1). In group 1, the removal generally was less than 50% even at high dose of ferrate (30 mg/L Fe), while in group 2 the removal exceeds 50% at moderate ferrate dose (20 mg/L Fe). In contrast, the removal of group 3 model compounds exceeds 50% even at a low dose of ferrate (10 mg/L Fe).

These findings further proved that ferrate is a selective oxidant thus could easily degrade specific types of model compounds which were also reported previously (Yang et al., 2012; Zhou and Jiang, 2015). The contribution of ferrate non-reactive species (i.e. ferric (Fe(III)) in the removal of model compounds was investigated in this study. Therefore, different doses of ferric chloride (as active iron equivalent to ferrate doses) were added to the reaction solution at pH=7.2 to mimic the removal in the coagulation process in the real application. As seen from Figure 6. 2, Fe(III) resulted from no removal to low removal of the selected CECs suggesting that their removal observed with ferrate treatment was mainly due to ferrate especially for group 2 and 3 compounds.

Higher removal was observed at lower pH for group 3 except PFOA, which was expected as ferrate is known to be a stronger oxidant at lower pH and thus the better removal. As the ferrate dose increase, the oxidant power of ferrate at lower pH also become less significant. No removal of PFOA was observed at acidic and neutral pH but only at basic pH strongly suggest that the removal was due to the coagulation at basic pH rather than oxidization.

In general, groups 1 and 2 have better removal at acidic and basic pH as compared to neutral pH which might be attributed to the stronger oxidizing power of ferrate at acidic pH and improved coagulation effect at basic pH.

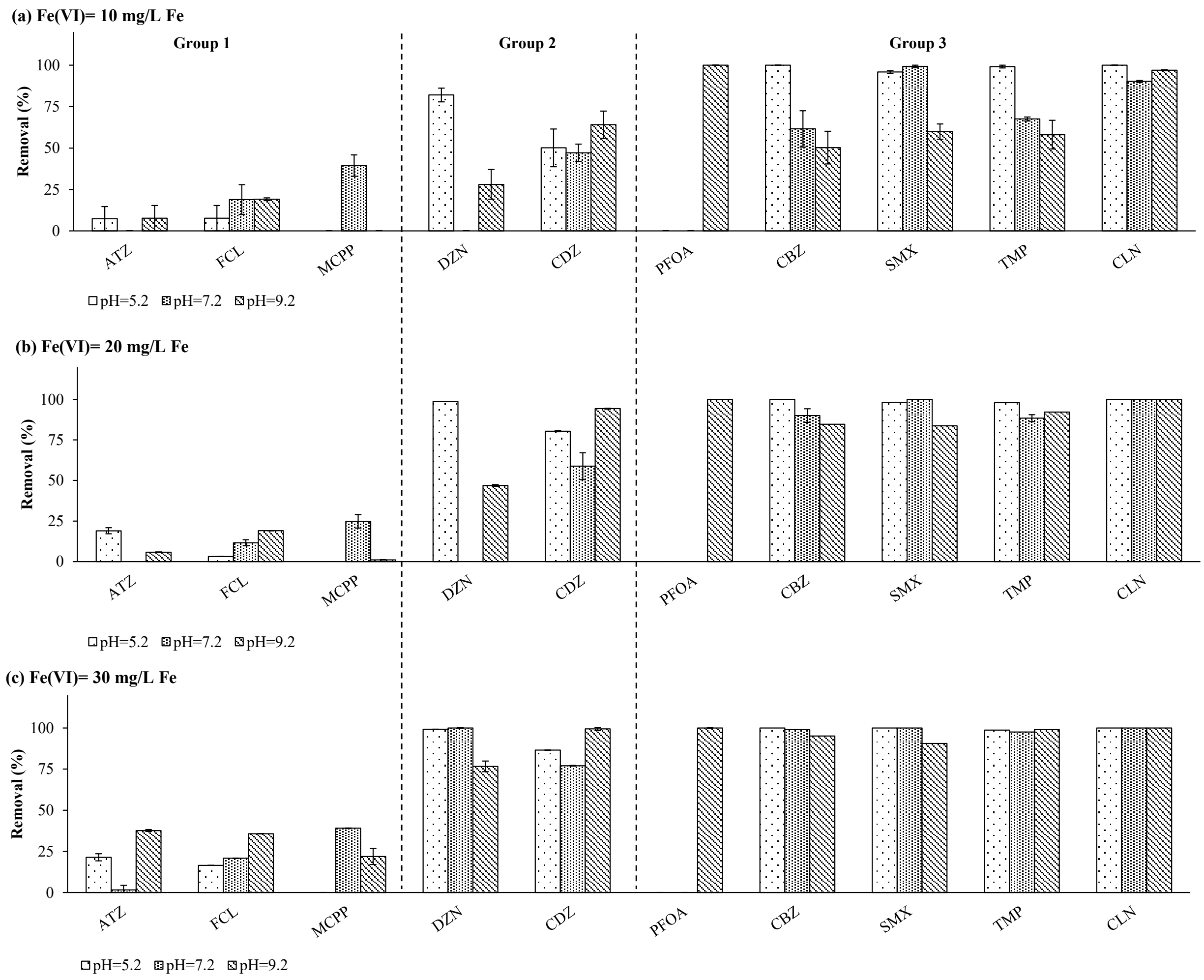

Figure 6. 1 Removal of selected MPs in buffered solutions (10 mM) with different pH values= 5.2, 7.2 and 9.2 with different doses of ferrate (a) Fe(VI) 10 mg/L Fe , (b) Fe(VI) 20 mg/L Fe and (c) Fe(VI) 30 mg/L Fe . The model compounds were spiked in mixture with fixed concentration of 50 μg/L

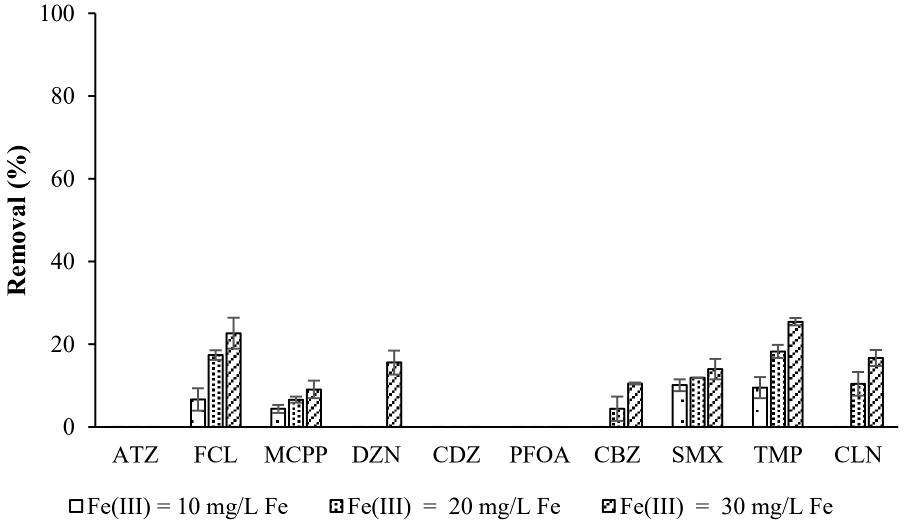

Figure 6. 2 Contribution of ferric (Fe(III)) in the removal of selected model compounds spiked in mixture in phosphate buffer solution (10 mM, pH= 7.2). Fe(III) was injected as an active iron equivalent to the used ferrate doses.

6.3.2 Kinetic study of DZN (group 2) and CLN (group 3)

One compound each from group 2 (DZN) and 3 (CLN) were selected as an indicator for the oxidation kinetic by ferrate. To the best of the author's knowledge, this is the first report of the kinetic study of DZN and CLN by ferrate. DZN might serve as an indicator for pesticides with moderate removal by ferrate technology while CLN indicator of the antibiotic pharmaceutical compound with high reactivity with ferrate. The kinetic experiments were conducted in a phosphate buffer solution with pH = 7.2 to mimic the pH condition of natural water and wastewater. The concentration of the tested compounds selected to be comparable with environmental detected concentration and fixed as 100 µg/L. Pseudo-order kinetic model was assumed to describe the kinetic data where the oxidant (i.e. ferrate) was added in excess.

Figure 6. 3 shows the degradation and kinetic modeling of DZN and ferrate. Ferrate 2 mg/L Fe (equal 36 µM Fe) removed 85% of DZN (100 µg/L) within 300 seconds with corresponded ferrate decay 53% (Figure 6. 3, b). The second-order kinetic model fit DZN oxidation data with

rate constant of DZN degradation as 1 x 10^{-4} (L/µg. s^{-1}) (equivalent to 41800 $M^{-1}s^{-1}$) with R^2=0.93 (Figure 6. 3, c). In comparison, sodium hypochlorite showed lower reactivity with DZN than ferrate with a rate constant of 1.6 $M^{-1}s^{-1}$ at pH = 9.5 (Zhang and Pehkonen, 1999). The ferrate-decay rate constant was found to be 2 x 10^{-6} (L/µg. s^{-1}) (equivalent to 0.1 x 10^{-3} $\mu M^{-1}s^{-1}$) which is smaller by 400 times than the rate constant of DZN degradation. That might prove the validity of pseudo-order kinetic assumption where the oxidant maintained in abundance during oxidation course. Direct photolysis also examined previously and showed poor reactivity with DZN (UV=2000 mJ/cm^2) and only removed 33% of DZN (200 µg/L) whereas UV/H_2O_2 (UV= 600 mJ/cm^2, H_2O_2= 25 mg/L) removed 96% of DZN at pH 7 (Shemer and Linden, 2006). Indeed, ferrate showed better performance than that of direct ozonation (1.58 mg/L O_3) which removed 89% of DZN (100 µg/L) within 30 minutes (pH~7)(Wu et al., 2007). That might suggest ferrate to be used as an alternative oxidant for degrading DZN which showed higher persistency to the aforementioned methods.

The CLN was removed >95% within the first 180 seconds by a ferrate dose of 2 mg/L Fe with only 40% of ferrate consumed (Figure 6. 4 a and b). The oxidation kinetic data found to fit properly with a second-order kinetic model for both CLN and ferrate (Figure 6. 4 c and d). The pseudo-second-order rate constant of CLN degradation was 14 x 10^{-4} (L/µg. s^{-1}) (605700 M^{-1} s^{-1}). The results revealed that the oxidation rate constant of CLN was higher than that of DZN by 14 times approximately under similar testing conditions.

The contribution of radical species (hydroxyl radical ($^{\bullet}OH$) and superoxide radical ($O_2^{\bullet-}$)) in the ferrate oxidation process of DZN and CLN was investigated for the first time in this study. Therefore, ferrate was spiked with and without superoxide radical scavengers (pBZQ) and hydroxyl radical scavenger (TBA) during DZN or CLN oxidation. As such, the results of this study showed that hydroxyl radical had no contribution to the degradation of DZN (Figure D. 1) while superoxide radical contributed significantly. In comparison, in ozone and UV-based techniques, hydroxyl radical contributed mainly to the DZN degradation process (Shemer and Linden, 2006; Wu et al., 2007). Of note, the degradation of DZN in the presence of pBZQ reduced by 51% which might indicate also the involvement of other species. In this study, it was evidenced that Fe(III) contributed partially to the removal of DZN (Figure 6. 2). However, the contribution of ferrate reactive species (Fe(V) and Fe(IV)) cannot be confirmed in this study and more experiments are required. Similar to DZN, $O_2^{\bullet-}$ was also the main contributor in the oxidation of CLN while $^{\bullet}OH$ showed no contribution. Additionally, the ferrate decay rate constant was found to be similar during the oxidation of both DZN and CLN with the calculated value of $2x\ 10^{-6}$ (L/µg. s^{-1}). This might further indicate that direct ferrate oxidation did not occur, and major oxidation occurred via superoxide species in ferrate technology. It should be stated that the role of radical species in the ferrate system was rarely addressed in the literature. Future studies might be required to further evaluate the involvement of other species in the ferrate system and evaluate the level of mineralization of the target compounds.

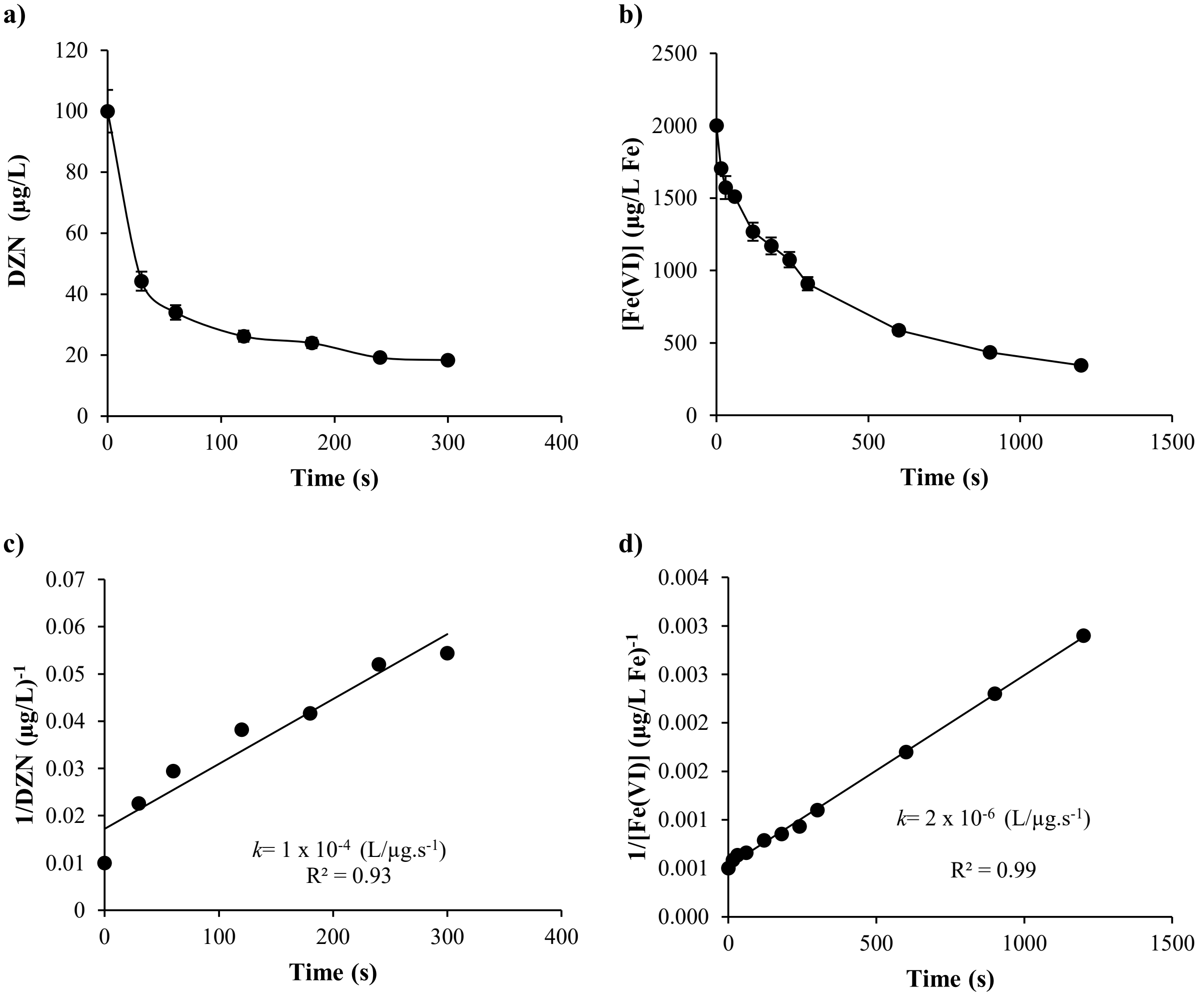

Figure 6. 3 Degradation of DZN by ferrate and kinetic modeling: a) DZN degradation (C_o= 100 µg/L) b) ferrate degradation (C_o = 2 mg/L Fe), c) DZN pseudo-second-order kinetic modeling d) ferrate pseudo-second order kinetic modeling. (DZN was spiked into phosphate-buffered solution (10 mM), pH=7.2).

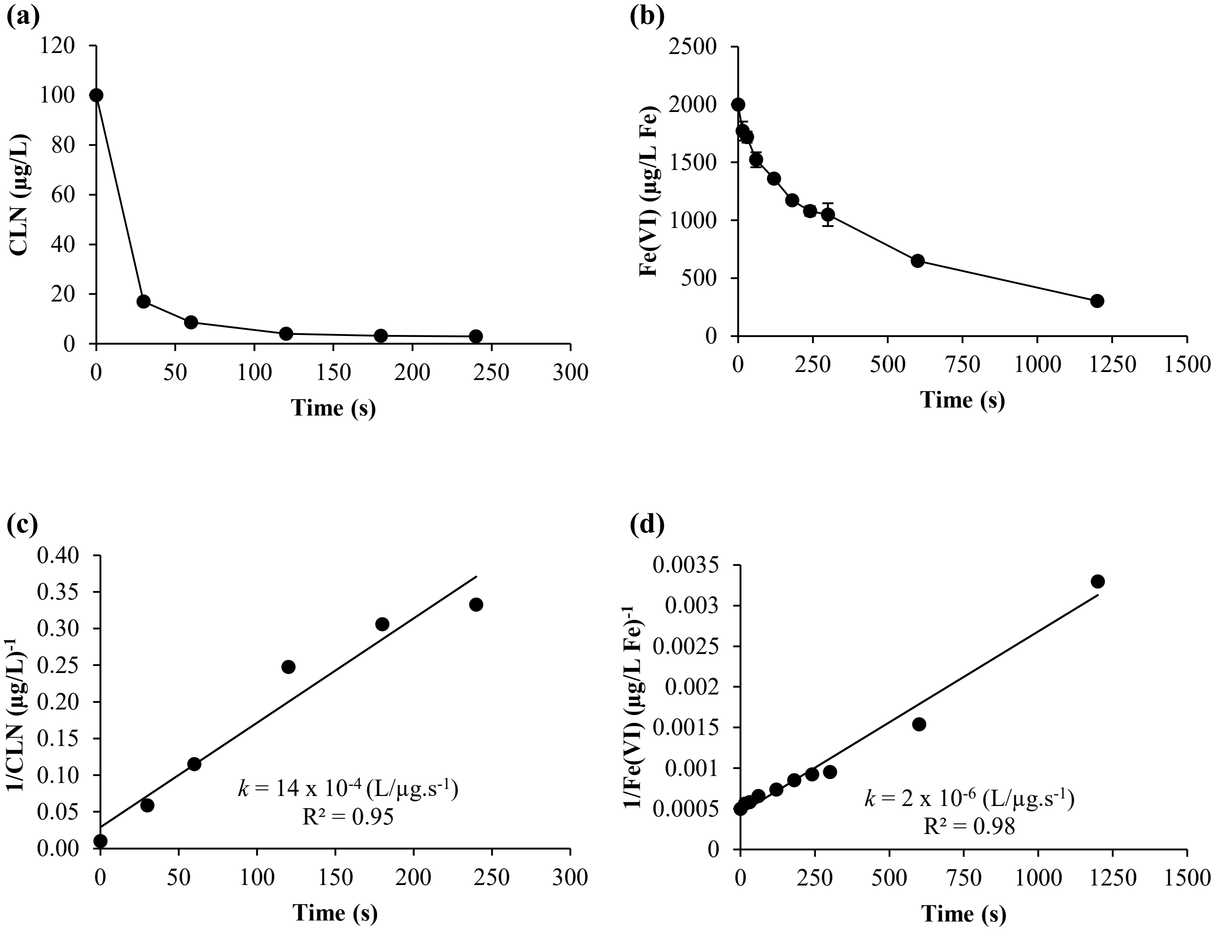

Figure 6. 4 Degradation of CLN by ferrate and kinetic modeling: a) CLN degradation (C_o= 100 µg/L) b) ferrate (C_o = 2 mg/L Fe), c) CLN Pseudo-second order kinetic modeling d) ferrate Pseudo-second order kinetic modeling. (CLN was spiked into phosphate buffered solution (10 mM), pH=7.2).

6.3.3 Ferrate-UV photo-degradation of selected MPs (MCPP and CDZ)

This study had explored the combination of ferrate-UV oxidation process to remove the poorly and moderately reactive model compounds as per the established classification in this study (section 6.3.1). Therefore, this section unveiled the degradation of MCPP (poorly reactive) and CDZ (moderately reactive) using fixed ferrate dose (178.6 µM equivalent= 10 mg/L Fe), a fixed concentration of model compounds (50 µg/L) and different doses of UV ranged from 0 to 221 mJ/cm^2. The removal of MCPP and CDZ by ferrate/UV processes was explored for the first time and no previous studies were found. The contribution of hydroxyl radical was also explored by spiking a set of samples with TBA ($^\bullet$OH scavenger). As such different sets of samples were prepared: UV ± TBA and UV/Ferrate ± TBA. As such, UV alone achieved better removal of MCPP than that attained by the UV/ferrate system with maximum removal of 60% at 221 mJ/cm^2 (Figure 6. 5 a). Similar photolysis hindrance by ferrate was reported previously where UV removed 89% of H_2S while UV/ferrate declined the removal to 65% (Talaiekhozani et al., 2016a). In principle, direct UV photolysis of model compound governs by molar absorbance of UV band which will raise the molecule to excited state thus leading to possible destabilization of the compound (Bolton and Stefan, 2002). Therefore, the presence of ferrate may cause shielding to MCPP molecules in this case thus hindering UV photolysis. In contrast, UV/Ferrate had removed 95% of CDZ while UV-alone achieved only 40% (Figure 6. 5 b). The degradation of CDZ (10 mg/L) examined previously using UV-alone and UV/TiO_2 (70 mg/L) which removed 90%of CDZ compared to 63% by UV alone with an exposure time of 75 minutes at pH= 6.73 (Saien and Khezrianjoo, 2008).

The pseudo-first-order kinetic was assumed which is widely used in previous studies to describe the degradation of model compounds using UV based process (Luo et al., 2018; Real et al., 2007; Shu et al., 2013). The kinetic modeling was performed based on equation 6.1(Bolton and Stefan, 2002). C_o is the initial concentration of the target compound and C the concentration at any time during the oxidation process and k time-based first-order rate constant and t is the time. By plotting ln C_o/C versus time k time based can be obtained. fluence based rate constant can be obtained by plotting ln C_o/C versus fluence doses (mJ/cm^2).

$$ln\left[\frac{C_o}{C}\right] = kt \qquad (6.1)$$

The pseudo-first order decay rate constant (fluence based) was obtained for MCPP and found to be 0.0037 cm^2/mJ (equal 0.008 s^{-1}) and 0.0005 cm^2/mJ (equal 0.0011 s^{-1}) using UV and UV/Ferrate respectively (Figure 6. 5 c). The degradation kinetic of MCPP (10 mg/L) at neutral pH was examined using different processes and the rate constants were reported as following UV (5400 mJ/cm^2) to be 0.0017 s^{-1}, UV/TiO_2 (5400 mJ/cm^2/100 mg/L) 0.0085 s^{-1}, UV/H_2O_2 (5400 mJ/cm^2/100 mg/L) 0.0135 s^{-1}, UV/persulfate (5400 mJ/cm^2/100 mg/L) 0.0052 s^{-1}, photo-Fenton (UV=5400 mJ/cm^2, Fe^{2+}=H_2O_2= 10 mg/L) 0.023 s^{-1}, Fenton (Fe^{2+}=10 mg/L, H_2O_2= 10 mg/L) 0.0065 s^{-1} (Martinez et al., 2016). This indicated that photo-catalytic process surpassed UV/ferrate therefore implementation of ferrate in MCPP oxidation might need further investigation to make it more feasible and effective.

CDZ degradation kinetic followed pseudo-first-order kinetic model and the rate constant (fluence-based) found to be 0.002 cm^2/mJ (equal 0.005 s^{-1}) and 0.014 cm^2/mJ (equal 0.03 s^{-1}) using UV and UV/Ferrate respectively (Figure 6. 5 d). The observed increment in the rate constant of DZN degradation by UV/Ferrate was 7 times higher than that achieved by UV alone which may attribute to the synergistic effect and promoting the formation of reactive species. This coincidence with what reported previously in the degradation of 2,4-dichlorophenol where the rate constant also increased from 0.0032 min^{-1} to 0.0222 min^{-1} by using UV and UV/ferrate respectively (ferrate 100 mg/L, 2, 4-dichlorophenol =20 mg/L, pH=7, UV= 0 to 712.8 mJ/cm^2) (Wu et al., 2020). Previous studies hypothesized that, the observed synergetic effect in the UV/ferrate process attributed to the formation of hydroxyl radical or Fe(V)/Fe(IV) reactive species (Aslani et al., 2017; Talaiekhozani et al., 2016a; Talaiekhozani et al., 2016b). In fact, this study investigated the $^{\bullet}OH$ contribution to the degradation of MCPP and CDZ in UV and UV/ferrate processes (Figure 6. 5, e and f). As such, in the UV-MCPP oxidation process, the $^{\bullet}OH$ radical contributed by 25% in the overall obtained oxidation rate constant (0.0036 cm^2/mJ) (Figure 6. 5, e) and while 75% expected to occur due to the direct UV photolysis which also reported previously (Shu et al., 2013). Furthermore, it was reported that UV-MCPP oxidation might be initiated by chlorine atom photolysis at benzene ring or direct $^{\bullet}$OH attack to the tertiary carbon atom of the propanoic moiety of MCPP (Semitsoglou-Tsiapou et al., 2016). Moreover, for CDZ, $^{\bullet}$OH contributed by 50% and 12% in the overall oxidation rate constants obtained by UV and UV/ferrate processes respectively (Figure 6. 5, f). Based on the observations of this study it can be stated that the $^{\bullet}$OH contribution in the UV/ferrate system was minimal and other reactive species were likely involved in the degradation process. A thorough study conducted by Wu and co-authors concluded that superoxide radical dominated the oxidation processes in the UV/ferrate system and mainly responsible for the observed degradation (Wu et al., 2020). In the same study, the formation of $O_2^{\bullet-}$ was confirmed by electron spin resonance (ESR) which showed increment by increasing UV radiation. In overall it can be stated that both $^{\bullet}$OH and $O_2^{\bullet-}$ were formed in the UV/ferrate process yet the latter dominated the UV/ferrate oxidation process.

(a) MCPP **(b)** CDZ

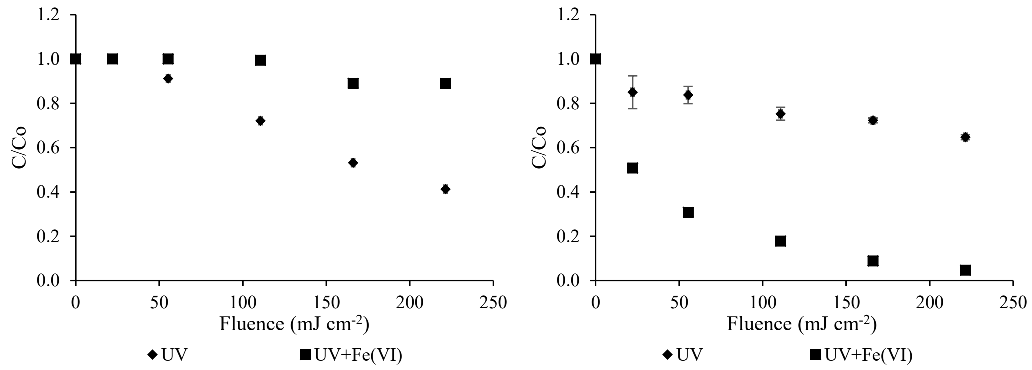

(c) MCPP **(d)** CDZ

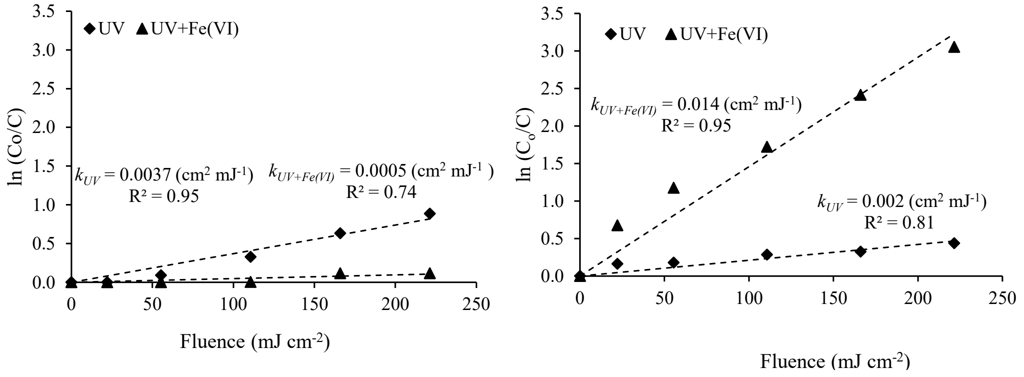

(e) MCPP **(f)** CDZ

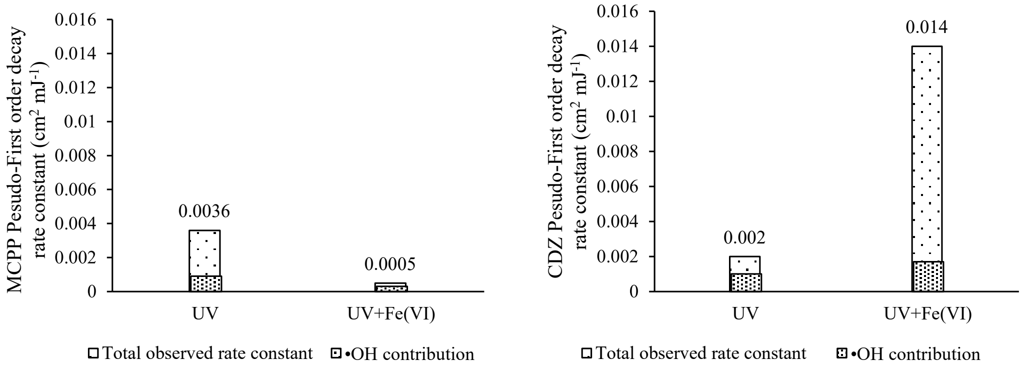

Figure 6. 5 Degradation and kinetic modeling of MCPP (50 µg/L) and CDZ (50 µg/L) treated by UV (0 to 250 mJ/cm^2) alone or by UV/ferrate (10 mg/L Fe): degradation of model compounds (a) MCPP, (b) CDZ; Pseudo-first order kinetic modeling (c) MCPP, (d) CDZ; Pseudo-first order decay rate constant with hydroxyl radical contribution (e) MCPP, (f) CDZ. The model compounds were spiked in a mixture in phosphate buffer solution (10 mM, pH=7).

6.4 Conclusions:

This study investigated the removal of selected model compounds presented in environmentally relevant concentrations using ferrate technologies. The selected model compounds showed different reactivity with ferrate and classified into three groups based on achieved removal: poorly reactive (removal <50%) model compounds: atrazine (ATZ), fluconazole (FLC), mecoprop (MCPP), moderately reactive (removal>50%): diazinon (DZN), carbendazim (CDZ), perfluorooctanoic acid (PFOA), and highly reactive (removal > 85%): carbamazepine (CBZ), sulfamethoxazole (SMX), trimethoprim (TMP) and clindamycin (CLN). The model compounds of groups 1 and 2 along with CLN showed less dependency on pH of the buffer solution. In contrast, PFOA was removed highly at alkaline pH and better removal was achieved at acidic pH for CBZ, SMX and TMP.

The oxidation kinetics of DZN and CLN was examined for the first-time using ferrate and the pseudo-second-order for both ferrate and the model compounds. A higher oxidation rate constant was obtained for CLN (14 x 10^{-4} (L/µg. s^{-1})) compared to that obtained for DZN (1 x 10^{-4} (L/µg. s^{-1})). The contribution of ferric species (Fe(III)), hydroxyl radical and superoxide radical species were all explored in this study. The results revealed that Fe(III) showed a small contribution (up to 25%) to the overall removal of tested compounds while hydroxyl radical showed no contribution. In contrast, superoxide radical contributed mainly to the removal of tested compounds in the ferrate system. The role of other reactive species in the ferrate system such as Fe(V) and Fe (IV) were not examined in this study and might require further investigation in future studies.

The degradation and kinetic of two model compounds (MCCP and CZN) were investigated using the UV/ferrate process. The results showed that the combination of UV/Ferrate improved the removal of CDZ by seven times (based on obtained fluence based rate constant). On the other hand, MCPP degradation declined by the combination of UV/Ferrate process which may due to shielding effects caused by the presence of ferrate molecules in the tested solution. The contribution of hydroxyl radical in the UV/ferrate system was investigated and found to have a minor contribution to the degradation process.

In overall this study showed that ferrate technology might be used successfully to remove the model compounds presented in the acidic, neutral or alkaline medium in environmentally relevant conditions.

6.5 References

Acero, J.L., Stemmler, K. and Von Gunten, U. 2000. Degradation kinetics of atrazine and its degradation products with ozone and OH radicals: A predictive tool for drinking water treatment. Environmental Science & Technology 34(4), 591-597.

Aslani, H., Nasseri, S., Nabizadeh, R., Mesdaghinia, A., Alimohammadi, M. and Nazmara, S. 2017. Haloacetic acids degradation by an efficient Ferrate/UV process: Byproduct analysis, kinetic study, and application of response surface methodology for modeling and optimization. Journal of Environmental Management 203, 218-228.

Benotti, M.J., Trenholm, R.A., Vanderford, B.J., Holady, J.C., Stanford, B.D. and Snyder, S.A. 2009. Pharmaceuticals and Endocrine Disrupting Compounds in US Drinking Water. Environmental Science & Technology 43(3), 597-603.

Bolton, J.R. and Stefan, M.I. 2002. Fundamental photochemical approach to the concepts of fluence (UV dose) and electrical energy efficiency in photochemical degradation reactions. Research on Chemical Intermediates 28(7-9), 857-870.

Chen, J., Xu, X., Zeng, X., Feng, M., Qu, R., Wang, Z., Nesnas, N. and Sharma, V.K. 2018. Ferrate(VI) oxidation of polychlorinated diphenyl sulfides: Kinetics, degradation, and oxidized products. Water Research 143, 1-9.

Feng, M., Cizmas, L., Wang, Z. and Sharma, V.K. 2017. Synergistic effect of aqueous removal of fluoroquinolones by a combined use of peroxymonosulfate and ferrate(VI). Chemosphere 177, 144-148.

Gombos, E., Barkacs, K., Felfoldi, T., Vertes, C., Mako, M., Palko, G. and Zaray, G. 2013. Removal of organic matters in wastewater treatment by ferrate (VI)-technology. Microchemical Journal 107, 115-120.

Hamza, R.A., Iorhemen, O.T. and Tay, J.H. 2016. Occurrence, impacts and removal of emerging substances of concern from wastewater. Environmental Technology & Innovation 5, 161-175.

Huber, M.M., Gobel, A., Joss, A., Hermann, N., Loffler, D., McArdell, C.S., Ried, A., Siegrist, H., Ternes, T.A. and von Gunten, U. 2005. Oxidation of pharmaceuticals during ozonation of municipal wastewater effluents: A pilot study. Environmental Science & Technology 39(11), 4290-4299.

Jiang, J.Q. 2013. The role of ferrate(VI) in the remediation of emerging micro pollutants. 2013 International Symposium on Environmental Science and Technology (2013 Isest) 18, 418-426.

Jiang, J.Q. 2015. The role of ferrate(VI) in the remediation of emerging micropollutants: a review. Desalination and Water Treatment 55(3), 828-835.

Jiang, J.Q., Zhou, Z. and Sharma, V.K. 2013. Occurrence, transportation, monitoring and treatment of emerging micro-pollutants in waste water - A review from global views. Microchemical Journal 110, 292-300.

Karlesa, A., De Vera, G.A.D., Dodd, M.C., Park, J., Espino, M.P.B. and Lee, Y. 2014. Ferrate(VI) Oxidation of beta-Lactam Antibiotics: Reaction Kinetics, Antibacterial Activity Changes, and Transformation Products. Environmental Science & Technology 48(17), 10380-10389.

Knopp, G., Prasse, C., Ternes, T.A. and Comel, P. 2016. Elimination of micropollutants and transformation products from a wastewater treatment plant effluent through pilot scale ozonation followed by various activated carbon and biological filters. Water Research 100, 580-592.

Lee, Y., Yoon, J. and von Gunten, U. 2005. Spectrophotometric determination of ferrate (Fe(Vl)) in water by ABTS. Water Research 39(10), 1946-1953.

Lee, Y., Zimmermann, S.G., Kieu, A.T. and von Gunten, U. 2009. Ferrate (Fe(VI)) Application for Municipal Wastewater Treatment: A Novel Process for Simultaneous Micropollutant Oxidation and Phosphate Removal. Environmental Science & Technology 43(10), 3831-3838.

Luo, S., Wei, Z., Spinney, R., Zhang, Z., Dionysiou, D.D., Gao, L., Chai, L., Wang, D. and Xiao, R. 2018. UV direct photolysis of sulfamethoxazole and ibuprofen: An experimental and modelling study. Journal of Hazardous Materials 343, 132-139.

Manoli, K., Nakhla, G., Ray, A.K. and Sharma, V.K. 2017. Enhanced oxidative transformation of organic contaminants by activation of ferrate(VI): Possible involvement of Fe-V/Fe-IV species. Chemical Engineering Journal 307, 513-517.

Martinez, S., Delgado, M. and Jarvis, P. 2016. Removal of Herbicide Mecoprop from Surface Water Using Advanced Oxidation Processes (AOPS). International Journal of Environmental Research 10(2), 291-296.

Peings, V., Pigot, T., Baylere, P., Sotiropoulos, J.M. and Frayret, J. 2017. Removal of pharmaceuticals by a potassium ferrate (VI) material: from practical implementation to reactivity prediction. Environmental Science-Water Research & Technology 3(4), 699-709.

Petrie, B., Barden, R. and Kasprzyk-Hordern, B. 2015. A review on emerging contaminants in wastewaters and the environment: Current knowledge, understudied areas and recommendations for future monitoring. Water Research 72, 3-27.

Real, F.J., Benitez, F.J., Acero, J.L. and Gonzalez, M. 2007. Removal of diazinon by various advanced oxidation processes. Journal of Chemical Technology and Biotechnology 82(6), 566-574.

Saien, J. and Khezrianjoo, S. 2008. Degradation of the fungicide carbendazim in aqueous solutions with UV/TiO2 process: Optimization, kinetics and toxicity studies. Journal of Hazardous Materials 157(2-3), 269-276.

Semitsoglou-Tsiapou, S., Templeton, M.R., Graham, N.J.D., Leal, L.H., Martijn, B.J., Royce, A. and Kruithof, J.C. 2016. Low pressure UV/H2O2 treatment for the degradation of the pesticides metaldehyde, clopyralid and mecoprop - Kinetics and reaction product formation. Water Research 91, 285-294.

Sharma, V.K. 2002. Potassium ferrate(VI): an environmentally friendly oxidant. Advances in Environmental Research 6(2), 143-156.

Sharma, V.K. 2013. Ferrate(VI) and ferrate(V) oxidation of organic compounds: Kinetics and mechanism. Coordination Chemistry Reviews 257(2), 495-510.

Sharma, V.K., Chen, L. and Zboril, R. 2016. Review on High Valent Fe-VI (Ferrate): A Sustainable Green Oxidant in Organic Chemistry and Transformation of Pharmaceuticals. Acs Sustainable Chemistry & Engineering 4(1), 18-34.

Shemer, H. and Linden, K.G. 2006. Degradation and by-product formation of diazinon in water during UV and UV/H2O2 treatment (vol 136, pg 553, 2003). Journal of Hazardous Materials 138(3), 638-638.

Shu, Z.Q., Bolton, J.R., Belosevic, M. and El Din, M.G. 2013. Photodegradation of emerging micropollutants using the medium-pressure UV/H2O2 Advanced Oxidation Process. Water Research 47(8), 2881-2889.

Sun, X.H., Zhang, Q., Liang, H., Ying, L., Meng, X.X. and Sharma, V.K. 2016. Ferrate(VI) as a greener oxidant: Electrochemical generation and treatment of phenol. Journal of Hazardous Materials 319, 130-136.

Talaiekhozani, A., Eskandari, Z., Bagheri, M. and Talaie, M.R. 2016a. Removal of H2S and COD using UV, ferrate and UV/ferrate from municipal wastewater. Journal of Human, Environment and Health Promotion 2(1), 1-8.

Talaiekhozani, A., Salari, M., Talaei, M.R., Bagheri, M. and Eskandari, Z. 2016b. Formaldehyde removal from wastewater and air by using UV, ferrate(VI) and UV/ferrate(VI). Journal of Environmental Management 184, 204-209.

Tankiewicz, M., Fenik, J. and Biziuk, M. 2010. Determination of organophosphorus and organonitrogen pesticides in water samples. Trac-Trends in Analytical Chemistry 29(9), 1050-1063.

Trapido, M., Epold, I., Bolobajev, J. and Dulova, N. 2014. Emerging micropollutants in water/wastewater: growing demand on removal technologies. Environmental Science and Pollution Research 21(21), 12217-12222.

Westerhoff, P., Yoon, Y., Snyder, S. and Wert, E. 2005. Fate of endocrine-disruptor, pharmaceutical, and personal care product chemicals during simulated drinking water treatment processes. Environmental Science & Technology 39(17), 6649-6663.

Wu, J.G., Luan, T.G., Lan, C.Y., Lo, W.H. and Chan, G.Y.S. 2007. Efficacy evaluation of low-concentration of ozonated water in removal of residual diazinon, parathion, methyl-parathion and cypermethrin on vegetable. Journal of Food Engineering 79(3), 803-809.

Wu, S., Liu, H., Lin, Y., Yang, C., Lou, W., Sun, J., Du, C., Zhang, D., Nie, L., Yin, K. and Zhong, Y. 2020. Insights into mechanisms of UV/ferrate oxidation for degradation of phenolic pollutants: Role of superoxide radicals. Chemosphere 244.

Wu, S.H., Li, H.R., Li, X., He, H.J. and Yang, C.P. 2018. Performances and mechanisms of efficient degradation of atrazine using peroxymonosulfate and ferrate as oxidants. Chemical Engineering Journal 353, 533-541.

Yang, B., Ying, G.G., Zhao, J.L., Liu, S., Zhou, L.J. and Chen, F. 2012. Removal of selected endocrine disrupting chemicals (EDCs) and pharmaceuticals and personal care products (PPCPs) during ferrate(VI) treatment of secondary wastewater effluents. Water Research 46(7), 2194-2204.

Zhang, K.J., Luo, Z., Zhang, T.Q., Gao, N.Y. and Ma, Y. 2015. Degradation Effect of Sulfa Antibiotics by Potassium Ferrate Combined with Ultrasound (Fe(VI)-US). Biomed Research International, 12.

Zhang, Q. and Pehkonen, S.O. 1999. Oxidation of diazinon by aqueous chlorine: Kinetics, mechanisms, and product studies. Journal of Agricultural and Food Chemistry 47(4), 1760-1766.

Zhou, Z.W. and Jiang, J.Q. 2015. Treatment of selected pharmaceuticals by ferrate(VI): Performance, kinetic studies and identification of oxidation products. Journal of Pharmaceutical and Biomedical Analysis 106, 37-45.

Chapter 7: Conclusions and Recommendations

7.1 Thesis overview

The combined sewer overflow is associated with wet weather flow (WWF) conditions in which a tremendous amount of combined sewer with limited or no treatment is sent directly to receiving water bodies. Different approaches have been proposed in the literature to mitigate the impacts of WWF, including physical and chemical processes or a combination of both. Enhanced primary treatment (EPT) using coagulant/flocculant was a more practical solution for existing wastewater treatment plants due to its easy retrofitting. Several coagulants might be used such as alum, poly-aluminum chloride, and ferric chloride. Ferrate has emerged as a multifunctional chemical that could act as a coagulant, disinfectant, and oxidant. It has the potential to be employed for WWF wastewater treatment to minimize the levels of suspended solids, turbidity, and microorganisms. Ferrate can also be used as a powerful oxidant to treat a wide range of pharmaceutical and personal care products (PPCPs) and pesticides which are present at higher concentrations in the influent and effluent wastewaters during WWF conditions due to surface runoff and the lack of removal during conventional wastewater treatment.

To achieve the target removal level of suspended solids and turbidity from WWF wastewater, several metal salt coagulants (alum, poly-aluminum chloride, and ferric chloride) were investigated in chapter 3. The doses and the operating conditions were optimized based on a factorial design. Bench-scale data were also scaled-up into a full application. Then, ferrate was thoroughly investigated in chapter 4 for its role in minimizing both the suspended solids and turbidity along with microbial level. It was explored in different possible treatment trains that rely on the application of ferrate as a coagulant, coagulant aid, and/or disinfectant. The disinfection kinetics parameters, which have special importance in real practice, were studied in chapter 5.

Moreover, the mode of action of ferrate for inactivating *E. coli* and flow cytometry analysis was studied in chapter 5. In chapter 6 the role of ferrate alone or in combination with UV for the degradation of selected PPCPs and pesticides was examined. In addition, the pH impact on the oxidation process and the contribution of oxygen reactive species were also highlighted.

7.2 Conclusions

The main conclusions of this research based on the main topics were listed as follows:

Optimization of metal salt coagulants for enhanced primary treatment during WWF

- Alum surpassed other coagulants (poly-aluminum chloride and ferric chloride), where an alum dose of 6 mg/L Al without any polymer achieved the target levels of TSS (<25 mg/L) and reduced turbidity and ortho-P by 87% and 71%, respectively.
- Three-factor ANOVA showed that TSS removal depended mostly on rapid mixing while COD and ortho-P removals depended on slow mixing and coagulant dose.
- Bench and full-scale applications of coagulant and coagulant aid exhibited comparable results especially for turbidity and TSS removals.

Ferrate as coagulant, coagulant aid, and disinfectant for treating wastewater during WWF

- The best removals of turbidity, TSS and, COD were achieved with ferrate used at a low dose (0.5 mg/L Fe) as a coagulant along with a cationic polymer (1.25 mg/L).
- ANOVA revealed that polymer addition and slow mixing had significant effects on the removal of turbidity, TSS and COD. On the other hand, rapid mixing had no direct effect on the removal of turbidity, while it affected significantly TSS and COD removals. General linear model equations were established and could predict the removal of TSS, turbidity and COD.

- Ferrate achieved a target level of TSS <25 mg/L, yet it failed to reduce the turbidity level to < 8 NTU.
- Ferrate as a coagulant aid with alum (ferrate = 10 mg/L Fe and alum 6 mg/L Al) achieved the target levels of TSS, turbidity and ferrate-induced iron particles in the treated effluent.
- Ferrate achieved the highest bacterial inactivation when used either with alum or at the post-dosing point.
- By using ferrate (10 mg/L Fe) as coagulant aid with alum (6 mg/L Al), the levels of TSS, turbidity and *E. coli* were simultaneously reduced and reached the target levels under the experimental conditions.

Ferrate disinfection kinetics study

- Ferrate exhibited high efficiency to inactivate the *E. coli* in the EPT effluent during WWF.
- Ferrate (5, 8 and 10 mg/L Fe) effectively removed *E. coli* within 3 to 10 minutes with log removals ranging from 1.7 to 4.2.
- Ferrate-decay followed second-order kinetics and *E. coli* inactivation was described successfully by the tested models: Chick-Watson, Hom and Collins-Selleck models with adjusted $R^2 \geq 0.94$.
- Flow cytometry (FCM) analysis revealed that, ferrate inactivated *E. coli* mainly by damaging or destructing the cell membrane while limited total cell lysis (limited oxidation of DNA) was achieved.
- The *in-situ* produced hydrogen peroxide during ferrate-decay was verified and equaled 20 to 26% of the ferrate initial dose.

- Ferrate imposed slight toxicity effects on the treated wastewater samples, which might be attributed to the formation of toxic compounds via the ferrate-oxidation process.

Degradation of micropollutants by ferrate and radical species contribution

- Ferrate showed high selectivity during the oxidation of the tested model compounds which were classified into three groups: group 1 poorly reactive (removal <50%) (includes: ATZ, FCL and MCPP), moderately reactive (removal>50%) (includes: DZN and CDZ), and highly reactive (removal > 85%) (includes: PFOA, CBZ, SMX and CLN).
- The model compounds of groups 1 and 2 along with CLN showed less dependence on pH of the buffer solution. In contrast, PFOA was removed highly at alkaline pH and better removals were achieved at acidic pH for CBZ, SMX and TMP.
- Ferrate-oxidation kinetics of DZN and CLN followed second order with oxidation rate constants 0.7314 $\mu M^{-1}s^{-1}$ and 0.0418 $\mu M^{-1}s^{-1}$, respectively.
- Ferric species (Fe(III)) (the final reduced form of ferrate) showed a small contribution (up to 25%) to the overall removal of the tested compounds while hydroxyl radicals showed no contribution. In contrast, superoxide radicals contributed mainly to the removal of tested compounds in the ferrate system.
- The combination of UV/ferrate improved the removal of CDZ by seven times (based on the obtained fluence based rate constant) while MCPP degradation decreased by the combination of UV/Ferrate process which may occur due to shielding effects caused by the presence of ferrate molecules in the tested solution. The contribution of hydroxyl radicals in the UV/ferrate system to the degradation process was minor.

7.3 Recommendations

- Bench-scale findings of this research should be entailed by a full-scale experiment for further confirmation.
- Evaluating the feasibility of using ferrate in the full-scale application requires further investigation.
- Ferrate should not be used as a primary coagulant for WWF wastewater due to it is poor coagulation properties especially for the removal of turbidity.
- A thorough investigation is required to evaluate the effect of alum/ferrate on the formed flocs characteristics.
- The *in-situ* generated H_2O_2 in the ferrate system should be always addressed and its potential benefits need further investigation.
- Flow cytometry analysis provides essential information on the viability of target bacteria and may be used as a complementary tool to evaluate the biocidal effect of the tested chemicals.
- Because ferrate imposed slight toxicity effects on the treated samples, the identification of the byproducts generated after the treatment and more comprehensive toxicity assays will be required in future experiments.
- The contribution of superoxide radical in the ferrate system was overlooked in most of the previous studies; therefore, it should be always considered in future studies.

Bibliography

Abughararah, Z.H. 1994. Effect of temperature on the kinetics of waste-water disinfection using ultraviolet-radiation. Journal of Environmental Science and Health Part a-Environmental Science and Engineering & Toxic and Hazardous Substance Control 29(3), 585-603.

Acero, J.L., Stemmler, K. and Von Gunten, U. 2000. Degradation kinetics of atrazine and its degradation products with ozone and OH radicals: A predictive tool for drinking water treatment. Environmental Science & Technology 34(4), 591-597.

Aguilar, M.I., Saez, J., Llorens, M., Soler, A., Ortuno, J.F., Meseguer, V. and Fuentes, A. 2005. Improvement of coagulation-flocculation process using anionic polyacrylamide as coagulant aid. Chemosphere 58(1), 47-56.

Al-Abduly, A. and Sharma, V.K. 2014. Oxidation of benzothiophene, dibenzothiophene, and methyl-dibenzothiophene by ferrate(VI). Journal of Hazardous Materials 279, 296-301.

Alalm, M.G., Tawfik, A. and Ookawara, S. 2015. Comparison of solar TiO2 photocatalysis and solar photo-Fenton for treatment of pesticides industry wastewater: Operational conditions, kinetics, and costs. Journal of Water Process Engineering 8, 55-63.

Alameddine, M., Al Umairi, A.R., Zakee Shaikh, M. and Gamal El-Din, M. 2020. Bench to Full-Scale Enhanced Primary Treatment of Municipal Wastewater under Wet Weather Flow for Minimized Pollution Load: Evaluation of Chemical Addition and Process Control Indicators. Canadian Journal of Civil Engineering.

Government of Alberta. 2018. Environmental Quality Guidelines for Alberta Surface Waters. Water Policy Branch, Alberta Evironment and Parks. Government of Alberta, Edmonton,Alberta.

Alsheyab, M., Jiang, J.-Q. and Stanford, C. 2010. Electrochemical generation of ferrate (VI): Determination of optimum conditions. Desalination 254(1-3), 175-178.

Altmann, J., Massa, L., Sperlich, A., Gnirss, R. and Jekel, M. 2016. UV_{254} absorbance as real-time monitoring and control parameter for micropollutant removal in advanced wastewater treatment with powdered activated carbon. Water research 94, 240-245.

Altmann, J., Zietzschmann, F., Geiling, E.-L., Ruhl, A.S., Sperlich, A. and Jekel, M. 2015. Impacts of coagulation on the adsorption of organic micropollutants onto powdered activated carbon in treated domestic wastewater. Chemosphere 125.

Alyaseri, I. and Zhou, J. 2016. Stormwater Volume Reduction in Combined Sewer Using Permeable Pavement: City of St. Louis. Journal of Environmental Engineering 142(4).

Amano, M., Lohwacharin, J., Dubechot, A. and Takizawa, S. 2018. Performance of integrated ferrate-polyaluminum chloride coagulation as a treatment technology for removing freshwater humic substances. Journal of Environmental Management 212, 323-331.

Anderson, M.J. (2015) Design of Experiments Simplified, Boca Raton, FL: CRC Press is an imprint of the Taylor & Francis Group, an Informa business.

Andoh, R.Y.G. and Saul, A.J. 2003. The use of hydrodynamic vortex separators and screening systems to improve water quality. Water Science and Technology 47(4), 175-183.

Anquandah, G.A.K., Sharma, V.K., Panditi, V.R., Gardinali, P.R., Kim, H. and Oturan, M.A. 2013. Ferrate(VI) oxidation of propranolol: Kinetics and products. Chemosphere 91(1), 105-109.

Antonelli, M., Rossi, S., Mezzanotte, V. and Nurizzo, C. 2006. Secondary effluent disinfection: PAA long term efficiency. Environmental Science & Technology 40(15), 4771-4775.

American Public Health Association (APHA).2017. Standard Methods for the Examination of Water and Wastewater, Washington, DC, USA.

Arlos, M.J., Braggb, L.M., Servos, M.R. and Parker, W.J. 2014. Simulation of the fate of selected pharmaceuticals and personal care products in a highly impacted reach of a Canadian watershed. Science of the Total Environment, 193-204.

Asghar, A., Raman, A.A.A. and Daud, W.M.A.W. 2015. Advanced oxidation processes for in-situ production of hydrogen peroxide/hydroxyl radical for textile wastewater treatment: a review. Journal of Cleaner Production 87, 826-838.

Aslani, H., Nasseri, S., Nabizadeh, R., Mesdaghinia, A., Alimohammadi, M. and Nazmara, S. 2017. Haloacetic acids degradation by an efficient Ferrate/UV process: Byproduct analysis, kinetic study, and application of response surface methodology for modeling and optimization. Journal of Environmental Management 203, 218-228.

Aubertin, N., Neveux, N., Gerardin, R. and Evrard, O. 1996. Synthesis of potassium sulfatoferrate and its use in wastewater treatment. Revue des Sciences de l'Eau 9(1), 17-30.

Autixier, L., Mailhot, A., Bolduc, S., Madoux-Humery, A.-S., Galarneau, M., Prevost, M. and Dorner, S. 2014. Evaluating rain gardens as a method to reduce the impact of sewer overflows in sources of drinking water. Science of the Total Environment 499, 238-247.

Avila, C., Jose Salas, J., Martin, I., Aragon, C. and Garcia, J. 2013. Integrated treatment of combined sewer wastewater and stormwater in a hybrid constructed wetland system in southern Spain and its further reuse. Ecological Engineering 50, 13-20.

Baghvand, A., Zand, A.D., Mehrdadi, N. and Karbassi, A. 2010. Optimizing coagulation process for low to high turbidity waters using aluminum and iron salts. American Journal of Environmental Sciences 6(5), 442-448.

Barbeau, B., Desjardins, R., Mysore, C. and Prevost, M. 2005. Impacts of water quality on chlorine and chlorine dioxide efficacy in natural waters. Water Research 39(10), 2024-2033.

Barbesti, S., Citterio, S., Labra, M., Baroni, M.D., Neri, M.G. and Sgorbati, S. 2000. Two and three-color fluorescence flow cytometric analysis of immunoidentified viable bacteria. Cytometry 40(3), 214-218.

Benotti, M.J., Trenholm, R.A., Vanderford, B.J., Holady, J.C., Stanford, B.D. and Snyder, S.A. 2009. Pharmaceuticals and Endocrine Disrupting Compounds in US Drinking Water. Environmental Science & Technology 43(3), 597-603.

Berney, M., Hammes, F., Bosshard, F., Weilenmann, H.-U. and Egli, T. 2007. Assessment and interpretation of bacterial viability by using the LIVE/DEAD BacLight kit in combination with flow cytometry. Applied and Environmental Microbiology 73(10), 3283-3290.

Berney, M., Vital, M., Huelshoff, I., Weilenmann, H.-U., Egli, T. and Hammes, F. 2008a. Rapid, cultivation-independent assessment of microbial viability in drinking water. Water Research 42(14), 4010-4018.

Berney, M., Vital, M., Hulshoff, I., Weilenmann, H.U., Egli, T. and Hammes, F. 2008b. Rapid, cultivation-independent assessment of microbial viability in drinking water. Water Research 42(14), 4010-4018.

Berney, M., Weilenmann, H.-U. and Egli, T. 2006. Flow-cytometric study of vital cellular functions in Escherichia coli during solar disinfection (SODIS). Microbiology-Sgm 152, 1719-1729.

Birch, H., Mikkelsen, P.S., Jensen, J.K. and Lutzhoft, H.C.H. 2011. Micropollutants in stormwater runoff and combined sewer overflow in the Copenhagen area, Denmark. Water Science and Technology 64(2), 485-493.

Bledzka, D., Gryglik, D., Olak, M., Gebicki, J.L. and Miller, J.S. 2010. Degradation of n-butylparaben and 4-tert-octylphenol in H2O2/UV system. Radiation Physics and Chemistry 79(4), 409-416.

Bolton, J.R. and Linden, K.G. 2003. Standardization of methods for fluence (UV dose) determination in bench-scale UV experiments. Journal of Environmental Engineering-Asce 129(3), 209-215.

Bolton, J.R. and Stefan, M.I. 2002. Fundamental photochemical approach to the concepts of fluence (UV dose) and electrical energy efficiency in photochemical degradation reactions. Research on Chemical Intermediates 28(7-9), 857-870.

Bunce, J.T., Ndam, E., Ofiteru, I.D., Moore, A. and Graham, D.W. 2018. A Review of Phosphorus Removal Technologies and Their Applicability to Small-Scale Domestic Wastewater Treatment Systems. Frontiers in Environmental Science 6.

Campo, N., De Flora, C., Maffettone, R., Manoli, K., Sarathy, S., Santoro, D., Gonzalez-Olmos, R. and Auset, M. 2020. Inactivation kinetics of antibiotic resistant Escherichia coli in secondary wastewater effluents by peracetic and performic acids. Water research 169, 115227.

Canonica, S., Meunier, L. and Von Gunten, U. 2008. Phototransformation of selected pharmaceuticals during UV treatment of drinking water. Water Research 42(1-2), 121-128.

Cao, B., Gao, B., Xu, C., Fu, Y. and Liu, X. 2010. Effects of pH on coagulation behavior and floc properties in Yellow River water treatment using ferric based coagulants. Chinese Science Bulletin 55(14), 1382-1387.

Chen, J., Xu, X., Zeng, X., Feng, M., Qu, R., Wang, Z., Nesnas, N. and Sharma, V.K. 2018. Ferrate(VI) oxidation of polychlorinated diphenyl sulfides: Kinetics, degradation, and oxidized products. Water Research 143, 1-9.

Chhetri, R.K., Bonnerup, A. and Andersen, H.R. 2016. Combined Sewer Overflow pretreatment with chemical coagulation and a particle settler for improved peracetic acid disinfection. Journal of Industrial and Engineering Chemistry 37, 372-379.

Chhetri, R.K., Flagstad, R., Munch, E.S., Hørning, C., Berner, J., Kolte-Olsen, A., Thornberg, D. and Andersen, H.R. 2015. Full scale evaluation of combined sewer overflows disinfection using performic acid in a sea-outfall pipe. Chemical Engineering Journal 270, 133-139.

Chhetri, R.K., Thornberg, D., Berner, J., Gramstad, R., Ojstedt, U., Sharma, A.K. and Andersen, H.R. 2014a. Chemical disinfection of combined sewer overflow waters using performic acid or peracetic acids. The Science of the total environment 490, 1065-1072.

Chhetri, R.K., Thornberg, D., Berner, J., Gramstad, R., Ojstedt, U., Sharma, A.K. and Andersen, H.R. 2014b. Chemical disinfection of combined sewer overflow waters using performic acid or peracetic acids. Sci. Total Environ. 490, 1065-1072.

Cho, M., Lee, Y., Choi, W., Chung, H.M. and Yoon, J. 2006. Study on Fe(VI) species as a disinfectant: Quantitative evaluation and modeling for inactivating Escherichia coli. Water Res. 40(19), 3580-3586.

Chys, M., Audenaert, W.T.M., Deniere, E., Mortier, S.v.T.r.s.F.C., Langenhove, H.V., Nopens, I., Demeestere, K. and Hulle, S.W.H.V. 2017. Surrogate-Based Correlation Models in View of Real-Time Control of Ozonation of Secondary Treated Municipal Wastewater - Model Development and Dynamic Validation. Environmental Science and Technology 51, 14233-14243.

City-of-Edmonton 2009 City of Edmonton Total Loadings Plan City of Edmonton Edmonton.

Collivignarelli, C., Bertanza, G. and Pedrazzani, R. 2000. A comparison among different wastewater disinfection systems: Experimental results. Environmental Technology 21(1), 1-16.

Collivignarelli, M.C., Abba, A., Benigna, I., Sorlini, S. and Torretta, V. 2018. Overview of the Main Disinfection Processes for Wastewater and Drinking Water Treatment Plants. Sustainability 10(1), 21.

Cornwell, D.A. and Bishop, M.M. 1983. Determining velocity gradients in laboratory and full-scale systems. American Water Works Association Journal 75(9), 470-475.

Coyle, E.E., Ormsbee, L.E. and Brion, G.M. 2014. Peracetic Acid as an Alternative Disinfection Technology for Wet Weather Flows. Water Environment Research 86(8), 687-697.

Czekalski, N., Imminger, S., Salhi, E., Veljkovic, M., Kleffel, K., Drissner, D., Hammes, F., Burgmann, H. and von Gunten, U. 2016. Inactivation of Antibiotic Resistant Bacteria and Resistance Genes by Ozone: From Laboratory Experiments to Full-Scale Wastewater Treatment. Environmental Science & Technology 50(21), 11862-11871.

David Jenkins, J.F.F., And Arnold and Menar, B. 1970 Review Paper:Chemical Processes for Phosphate Removal, pp. 369-389., Water Research Pergamon Press.

De Laat, J. and Gallard, H. 1999. Catalytic decomposition of hydrogen peroxide by Fe(III) in homogeneous aqueous solution: Mechanism and kinetic modeling. Environmental Science & Technology 33(16), 2726-2732.

Del Rio, H., Suarez, J., Puertas, J. and Ures, P. 2013. PPCPs wet weather mobilization in a combined sewer in NW Spain. Science of the Total Environment 449, 189-198.

Dempsey, B.A., Sheu, H., Tanzeer Ahmed, T.M.T. and Mentink, J. 1985. Polyaluminum Chloride and Alum Coagulation of Clay-Fulvic Aicd Suspensions. American Water Works Association 77(3), 74-80.

Deng, Y., Jung, C., Liang, Y., Goodey, N. and Waite, T.D. 2018. Ferrate(VI) decomposition in water in the absence and presence of natural organic matter (NOM). Chemical Engineering Journal 334, 2335-2342.

Ding, L., Liu, T.X. and Li, X.Z. 2014. Removal of CH3SH with in-situ generated ferrate(VI) in a wet-scrubbing reactor. Journal of Chemical Technology and Biotechnology 89(3), 455-461.

Doane, T.A. and Horwath, W.R. 2010. Eliminating interference from iron(III) for ultraviolet absorbance measurements of dissolved organic matter. Chemosphere 78(11), 1409-1415.

Dong, F., Liu, J., Li, C., Lin, Q., Zhang, T., Zhang, K. and Sharma, V.K. 2019. Ferrate(VI) pre-treatment and subsequent chlorination of blue-green algae: Quantification of disinfection byproducts. Environment International 133.

Duan, J.M. and Gregory, J. 2003. Coagulation by hydrolysing metal salts. Advances in Colloid and Interface Science 100, 475-502.

Duchesne, S., Mailhot, A., Dequidt, E. and Villeneuve, J.-P. 2001. Mathematical modeling of sewer under surcharge for real time control of combined sewer overflows. Urban Water 3, 241-252.

Ebeling, J.M. and Ogden, S.R. 2004. Application of chemical coagulation aids for the removal of suspended solids (TSS) and phosphorus from the microscreen effluent discharge of an intensive recirculating aquaculture system. North American Journal of Aquaculture 66(3), 198-207.

El Samrani, A.G., Lartiges, B.S. and Villieras, F. 2008a. Chemical coagulation of combined sewer overflow: heavy metal removal and treatment optimization. Water research 42(4-5), 951-960.

El Samrani, A.G., Lartiges, B.S. and Villieras, F. 2008b. Chemical coagulation of combined sewer overflow: Heavy metal removal and treatment optimization. Water Res. 42(4-5), 951-960.

Elnakar, H. and Buchanan, I. 2019. The role of mixing in potassium ferrate(VI) consumption kinetics and disinfection of bypass wastewater. Journal of Environmental Management 231, 515-523.

Environment and Climate Change Canada (ECCC). 2019a. Wastewater Systems Effluent Regulations-2016 Status Report. Environment Canada, Gatineau, Quebec.

Environment and Climate Change Canada (ECCC). 2019b. Wastewater Systems Effluent Regulations Reported Data Environment. Canada, Gatineau, Quebec.

Environment and Climate Change Canada (ECCC). 2019c. Canadian Environmental Protection Act, 1999, Federal Environmental Quality Guidelines – Iron. National Guidelines and Standards Office, Environment Canada, Gatineau, Quebec.

EPA 1999 Combined Sewer Overflows Guidelines for Monitoring and Modeling. Agency, W.M.E.P. (ed).

Exall, K. and Marsalek, J. 2013. A Coagulant Survey for Chemically Enhanced Primary Treatment of Synthetic CSOs. Water Air and Soil Pollution 224(2), 9.

Fan, J., Lin, B.-H., Chang, C.-W., Zhang, Y. and Lin, T.-F. 2018. Evaluation of potassium ferrate as an alternative disinfectant on cyanobacteria inactivation and associated toxin fate in various waters. Water Research 129, 199-207.

Fang, R., Cheng, X. and Xu, X. 2010. Synthesis of lignin-base cationic flocculant and its application in removing anionic azo-dyes from simulated wastewater. Bioresource Technology 101(19), 7323-7329.

Faria, E.C., Brown, B.J.T. and Snook, R.D. 2004. Water toxicity monitoring using Vibrio fischeri: a method free of interferences from colour and turbidity. Journal of Environmental Monitoring 6(2), 97-102.

Feng, M., Cizmas, L., Wang, Z. and Sharma, V.K. 2017a. Activation of ferrate(VI) by ammonia in oxidation of flumequine: Kinetics, transformation products, and antibacterial activity assessment. Chemical Engineering Journal 323, 584-591.

Feng, M., Cizmas, L., Wang, Z. and Sharma, V.K. 2017b. Synergistic effect of aqueous removal of fluoroquinolones by a combined use of peroxymonosulfate and ferrate(VI). Chemosphere 177, 144-148.

Feng, M. and Sharma, V.K. 2018. Enhanced oxidation of antibiotics by ferrate(VI)-sulfur(IV) system: Elucidating multi-oxidant mechanism. Chemical Engineering Journal 341, 137-145.

Gan, W.H., Sharrna, V.K., Zhang, X., Yang, Y. and Yang, X. 2015. Investigation of disinfection byproducts formation in ferrate(VI) pre-oxidation of NOM and its model compounds followed by chlorination. Journal of Hazardous Materials 292, 197-204.

Gandhi, R., Ray, A.K., Sharma, V.K. and Nakhla, G. 2014. Treatment of Combined Sewer Overflows Using Ferrate (VI). Water Environment Research 86(11), 2202-2211.

Ganguly, P., Byrne, C., Breen, A. and Pillai, S.C. 2018. Antimicrobial activity of photocatalysts: Fundamentals, mechanisms, kinetics and recent advances. Applied Catalysis B-Environmental 225, 51-75.

Gasperi, J., Garnaud, S., Rocher, V. and Moilleron, R. 2008. Priority pollutants in wastewater and combined sewer overflow. The Science of the total environment 407(1), 263-272.

Gasperi, J., Laborie, B. and Rocher, V. 2012. Treatment of combined sewer overflows by ballasted flocculation: Removal study of a large broad spectrum of pollutants. Chem. Eng. J. 211, 293-301.

Gasperi, J., Rocher, V., Gilbert, S., Azimi, S. and Chebbo, G. 2010. Occurrence and removal of priority pollutants by lamella clarification and biofiltration. Water Research 44(10), 3065-3076.

Ghernaout, D. and Naceur, M.W. 2011. Ferrate(VI): In situ generation and water treatment - A review. Desalination and Water Treatment 30(1-3), 319-332.

Ghosh, M., Manoli, K., Renaud, J.B., Sabourin, L., Nakhla, G., Sharma, V.K. and Ray, A.K. 2019. Rapid removal of acesulfame potassium by acid-activated ferrate(VI) under mild alkaline conditions. Chemosphere 230, 416-423.

Gibson, J., Farnood, R. and Seto, P. 2016a. Chemical pretreatment of combined sewer overflows for improved UV disinfection. Water Science and Technology 73(2), 375-381.

Gibson, J., Farnood, R. and Seto, P. 2016b. Chemical pretreatment of combined sewer overflows for improved UV disinfection. Water science and technology : a journal of the International Association on Water Pollution Research 73(2), 375-381.

Gillespie, S., Lipphaus, P., Green, J., Parsons, S., Weir, P., Juskowiak, K., Jefferson, B., Jarvis, P. and Nocker, A. 2014. Assessing microbiological water quality in drinking water distribution systems with disinfectant residual using flow cytometry. Water Research 65, 224-234.

Gombos, E., Barkacs, K., Felfoldi, T., Vertes, C., Mako, M., Palko, G. and Zaray, G. 2013. Removal of organic matters in wastewater treatment by ferrate (VI)-technology. Microchemical Journal 107, 115-120.

Gombos, E., Felfoeldi, T., Barkacs, K., Vertes, C., Vajna, B. and Zaray, G. 2012. Ferrate treatment for inactivation of bacterial community in municipal secondary effluent. Bioresource Technology 107, 116-121.

Goodwill, J.E., Jiang, Y.J., Reckhow, D.A., Gikonyo, J. and Tobiason, J.E. 2015. Characterization of Particles from Ferrate Preoxidation. Environmental Science & Technology 49(8), 4955-4962.

Government of Alberta 2018 Environmental Quality Guidelines for Alberta Surface Waters, Water Policy Branch Alberta Environment and Parks Edmonton, Alberta.

Graham, N.J.D., Khoi, T.T. and Jiang, J.Q. 2010. Oxidation and coagulation of humic substances by potassium ferrate. Water Science and Technology 62(4), 929-936.

Grayson, R.B., Finlayson, B.L., Gippel, C.J. and Hart, B.T. 1996. The potential of field turbidity measurements for the computation of total phosphorus and suspended solids loads. Journal of Environmental Management 47(3), 257-267.

Gregori, G., Citterio, S., Ghiani, A., Labra, M., Sgorbati, S., Brown, S. and Denis, M. 2001. Resolution of viable and membrane-compromised bacteria in freshwater and marine waters based on analytical flow cytometry and nucleic acid double staining. Applied and Environmental Microbiology 67(10), 4662-4670.

Gromaire, M.C., Garnaud, S., Saad, M. and Chebbo, G. 2001. Contribution of different sources to the pollution of wet weather flows in combined sewers. Water Research 35(2), 521-533.

Guida, M., Mattei, M., Della Rocca, C., Melluso, G. and Meric, S. 2007. Optimization of alum-coagulation/flocculation for COD and TSS removal from five municipal wastewater. Desalination 211(1-3), 113-127.

Gyurek, L.L. and Finch, G.R. 1998. Modeling water treatment chemical disinfection kinetics. Journal of Environmental Engineering-Asce 124(9), 783-793.

Haas, C.N. and Karra, S.B. 1984. kinetics of microbial inactivation by chlorine .2. kinetics in the presence of chlorine demand. Water Research 18(11), 1451-1454.

Hamza, R.A., Iorhemen, O.T. and Tay, J.H. 2016. Occurrence, impacts and removal of emerging substances of concern from wastewater. Environmental Technology & Innovation 5, 161-175.

Han, Q., Wang, H.J., Dong, W.Y., Liu, T.Z. and Yin, Y.L. 2014. Suppression of bromate formation in ozonation process by using ferrate(VI): Batch study. Chemical Engineering Journal 236, 110-120.

Han, Q., Wang, H.J., Dong, W.Y., Liu, T.Z., Yin, Y.L. and Fan, H.K. 2015. Degradation of bisphenol A by ferrate(VI) oxidation: Kinetics, products and toxicity assessment. Chemical Engineering Journal 262, 34-40.

Hannouche, A., Chebbo, G., Ruban, G., Tassin, B., Lemaire, B.J. and Joannis, C. 2011. Relationship between turbidity and total suspended solids concentration within a combined sewer system. Water Science and Technology 64(12), 2445-2452.

Hassaballah, A.H., Nyitrai, J., Hart, C.H., Dai, N. and Sassoubre, L.M. 2019. A pilot-scale study of peracetic acid and ultraviolet light for wastewater disinfection. Environmental Science-Water Research & Technology 5(8), 1453-1463.

Haydar, S. and Aziz, J.A. 2009. Characterization and treatability studies of tannery wastewater using chemically enhanced primary treatment (CEPT)-A case study of Saddiq Leather Works. Journal of Hazardous Materials 163(2-3), 1076-1083.

Henao, L.D., Cascio, M., Turolla, A. and Antonelli, M. 2018. Effect of suspended solids on peracetic acid decay and bacterial inactivation kinetics: Experimental assessment and definition of predictive models. Science of the Total Environment 643, 936-945.

Hernandez, M.A.C., May, A., Bonakdapour, A., Mohseni, M. and Wilkinson, D.P. 2017. Analytical quantification of electrochemical ferrates for drinking water treatments. Canadian Journal of Chemistry 95(1), 105-112.

Hollender, J., Zimmermann, S.G., Koepke, S., Krauss, M., McArdell, C.S., Ort, C., Singer, H., von Gunten, U. and Siegrist, H. 2009. Elimination of Organic Micropollutants in a Municipal Wastewater Treatment Plant Upgraded with a Full-Scale Post-Ozonation Followed by Sand Filtration. Environmental Science & Technology 43(20), 7862-7869.

Hu, J., Chu, W., Sui, M., Xu, B., Gao, N. and Ding, S. 2018. Comparison of drinking water treatment processes combinations for the minimization of subsequent disinfection by-products formation during chlorination and chloramination. Chem. Eng. J. 335, 352-361.

Hu, L., Page, M.A., Sigstam, T., Kohn, T., Marinas, B.J. and Strathmann, T.J. 2012a. Inactivation of Bacteriophage MS2 with Potassium Ferrate(VI). Environmental Science & Technology 46(21), 12079-12087.

Hu, L., Page, M.A., Sigstam, T., Kohn, T., Mariñas, B.J. and Strathmann, T.J. 2012b. Inactivation of Bacteriophage MS2 with Potassium Ferrate(VI). Environ. Sci. Technol. 46(21), 12079-12087.

Huang, C.C., Hu, Y., Wang, L., Wang, Y.F., Li, N., Guo, Y.Q., Feng, Y.Y. and Xiao, L.H. 2017. Environmental Transport of Emerging Human-Pathogenic Cryptosporidium Species and Subtypes through Combined Sewer Overflow and Wastewater. Applied and Environmental Microbiology 83(16), 11.

Huang, Y., Nie, Z., Wang, C., Li, Y., Xu, M. and Hofmann, R. 2018. Quenching H2O2 residuals after UV/H2O2 oxidation using GAC in drinking water treatment. Environmental Science-Water Research & Technology 4(10), 1662-1670.

Huber, M.M., Gobel, A., Joss, A., Hermann, N., Loffler, D., McArdell, C.S., Ried, A., Siegrist, H., Ternes, T.A. and von Gunten, U. 2005a. Oxidation of pharmaceuticals during ozonation of municipal wastewater effluents: A pilot study. Environmental Science & Technology 39(11), 4290-4299.

Huber, M.M., Korhonen, S., Ternes, T.A. and von Gunten, U. 2005b. Oxidation of pharmaceuticals during water treatment with chlorine dioxide. Water Research 39(15), 3607-3617.

Hussain, S., Aziz, H.A., Isa, M.H., Ahmad, A., Van Leeuwen, J., Zou, L., Beecham, S. and Umar, M. 2011. Orthophosphate removal from domestic wastewater using limestone and granular activated carbon. Desalination 271(1-3), 265-272.

Irfan, M., Butt, T., Imtiaz, N., Abbas, N., Khan, R.A. and Shafique, A. 2017. The removal of COD, TSS and colour of black liquor by coagulation-flocculation process at optimized pH, settling and dosing rate. Arabian Journal of Chemistry 10, S2307-S2318.

Jain, A., Sharma, V.K. and Mbuya, O.S. 2009. Removal of arsenite by Fe(VI), Fe(VI)/Fe(III), and Fe(VI)/Al(III) salts: Effect of pH and anions. Journal of Hazardous Materials 169(1-3), 339-344.

Jalliffier-Verne, I., Leconte, R., Huaringa-Alvarez, U., Madoux-Humery, A.S., Galarneau, M., Servais, P., Prevost, M. and Dorner, S. 2015. Impacts of global change on the concentrations and dilution of combined sewer overflows in a drinking water source. Science of the Total Environment 508, 462-476.

Jeon, J.C., Jung, Y.J., Kwon, K.H. and Min, K.S. 2017. Enhanced water quality of CSOs with different coagulant treatment. Desalin. Water Treat. 63, 469-477.

Jessen, A., Randall, A., Reinhart, D. and Daly, L. 2008. Effectiveness and Kinetics of Ferrate as a Disinfectant for Ballast Water. Water Environment Research 80(6), 561-569.

Jiang Chengchun, L.C., and Wang Shichao (2008) Ferrates Synthesis,Properties, and Applications in Water and Wastewater Treatment. K.Sharma, V. (ed), pp. 94-101, American Chemical Society.

Jiang, J.-Q., Zhou, Z., Patibandla, S. and Shu, X. 2013a. Pharmaceutical removal from wastewater by ferrate(VI) and preliminary effluent toxicity assessments by the zebrafish embryo model. Microchemical Journal 110, 239-245.

Jiang, J.K. and Graham, N.J.D. 2010. Enhanced Coagulation Using Al/Fe(III) Coagulants: Effect of Coagulant Chemistry on the Removal of Colour-Causing NOM. Environmental Technology 17, 937-950.

Jiang, J.Q. 2013. The role of ferrate(VI) in the remediation of emerging micro pollutants. 2013 International Symposium on Environmental Science and Technology (2013 Isest) 18, 418-426.

Jiang, J.Q. 2014. Advances in the development and application of ferrate(VI) for water and wastewater treatment. Journal of Chemical Technology and Biotechnology 89(2), 165-177.

Jiang, J.Q. 2015. The role of ferrate(VI) in the remediation of emerging micropollutants: a review. Desalination and Water Treatment 55(3), 828-835.

Jiang, J.Q., Durai, H.B.P., Winzenbacher, R., Petri, M. and Seitz, W. 2015a. Drinking water treatment by in situ generated ferrate(VI). Desalination and Water Treatment 55(3), 731-739.

Jiang, J.Q. and Lloyd, B. 2002. Progress in the development and use of ferrate(VI) salt as an oxidant and coagulant for water and wastewater treatment. Water Research 36(6), 1397-1408.

Jiang, J.Q., Lloyd, B. and Grigore, L. 2001. Preparation and evaluation of potassium ferrate as an oxidant and coagulant for potable water treatment. Environmental Engineering Science 18(5), 323-328.

Jiang, J.Q., Wang, S. and Panagoulopoulos, A. 2006. The exploration of potassium ferrate(VI) as a disinfectant/coagulant in water and wastewater treatment. Chemosphere 63(2), 212-219.

Jiang, J.Q., Wang, S. and Panagoulopoulos, A. 2007. The role of potassium ferrate(VI) in the inactivation of Escherichia coli and in the reduction of COD for water remediation. Desalination 210(1-3), 266-273.

Jiang, J.Q., Zhou, Z. and Sharma, V.K. 2013b. Occurrence, transportation, monitoring and treatment of emerging micro-pollutants in waste water - A review from global views. Microchemical Journal 110, 292-300.

Jiang, W., Chen, L., Batchu, S.R., Gardinali, P.R., Jasa, L., Marsalek, B., Zboril, R., Dionysiou, D.D., O'Shea, K.E. and Sharma, V.K. 2014a. Oxidation of Microcystin-LR by Ferrate(VI): Kinetics, Degradation Pathways, and Toxicity Assessments. Environmental Science & Technology 48(20), 12164-12172.

Jiang, W.J., Zhu, L.F., Sharma, V.K., Batchu, S.R., Gardinali, P.R., Dionysiou, D.D. and O'Shea, K.E. 2014b. Oxidation of microcystin-LR by ferrate(VI): Intermediates, degradation pathways, and toxicity assessments. Abstracts of Papers of the American Chemical Society 247, 1.

Jiang, Y., Goodwill, J.E., Tobiason, J.E. and Reckhow, D.A. 2015b. Effect of Different Solutes, Natural Organic Matter, and Particulate Fe(III) on Ferrate(VI) Decomposition in Aqueous Solutions. Environmental Science & Technology 49(5), 2841-2848.

Jiang, Y.J., Goodwill, J.E., Tobiason, J.E. and Reckhow, D.A. 2015c. Effect of Different Solutes, Natural Organic Matter, and Particulate Fe(III) on Ferrate(VI) Decomposition in Aqueous Solutions. Environmental Science & Technology 49(5), 2841-2848.

Jiang, Y.J., Goodwill, J.E., Tobiason, J.E. and Reckhow, D.A. 2016a. Bromide oxidation by ferrate(VI): The formation of active bromine and bromate. Water Research 96, 188-197.

Jiang, Y.J., Goodwill, J.E., Tobiason, J.E. and Reckhow, D.A. 2016b. Impacts of ferrate oxidation on natural organic matter and disinfection byproduct precursors. Water Research 96, 114-125.

Jimenez-Del-Rio, M., Suarez-Cedeno, G. and Velez-Pardo, C. 2010. Using paraquat to generate anion free radicals and hydrogen peroxide in in vitro: antioxidant effect of vitamin e a procedure to teach theoretical and experimental principles of reactive oxygen species biochemistry. Biochemistry and Molecular Biology Education 38(2), 104-109.

Johnson, A.C. and Williams, R.J. 2004. A Model To Estimate Influent and Effluent Concentrations of Estradiol, Estrone, and Ethinylestradiol at Sewage Treatment Works. Environmental Science and Technology 38, 3649-3658.

Jolis, D. and Ahmad, M.L. 2004. Evaluation of high-rate clarification for wet-weather-only treatment facilities. Water Environment Research 76(5), 474-480.

Jun, M. and Wei, L. 2002. Effectiveness of ferrate (VI) preoxidation in enhancing the coagulation of surface waters. Water Research 36(20), 4959-4962.

Jung, C., Oh, J. and Yoon, Y. 2015. Removal of acetaminophen and naproxen by combined coagulation and adsorption using biochar: influence of combined sewer overflow components. Environmental science and pollution research international 22(13), 10058-10069.

Karlesa, A., De Vera, G.A.D., Dodd, M.C., Park, J., Espino, M.P.B. and Lee, Y. 2014. Ferrate(VI) Oxidation of beta-Lactam Antibiotics: Reaction Kinetics, Antibacterial Activity Changes, and Transformation Products. Environmental Science & Technology 48(17), 10380-10389.

Kay, P., Hughes, S.R., Ault, J.R., Ashcroft, A.E. and Brown, L.E. 2016. Widespread, routine occurrence of pharmaceuticals in sewage effluent, combined sewer overflows and receiving waters. Environmental Pollution 220, 1447e1455.

Keen, O.S., Dotson, A.D. and Linden, K.G. 2013. Evaluation of Hydrogen Peroxide Chemical Quenching Agents following an Advanced Oxidation Process. Journal of Environmental Engineering-Asce 139(1), 137-140.

Kelly, C.J., Tumsaroj, N. and Lajoie, C.A. 2004. Assessing wastewater metal toxicity with bacterial bioluminescence in a bench-scale wastewater treatment system. Water Research 38(2), 423-431.

Kerr, J.L., Guo, Z., Smith, D.W., Goss, G.G. and Belosevic, M. 2008. Use of goldfish to monitor wastewater and resue water for xenobiotics. Journal of Environmental Engineering and Science 7.

Kim, M.-K. and Zoh, K.-D. 2016. Occurrence and removals of micropollutants in water environment. Environmental Engineering Research 21(4), 319-332.

Knopp, G., Prasse, C., Ternes, T.A. and Comel, P. 2016. Elimination of micropollutants and transformation products from a wastewater treatment plant effluent through pilot scale ozonation followed by various activated carbon and biological filters. Water Research 100, 580-592.

Koeck-Schulmeyer, M., Villagrasa, M., Lopez de Alda, M., Cespedes-Sanchez, R., Ventura, F. and Barcelo, D. 2013. Occurrence and behavior of pesticides in wastewater treatment plants and their environmental impact. Science of the Total Environment 458, 466-476.

Kok, S. 2004. Wet-weather flow management in the Great Lakes Areas of Concern. Water Quality Research Journal of Canada 39(4), 319-330.

Kolar, M., Novak, P., Siskova, K.M., Machala, L., Malina, O., Tucek, J., Sharma, V.K. and Zboril, R. 2016. Impact of inorganic buffering ions on the stability of Fe(VI) in aqueous solution: role of the carbonate ion. Physical Chemistry Chemical Physics 18(6), 4415-4422.

Kowalska, E., Janczarek, M., Hupka, J. and Grynkiewicz, M. 2004. H2O2/UV enhanced degradation of pesticides in wastewater. Water Science and Technology 49(4), 261-266.

Kralchevska, R.P., Prucek, R., Kolarik, J., Tucek, J., Machala, L., Filip, J., Sharma, V.K. and Zboril, R. 2016. Remarkable efficiency of phosphate removal: Ferrate(VI)-induced in situ sorption on core-shell nanoparticles. Water Research 103, 83-91.

Krupinska, I. 2018. Removal of natural organic matter from groundwater by coagulation using prehydrolysed and non- prehydrolysed coagulants. Desalin. Water Treat. 132, 244-252.

Kwon, J.H., Kim, I.K., Park, K.Y., Kim, Y.D. and Cho, Y.H. 2014. Removal of phosphorus and coliforms from secondary effluent using ferrate(VI). Ksce Journal of Civil Engineering 18(1), 81-85.

Laidler, K.J. 1984. The development of the arrhenius equation. Journal of Chemical Education 61(6), 494-498.

Lambert, R.J.W. 2003. A model for the thermal inactivation of micro-organisms. Journal of Applied Microbiology 95(3), 500-507.

Lambert, R.J.W., Johnston, M.D. and Simons, E.A. 1999. A kinetic study of the effect of hydrogen peroxide and peracetic acid against Staphylococcus aureus and Pseudomonas aeruginosa using the Bioscreen disinfection method. Journal of Applied Microbiology 87(5), 782-786.

Lan, B.Y., Wang, Y.X., Wang, X., Zhou, X.T., Kang, Y. and Li, L.S. 2016. Aqueous arsenic (As) and antimony (Sb) removal by potassium ferrate. Chemical Engineering Journal 292, 389-397.

Launay, M.A., Dittmer, U. and Steinmetz, H. 2016a. Organic micropollutants discharged by combined sewer overflows - Characterisation of pollutant sources and stormwater-related processes. Water Res. 104, 82-92.

Launay, M.A., Dittmer, U. and Steinmetz, H. 2016b. Organic micropollutants discharged by combined sewer overflowseCharacterisation of pollutant sources and stormwater-related processes. Water research 104, 82-92.

Lee, Y., Cho, M., Kim, J.Y. and Yoon, J. 2004. Chemistry of ferrate (Fe(VI)) in aqueous solution and its applications as a green chemical. J. Ind. Eng. Chem. 10(1), 161-171.

Lee, Y., Imminger, S., Czekalski, N., von Gunten, U. and Hammes, F. 2016. Inactivation efficiency of Escherichia coli and autochthonous bacteria during ozonation of municipal wastewater effluents quantified with flow cytometry and adenosine tri-phosphate analyses. Water Research 101, 617-627.

Lee, Y., Kissner, R. and von Gunten, U. 2014. Reaction of Ferrate(VI) with ABTS and Self-Decay of Ferrate(VI): Kinetics and Mechanisms. Environmental Science & Technology 48(9), 5154-5162.

Lee, Y. and von Gunten, U. 2010. Oxidative transformation of micropollutants during municipal wastewater treatment: Comparison of kinetic aspects of selective (chlorine, chlorine dioxide, ferrate(VI), and ozone) and non-selective oxidants (hydroxyl radical). Water Research 44(2), 555-566.

Lee, Y., Yoon, J. and von Gunten, U. 2005. Spectrophotometric determination of ferrate (Fe(Vl)) in water by ABTS. Water Research 39(10), 1946-1953.

Lee, Y., Zimmermann, S.G., Kieu, A.T. and von Gunten, U. 2009. Ferrate (Fe(VI)) Application for Municipal Wastewater Treatment: A Novel Process for Simultaneous Micropollutant Oxidation and Phosphate Removal. Environmental Science & Technology 43(10), 3831-3838.

Lefevre, F., Audic, J.M. and Ferrand, F. 1992. peracetic-acid disinfection of secondary effluents discharged off coastal seawater. Water Science and Technology 25(12), 155-164.

Li, C., Dong, F., Feng, L., Zhao, J., Zhang, T., Cizmas, L. and Sharma, V.K. 2017a. Bacterial community structure and microorganism inactivation following water treatment with ferrate(VI) or chlorine. Environmental Chemistry Letters 15(3), 525-530.

Li, C., Li, X.Z., Graham, N. and Gao, N.Y. 2008. The aqueous degradation of bisphenol A and steroid estrogens by ferrate. Water Research 42(1-2), 109-120.

Li, H., Gyurek, L.L., Finch, G.R., Smith, D.W. and Belosevic, M. 2001. Effect of temperature on ozone inactivation of Cryptosporidium parvum in oxidant demand-free phosphate buffer. Journal of Environmental Engineering-Asce 127(5), 456-467.

Li, J.G., Dhanvantari, S., Averill, D. and Biswas, N. 2003. Windsor combined sewer overflow treatability study with chemical coagulation. Water Quality Research Journal of Canada 38(2), 317-334.

Li, J.G., Horneck, H., Averill, D., McCorquodale, J.A. and Biswas, N. 2004. High-Rate Retention Treatment Basins for CSO Control in Windsor, Ontario. Water Quality Research Journal of Canada 39(4), 449–456.

Li, X., Liu, Y., Liu, F., Liu, A. and Feng, Q. 2017b. Comparison of ferric chloride and aluminum sulfate on phosphorus removal and membrane fouling in MBR treating BAF effluent of municipal wastewater. Journal of Water Reuse and Desalination 7(4), 442-448.

Liang, Y.M., Zhang, Z.L., Yang, X. and Liu, W. 2013. Effect of Suspended Solids on the Sequential Disinfection of Secondary Effluent by UV Irradiation and Chlorination. Journal of Environmental Engineering 139(12), 1482-1487.

Liberti, L., Lopez, A., Notarnicola, M., Barnea, N., Pedahzur, R. and Fattal, B. 2000. Comparison of advanced disinfecting methods for municipal wastewater reuse in agriculture. Water Science and Technology 42(1-2), 215-220.

Licht, S. and Yu, X.W. 2005. Electrochemical alkaline Fe(VI) water purification and remediation. Environmental Science & Technology 39(20), 8071-8076.

Lim, M. and Kim, M.-J. 2010. Effectiveness of Potassium Ferrate (K2FeO4) for Simultaneous Removal of Heavy Metals and Natural Organic Matters from River Water. Water Air and Soil Pollution 211(1-4), 313-322.

Lin, S.H. and Lo, C.C. 1997. Fenton process for treatment of desizing wastewater. Water Research 31(8), 2050-2056.

Liu, J., Zhang, Z.H., Chen, Q.H. and Zhang, X.H. 2018. Synergistic effect of ferrate (VI)-ozone integrated pretreatment on the improvement of water quality and fouling alleviation of ceramic UF membrane in reclaimed water treatment. Journal of Membrane Science 567, 216-227.

Lucas, W.C. and Sample, D.J. 2015. Reducing combined sewer overflows by using outlet controls for Green Stormwater Infrastructure: Case study in Richmond, Virginia. Journal of Hydrology 520, 473-488.

Luo, S., Wei, Z., Spinney, R., Zhang, Z., Dionysiou, D.D., Gao, L., Chai, L., Wang, D. and Xiao, R. 2018. UV direct photolysis of sulfamethoxazole and ibuprofen: An experimental and modelling study. Journal of Hazardous Materials 343, 132-139.

Luo, Z.Y., Strouse, M., Jiang, J.Q. and Sharma, V.K. 2011. Methodologies for the analytical determination of ferrate(VI): A Review. J. Environ. Sci. Health Part A-Toxic/Hazard. Subst. Environ. Eng. 46(5), 453-460.

Lv, D., Zheng, L., Zhang, H. and Deng, Y. 2018. Coagulation of colloidal particles with ferrate(vi). Environmental Science-Water Research & Technology 4(5), 701-710.

Macova, Z., Bouzek, K., Hives, J., Sharma, V.K., Terryn, R.J. and Baum, J.C. 2009. Research progress in the electrochemical synthesis of ferrate(VI). Electrochimica Acta 54(10), 2673-2683.

Madoux-Humery, A.-S., Dorner, S., Sauve, S., Aboulfadl, K., Galarneau, M., Servais, P. and Prevost, M. 2013. Temporal variability of combined sewer overflow contaminants: Evaluation of wastewater micropollutants as tracers of fecal contamination. Water Research 47(13), 4370-4382.

Madoux-Humery, A.-S., Dorner, S., Sauve, S., Aboulfadl, K., Galarneau, M., Servais, P. and Prevost, M. 2016a. The effects of combined sewer overflow events on riverine sources of drinking water. Water Research 92, 218-227.

Madoux-Humery, A.S., Dorner, S., Sauve, S., Aboulfadl, K., Galarneau, M., Servais, P. and Prevost, M. 2016b. The effects of combined sewer overflow events on riverine sources of drinking water. Water research 92, 218-227.

Makky, E.A., Park, G.-S., Choi, I.-W., Cho, S.-I. and Kim, H. 2011. Comparison of Fe(VI) (FeO42-) and ozone in inactivating Bacillus subtilis spores. Chemosphere 83(9), 1228-1233.

Malachova, K., Sezimova, H. and Rozinek, R. 2014. Detection of genotoxicity and toxicity of wastewater treatment plant (WTP) effluents after pretreatment with ferrate (VI). Toxicol. Lett. 229, S117-S118.

Malik, S.N., Ghosh, P.C., Vaidya, A.N., Waindeskar, V., Das, S. and Mudliar, S.N. 2017. Comparison of coagulation, ozone and ferrate treatment processes for color, COD and toxicity removal from complex textile wastewater. Water Science and Technology 76(5), 1001-1010.

Manoli, K., Maffettone, R., Sharma, V.K., Santoro, D., Ray, A.K., Passalacqua, K.D., Carnahan, K.E., Wobus, C.E. and Sarathy, S. 2020. Inactivation of Murine Norovirus and Fecal Coliforms by Ferrate(VI) in Secondary Effluent Wastewater. Environmental Science & Technology 54(3), 1878-1888.

Manoli, K., Nakhla, G., Feng, M., Sharma, V.K. and Ray, A.K. 2017a. Silica gel-enhanced oxidation of caffeine by ferrate(VI). Chemical Engineering Journal 330, 987-994.

Manoli, K., Nakhla, G., Ray, A.K. and Sharma, V.K. 2017b. Enhanced oxidative transformation of organic contaminants by activation of ferrate(VI): Possible involvement of Fe-V/Fe-IV species. Chemical Engineering Journal 307, 513-517.

Manoli, K., Nakhla, G., Ray, A.K. and Sharma, V.K. 2017c. Oxidation of Caffeine by Acid-activated Ferrate(VI): Effect of Ions and Natural Organic Matter. Aiche Journal 63(11), 4998-5006.

Margot, J., Rossi, L., Barry, D.A. and Holliger, C. 2015. A review of the fate of micropollutants in wastewater treatment plants. Wiley Interdisciplinary Reviews: Water 2(5), 457-487.

Marques, R.d.O. and Ferreira Filho, S.S. 2017. Flocculation kinetics of low-turbidity raw water and the irreversible floc breakup process. Environmental Technology 38(7), 901-910.

Marsalek, J. and Rochfort, Q. 2004. Urban wet-weather flows: Sources of fecal contamination impacting on recreational waters and threatening drinking-water sources. Journal of Toxicology and Environmental Health-Part a-Current Issues 67(20-22), 1765-1777.

Martinez, S., Delgado, M. and Jarvis, P. 2016. Removal of Herbicide Mecoprop from Surface Water Using Advanced Oxidation Processes (AOPS). International Journal of Environmental Research 10(2), 291-296.

Masi, F., Rizzo, A., Bresciani, R. and Conte, G. 2017. Constructed wetlands for combined sewer overflow treatment: Ecosystem services at Gorla Maggiore, Italy. Ecological Engineering 98, 427-438.

Matin, A.R., Yousefzadeh, S., Ahmadi, E., Mahvi, A., Alimohammadi, M., Aslani, H. and Nabizadeh, R. 2018. A comparative study of the disinfection efficacy of H2O2/ferrate and UV/ H2O2/ferrate processes on inactivation of Bacillus subtilis spores by response surface methodology for modeling and optimization. Food and Chemical Toxicology 116, 129-137.

Mbaeze MC, A.V.a.O.N. 2017. Comparative Assessment of Performance of Aluminium Sulphate (Alum) and Ferrous Sulphate as Coagulants in Water Treatment Modern Chemistry & Applications 5(4).

McFadden, M., Loconsole, J., Schockling, A., Nerenberg, R. and Pavissich, J.P. 2017. Comparing peracetic acid and hypochlorite for disinfection of combined sewer overflows: Effects of suspended-solids and pH. Sci. Total Environ. 599, 533-539.

McIntyre, J.K., Winters, N., Rozmyn, L., Haskins, T. and Stark, J.D. 2019. Metals leaching from common residential and commercial roofing materials across four years of weathering and implications for environmental loading. Environmental Pollution 255.

Mohammed, S. and Shanshool, H.A. 2009 Phosphorus Removal from Water and Waste Water by Chemical Precipitation Using Alum and Calcium Chloride.

Mohtadi, M.F. and Rao, P.N. 1973. Effect of Temperature on Flocculation of Aqueous Dispersions. Water Research Pergamon Press 7, 747-767.

Mutzner, L., Staufer, P. and Ort, C. 2016. Model-based screening for critical wet-weather discharges related tomicropollutants from urban areas. Water research 104.

Najm, I. 2006. An alternative interpretation of disinfection kinetics. Journal American Water Works Association 98(10), 93-+.

Nikolic-Bujanovic, L., Cekerevac, M., Tomic, M. and Zdravkovic, M. 2016. Ibuprofen removal from aqueous solution by in situ electrochemically generated ferrate(VI): proof-of-principle. Water Science and Technology 73(2), 389-395.

Ning, B., Graham, N., Zhang, Y., Nakonechny, M. and Gamal El-Din, M. 2007. Degradation of Endocrine Disrupting Chemicals by Ozone/AOPs. Ozone: Science & Engineering 29(3), 153-176.

Noorhasan, N., Patel, B. and Sharma, V.K. 2010. Ferrate(VI) oxidation of glycine and glycylglycine: Kinetics and products. Water Research 44(3), 927-935.

Olmez-Hanci, T., Arslan-Alaton, I. and Dursun, D. 2014. Investigation of the toxicity of common oxidants used in advanced oxidation processes and their quenching agents. Journal of Hazardous Materials 278, 330-335.

Onen, V., Beyazyuz, P. and Yel, E. 2018. Removal of Turbidity from Travertine Processing Wastewaters by Coagulants, Flocculants and Natural Materials. Mine Water and the Environment 37(3), 482-492.

Owoseni, M.C., Olaniran, A.O. and Okoh, A.I. 2017. Chlorine Tolerance and Inactivation of Escherichia coli recovered from Wastewater Treatment Plants in the Eastern Cape, South Africa. Applied Sciences-Basel 7(8).

Pachuau, L., Lee, S.M. and Tiwari, D. 2013. Ferrate(VI) in wastewater treatment contaminated with metal(II)-iminodiacetic acid complexed species. Chemical Engineering Journal 230, 141-148.

Passerat, J., Ouattara, N.K., Mouchel, J.-M., Rocher, V. and Servais, P. 2011. Impact of an intense combined sewer overflow event on the microbiological water quality of the Seine River. Water Research 45(2), 893-903.

Peings, V., Pigot, T., Baylere, P., Sotiropoulos, J.M. and Frayret, J. 2017. Removal of pharmaceuticals by a potassium ferrate (VI) material: from practical implementation to reactivity prediction. Environmental Science-Water Research & Technology 3(4), 699-709.

Petala, M., Samaras, P., Kungolos, A., Zouboulis, A., Papadopoulos, A. and Sakellaropoulos, G.P. 2006. The effect of coagulation on the toxicity and mutagenicity of reclaimed municipal effluents. Chemosphere 65(6), 1007-1018.

Petrie, B., Barden, R. and Kasprzyk-Hordern, B. 2015. A review on emerging contaminants in wastewaters and the environment: Current knowledge, understudied areas and recommendations for future monitoring. Water Research 72, 3-27.

Phillips, P.J., Chalmers, A.T., Gray, J.L., Kolpin, D.W., Foreman, W.T. and Wall, G.R. 2012a. Combined Sewer Overflows: An Environmental Source of Hormones and Wastewater Micropollutants. Environ. Sci. Technol. 46(10), 5336-5343.

Phillips, P.J., Chalmers, A.T., Gray, J.L., Kolpin, D.W., Foreman, W.T. and Wall, G.R. 2012b. Combined sewer overflows: an environmental source of hormones and wastewater micropollutants. Environmental science & technology 46(10), 5336-5343.

Pifer, A.D. and Fairey, J.L. 2014. Suitability of Organic Matter Surrogates to Predict Trihalomethane Formation in Drinking Water Sources. Environemntal Engineering Science 31.

Ramseier, M.K., von Gunten, U., Freihofer, P. and Hammes, F. 2011. Kinetics of membrane damage to high (HNA) and low (LNA) nucleic acid bacterial clusters in drinking water by ozone, chlorine, chlorine dioxide, monochloramine, ferrate(VI), and permanganate. Water Research 45(3), 1490-1500.

Ratnaweera, H. and Fettig, J. 2015. State of the Art of Online Monitoring and Control of the Coagulation Process. Water 7(11), 6574-6597.

Ravi Kumar Chhetri, D.T., Jesper Berner, Robin Gramstadd, Ulrik Öjstedt, Anitha Kumari Sharma, Henrik Rasmus Andersena 2016 Chemical disinfection of combined sewer overflow waters using performic acid or peracetic acids pp. 1065-1072, Elsevier B.V.

Real, F.J., Benitez, F.J., Acero, J.L. and Gonzalez, M. 2007. Removal of diazinon by various advanced oxidation processes. Journal of Chemical Technology and Biotechnology 82(6), 566-574.

Rechenburg, A., Koch, C., Classen, T. and Kistemann, T. 2006. Impact of sewage treatment plants and combined sewer overflow basins on the microbiological quality of surface water. Water Science and Technology 54(3), 95-99.

Richardson, S.D., Plewa, M.J., Wagner, E.D., Schoeny, R. and DeMarini, D.M. 2007. Occurrence, genotoxicity, and carcinogenicity of regulated and emerging disinfection by-products in drinking water: A review and roadmap for research. Mutation Research-Reviews in Mutation Research 636(1-3), 178-242.

Rizzo, L., Lofrano, G., Gago, C., Bredneva, T., Lannece, P., Pazos, M., Krasnogorskaya, N. and Carotenuto, M. 2018. Antibiotic contaminated water treated by photo driven advanced oxidation processes: Ultraviolet/H2O2 vs ultraviolet/peracetic acid. Journal of Cleaner Production 205, 67-75.

Rong, H., Gao, B., Dong, M., Zhao, Y., Sun, S., YanWang, Yue, Q. and Li, Q. 2013. Characterization of size, strength and structure of aluminum-polymer dual-coagulant flocs under different pH and hydraulic conditions. Journal of Hazardous Materials 252, 330-337.

Ryu, J., Oh, J., Snyder, S.A. and Yoon, Y. 2014a. Determination of micropollutants in combined sewer overflows and their removal in a wastewater treatment plant (Seoul, South Korea). Environmental monitoring and assessment 186(5), 3239-3251.

Ryu, J., Oh, J., Snyder, S.A. and Yoon, Y. 2014b. Determination of micropollutants in combined sewer overflows and their removal in a wastewater treatment plant (Seoul, South Korea). Environ. Monit. Assess. 186(5), 3239-3251.

Saien, J. and Khezrianjoo, S. 2008. Degradation of the fungicide carbendazim in aqueous solutions with UV/TiO2 process: Optimization, kinetics and toxicity studies. Journal of Hazardous Materials 157(2-3), 269-276.

Saritha, V., Srinivas, N. and Vuppala, S. 2017. Analysis and optimization of coagulation and flocculation process. Applied Water Science 7, 451-460.

Sarkar, S., Kamilya, D. and Mal, B.C. 2007. Effect of geometric and process variables on the performance of inclined plate settlers in treating aquacultural waste. Water research 41, 993-1000.

Segura, P.A., Francois, M., Gagnon, C. and Sauve, S. 2009. Review of the Occurrence of Anti-infectives in Contaminated Wastewaters and Natural and Drinking Waters. Environmental Health Perspectives 117(5), 675-684.

Semitsoglou-Tsiapou, S., Templeton, M.R., Graham, N.J.D., Leal, L.H., Martijn, B.J., Royce, A. and Kruithof, J.C. 2016. Low pressure UV/H2O2 treatment for the degradation of the pesticides metaldehyde, clopyralid and mecoprop - Kinetics and reaction product formation. Water Research 91, 285-294.

Shah, M. and Pathak, K. 2010. Development and Statistical Optimization of Solid Lipid Nanoparticles of Simvastatin by Using 2(3) Full-Factorial Design. Aaps Pharmscitech 11(2), 489-496.

Shao, B., Dong, H., Feng, L., Qiao, J. and Guan, X. 2020. Influence of sulfite / Fe(VI) molar ratio on the active oxidants generation in Fe(VI)/sulfite process. Journal of hazardous materials 384, 121303-121303.

Shao, B., Dong, H., Sun, B. and Guan, X. 2019. Role of Ferrate(IV) and Ferrate(V) in Activating Ferrate(VI) by Calcium Sulfite for Enhanced Oxidation of Organic Contaminants. Environmental Science & Technology 53(2), 894-902.

Sharma, V.K. 2002. Potassium ferrate(VI): an environmentally friendly oxidant. Advances in Environmental Research 6(2), 143-156.

Sharma, V.K. 2007. Disinfection performance of Fe(VI) in water and wastewater: a review. Water Science and Technology 55(1-2), 225-232.

Sharma, V.K. 2011. Oxidation of inorganic contaminants by ferrates (VI, V, and IV)-kinetics and mechanisms: A review. Journal of Environmental Management 92(4), 1051-1073.

Sharma, V.K. 2013. Ferrate(VI) and ferrate(V) oxidation of organic compounds: Kinetics and mechanism. Coordination Chemistry Reviews 257(2), 495-510.

Sharma, V.K. and Bielski, B.H.J. 1991. reactivity of ferrate(vi) and ferrate(v) with amino-acids. Inorganic Chemistry 30(23), 4306-4310.

Sharma, V.K., Chen, L. and Zboril, R. 2016. Review on High Valent Fe-VI (Ferrate): A Sustainable Green Oxidant in Organic Chemistry and Transformation of Pharmaceuticals. Acs Sustainable Chemistry & Engineering 4(1), 18-34.

Sharma, V.K., Graham, N.J.D., Li, X.Z. and Yuan, B.L. 2010. Ferrate(VI) enhanced photocatalytic oxidation of pollutants in aqueous TiO2 suspensions. Environmental Science and Pollution Research 17(2), 453-461.

Sharma, V.K., Kazama, F., Jiangyong, H. and Ray, A.K. 2005. Ferrates (iron(VI) and iron(V)): Environmentally friendly oxidants and disinfectants. Journal of Water and Health 3(1), 45-58.

Sharma, V.K., Liu, F., Tolan, S., Sohn, M., Kim, H. and Oturan, M.A. 2013. Oxidation of beta-lactam antibiotics by ferrate(VI). Chemical Engineering Journal 221, 446-451.

Sharma, V.K., Sohn, M., Anquandah, G.A.K. and Nesnas, N. 2012. Kinetics of the oxidation of sucralose and related carbohydrates by ferrate(VI). Chemosphere 87(6), 644-648.

Sharma, V.K., Zboril, R. and Varma, R.S. 2015. Ferrates: Greener Oxidants with Multimodal Action in Water Treatment Technologies. Accounts of Chemical Research 48(2), 182-191.

Shemer, H. and Linden, K.G. 2006. Degradation and by-product formation of diazinon in water during UV and UV/H2O2 treatment (vol 136, pg 553, 2003). Journal of Hazardous Materials 138(3), 638-638.

Shu, Z., Bolton, J.R., Belosevic, M. and Din, M.G.E. 2013a. Photodegradation of emerging micropollutants using the medium-pressure UV/H_2O_2 Advanced Oxidation Process. Water research 47, 2881-2889.

Shu, Z.Q., Bolton, J.R., Belosevic, M. and El Din, M.G. 2013b. Photodegradation of emerging micropollutants using the medium-pressure UV/H2O2 Advanced Oxidation Process. Water Research 47(8), 2881-2889.

Sigstam, T., Rohatschek, A., Zhong, Q.X., Brennecke, M. and Kohn, T. 2014. On the cause of the tailing phenomenon during virus disinfection by chlorine dioxide. Water Research 48, 82-89.

Siskova, K.M., Jancula, D., Drahos, B., Machala, L., Babica, P., Alonso, P.G., Travnicek, Z., Tucek, J., Marsalek, B., Sharma, V.K. and Zboril, R. 2016. High-valent iron (Fe-VI, Fe-V, and Fe-IV) species in water: characterization and oxidative transformation of estrogenic hormones. Physical Chemistry Chemical Physics 18(28), 18802-18810.

Smoczynski, L., Munska, K.T., Kosobucka, M. and Pierozynski, B. 2014. Phosphorus and COD Removal from Chemically and Electrichemically Coagualated Wastewater. Environmental Protection Engineering 40(3), 63-73.

Song, Y.L., Deng, Y. and Jung, C.I. 2016. Mitigation and degradation of natural organic matters (NOMs) during ferrate(VI) application for drinking water treatment. Chemosphere 146, 145-153.

Soonthornnonda, P. and Christensen, E.R. 2008. Source apportionment of pollutants and flows of combined sewer wastewater. Water Research 42(8-9), 1989-1998.

Stampi, S., De Luca, G. and Zanetti, F. 2001. Evaluation of the efficiency of peracetic acid in the disinfection of sewage effluents. Journal of Applied Microbiology 91(5), 833-838.

Stanford, C., Jiang, J.Q. and Alsheyab, M. 2010. Electrochemical Production of Ferrate (Iron VI): Application to the Wastewater Treatment on a Laboratory Scale and Comparison with Iron (III) Coagulant. Water Air and Soil Pollution 209(1-4), 483-488.

Sui, Q., Huang, J., Deng, S., Yu, G. and Fan, Q. 2010. Occurrence and removal of pharmaceuticals, caffeine and DEET in wastewater treatment plants of Beijing, China. Water research 44(2), 417-426.

Sumant, K., Ghosh, N.C. and Kazmi, A.A. 2016. Ballasted sand flocculation for water, wastewater and CSO treatment. Environmental Technology Reviews 5(1), 57-67.

Sun, X.H., Zhang, Q., Liang, H., Ying, L., Meng, X.X. and Sharma, V.K. 2016. Ferrate(VI) as a greener oxidant: Electrochemical generation and treatment of phenol. Journal of Hazardous Materials 319, 130-136.

Szabo, J.G., Buchberger, S.G. and Bishop, P.L. 2005. Performance of wet weather treatment facility for control of combined sewer overflows: Case study in Cincinnati, Ohio. Journal of Environmental Engineering-Asce 131(3), 375-386.

Talaiekhozani, A., Eskandari, Z., Bagheri, M. and Talaie, M.R. 2016a. Removal of H2S and COD using UV, ferrate and UV/ferrate from municipal wastewater. Journal of Human, Environment and Health Promotion 2(1), 1-8.

Talaiekhozani, A., Salari, M., Talaei, M.R., Bagheri, M. and Eskandari, Z. 2016b. Formaldehyde removal from wastewater and air by using UV, ferrate(VI) and UV/ferrate(VI). Journal of Environmental Management 184, 204-209.

Tankiewicz, M., Fenik, J. and Biziuk, M. 2010. Determination of organophosphorus and organonitrogen pesticides in water samples. Trac-Trends in Analytical Chemistry 29(9), 1050-1063.

Tao, W.D., Bays, J.S., Meyer, D., Smardon, R.C. and Levy, Z.F. 2014. Constructed Wetlands for Treatment of Combined Sewer Overflow in the US: A Review of Design Challenges and Application Status. Water 6(11), 3362-3385.

Teksoy, A., Alkan, U., Eleren, S.C., Topac, B.S., Sagban, F.O.T. and Baskaya, H.S. 2011. Comparison of indicator bacteria inactivation by the ultraviolet and the ultraviolet/hydrogen peroxide disinfection processes in humic waters. Journal of Water and Health 9(4), 659-669.

Thompson, G.W., Ockerman, L.T. and Schreyer, J.M. 1951. preparation and purification of potassium ferrate .6. Journal of the American Chemical Society 73(3), 1379-1381.

Tiwari, D., Sailo, L., Choi, S.I., Yoon, Y.Y. and Lee, S.M. 2017. Efficient oxidative removal of 4-tert-octylphenol and 17 alpha-ethynylestradiol from aqueous solutions using ferrate(VI). Korean Journal of Chemical Engineering 34(3), 734-740.

Tolouei, S., Jean-Baptiste Burneta, Autixiera, L., Taghipoura, M., Bonsteelb, J., Duy, S.V., Sauve, S., Prevost, M. and Dorner, S. 2019. Temporal variability of parasites, bacterial indicators, and wastewatermicropollutants in a water resource recovery facility under variousweather conditions. Water research 148, 446-458.

Tondera, K., Klaer, K., Gebhardt, J., Wingender, J., Koch, C., Horstkott, M., Strathmann, M., Jurzik, L., Hamza, I.A. and Pinnekamp, J. 2015a. Reducing pathogens in combined sewer overflows using ozonation or UV irradiation. International journal of hygiene and environmental health 218(8), 731-741.

Tondera, K., Klaer, K., Gebhardt, J., Wingender, J., Koch, C., Horstkott, M., Strathmann, M., Jurzik, L., Hamza, I.A. and Pinnekamp, J. 2015b. Reducing pathogens in combined sewer overflows using ozonation or UV irradiation. International Journal of Hygiene and Environmental Health 218(8), 731-741.

Tondera, K., Klaer, K., Koch, C., Hamza, I.A. and Pinnekamp, J. 2016a. Reducing pathogens in combined sewer overflows using performic acid. International journal of hygiene and environmental health 219(7 Pt B), 700-708.

Tondera, K., Klaer, K., Koch, C., Hamza, I.A. and Pinnekamp, J. 2016b. Reducing pathogens in combined sewer overflows using performic acid. International Journal of Hygiene and Environmental Health 219(7), 700-708.

Trapido, M., Epold, I., Bolobajev, J. and Dulova, N. 2014. Emerging micropollutants in water/wastewater: growing demand on removal technologies. Environmental Science and Pollution Research 21(21), 12217-12222.

Trinh, T.K. and Kang, L.S. 2015. Coagulation of phosphorus: effects of Al(III) species (Al-a, Al-b, and Al-c). Desalination and Water Treatment 53(2), 485-492.

von Gunten, U. 2018. Oxidation Processes in Water Treatment: Are We on Track? Environ. Sci. Technol. 52(9), 5062-5075.

Vuong, T. and Monson, P.A. 1998. Surface roughness effects in molecular models of adsorption in heterogeneous porous solids. Langmuir 14(17), 4880-4886.

Wang, C.J., Hofmann, M., Safari, A., Viole, I., Andrews, S. and Hofmann, R. 2019. Chlorine is preferred over bisulfite for H2O2 quenching following UV-AOP drinking water treatment. Water Research 165, 6.

Wang, H.Y., Liu, Y.B. and Jiang, J.Q. 2016a. Reaction kinetics and oxidation product formation in the degradation of acetaminophen by ferrate (VI). Chemosphere 155, 583-590.

Wang, K.M., Shu, J., Wang, S.J., Hong, T.Y., Xu, X.P. and Wang, H.Y. 2020. Efficient electrochemical generation of ferrate(VI) by iron coil anode imposed with square alternating current and treatment of antibiotics. Journal of Hazardous Materials 384.

Wang, W., Xu, Z., Li, H. and Jin, W. 2015a. Optimization of coagulation–flocculation process for combined sewer overflow wastewater treatment using response surface methodology. Desalination and Water Treatment 57(32), 14824-14832.

Wang, W.-g., Xu, Z.-x., Li, H.-z. and Jin, W. 2016b. coagulation characteristics of organic pollutants removal in cso wastewater treatment. Environmental Engineering and Management Journal 15(1), 75-80.

Wang, Y.L., Liu, H.J., Liu, G.G., Xie, Y.H. and Gao, S.Y. 2015b. Oxidation of diclofenac by potassium ferrate (VI): Reaction kinetics and toxicity evaluation. Science of the Total Environment 506, 252-258.

Wei, N., Zhang, Z.G., Liu, D., Wu, Y., Wang, J. and Wang, Q.H. 2015. Coagulation behavior of polyaluminum chloride: Effects of pH and coagulant dosage. Chinese Journal of Chemical Engineering 23(6), 1041-1046.

Westerhoff, P., Yoon, Y., Snyder, S. and Wert, E. 2005. Fate of endocrine-disruptor, pharmaceutical, and personal care product chemicals during simulated drinking water treatment processes. Environmental Science & Technology 39(17), 6649-6663.

Wojtenko, I., Stinson, M.K. and Field, R. 2001a. Challenges of Combined Sewer Overflow Disinfection by Ultraviolet Light Irradiation. Critical Reviews in Environmental Science and Technology 31(3), 223-239.

Wojtenko, I., Stinson, M.K. and Field, R. 2001b. Performance of Ozone as a Disinectant for Combined Sewer Overflow. Critical Reviews in Environmental Science and Technology 31(4), 295-309.

Wu, J.G., Lan, C.Y. and Chan, G.Y.S. 2009. Organophosphorus pesticide ozonation and formation of oxon intermediates. Chemosphere 76(9), 1308-1314.

Wu, J.G., Luan, T.G., Lan, C.Y., Lo, W.H. and Chan, G.Y.S. 2007. Efficacy evaluation of low-concentration of ozonated water in removal of residual diazinon, parathion, methyl-parathion and cypermethrin on vegetable. Journal of Food Engineering 79(3), 803-809.

Wu, S., Liu, H., Lin, Y., Yang, C., Lou, W., Sun, J., Du, C., Zhang, D., Nie, L., Yin, K. and Zhong, Y. 2020. Insights into mechanisms of UV/ferrate oxidation for degradation of phenolic pollutants: Role of superoxide radicals. Chemosphere 244.

Wu, S.H., Li, H.R., Li, X., He, H.J. and Yang, C.P. 2018. Performances and mechanisms of efficient degradation of atrazine using peroxymonosulfate and ferrate as oxidants. Chemical Engineering Journal 353, 533-541.

Xiao, Y.H., Sara-Aho, T., Hartikainen, H. and Vahatalo, A.V. 2013. Contribution of ferric iron to light absorption by chromophoric dissolved organic matter. Limnology and Oceanography 58(2), 653-662.

Xu, Z.H., Wang, J.M., Shao, H.B., Tang, Z. and Zhang, J.Q. 2007. Preliminary investigation on the physicochemical properties of calcium ferrate(VI). Electrochemistry Communications 9(3), 371-377.

Yan, X., Sun, J., Kenjiahan, A., Dai, X., Ni, B.-J. and Yuan, Z. 2020. Rapid and strong biocidal effect of ferrate on sulfidogenic and methanogenic sewer biofilms. Water Research 169.

Yang, B., Ying, G.-G., Zhao, J.-L., Zhang, L.-J., Fang, Y.-X. and Nghiem, L.D. 2011. Oxidation of triclosan by ferrate: Reaction kinetics, products identification and toxicity evaluation. Journal of Hazardous Materials 186(1), 227-235.

Yang, B., Ying, G.G., Zhao, J.L., Liu, S., Zhou, L.J. and Chen, F. 2012. Removal of selected endocrine disrupting chemicals (EDCs) and pharmaceuticals and personal care products

(PPCPs) during ferrate(VI) treatment of secondary wastewater effluents. Water Research 46(7), 2194-2204.

Yang, K., Li, Z., Zhang, H., Qian, J. and Chen, G. 2010. Municipal wastewater phosphorus removal by coagulation. Environmental Technology 31(6), 601-609.

Yang, T., Wang, L., Liu, Y., Huang, Z., He, H., Wang, X., Jiang, J., Gao, D. and Ma, J. 2019. Comparative study on ferrate oxidation of BPS and BPAF: Kinetics, reaction mechanism, and the improvement on their biodegradability. Water Research 148, 115-125.

Yao, C.C.D. and Haag, W.R. 1991. Rate constants for direct reactions of ozone with several drinking-water contaminants. water research 25(7), 761-773.

Yates, B.J., Zboril, R. and Sharma, V.K. 2014. Engineering aspects of ferrate in water and wastewater treatment - a review. Journal of Environmental Science and Health Part a-Toxic/Hazardous Substances & Environmental Engineering 49(14), 1603-1614.

Yoon, J., Lee, Y. and Kim, S. 2001. Investigation of the reaction pathway of OH radicals produced by Fenton oxidation in the conditions of wastewater treatment. Water Science and Technology 44(5), 15-21.

Young, S., Stanley, S.J. and Smith, D.W. 2000. Effect of mixing on the kinetics of polymer-aided flocculation. Journal of Water Services Research and Technology-Aqua 49(1), 1-8.

Yu, M.R., Chang, Y.Y., Keller, A.A. and Yang, J.K. 2013. Application of ferrate for the treatment of metal-sulfide. Journal of Environmental Management 116, 95-100.

Yu, W., Li, G., Xu, Y. and Yang, X. 2009. Breakage and re-growth of flocs formed by alum and PACl. Powder Technology 189(3), 439-443.

Yu, W.-z., Gregory, J., Campos, L. and Li, G. 2011. The role of mixing conditions on floc growth, breakage and re-growth. Chemical Engineering Journal 171(2), 425-430.

Yu, W.Z., Yang, Y.J. and Graham, N. 2016. Evaluation of ferrate as a coagulant aid/oxidant pretreatment for mitigating submerged ultrafiltration membrane fouling in drinking water treatment. Chemical Engineering Journal 298, 234-242.

Yuan, B.L., Qu, J.H. and Fu, M.L. 2002. Removal of cyanobacterial microcystin-LR by ferrate oxidation-coagulation. Toxicon 40(8), 1129-1134.

Yukselen, M.A. and Gregory, J. 2004. The effect of rapid mixing on the break-up and re-formation of flocs. Journal of Chemical Technology & Biotechnology 79(7), 782-788.

Zaharia, C., Suteu, D., Muresan, A., Muresan, R. and Popescu, A. 2009. Textile wastewater treatment by homogeneous oxidation with hydrogen peroxide. Environmental Engineering and Management Journal 8(6), 1359-1369.

Zhan, X., Gao, B., Wang, Y. and Yue, Q. 2011. Influence of velocity gradient on aluminum and iron floc property for NOM removal from low organic matter surfacewater by coagulation. Chemical Engineering Journal 166(1), 116-121.

Zhang, J., Zhu, L., Shi, Z. and Gao, Y. 2017. Rapid removal of organic pollutants by activation sulfite with ferrate. Chemosphere 186, 576-579.

Zhang, K., Deletic, A., Page, D. and McCarthy, D.T. 2015a. Surrogates for herbicide removal in stormwater biofilters. Water research 81, 64-71.

Zhang, K.J., Luo, Z., Zhang, T.Q., Gao, N.Y. and Ma, Y. 2015b. Degradation Effect of Sulfa Antibiotics by Potassium Ferrate Combined with Ultrasound (Fe(VI)-US). Biomed Research International, 12.

Zhang, Q. and Pehkonen, S.O. 1999. Oxidation of diazinon by aqueous chlorine: Kinetics, mechanisms, and product studies. Journal of Agricultural and Food Chemistry 47(4), 1760-1766.

Zhang, T., Dong, F., Luo, F. and Li, C. 2018. Degradation of sulfonamides and formation of trihalomethanes by chlorination after pre-oxidation with Fe(VI). Journal of Environmental Sciences 73, 89-95.

Zhao, J., Liu, Y., Wang, Q., Fu, Y., Lu, X. and Bai, X. 2018a. The self-catalysis of ferrate (VI) by its reactive byproducts or reductive substances for the degradation of diclofenac: Kinetics, mechanism and transformation products. Separation and Purification Technology 192, 412-418.

Zhao, J., Wang, Q., Fu, Y., Peng, B. and Zhou, G. 2018b. Kinetics and mechanism of diclofenac removal using ferrate(VI): roles of Fe3+, Fe2+, and Mn2+. Environmental Science and Pollution Research 25(23), 22998-23008.

Zheng, L. and Deng, Y. 2016. Settleability and characteristics of ferrate(VI)-induced particles in advanced wastewater treatment. Water Research 93, 172-178.

Zhou, J.H., Chen, K.B., Hong, Q.K., Zeng, F.C. and Wang, H.Y. 2017. Degradation of chloramphenicol by potassium ferrate (VI) oxidation: kinetics and products. Environmental Science and Pollution Research 24(11), 10166-10171.

Zhou, Y., Liang, Z. and Wang, Y. 2008. Decolorization and COD removal of secondary yeast wastewater effluents by coagulation using aluminum sulfate. Desalination 225(1-3), 301-311.

Zhou, Z. and Jiang, J.Q. 2015a. Reaction kinetics and oxidation products formation in the degradation of ciprofloxacin and ibuprofen by ferrate(VI). Chemosphere 119, S95-S100.

Zhou, Z.W. and Jiang, J.Q. 2015b. Treatment of selected pharmaceuticals by ferrate(VI): Performance, kinetic studies and identification of oxidation products. Journal of Pharmaceutical and Biomedical Analysis 106, 37-45.

Zhu, W., Seth, R. and Lalman, J. 2007. Evaluation of a micro carrier weighted coagulation flocculation process for the treatment of combined sewer overflow. Environmental Technology 28(7), 761-770.

Ziska, A.D., Park, M., Anumol, T. and Snyder, S.A. 2016. Predicting trace organic compound attenuation with spectroscopic parameters in powdered activated carbon processes. Chemosphere 156, 163-171.

Zondervan, E. and Roffel, B. 2007. Evaluation of different cleaning agents used for cleaning ultra tiltration membranes fouled by surface water. Journal of Membrane Science 304(1-2), 40-49.

Appendix A

Table A. 1 Calculations of metal-equivalent coagulant doses.

Coagulant	**Coagulant Molecular Weight (MW) (g/mol)**	**Active Species: Molecular Weight (g/mol)**	**Coagulant dose (mg/L)**	**Metal concentration (mM)** $= \left(\frac{\text{Coagulant dose } (\frac{mg}{L})}{\text{Coagulant MW } (\frac{mg}{mol})}\right) \times n^*$	**Metal-equivalent Dose (mg Al or Fe/L)**
Aluminum Sulfate: Alum ($Al_2O_{12}S_3.18H_2O$)	666.42	Al: 27 g/mol	25	0.07	2.03
			50	0.15	4.05
			75	0.23	6.08
			100	0.30	8.10
			125	0.37	10.14
			150	0.45	12.15
Ferric Chloride ($FeCl_3$)	162.2	Fe: 55.84 g/mol	24.34	0.15	8.38
			60.85	0.37	20.95
	Density (g/mL)	**Metal-equivalent Dose** (mg Al/L)	**Volume of PACl required in 2 L Jar** (mL)	**Mass of PACl required in 2 L Jar** (mg)	**Coagulant dose** (mg/L of PACl)
Polyhydroxyl Aluminum Chloride ** (PACl)	1.37	4.05	0.061	83.57	41.78
		10.14	0.154	210.98	105.49

Notes:

* n= mol of Active species in 1 mol of coagulant.

** PACl (Clear PAC 180) with a Specific Gravity of 1.37 (according to the manufacturer) was obtained in a solution form and was characterized in the lab for Al content. Results indicated the Al content of PACl as 131589.16 mg Al/L and calculations were made accordingly.

Reference equations for Alum and $FeCl_3$ in wastewater:

$$Al_2(SO_4)_3 \cdot 18H_2O + 3Ca(HCO_3)_2 \Leftrightarrow 3CaSO_4 + 2Al(OH)_3 + 6CO_2 + 18H_2O$$

$$2FeCl_3 + 6H_2O + 3Ca(HCO_3)_2 \Leftrightarrow 3CaCl_2 + 2Fe(OH)_3 + 6CO_2 + 12H_2O$$

Table A. 2 Conversion of mixing conditions from rpm, min to Gt (Based on B-KER2 – Phipps & Bird Specifications).

Factor	**Level**	**Speed**		**Time**		**Gt**
		rpm	**G (s^{-1})**	**T (min)**	**t (s)**	
Rapid Mixing	High	300	380	3	180	68400
	Low	150	155	1	60	9300
Slow Mixing	High	30	23	20	1200	27600
	Low	15	10	10	600	6000

Table A. 3 Chemical and physical properties of the polymers used in this study.

Polymer	Chemical Composition	Concentration %	Type	Density (g/cm^3)	pH
A	Distllates (petroluem , hyrdotreated light	20 to 23	Anionic	1	6 to 8
	Alcohol, c12-14, ethoxylated	0 to 3			
	Alcohol, c10-16, ethoxylated	0 to 3			
	Alcohol, c12-16, ethoxylated	0 to 3			
	Alcohol, c13-15, ethoxylated, branched and linear	0 to 3			
B	Distillates (petroleum) , hydrotreated naphthenic acid	15 to 40	Anionic	1.1	3.9-4.4
	Alcohol, c12-15,ethoxylated, propoxylayted	1 to 5			
C	Distillates petroluem, hyrdotreated light	22 to 25	Anionic	1.1	6 to 9.5
	Alcohol, c10-16, ethoxylated	0 to 3.6			
	Alcohol, c12-14, ethoxylated	0 to 3.6			
	Alcohol, c12-16, ethoxylated	0 to 3.6			
	(Z)-octadec-9-enylyamine, ethoxylayted	1.2 to 1.6			
	Ammonium acetate	2 to 10			
D	Distillates petroluem, hyrdotreated light	22 to 25	Anionic	1.1	5 to 8 at 5 g/L
	Alcohol, c12-16, ethoxylated	0 to 3.6			
	Alcohol, c12-14, ethoxylated	0 to 3.6			
	Alcohol, c10-16, ethoxylated	0 to 3.6			
	(Z)-octadec-9-enylyamine,ethoxylayted	1.2 to 1.6			
	Ammonium acetate	2 to 10			
E	Distillates (petroleum), hydrotreated naphthenic acid	20 to 45	Anionic	1.1	5 to 8 at 5 g/L
	Poly(oxy-1,2-ethanediyl), a-tridecyl-w-hydroxy-,branched	<3			
F	Poly(oxy-1,2-ethanediyl), a-tridecyl-w-hydroxy-,branched	<3	Anionic	1.1	5 to 8 at 5 g/L
	Distillates (petroleum), hydrotreated naphthenic acid	20 to 45			
G	Distillates (petroleum) hydrotreated light	<30%	Anionic	1	6 to 8
	Alcohol, C12-16, Ethoxylated	<5%			
	Alcohol, C12-14, Ethoxylated	<5%			
	Alcohol, C10-16, Ethoxylated	<5%			
H	Distillates (Petroleum) Hydrotreated Light	20 to 28 %	Anionic	1	6 to 8
	Alcohol, C10-16, Ethoxylated	<5%			
	Alcohol, C12-16, Ethoxylated	<5%			
Cationic	COCO DIETHANOLAMIDE	>=0.5 < 1 %	Cationic	0.62	4 at 10 g/L

Table A. 4 Effects coefficients of the Three-Factor ANOVA test showing the statistical significance levels of the three factors: A=rapid mixing, B=slow mixing, and C=coagulant dose with p-value= 0.05, on the removal of tested parameters.

	Alum							
Factors	**Turbidity % Removal**		**TSS % Removal**		**COD % Removal**		**Ortho-P % Removal**	
	p-value	Effect *(±1.38)*	p-value	Effect *(±1.38)*	p-value	Effect *(±3.63)*	p-value	Effect *(±1.11)*
Rapid Mixing A	**0.000**	-5.71	**0.000**	-7.32	0.103	-6.15	0.051	-2.28
Slow Mixing B	0.151	1.24	0.207	1.78	**0.000**	-19.30	0.878	-0.17
Coagulant Dose C	**0.000**	5.53	**0.017**	3.52	0.278	-4.03	**0.000**	18.35
Rapid Mixing & Slow Mixing AB	**0.009**	-2.37	**0.000**	-6.78	**0.001**	-13.79	0.159	-1.61
Rapid Mixing & Coagulant Dose AC	**0.004**	-2.63	**0.019**	-3.47	**0.033**	-8.20	0.829	0.24
Slow Mixing & Coagulant Dose BC	**0.026**	-1.99	**0.004**	-4.35	**0.000**	-21.09	**0.000**	-17.02
Rapid Mixing & Slow Mixing & Coagulant Dose ABC	0.618	0.42	0.134	2.13	0.115	-5.94	0.051	2.28
	PACl							
	Turbidity % Removal		**TSS % Removal**		**COD % Removal**		**Ortho-P % Removal**	
	p-value	Effect *(±1.38)*	p-value	Effect *(±1.40)*	p-value	Effect *(±3.20)*	p-value	Effect *(±2.05)*
Rapid Mixing A	**0.015**	-1.24	**0.001**	-5.40	0.046	-6.75	0.924	-0.20
Slow Mixing B	**0.000**	3.84	0.772	0.41	**0.000**	-16.60	**0.007**	-6.09
Coagulant Dose C	**0.000**	11.32	**0.002**	4.89	**0.003**	10.61	**0.000**	22.29
Rapid Mixing & Slow Mixing AB	**0.005**	-1.48	**0.000**	-10.35	0.216	-4.07	0.282	2.26
Rapid Mixing & Coagulant Dose AC	**0.000**	2.94	**0.000**	8.98	0.360	-2.98	**0.027**	4.83
Slow Mixing & Coagulant Dose BC	**0.000**	-5.65	**0.000**	-5.95	**0.004**	-10.27	**0.000**	-27.74
Rapid Mixing & Slow Mixing & Coagulant Dose ABC	**0.000**	2.89	0.501	-0.96	0.080	5.85	**0.005**	6.39
	FeCl$_3$							
	Turbidity % Removal		**TSS % Removal**		**COD % Removal**		**Ortho-P % Removal**	
	p-value	Effect *(±1.38)*	p-value	Effect *(±1.35)*	p-value	Effect *(±3.55)*	p-value	Effect *(±1.34)*
Rapid Mixing A	**0.006**	-2.14	0.265	-1.54	0.057	-7.10	**0.000**	12.11
Slow Mixing B	**0.001**	2.61	**0.000**	-5.93	**0.000**	-18.81	**0.000**	-23.54
Coagulant Dose C	**0.000**	9.30	0.484	0.96	0.987	0.06	**0.000**	16.27
Rapid Mixing & Slow Mixing AB	0.479	-0.51	0.366	-1.24	**0.000**	-20.98	**0.000**	14.40
Rapid Mixing & Coagulant Dose AC	0.871	-0.12	**0.000**	9.48	0.852	0.67	**0.000**	14.13
Slow Mixing & Coagulant Dose BC	0.741	0.24	**0.000**	-12.76	**0.004**	-11.48	**0.000**	-41.41
Rapid Mixing & Slow Mixing & Coagulant Dose ABC	0.358	-0.67	0.294	1.45	0.757	1.11	**0.000**	15.50

Table A. 5 ANOVA models.

	Turbidity % Removal by:
Alum	$88.57 - 5.71 A - 2.37 AB - 2.63 AC - 1.99 BC$
PACl	$89.49 - 1.24 A + 6.84 B + 11.32 C - 1.48 AB + 2.94 AC - 5.65 BC + 2.89 ABC$
FeCl$_3$	$81.46 - 2.14A + 2.61 B + 9.30 C$
	COD % Removal by:
Alum	$58.33 - 19.30 B - 13.79 AB - 8.20 AC - 21.09 BC$
PACl	$63.47 - 6.75 A - 16.60 B + 10.61 C - 10.27 BC$
FeCl$_3$	$57.52 - 18.81 B - 20.98 AB - 11.48 BC$
	OP % Removal by:
Alum	$80.88 + 18.35 C - 17.02 BC$
PACl	$68.36 - 6.09 B + 22.29 CB + 4.83 AC - 27.74 BC + 6.39 ABC$
FeCl$_3$	$57.17 + 12.11 A - 23.54 B + 16.27 C + 14.40 AB + 14.13 AC - 41.41 BC + 15.50 ABC$

Table A. 6 Water quality parameters of untreated and treated samples during full-scale application of Alum and Alum + Polymer A at the WWTP.

Sample ID	**Date**	**Flow rate (MLD)**	**HRT (hr)**	**Turbidity (NTU)**	**TSS (mg/L)**	**OP (mg/L)**	**% UVT**
PI*	18-Aug	131.5	2.92	126	208	11.25	24
PI	19-Aug	239	1.61	86.45	200	6.65	33
Alum (100 mg/L)	19-Aug			26	26	1	44
PI	24-Aug	250.7	1.53	164	240	9.9	30
EPT Effluent**	24-Aug			73.55	54	9	36
PI	13-Sep	259.7	1.48	165.5	188	7.75	36
EPT Effluent	13-Sep			72.1	32	8.88	48
PI	13-Sep	320	1.2	120.5	244	7.25	42
Alum + Polymer (A) (75/1.45) mg/L	13-Sep			30.75	38	2	45
PI	13-Sep	263	1.46	113.5	138	7.125	46
Alum + Polymer (A) (75/1.45) mg/L	13-Sep			23.35	26	0.88	51
PI	14-Sep	214	1.79	190	364	8.88	40
EPT Effluent	14-Sep			67.1	40	4.75	51
PI	14-Sep	269	1.43	149	200	6.75	44
Alum 75	14-Sep			42.9	44	1.38	52
PI	19-Sep	192	1	164.5	218	5.06	50
PI	19-Sep						
Alum + Polymer (B) (75/1.1) mg/L	19-Sep			21.2	28	0.88	53
PI	19-Sep	272	0.71	154	180	4	56
Alum + Polymer (B) (75/1.1) mg/L	19-Sep			68.55	64	0.5	68
PI	19-Sep	232	0.83	177.5	176	6.12	46
EPT Effluent	19-Sep			82.75	60	7.88	48
PI	19-Sep	306	0.63	215	360	2.63	62
Alum + Polymer (B) (75/1.1) mg/L	19-Sep			62.8	98	0.5	65
PI	20-Sep	144.7	1.33	190	248	9.38	38
EPT Effluent	20-Sep			197.5	150	8.5	41
PI	20-Sep	179.3	1.07	191.5	280	5.75	41
Alum + Polymer (B) (75/0.75) mg/L	20-Sep			57.3	56	2.5	45
PI	20-Sep	162.5	1.18	170.5	280	7.75	42
Alum + Polymer (B) (75/0.75) mg/L	20-Sep			35.15	40	1.38	45
PI	21-Sep	247.7	0.78	124.5	200	0.88	57
Alum + Polymer (B) (75/0.75) mg/L	21-Sep			14.085	14	0.25	62
PI	01-Oct	226	0.85	221	296	9.1	33
EPT Effluent	01-Oct			124	76	9.9	41
PI	02-Oct	167	1.15	147	244	11.1	43
Alum + Polymer (A) (75/0.75) mg/L	02-Oct			39.55	48	3.9	47

Notes:

* PI = Primary Influent to the WWTP.

** EPT Effluent = effluent from the primary clarifier without any chemical addition (i.e., after mixing and settling only).

Appendix B

Table B. 1 Water quality parameters of wet weather flow samples (average values ± standard deviation).

Parameter	**Values**
pH	7.5 ± 0.31
Turbidity (NTU)	101.1 ± 8.19
TSS (mg/L)	157.3 ± 10.34
COD (mg/L)	318.3 ± 33.49
Alkalinity (mg/L $CaCO_3$)	224.8 ± 28.27
OP (mg/L)	8.1 ± 3.04
UV_{245} (cm^{-1})	0.2 ± 0.08
UVT%	60.6 ± 10.75
***E. coli* (CFU/100 mL)**	$2.26 \times 10^6 \pm 4.02 \times 10^5$

Table B. 2 Average pH values of untreated and treated samples for different mixing conditions using different doses of ferrate with and without cationic polymer.

Sample ID	**pH**			
Mixing condition (rapid/slow)	Gt (68400/27600)	Gt (68400/6000)	Gt (9300/27600)	Gt (9300/6000)
No Chemical	7.5	7.9	7.2	7.3
Fe(VI) 0.5 mg/L	7.6	7.4	6.9	7.4
Fe(VI) 0.5 mg/L + Polymer	7.6	7.3	7.39	7.3
Fe(VI) 8 mg/L	7.6	7.3	7.4	7.4
Fe(VI) 8mg/L + Polymer	7.6	7.4	7.4	7.4
Polymer only	7.6	7.4	7.4	7.4

Table B. 3 Average alkalinity concentration (mg/L $CaCO_3$) of untreated and treated samples for different mixing conditions using different doses of ferrate with and without cationic polymer.

Sample ID	**Alkalinity (mg/L $CaCO_3$)**			
Mixing condition (rapid/slow)	Gt(68400/27600)	Gt(68400/6000)	Gt(9300/27600)	Gt(9300/6000)
No Chemical	213.6	191	189	179
Fe(VI) 0.5 mg/L	214.75	202	208	173
Fe(VI) 0.5 mg/L + Polymer	214.4	198	181	175
Fe(VI) 8 mg/L	214.9	200	194	173
Fe(VI) 8mg/L + Polymer	216.6	201	194	170
Polymer only	217.6	202	191	181

Table B. 4 Average TVSS removal percentage (%) untreated and treated samples for different mixing conditions using different doses of ferrate with and without cationic polymer.

Sample ID	**TVSS (mg/L)**			
Mixing condition (rapid/slow)	Gt(68400/27600)	Gt(68400/6000)	Gt(9300/27600)	Gt(9300/6000)
No Chemical	39	70	66	73
Fe(VI) 0.5 mg/L	42	72	86	78
Fe(VI) 0.5 mg/L + Polymer	54	74	73	78
Fe(VI) 8 mg/L	55	87	81	79
Fe(VI) 8mg/L + Polymer	43	69	65	75
Polymer only	85	89	87	100

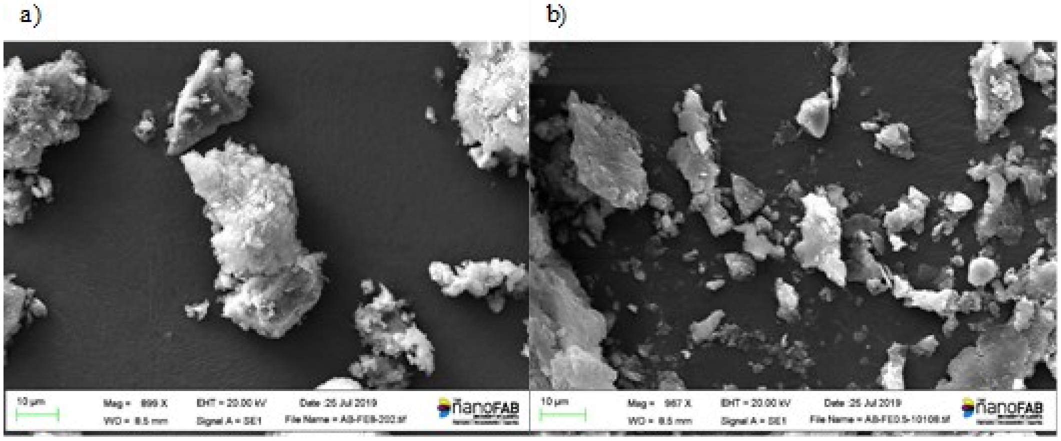

Figure B. 1 SEM image for flocs generated by ferrate treatment of wet weather flow (WWF) samples: (a) ferrate dose of 0.5 mg/L+ polymer (1.25 mg/L) and (b) ferrate dose of 8 mg/L+ polymer (1.25 mg/L)

Table B. 5 EDX data of elemental distribution in flocs samples generated after treating WWF sample by two dosing conditions: 0.5 mg/L Fe and 8 mg/L Fe both with cationic polymer (1.25 mg/L)

Element	**Ferrate 0.5 mg/L Fe +polymer (1.25 mg/L)**		**Element**	**Ferrate 8 mg/L Fe +polymer (1.25 mg/L)**	
	Wt%	σ[1]		Wt%	σ
O	53.5	0.3	O	57.1	0.3
Si	14.8	0.2	Si	11	0.1
Ca	6	0.1	Fe	10.7	0.2
Al	5.5	0.1	Ca	5.4	0.1
Cl	4.9	0.1	Al	4.7	0.1
Na	4.9	0.2	S	2.2	0.1
Fe	4.2	0.2	Na	2.1	0.1
Mg	3.6	0.1	K	1.9	0.1
K	2.7	0.1	Mg	1.8	0.1
S	NA[2]	NA	Cl	1.6	0.1
P	NA	NA	P	1.6	0.1

[1] standard deviation, [2]not available

Table B. 6 Average OP removal percentage (%) untreated and treated samples for different mixing conditions and chemical combination.

Sample ID	**OP%**			
Mixing condition (rapid/slow)	Gt (68400/27600)	Gt (68400/6000)	Gt (9300/27600)	Gt (9300/6000)
No Chemical	4	NA[1]	6	12
Fe(VI) 0.5 mg/L	13	7	16	15
Fe(VI) 0.5 mg/L + Polymer	24	9	24	13
Fe(VI) 8 mg/L	27	NA	35	19
Fe(VI) 8mg/L + Polymer	31	41	NA	14
Polymer only	15	0	18	16

[1]NA= not analyzed

Table B. 7 Average UVT% untreated and treated samples for different mixing conditions and chemical combination.

Sample ID	**UVT%**			
Mixing condition (rapid/slow)	Gt (68400/27600)	Gt (68400/6000)	Gt (9300/27600)	Gt (9300/6000)
No Chemical	55	68	65	NA
Fe(VI) 0.5 mg/L	53	69	65	NA
Fe(VI) 0.5 mg/L + Polymer	55	69	64	NA
Fe(VI) 8 mg/L	56	69	64	NA
Fe(VI) 8mg/L + Polymer	55	70	64	NA
Polymer only	58	71	65	NA

[1]NA= not analyzed

Table B. 8 Complete matrix used to analyze two-level full factorial (23) design with coding system for main and interaction effects and corresponding responses of turbidity removal (%), TSS removal (%) ,and COD removal (%), (high level coded as 1, low level coded as -1).

Standard	**Main effects**			**Interaction Effects**				**Response**		
	A	B	C	AB	AC	BC	ABC	Turbidity (%)	TSS (%)	COD (%)
1	1	1	1	1	1	1	1	73.6	79.9	70.2
2	-1	-1	-1	1	1	1	-1	55.2	82.1	38.8
3	-1	1	1	-1	-1	1	-1	78.8	77.7	56.2
4	1	-1	-1	-1	-1	1	1	44.8	75.5	44.6
5	1	1	-1	1	-1	-1	-1	60.1	74.4	66.9
6	-1	-1	1	1	-1	-1	1	64.5	78.1	50.0
7	1	-1	1	-1	1	-1	-1	82.8	86.7	61.8
8	-1	1	-1	-1	1	-1	1	76.1	66.9	42.5

Table B. 9 Effect coefficient ANOVA results for statistically tested effects of the factors (A= rapid mixing; B= slow mixing; and C= polymer addition) on turbidity removal, p-value =0.05.

Factors	Effect	SS	df	MS	F	p-value
A	-3.319	44.07612	1	44.07612	2.146596	0.18105
B	10.359	429.2486	1	429.2486	20.90527	0.00182
C	15.910	1012.472	1	1012.472	49.30944	0.00011
AB	-7.250	210.2346	1	210.2346	10.23885	0.012616
AC	9.844	387.5817	1	387.5817	18.876	0.002463
BC	-7.775	241.8119	1	241.8119	11.77672	0.008932
ABC	-4.478	80.21287	1	80.21287	3.906528	0.083501
Error		164.2643	8	20.53304		
Total		2569.902	15	171.3268		

Table B. 10 ANOVA results for statistically significant effect of the factors (A= rapid mixing; B= slow mixing; and C= polymer addition) on TSS removal, p-value =0.05.

Factor	Effect	SS	df	MS	F	p-value
A	2.936	68.97827	1	68.97827	4.780792	0.038763
B	-5.890	277.4911	1	277.4911	19.23254	0.000198
C	5.899	278.3648	1	278.3648	19.2931	0.000195
AB	1.931	29.83403	1	29.83403	2.067757	0.163355
AC	2.473	48.9418	1	48.9418	3.392091	0.077902
BC	2.293	42.06318	1	42.06318	2.915343	0.100647
ABC	-5.110	208.8672	1	208.8672	14.47631	0.000862
Error		346.277	24	14.42821		
Total		1300.817	31	41.96185		

Table B. 11 ANOVA results for statistically significant effect of the factors (A= rapid mixing; B= slow mixing; and C= polymer addition) on COD removal, p- value =0.05.

Factors	**Effect**	**SS**	**df**	**MS**	**F**	**p-value**
A	14.008	1569.736	1	1569.736	55.12949	0
B	10.159	825.7019	1	825.7019	28.99884	0
C	11.360	1032.325	1	1032.325	36.25549	0
AB	5.178	214.462	1	214.462	7.531955	0.011292
AC	-1.143	10.44927	1	10.44927	0.366981	0.550341
BC	-2.855	65.21448	1	65.21448	2.290347	0.143239
ABC	-4.108	134.9801	1	134.9801	4.740532	0.039522
Error		683.3669	24	28.47362		
Total		4536.236	31	146.3302		

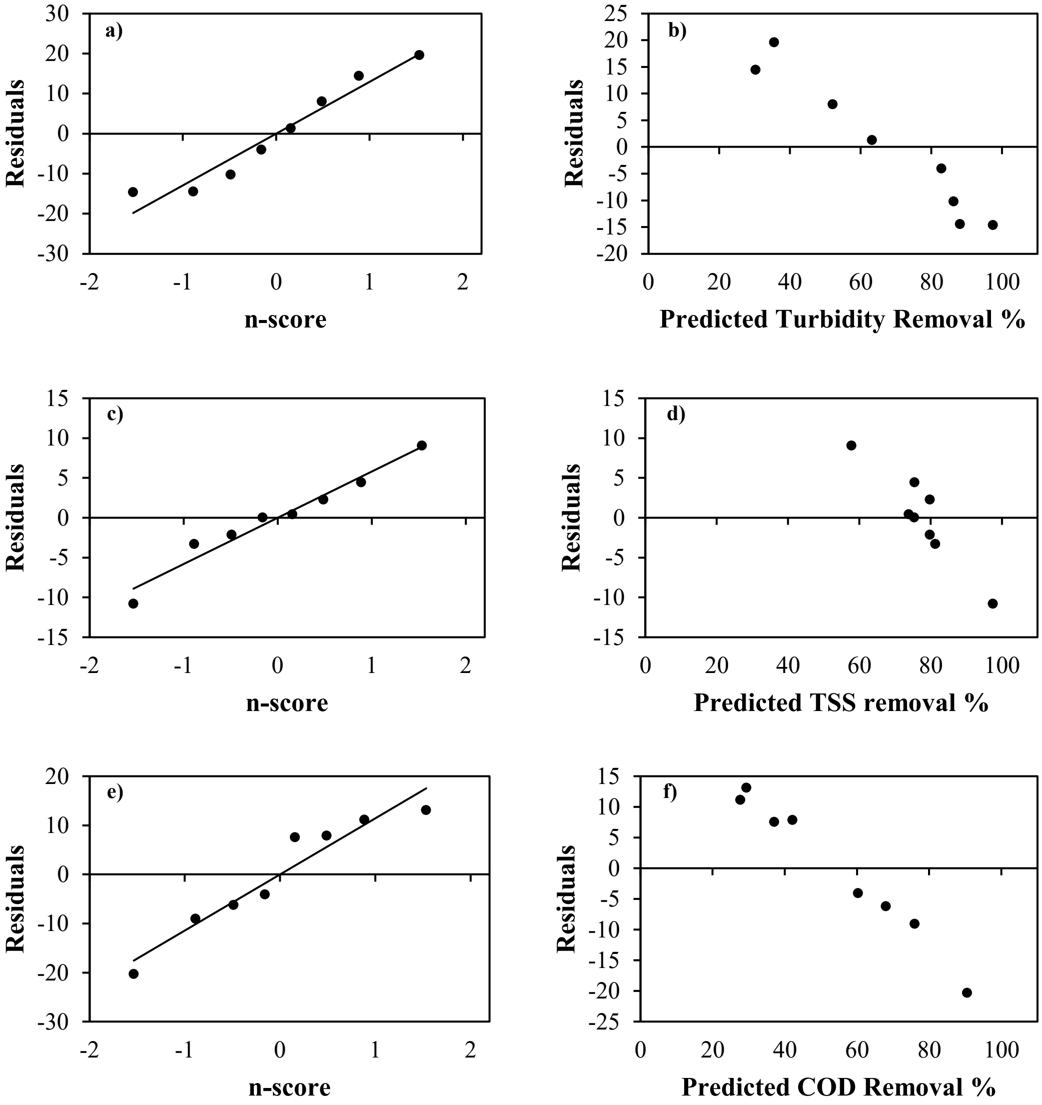

Figure B. 2 Normal probability plots for residuals and residual versus predicted removals: a, b for turbidity removal, c, d for TSS removal and e, f for COD removal. Note: n-score values were calculated using excel equation NORMSINV(P) and P calculated by using equation P=(i-0.5)/n , where i is ranking number of residual measurement in ascending order, n is total number of measurements.

Appendix C

Table C. 1 Two-Way ANOVA results evaluate statistical significance impact on E. coli inactivation from three factors: A= ferrate dose (10, 5 mg/L), B=Temperature (temperature 19 ,9 °C), C= contact time (10,3 minutes).

	SS	*df*	*MS*	*F*	*p-value*	*sig*
A	14.6	1.0	14.6	78.2	0.0	yes
B	1.0	1.0	1.0	5.5	0.0	yes
C	0.6	1.0	0.6	3.0	0.1	no
A x B	1.1	1.0	1.1	5.6	0.0	yes
A x C	0.2	1.0	0.2	1.3	0.3	no
B x C	0.4	1.0	0.4	1.9	0.2	no
A x B x C	0.4	1.0	0.4	2.2	0.2	no
Within	1.5	8.0	0.2			
Total	19.8	15.0	1.3			

Table C. 2 ANOVA test summary for temperature effect on the ferrate-decay rate constant determined under different temperatures

Sources	SS	df	MS	F	*P value*
Between Groups	0.04	1.00	0.04	0.29	0.62
Within Groups	0.52	4.00	0.13		
Total	0.55	5.00	0.11		

Table C. 3 The calculated half-life of ferrate corresponded to different doses under different temperatures during the disinfection kinetic experiment.

	$t_{1/2}$, min	
Temperature C◦	**19**	**9**
Ferrate (10 mg/L Fe)	0.66	0.72
Ferrate (8 mg/L Fe)	0.48	0.62
Ferrate (5 mg/L Fe)	0.20	0.35

Table C. 4 The obtained p-values based on the Goodness of fit test using Anderson-Darling Test rejection p-value= 0.05.

Fe(VI) (mg/L Fe)	**5**		**8**		**10**	
Temperature (°C)	9	19	9	19	9	19
Collins-Selleck	0.51	1.00	0.83	0.98	0.74	0.69
Chick-Watson	0.62	0.69	0.89	0.90	0.79	0.49
Hom	0.51	1.00	0.92	0.98	0.84	0.69

Table C. 5 summary of previous studies examined ferrate inactivation kinetic of different microorganisms using different water matrices.

Microorganism/ disinfectant	**Water matrix**	**Disinfection model/ rate constant (*k*) L/(mg min)**	**Reference**
***E. coli* /ferrate**	PBS[1]	Chick-Watson/ k=0.625	(Cho et al., 2006)
***E. coli* / ferrate**	model tap water	Chick-Watson k=0.687	(Jiang et al., 2007)
***E. coli* /ferrate**	ballast water (model water)	Chick-Watson/ k=0.39 Hom / k=2.345	(Jessen et al., 2008)
Bacillus subtilis spores/ ferrate and ozone	PBS	Delayed Chick-Watson/ k_{ferrate} =0.034 k_{ozone} = 0.9	(Makky et al., 2011)
Bacteriophage MS2/ ferrate	PBS	Chick-Watson k= 2.27	(Hu et al., 2012)
Total coliform / ferrate	SE[2]	Chick-Watson k= 0.493	(Kwon et al., 2014)
***E. coli*/ ferrate**	wastewater of WWF[3]	Chick-Watson/ k= NA[4] Hom / k= NA	(Elnakar and Buchanan, 2019)
Murine Norovirus (MNV) and Fecal Coliforms/ferrate	SE / PBS	Chick-Watson/ $K_{\mathrm{MNV,PBS}}$= 0.075 $K_{\mathrm{MNV},SEW}$=.135 $K_{FC,SEW}$=2.08	(Manoli et al., 2020)
***E. coli*/ ozone**	SE/PBS	Chick-Watson/ K_{PBS}= 8.04 x 10^3 K_{SE}= 1.92 x 10^3	(Czekalski et al., 2016)
***E. coli* / peracetic acid (PAA) and performic acid (PFA)**	SE	Chick-Watson k_{PAA}= 0.148 x 10^{-3} k_{PFA}= 0.148 x 10^{-3}	(Campo et al., 2020)
***E. coli*/ chlorine**	SE	Chick-Watson k =0.151	(Owoseni et al., 2017)

---

[1] phosphate buffer solution, [2] wastewater of secondary effluent, [3] wet weather flow sample, [4] not available

Table C. 6 ANOVA test summary for temperature effect on E. coli inactivation rate constant in the ferrate disinfection process determined under different temperatures

Sources	SS	df	MS	F	*P value*
Between Groups	0.13	1.00	0.13	4.10	0.11
Within Groups	0.13	4.00	0.03		
Total	0.25	5.00	0.05		

Appendix D

Table D. 1 The concentration of the stock solutions for the selected model compounds

Model compound	**Stock solution concentration (mg/L)**
atrazine	25
fluconazole	100
mecoprop	100
diazinon	25
carbendazim	5
perfluorooctanoic acid	100
carbamazepine	10
sulfamethoxazole	100
trimethoprim	100
clindamycin,	25

Table D. 2 Physicochemical properties of the selected MPs with chemical formula, class, p*Ka*, $\log k_{ow}$ and chemical structure.

No.	**Model Compound**	**Formula**	**Class**	**pK_a**	**$\log K_{ow}$**	**Chemical structure**
1	Carbendazim	$C_9H_9N_3O_2$	Antifungal	4.2-4.29	1.49-1.52	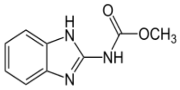
2	Fluconazole	$C_{13}H_{12}N_6OF_2$	Antifungal	2.27	0.25	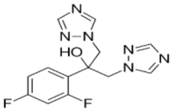
3	Atrazine	$C_8H_{14}N_5Cl$	herbicide	1.6	2.61	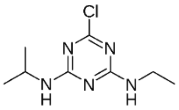
4	Mecoprop	$C_{10}H_{11}O_3Cl$	herbicide	3.78	3.3	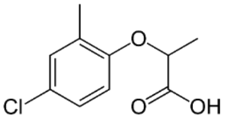
5	Diazinon	$C_{12}H_{21}N_2O_3PS$	insecticide	2.6	3.81	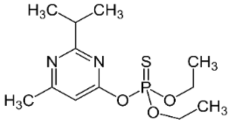
6	Perfluorooctanoic acid (PFOA)	$C_8HF_{15}O_2$	surfactant	1.3	1.92-2.59	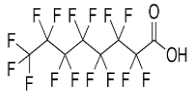
7	Carbamazepine	$C_{15}H_{12}N_2O$	anticonvulsant	13.9	2.45	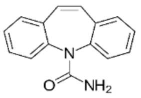
8	Sulfamethoxazole	$C_{10}H_{11}N_3O_3S$	antibiotic	1.7,5.6	0.89	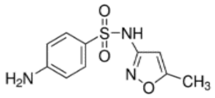
9	Trimethoprim	$C_{14}H_{18}N_4O_3$	antibiotic	7.12	0.91	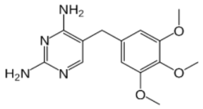
10	Clindamycin	$C_{18}H_{33}N_2O_5SCl$	antibiotic	7.79	2.16	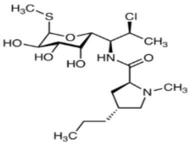

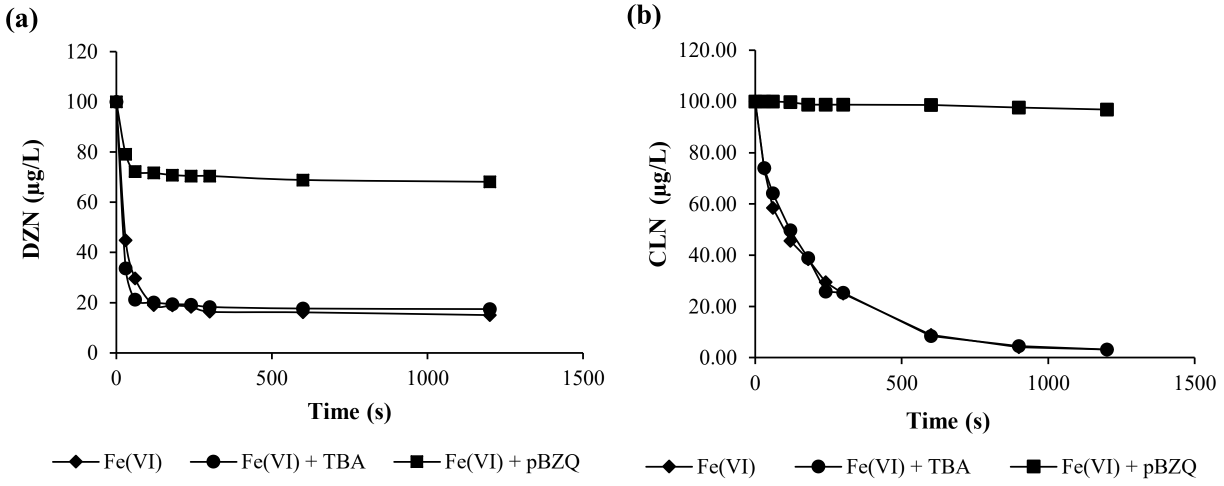

Figure D. 1 Radical species contribution in the degradation of model compounds by ferrate: a) CLN (C_o=100 µg/L), ferrate Fe(VI)= 1 mg/L Fe), b) DZN (C_o=100 µg/L), (Fe(VI)= 3 mg/L Fe). Ferrate alone denoted as Fe(VI), ferrate with hydroxyl radical scavenger tert-Bytyl alcohol (TBA) denoted as Fe(VI) +TBA and ferrate with superoxide radical scavenger para-benzoquinone denoted as Fe(VI) + pBZQ. The concentration of radical scavengers was 1 mM